SEPARATION OF TRACE PALLADIUM CHLORO COMPLEXES FROM WASTEWATER OF ELECTROLESS PLATING PROCESS VIA HOLLOW FIBER SUPPORTED LIQUID MEMBRANE

Miss Vanee Mohdee

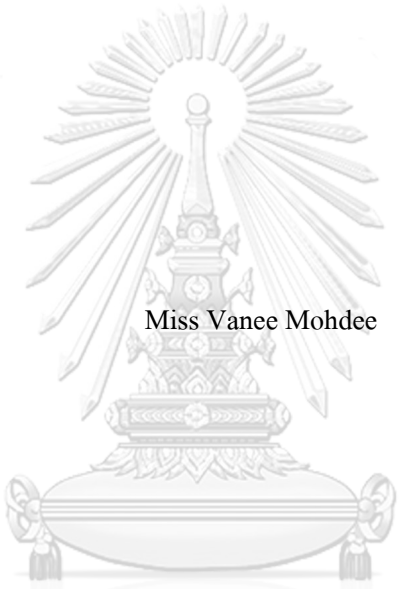

จุฬาลงกรณ์มหาวิทยาลัย
CHULALONGKORN UNIVERSITY

A Dissertation Submitted in Partial Fulfillment of the Requirements
for the Degree of Doctor of Engineering in Chemical Engineering
Department of Chemical Engineering
FACULTY OF ENGINEERING
Chulalongkorn University
Academic Year 2019

Copyright of Chulalongkorn University

กระบวนการแยกแพลเลเดียมคลอโรคอมเพล็กซ์จากน้ำเสียของกระบวนการเคลือบโดยไม่ใช้ไฟฟ้าด้วยเยื่อแผ่นเหลวที่พยุงด้วยเส้นใยกลวง

น.ส.วาณี หมอดี

จุฬาลงกรณ์มหาวิทยาลัย
CHULALONGKORN UNIVERSITY

วิทยานิพนธ์นี้เป็นส่วนหนึ่งของการศึกษาตามหลักสูตรปริญญาวิศวกรรมศาสตรดุษฎีบัณฑิต
สาขาวิชาวิศวกรรมเคมี ภาควิชาวิศวกรรมเคมี
คณะวิศวกรรมศาสตร์ จุฬาลงกรณ์มหาวิทยาลัย
ปีการศึกษา 2562
ลิขสิทธิ์ของจุฬาลงกรณ์มหาวิทยาลัย

Thesis Title	SEPARATION OF TRACE PALLADIUM CHLORO COMPLEXES FROM WASTEWATER OF ELECTROLESS PLATING PROCESS VIA HOLLOW FIBER SUPPORTED LIQUID MEMBRANE
By	Miss Vanee Mohdee
Field of Study	Chemical Engineering
Thesis Advisor	Professor URA PANCHAROEN
Thesis Co Advisor	Assistant Professor SUPHOT PHATANASRI

Accepted by the FACULTY OF ENGINEERING, Chulalongkorn University in Partial Fulfillment of the Requirement for the Doctor of Engineering

..... Dean of the FACULTY OF ENGINEERING

(Professor SUPOT TEACHAVORASINSKUN)

DISSERTATION COMMITTEE

..... Chairman

(Assistant Professor Sirikul Chunsawang)

..... Thesis Advisor

(Professor URA PANCHAROEN)

..... Thesis Co-Advisor

(Assistant Professor SUPHOT PHATANASRI)

..... Examiner

(Assistant Professor APINAN SOOTTITANTAWAT)

..... Examiner

(Associate Professor KASIDIT NOOTONG)

..... Examiner

(Assistant Professor Kreangkrai Maneeintr)

จุฬาลงกรณ์มหาวิทยาลัย
Chulalongkorn University

วาณี หมอดี : กระบวนการแยกแพลเลเดียมคลอโรคอมเพล็กซ์จากน้ำเสียของกระบวนการเคลือบโดยไม่ใช้ไฟฟ้าด้วยเยื่อแผ่นเหลวที่พยุงด้วยเส้นใยกลวง. (SEPARATION OF TRACE PALLADIUM CHLORO COMPLEXES FROM WASTEWATER OF ELECTROLESS PLATING PROCESS VIA HOLLOW FIBER SUPPORTED LIQUID MEMBRANE) อ.ที่ปรึกษาหลัก : ศ.อุรา ปานเจริญ, อ.ที่ปรึกษาร่วม : ผศ.สุพจน์ พัฒนะศรี

งานวิจัยนี้ศึกษาการแยกแพลเลเดียมจากน้ำเสียของกระบวนการเคลือบโดยไม่ใช้ไฟฟ้า (ซึ่งประกอบด้วยโลหะทองแดงและนิกเกิลปะปนอยู่ด้วย) ด้วยเยื่อแผ่นเหลวที่พยุงด้วยเส้นใยกลวง ปัจจัยที่ศึกษา ได้แก่ ชนิดและความเข้มข้นของสารสกัดและสารนำกลับ, ความเป็นกรด-ด่างของสารละลายป้อนและอัตราการไหลของสารละลายป้อนและสารนำกลับ ผลการทดลองพบว่า สามารถสกัดและนำกลับแพลเลเดียมคลอโรคอมเพล็กซ์ได้สูงถึง >99% และ 87.09% ตามลำดับ โดยใช้ Aliquat 336 ละลายในตัวทำละลาย cyclohexane ความเข้มข้น 6% โดยปริมาตรเป็นสารสกัด, ค่าความเป็นกรด-ด่างของสารละลายป้อนเท่ากับ 2, สารละลายผสมระหว่างไทโอยูเรีย 0.5 โมลาร์ และกรดไฮโดรคลอริก 0.1 โมลาร์ เป็นสารนำกลับและอัตราการไหลของสารป้อนและสารนำกลับเท่ากับ 100 มิลลิลิตร/นาที ขั้นตอนควบคุมอัตราการถ่ายเทมวลผ่านระบบเยื่อแผ่นเหลวที่พยุงด้วยเส้นใยกลวง คือ การแพร่ซึมของสารประกอบเชิงซ้อนของไอออนแพลเลเดียมและสารสกัด Aliquat 336 ผ่านเยื่อแผ่นเหลว นอกจากนี้ แบบจำลองการถ่ายเทมวลสามารถใช้คำนวณความเข้มข้นของไอออนแพลเลเดียมที่เวลาต่างๆ ได้ โดยผลที่ได้จากการคำนวณพบว่ามีความสอดคล้องกับผลการทดลอง

จุฬาลงกรณ์มหาวิทยาลัย
CHULALONGKORN UNIVERSITY

สาขาวิชา วิศวกรรมเคมี ลายมือชื่อนิสิต .....

ปีการศึกษา 2562 ลายมือชื่อ อ.ที่ปรึกษาหลัก .....

ลายมือชื่อ อ.ที่ปรึกษาร่วม .....

5971475321 : MAJOR CHEMICAL ENGINEERING

KEYWORD: Extraction, Palladium separation, Mass transfer, HFSLM, Solubility

Vanee Mohdee : SEPARATION OF TRACE PALLADIUM CHLORO COMPLEXES FROM WASTEWATER OF ELECTROLESS PLATING PROCESS VIA HOLLOW FIBER SUPPORTED LIQUID MEMBRANE. Advisor: Prof. URA PANCHAROEN Co-advisor: Asst. Prof. SUPHOT PHATANASRI

The separation of palladium (Pd (II)) from wastewater containing copper (Cu (II)) and nickel (Ni (II)) is investigated via hollow fiber supported liquid membrane (HFSLM). The viability to separate Pd (II) was established by controlling the influence of operating conditions viz. aqueous feed acidity, carrier concentration, types of stripping solution as well as flows rate of feed and stripping solutions. A complete separation of Pd (II) acheiving >99% extraction and 87.09% recovery was demonstrated under optimum conditions of 6%(v/v) Aliquat 336, pH 2 as aqueous feed acidity, 0.5 M thiourea mixed with 0.1 M HCl as a strippant and 100 mL/min flow rate for both feed and stripping solutions. Transportation of Pd (II) across HFSLM was also investigated. The mass transfer in the LMs was found to be the rate controlling step. An analysis of mass is presented to study the transport phenomena of Pd (II) across HFSLM. Results indicate that the model proves to be an effective approach for predicting the transportation of Pd (II) across the system. It is significant that the model predictions were found to be in good agreement with the obtained experimental data.

จุฬาลงกรณ์มหาวิทยาลัย
Chulalongkorn University

Field of Study:	Chemical Engineering	Student's Signature .....
Academic Year:	2019	Advisor's Signature .....
		Co-advisor's Signature .....

ACKNOWLEDGEMENTS

Foremost, my deep gratitude goes first to my supervisor, Professor Ura Pancharoen, who expertly guided and contributed me through my Ph.D. study. Under his supervision, I learned how to define a research problem, find a solution to it, and finally publish the results. I also wish to express my sincere appreciation to Assist.Prof. Suphot Phatanasri, my Co-advisor, for giving an encouragement and insightful suggestions throughout my thesis.

Besides my advisor, I would like to express the gratitude to my dissertation committee members: Assist.Prof. Sirikul Chunsawang, Assist.Prof. Apinan Soottitantawat, Assoc.Prof. Kasidit Nootong and Assist.Prof. Kreangkrai Maneeintr, for theirs invaluable advice that shaped my final dissertation.

My grateful thanks are also extended to the funding sources of my research. I profoundly appreciate the support from the Thailand Research Fund and Chulalongkorn University under the Research and Researchers for Industries (RRi) Ph.D. Program (Grant No. PHD58I0081). Thanks are also given to the Separation Laboratory, Department of Chemical Engineering, Faculty of Engineering, Chulalongkorn University as well as to the Mektec Manufacturing Corporation (Thailand) Ltd. Without their valuable support and funding, this project could not have reached its goal.

I would always remember my friends and fellow lab mates too for the fun-time we spent together for their continued support me well throughout the entire research program.

Last but not least, I wish to acknowledge the support and great love of my father, my mother and my brother who remembered me in their prayers for the ultimate success. They kept me going on and this work would not have been possible without their warm love, continued patience, and endless support.

Vanee Mohdee

จุฬาลงกรณ์มหาวิทยาลัย
CHULALONGKORN UNIVERSITY

TABLE OF CONTENTS

Page

..... iii

ABSTRACT (THAI)..... iii

..... iv

ABSTRACT (ENGLISH)..... iv

ACKNOWLEDGEMENTS.....v

TABLE OF CONTENTS..... vi

LIST OF TABLES..... xiii

LIST OF FIGURES xvi

NOMENCLATURES xx

CHAPTER I.....1

INTRODUCTION 1

1.1 General introduction.....1

1.1.1 Extractants.....3

1.1.2 Diluents 5

1.1.3 Feed solutions 5

1.1.4 Stripping solutions 5

1.1.5 Transportation of metal ions across HFSLM.....6

1.1.6 Mass transfer across HFSLM.....8

1.1.7 Flow patterns of HFSLM 11

1.1.9 Properties of HFSLM.....13

1.1.10 Aqueous feed acidity.....14

จุฬาลงกรณ์มหาวิทยาลัย
CHULALONGKORN UNIVERSITY

1.1.11 Carrier concentration....14
1.1.12 Flow rates of both aqueous solutions....14
1.1.13 Flow patterns of aqueous solutions....15
1.1.14 Mathematical modelling....15
1.1.15 Solubility....15
1.2 Objectives of the dissertation....16
1.3 Scope of the dissertation....16
1.4 Expected results....17
1.5 Description of the dissertation....17
CHAPTER II....20
2.1 Graphical Abstract....21
2.2 Abstract....21
2.3 Introduction....22
2.4 Theoretical background....25
2.4.1 Conservation equations of mass....28
2.4.2 Mass transportation across HFSLM system....33
2.5 Experimental....35
2.5.1 Reagents and chemical compounds....35
2.5.2 Experimental apparatus....36
2.5.3 Experimental procedures....36
2.6 Results and discussion....37
2.6.1 Effect of aqueous feed acidity....37
2.6.2 Effect of carrier concentration....40
2.6.3 Slope analysis....42

จุฬาลงกรณ์มหาวิทยาลัย
CHULALONGKORN UNIVERSITY

2.6.4 Statistical analysis 43

2.6.5 Effect of type of strippants 46

2.6.6 Effect of flow rate in Pd (II) transportation 48

2.6.7 Numerical solution 50

2.6.8 Evaluation of mass transfer coefficient 54

2.7 Conclusion 54

2.8 Funding 55

2.9 Nomenclature 55

2.10 References 56

2.11 Recommendations for future research 62

CHAPTER III 63

3.1 Abstract 64

3.2 Graphical Abstract 65

3.3 Introduction 65

3.4 Experimental 67

3.4.1 Reagents and solutions 67

3.4.2 Procedure 67

3.5 Design of the experiment 68

3.6 Statistical analysis 69

3.7 Thermodynamics study 69

3.8 Kinetic study 72

3.9 Results and discussion 73

3.9.1 Influence of Aliquat 336 concentration on Pd (II) extraction 73

3.9.2 Influence of pH on Pd (II) extraction 73

จุฬาลงกรณ์มหาวิทยาลัย
Chulalongkorn University

3.9.3 Influence of stirring speed on Pd (II) extraction 75

3.9.4 Influence of reaction time on Pd (II) extraction.....76

3.9.5 Thermodynamics study on Pd (II) extraction 77

3.9.6 Isotherm model 80

3.9.7 Kinetic study on Pd (II) extraction.....82

3.9.8 Selection of lower, middle and upper levels for the design variables.....83

3.9.9 ANOVA results and regression model: response surface analysis 83

3.9.10 Response surface plot.....85

3.10 Conclusion.....87

3.11 Acknowledgements 87

3.12 References 88

CHAPTER IV 98

4.1 Abstract 99

4.2 Introduction 99

4.3 Experimental 101

4.3.1 Reagents and solutions.....101

4.3.2 Procedure 102

4.3.4 Kinetics study.....103

4.4 Results and discussion.....104

4.4.1 Influence of types of solvating extractant 104

4.4.2 Influence of Aliquat 336 concentration 105

4.4.3 Influence of HCl concentration.....106

4.4.4 Influence of types of strippants.....107

4.4.5 Thermodynamics study on Pd (II) ions solvating system.....111

จุฬาลงกรณ์มหาวิทยาลัย
CHULALONGKORN UNIVERSITY

4.4.6 Kinetics study on Pd (II) ions solvating system....113
4.4.7 Mechanism and model....114
4.5 Conclusion....119
4.6 Acknowledgments....120
4.7 Funding....120
4.8 References....120
CHAPTER V....129
5.1 Graphical abstract....130
5.2 Abstract....130
5.3 Introduction....131
5.4 Solubility modelling....132
5.4.1 The Apelblat equation....132
5.4.2 Buchowski–Książ̇czak λh equation....133
5.4.3 NRTL model....133
5.4.4 The apparent thermodynamic parameters for DMBA dissolution....134
5.5 Experimental....136
5.5.1 Materials....136
5.5.2 Characterization of DMBA....138
5.5.3 Measurement of DMBA solubility....138
5.6 Results and discussion....140
5.6.1 Solid phase properties of DMBA....140
5.6.2 Solubility data....141
5.6.3 Solvent selection....143
5.6.4 Effect of solvent properties....145

จุฬาลงกรณ์มหาวิทยาลัย
Chulalongkorn University

5.6.5 Correlation of DMBA solubility 147

5.6.6 Model comparison.....151

5.6.7 Apparent thermodynamic parameters for DMBA dissolution 156

5.6.8 Thermodynamic functions of mixing.....159

5.7 Conclusion.....160

5.8 Declaration of competing interest 161

5.9 Acknowledgement.....161

5.10 Reference.....161

5.11 Notation 166

CHAPTER VI 167

6.1 Conclusion.....167

6.2 Limitation 169

6.3 Recommendations for future research.....169

APPENDICES 171

APPENDIX A 172

List of publications.....172

APPENDIX B 174

B.1 Graphical abstract 175

B.2 Abstract.....176

B.3 Introduction 176

B.4 Experimental.....178

B.5 Results and discussion 180

B.6 Conclusion 208

B.7 Acknowledgement 209

จุฬาลงกรณ์มหาวิทยาลัย
Chulalongkorn University

B.8 Nomenclature.....209

B.9 References 210

REFERENCES 227

VITA 229

จุฬาลงกรณ์มหาวิทยาลัย
Chulalongkorn University

LIST OF TABLES

Table **Page**

Table 1.1 Summary of previous research on Pd (II) separation via different methods…….……2

Table 1.2 The characteristics of obtained wastewater……..…….5

Table 1.3 Properties of the HF module……...13

Table 2.1 Summary of previous research on mass separation via HFSLM…….…..….24

Table 2.2 Detailed information on the materials…….……..……..35

Table 2.3 The characteristics of the HF module…….36

Table 2.4 Separation factor of Pd (II) over Cu (II) and Ni (II) against feed acidity……...40

Table 2.5 Distribution ratio against concentration of Aliquat 336……..……42

Table 2.6 Analysis of variance……..……..44

Table 2.7 Distribution ratio and separation factor of each metal at various flow rates……..49

Table 3.1 Summary of previous research on palladium separation……...….66

Table 3.2 Five independent variables and levels used for CCD…….……69

Table 3.3 Relationship between adsorption and extraction process……...…….72

Table 3.4 Thermodynamic data for the Pd-Aliquat 336 system…….……79

Table 3.5 Comparison of Langmuir, Freundlich and Temkin constants of Pd (II) ions Extraction……...……82

Table 3.6 The reaction rate order of Pd (II) ions LLE……...…….82

Table 4.1 Summary of previous research on SX of Pd (II) ions……...100

Table 4.2 Sources and %purity of materials used…….101

Table 4.3 Palladium chlorocomplexes's stability constant……...……105

Table 4.4 Stripping efficiency of Pd (II) ions solvating system using various strippants…….....108

Table 4.5 Stripping efficiency of Pd (II) ions solvating system using various synergistic strippants…….110

Table 4.6 Thermodynamic data for the Pd-Aliquat 336 system……..…….113

Table 4.7 The reaction rate order of Pd (II) ions solvating system…….……..113

Table 5.1 Detailed information on DMBA……...137

จุฬาลงกรณ์มหาวิทยาลัย
Chulalongkorn University

Table 5.2 Detailed information on the solvents……137

Table 5.3 Experimental mole fraction solubility (x_e) of DMBA in different solvents at elevated temperature range from T = (298.15 to 353.15) K at atmospheric pressure (101.325 kPa)……143

Table 5.4 The polarity index of different solvents……144

Table 5.5 Physicochemical properties of selected solvents……..145

Table 5.6 Apelblat equation parameters for DMBA in various solvents……..148

Table 5.7 The λh equation parameters for DMBA in various solvents……149

Table 5.8 NRTL parameters for DMBA in various solvents……150

Table 5.9 Experimental mole fraction solubility (x_e) and correlated solubility (x_c) of DMBA in different solvents at elevated temperature range from T = (298.15 to 353.15) K at atmospheric pressure (101.325 kPa)……153

Table 5.10 Thermodynamic parameters $\Delta_{sol}H$ (kJ·mol^{-1}) and $\Delta_{sol}S$ (J·mol^{-1}·K^{-1}) for DMBA in various solvents at different temperatures and at atmospheric pressure (101.325 kPa)……...158

Table 5.11 Gibbs free energy of mixing of DMBA in selected solvents……..160

Table B.1 Detailed information of DMPA……178

Table B.2 Detailed information of materials used……179

Table B.3 Experimental mole fraction solubility of DMPA in different solvents at temperature range from T = (298.15 to 353.15) K and 101.32 kPa……182

Table B.4 The Apelblat equation parameters for DMPA in various solvents…….…….183

Table B.5 The λh equation parameters for DMPA in various investigated solvents……...184

Table B.6 NRTL parameters for DMPA in various solvents……186

Table B.7 Experimental mole fraction solubility (x_e) and correlated solubility (x_c) of DMPA in different solvents at temperature range from T = (298.15 to 353.15) K and atmospheric pressure (101.325 kPa)……..……191

Table B.8 Apparent thermodynamic parameters: molar enthalpy, $\Delta_{sol}H$ (kJ·mol^{-1}), and molar entropy, Δ_{sol}S (J·mol^{-1}·K^{-1}), for DMPA in various solvents at different temperatures and 101.32 kPa……199

Table B.9 Excess enthalpy of DMPA in selected solvents at various temperatures

จุฬาลงกรณ์มหาวิทยาลัย
Chulalongkorn University

and 101.32 kPa……..……..202

Table B.10 Gibbs free energy of mixing ($\Delta_{mix}G$) of DMPA in selected solvents……..……..204

Table B.11 The polarity index of solvents used……206

Table B.12 Physicochemical properties of selected solvents……207

จุฬาลงกรณ์มหาวิทยาลัย
CHULALONGKORN UNIVERSITY

LIST OF FIGURES

Figure **Page**

Figure 1.1 Facilitated coupled transport of ions through the liquid membrane……8

Figure 2.1 Chemical structure of Aliquat 336……24

Figure 2.2 Schematic diagram for separation via HFSLM……26

Figure 2.3 Schematic diagram of a single hollow fiber……28

Figure 2.4 Schematic diagram of the HFSLM system……37

Figure 2.5 Influence of feed acidity on metal extraction and stripping (Extractant: 2%(v/v) of Aliquat 336, Strippant: 2 M of HNO_3, Flow rate: 100 mL/min for both feed and stripping solutions)……39

Figure 2.6 Pourbaix diagram of each metal……40

Figure 2.7 Influence of Aliquat 336 concentration on Pd (II) extraction. (Feed acidity: pH 2, Strippant: 2 M of HNO3, Flow rate: 100 mL/min for both feed and stripping solutions)……41

Figure 2.8 Slope analysis of each metal……43

Figure 2.9 Contour plot and surface plot of %Pd (II) extraction versus concentration of Aliquat 336 and pH of feed solution……45

Figure 2.10 The predicted values of %Pd (II) extraction in comparison to experimental results……46

Figure 2.11 Influence of stripping solutions on metal ions recovery. (Feed acidity: pH 2, Extractant: 6%(v/v) of Aliquat 336, Flow rate: 100 mL/min for both feed and stripping solutions)……47

Figure 2.12 Influence of flow rate on metal ions recovery. (Feed acidity: pH 2, Extractant: 6%(v/v) of Aliquat 336, Strippant: 0.5 M Thiourea mixed with 0.1 M HCl)……49

Figure 2.13 Concentration profile of Pd (II) via finite difference method along the tube, LMs, and shell side via HFSLM system: (a) concentration distribution (b) concentration profile in r-direction and (c) concentration profile in z-direction……51

Figure 2.14 Numerical results compared with experimental results for Pd (II) in both

จุฬาลงกรณ์มหาวิทยาลัย
Chulalongkorn University

feed and stripping phases…….52

Figure 2.15 Numerical results compared with experimental results in the stripping phase using thiourea solution and synergistic solutions (0.5 M thiourea mixed with 0.1 M HCl)……..53

Figure 2.16 Numerical results compared with experimental results in the feed phase applied to Ta [36] and Nd [8]……...53

Figure 2.17 Linear relationship between $1/P$ vs. $1/K_d$ for Pd (II) transportation……54

Figure 3.1 Influence of concentration of Aliquat 336 on Pd (II) extraction……...73

Figure 3.2 Influence of pH of feed solution on Pd (II) extraction using 0.6 M of Aliquat 336 dissolved in cyclohexane……...75

Figure 3.3 Influence of stirring speed on Pd (II) extraction using 0.6 M of Aliquat 336 dissolved in cyclohexane……...76

Figure 3.4 Influence of reaction time on Pd (II) extraction using 0.6 M of Aliquat 336 dissolved in cyclohexane……..77

Figure 3.5 Influence of reaction temperature on Pd (II) extraction using 0.6 M of Aliquat 336 dissolved in cyclohexane……...78

Figure 3.6 Plot of ln K_{eq} vs 1/T……...79

Figure 3.7 Parameter constants; a Langmuir model, b Freundlich model and c Temkin model……..80

Figure 3.8 First-order reaction rate plot of Pd (II) LLE……..83

Figure 4.1 Influence of extractants on Pd (II) ions solvating system using 2%v/v of extractant……..105

Figure 4.2 Influence of concentration of Aliquat 336 on Pd (II) ions solvating system……...106

Figure 4.3 Influence of chloride medium concentration on Pd (II) ions extracted via solvating system……107

Figure 4.4 Influence of synergistic strippants on Pd (II) ions solvating system……...110

Figure 4.5 Influence of reaction temperature on Pd (II) ions solvating system. (Solid line: % Pd extraction and dash line: % Pd stripping)……112

Figure 4.6 Plot of ln K_{eq} versus $1/T$……...112

Figure 4.7 Graphical plot of kinetics study on Pd (II) ions solvating system

จุฬาลงกรณ์มหาวิทยาลัย
Chulalongkorn University

(a) Pd (II) extraction reaction and (b) Pd (II) stripping reaction…….114

Figure 4.8 Mechanism of Pd (II) ions stripping in an aqueous/organic two-phase system……..115

Figure 4.9 Mechanism of synergistic strippants solution, thiourea + HCl……116

Figure 4.10 Influence of pH on P_{app}.

(Symbols: experimental value and line: calculated value)……..118

Figure 4.11 Influence of reaction temperature on Pd (II) ions distribution ratio……..119

Figure 5.1 The chemical structure of 2,2-Bis(hydroxymethyl)butyric acid……..131

Figure 5.2 Thermal analysis (DSC) of DMBA (2A – before recrystallization

and 2B – after recrystallization)……..141

Figure 5.3 Mole fraction solubility (xe) of DMBA in various solvents,

as a function of temperature…….142

Figure 5.4 Solubility spectra of DMBA in selected solvents at 298.15 K as a function of

(a) solvent polarity, (b) hydrogen bond donor propensity,

(c) hydrogen bond acceptor propensity and (d) cohesive energy density…….....146

Figure 5.5 Experimental mole fraction solubility (x_e) and the calculated

mole fraction solubility ($x_{e,\ NRTL}$) of DMBA in various solvents,

as a function of temperature…….151

Figure 5.6 Experimental mole fraction solubility (x_e) and the calculated

mole fraction solubility of DMBA in various solvents,

as a function of temperature……152

Figure B.1 The chemical structure of DMPA……...177

Figure B.2 Mole fraction solubility (x_e) of DMPA in different solvents,

as a function of temperature……..181

Figure B.3 Experimental mole fraction solubility (x_e) and the calculated

mole fraction solubility of DMPA in different solvents,

as a function of temperature……187

Figure B.4 DSC thermograms of DMPA: Before recrystallization (1A) and

after recrystallization (1B)……..196

Figure B.5 DSC thermograms of DMPA: Original sample and equilibrium bottom solid phases

in different solvents…….197

จุฬาลงกรณ์มหาวิทยาลัย
Chulalongkorn University

Figure B.6 Dissolution properties of DMPA as a function of temperature,
in various mono solvent……..200
Figure B.7 Excess enthalpy of solutions as a function of temperature…….203
Figure B.8 Gibbs free energy of mixing as a function of temperature……..205
Figure B.9 Solubility spectra of DMPA in selected solvents at 298.15 K as a function of
solvent polarity, hydrogen bond donor propensity,
hydrogen bond acceptor propensity and cohesive energy density……..208

จุฬาลงกรณ์มหาวิทยาลัย
CHULALONGKORN UNIVERSITY

NOMENCLATURES

A	membrane area (cm^2)
A_f	cross sectional area of hollow fiber (cm^2)
A_p	cross sectional area of hollow fiber ring (cm^2)
A_s	cross sectional area of stripping phase (cm^2)
C_e	equilibrium concentration of Pd (II) (mg/L)
d_i	inner diameter of the hollow fiber (cm)
d_o	outer diameter of the hollow fiber (cm)
$\mathcal{D}$	diffusion coefficient of Pd (II)
k_d	distribution coefficient
k_f	rate constant of extraction reaction ($cm^3 \cdot mg^{-1} \cdot min^{-1}$)
k_{LMs}	mass transfer coefficient in the membrane phase ($cm \cdot min^{-1}$)
k_s	rate constant of stripping reaction ($cm^3 \cdot mg^{-1} \cdot min^{-1}$)
L	length of the hollow fiber (cm)
N	numbers of hollow fibers in the module
q_f	volumetric flow rate of feed solution ($cm^3 \cdot min^{-1}$)
q_s	volumetric flow rate of stripping solution ($cm^3 \cdot min^{-1}$)
r_i	inner radius of the hollow fiber (cm)
r_o	outter radius of the hollow fiber (cm)
a_i	activity of DMPA
a_s	activities of solid

จุฬาลงกรณ์มหาวิทยาลัย
CHULALONGKORN UNIVERSITY

a_w	activities of liquid
A, B and C	empirical parameters (the Apelblat equation)
g_{12} and g_{21}	equation parameters (NRTL model)
H^E	excess enthalpy of solutions (kJ·mol^{-1})
K_i	dissolution equilibrium constants
K_F	Freundlich isotherm constants (mg/g)
K_L	Langmuir isotherm constant
K_T	Temkin isotherm constant (mg/g)
n	total experimental points
q_e	amount of metal ion adsorbed or extracted per weight of carrier (mg/g)
q_{max}	maximum adsorbed or extracted capacity
R	gas constant (J· mol^{-1}· K^{-1})
T_m	melting temperature (K)
x	mole fraction solubility of solute in solvent
x_c	the calculated molar fraction of solubility
x_e	the experimental molar fraction of solubility
λ and h	empirical parameters (Buchowski–Książczak λh equation)
$\Delta_{fus}H$	fusion enthalpy of DMPA (kJ· mol^{-1})
$\Delta_{sol}H$	molar enthalpy of dissolutions (kJ· mol^{-1})
$\Delta_{sol}S$	molar entropy of dissolutions (J· mol^{-1}· K^{-1})
α_{ij}	the solution non-randomnes

จุฬาลงกรณ์มหาวิทยาลัย
Chulalongkorn University

CHAPTER I

INTRODUCTION

1.1 General introduction

Palladium has been widely used in diverse industrial applications such as jewelry, automotive, electronic and chemical processes owing to its unique properties [1, 2]. Generally, industrial wastewater, as secondary resources, such as that caused by the electroless plating process in the flexible printed circuit board manufacturers, still contains palladium ions (Pd (II)) and other precious metals at a trace level of concentration. Therefore, separation of Pd (II) from industrial wastewater is a technologically challenging ascribe to its valuable metal residue, its limited resources and its high demand [3, 4]. Several conventional methods have been highlighted in the process of wastewater treatment for the separation of target metal ions i.e. precipitation, solvent extraction, adsorption and ion exchange [5-7]. Solvent extraction (SX), one of a conventional method, has been widely used in hydrometallurgical process owing to its high efficiency of purification and simple operation [8]. However, the limitation of SX was found to be ineffective and difficulty in separating the target specie at a trace concentration level [9]. Thus, the separation and recovery of trace concentration of Pd (II) is valuable and difficult to seek an appropriate method.

จุฬาลงกรณ์มหาวิทยาลัย
Chulalongkorn University

Of late, liquid membranes (LMs) have received much attention, involving the separation and removal of target organic and inorganic species [10]. Hollow fiber supported liquid membrane (HFSLM), especially, is a promising system for processing target metals ions. It has been shown to have effectively separated trace levels of target metals owing to its high surface area of the LMs modules (approximately 104 m^2/m^3) [11]. The advantages of HFSLM over conventional methods are its high efficiency,

high selectivity, high contact area, use less amount of chemical solutions as well as lower energy consumption and costs [12, 13]. HFSLM is seen as having high selectivity allowing simultaneous extraction and stripping processes in a single-step of operation. Moreover, it can be regarded as a green technology over conventional methods on account of its reusability of LMs and zero discharge of effluent. In **Table 1.1**, a summary of previous studies on Pd (II) separation via different methods is presented.

Table 1.1 Summary of previous research on Pd (II) separation via different methods.

Feed solution	Extractant	Diluent	Methods	%Extraction	Ref.
Synthesized feed	diglycolthioamide	Kerosene	SX	N/A	[1]
Synthesized feed	piperidine-based	toluene	SX	>90%	[2]
waste PCBs (powder)	Sc-CO_2	acetone	SCWO	>93.7%	[3]
Synthesized feed	NTH	hexane	HFSLM	N/A	[14]
Industrial wastewater	LIX 84-I	kerosene	HFSLM	100%	[15]
Synthesized feed	Alamine 300	kerosene	SX	98%	[16]
Synthesized feed	CYANEX 471X	kerosene	SX	72%	[17]
Synthesized feed	Aliquat 336	benzene	SX	>99%	[18]
Synthesized feed	Cyphos®IL 101	toluene	SX	97.6%	[19]

Note: SX = solvent extraction, Sc-CO_2 = supercritical carbon dioxide, SCWO = supercritical water oxidation-extraction process, HFSLM = hollow fiber supported liquid membrane.

HFSLM is a cutting edge system that has been well applied in separation processes [20-27]. It is seen as a promising system for processing target species. HFSLM has high selectivity allowing simultaneous extraction and stripping processes in a single-step.

จุฬาลงกรณ์มหาวิทยาลัย
Chulalongkorn University

1.1.1 Extractants

The extractant used as a carrier for supported liquid membrane (SLM) is basically an organic solvent. Metal ion transfer through SLM can be described as regards the solvent extraction chemistry. The chemistry of extraction reaction can be classified as follows: [28-30]

Extraction by Compound Formation

Extraction reaction via compound formation mechanism occurred when extractants which exhibited chelating properties or acidic properties is employed. The mechanism of extraction via compound extraction is shown in Eq.(1.1):

$$M^{n+}(aq) + nHR(org) \longleftrightarrow MR_n(org) + nH^{+}(aq) \quad (1.1)$$

Chelating extractants: These types of extractants will be reacting with cation species. It's chemically bond to cation species at two sites in the same manner as holding an object between the ends of the thumb and the index finger. Hydrogen ion (H^{+}) is released into the feed solution when the chelating extractants bond with cation species. The efficiency of extraction increased with increasing pH of feed solution. As the pH of feed solution decreased, stripping reaction favorably occur. Examples of chelating extractants is LIX-84I, LIX 64N and LIX 62N, etc.

จุฬาลงกรณ์มหาวิทยาลัย
Chulalongkorn University

Acidic extractants: Acidic extractant is organic acids and their derivatives and related to proton donors. Acidic extractants react with cation in the feed solution as same as chelating extractants. Some commercially acidic extractants are D2EHPA, PC88A, Cyanex 272 (phosphoric acid derivatives) and so forth. These types of extractants have been widely used in hydrometallurgical process for the extraction of various metal ions such as Cu, Ni, Fe, Mn and etc.

Extraction by Ion-Pair Formation

Basic extractants (anion-exchangers) are utilized to extract metal ions via ion-pair formation chemistry. Basic extractants contain primary, secondary, tertiary amines, and their derivatives, quaternary amine salts and other proton acceptors. Amine based extractants will be expressed two modes of action during extraction via ion pair formation chemistry. Initially, Amine based extractants (as a free base form) are able to extract acid from the aqueous solution. Then, by anion exchange reaction, metal ions are extracted. Basic extractants, for example, Alamine 336, Aliquat 336, Alamine 304 and so forth. Extraction mechanism of Pd (II) from 0.1 M HCl with Aliquat 336 can be expressed as follows: [18]

$$2R_3N^+CH_3Cl^- + PdCl_4^{2-} \longleftrightarrow 2R_3N^+CH_3PdCl_4^{2-} + 2Cl^- \qquad (1.2)$$

Extraction by Solvation

The solvating extractants/neutral extractants, also known as selective extractants, are weakly basic and thus they extract either neutral metal complexes or acids by forming a solvate. These types of extractants are organic species with electron donor or acceptor properties, or solvating carriers. Solvating extractants will coordinate with certain neutral metal ions by replacing water molecules of hydration around neutral metal ions. Thereby, hydrophobic ions are formed. Some solvating extractants are MIBK, TBP, TOPO etc. The extraction mechanism for extraction reaction via solvation is shown in Eqs.(1.3) and (1.4): [31-33]

$$M_nX + yS \longleftrightarrow MX_nS_y \qquad (1.3)$$

$$HMX_{n+1} + xS \longleftrightarrow (HS_n) + (MX_{n+1})^- \qquad (1.4)$$

1.1.2 Diluents

Diluents have been applied to diminish the viscosity of solvents, which leads to the diffusivity of the solute complex within the membrane. Generally, diluents are inert solvents. Its properties should have high dielectric constant, low viscosity, high boiling point, low toxicity and cheap. Diluents play a significant on the extraction of metals regarding both physical and chemical interactions that exist between diluent and extractant. Various types of diluents are widely used in hydrometallurgical processes such as kerosene, toluene, hexane, cyclohexane, etc. [34]. Solvent physical properties have an influence on metal ions extraction. As the dipole moment and dielectric constant of diluents decreased, extraction efficiency increased.

1.1.3 Feed solutions

Wastewater of electroless plating process was obtained from Mektec Manufacturing CO., Ltd., Thailand. The characteristics of obtained wastewater were described in **Table 1.2**.

Table 1.2 The characteristics of obtained wastewater.

Color	pH	Pd (II) (ppm)	Cu (II) (ppm)	Ni (II) (ppm)
colorless	6-7	10.269	3.757	0.144

1.1.4 Stripping solutions

As regards metal recovery and the regeneration of an extractant, a stripping reaction is significant. Therefore, types and concentrations of stripping solutions play an essential role in the performance of metal recovery across HFSLM system. Thus, the selection of stripping solutions depends on both the target species of metal extracted and the types of extractants used.

In the case of target specie was metal cations, an acidic extractant or a chelating extractant were employed. Therefore, an acidic stripping solution is required. The mechanism occurred via acidic stripping solutions was described as follows: Hydrogen ions in acidic stripping solution substituted metal cations in the organometallic complex. Subsequently, the free metal cations are captured by the stripping solutions.

Regards metal anions extraction, the basic extractant or neutral extractant is applied. Accordingly, a basic stripping solution is required. The mechanism that occurred via basic stripping solutions was described as follows: Anions in basic stripping solution substituted metal anions in the organometallic complex and released metal anions into the stripping solutions.

Many types of researches have been attempted in creating and improving novel extractants. Meanwhile, few studies have investigated the enhancement of stripping efficiency. It is observed that an increase in stripping concentration resulting in higher stripping efficiency. In order to enhance the stripping efficiency, synergistic strippants is introduced. Thus, the synergistic solution is proposed to improve the effectiveness as well as selectivity of the processes of separation.

จุฬาลงกรณ์มหาวิทยาลัย
Chulalongkorn University

1.1.5 Transportation of metal ions across HFSLM

The transport phenomena of target species diffuse through the LMs phase can be achieved either via passive transport or active transport (or facilitated) [35-36].

Passive transport

Passive transport is a simply diffusing of solute across the LMs phase due to their concentration gradient in the feed phase and the stripping phase. It is limited by the equilibrium condition between the two aqueous phases, and is mainly used when

one species in a liquid mixture is soluble in the organic phase, whereas the other are not, leading to a separation.

Facilitated transport

In facilitated transport, membrane phase contains a carrier dissolved in an organic solvent. The carrier acts as a catalyst because it increases the solubility of the chemical space in the membrane by promoting the transfer speed. The driving force of facilitated transport is the concentration gradient between the feed phase and the stripping phase. Facilitated transport can be divided as follows:

- *Co-transport*: In this case, the neutral carrier is employed and the feed solutions contain a pair of cations and anions (M^{m+} mX^{-}) associated and extracted (dissociated) reversibly by carrier (L). The cation and anion migrate in the same direction of the source phase to the stripping phase owing to the concentration gradient. The mechanism of this type of transport is shown below:

$$M^{m+}_{(aq)} + mX^{-}_{(aq)} + L_{(org)} \longleftrightarrow (ML^{m+}\ mX^{-})_{org} \qquad (1.5)$$

จุฬาลงกรณ์มหาวิทยาลัย
CHULALONGKORN UNIVERSITY

- *Counter Transport*: In this case, the carrier can be acidic or basic nature. It's possible to find counter transport of anions or cations. For counter cation transport, the carrier in the membrane phase is an acid, and this process is done by a cation-exchange proton (pH pump), cations migrate in the opposite direction protons (high pH to low pH). The mechanism of counter cations transport is described in Eq.(1.6).

$$M^{m+}_{(aq)} + mHL_{(org)} \longleftrightarrow (ML_m)_{org} + mH^{+}_{(aq)} \qquad (1.6)$$

In the case counter facilitated transport of anions, the carrier in the LMs phase exchanged an anion (basic agent) by interaction with the substrate at the interface

between feed and LMs phases. Thus, a neutral entity (A^-L^+) was formed. Thereafter, A^-L^+ diffused through the LMs phase to the interface between LMs and stripping phases. The anion, A^-, is released and diffuses to the stripping phase, whereas the cationic species, L^+, associates with another anion X^- present in the stripping phase to form LX. Subsequently, LX diffuses through the LMs in the opposite direction of A^-. Anions facilitated transport is governed by the association between the substrate and carrier, the gradient of the concentration of anion X and electroneutrality of the feed and stripping phases. The mechanism of counter anions transport is described in Eq.(1.7). In **Fig. 1.1**, the facilitated transport of ions through LMs is depicted [36].

$$A^-_{(aq)} + XL_{(org)} \longleftrightarrow (A^-L^+)_{org} + X^-_{(org)} \qquad (1.7)$$

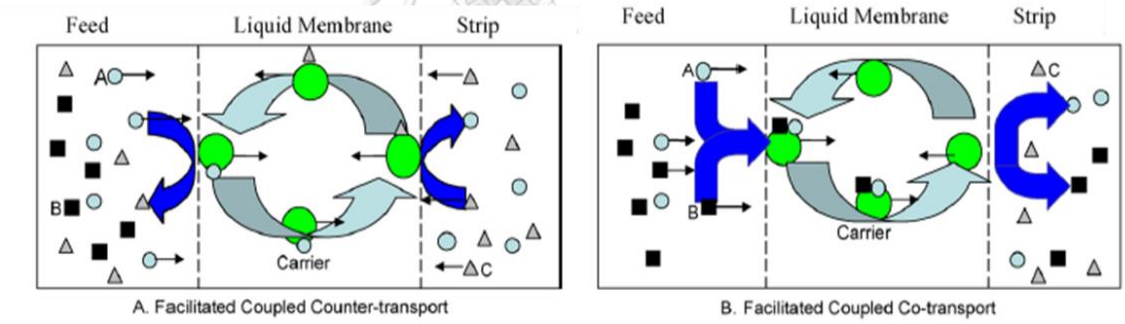

Fig. 1.1 Facilitated coupled transport of ions through the liquid membrane.

1.1.6 Mass transfer across HFSLM

The overall mass transfer resistance across HFSLM is considered based on the summation of each individual mass transfer resistances which are (1) the liquid phase resistance in the feed phase (2) the interfacial resistance of the extraction reaction (3)

the membrane phase resistance (4) the shell-side resistance (5) the resistance of the stripping reaction and (6) the strip-side resistance as can be written in Eq.(1.8). [37]

$$\frac{1}{K} = \frac{1}{k_a} + \frac{1}{k_e} + \frac{1}{m_f k_m} + \frac{1}{m_f k_o} + \frac{1}{m_f k_s} + \frac{1}{(m_f/k_s)k_{as}} \quad (1.8)$$

where k_a is the mass transfer coefficient in the feed phase, k_e is the mass transfer due to extraction reaction rate, k_s is the mass transfer due to stripping reaction rate, k_m is the mass transfer coefficient of the complex species in the LMs phase, k_o is the mass transfer coefficient in the shell side and k_{as} is the mass transfer coefficient in the stripping solution. The partition coefficient of target metal is the ratio between concentrations of target metal ions in the organic phase divided by the concentration of target metal ions in the feed phase.

Based on the concept of instantaneously stripping reaction was found to occurr, the mass transfer resistance of the stripping side can be negligible. Thus, the total mass transfer resistances can be simplified, as shown in Eq.(1.9).

จุฬาลงกรณ์มหาวิทยาลัย
CHULALONGKORN UNIVERSITY

$$\frac{1}{K} = \frac{1}{k_a} + \frac{1}{k_e} + \frac{1}{m_f k_m} + \frac{1}{m_s k_o} \quad (1.9)$$

Eq.(1.10), the mass transfer coefficient in the aqueous phase is given.

$$k_a = 1.62 \frac{D_f}{d_i} \left(\frac{d_i^2 v_f}{D_f}\right)^{0.33} \quad (1.10)$$

where D_f is the diffusivity of metal ions in feed phase (cm^2/s), v_f is the velocity of feed solution (cm/s) and d_i is the inner diameter of the fiber (cm).

The mass transfer coefficient in the LMs phase can be calculated, as shown in Eq.(1.11):

$$k_m = \frac{D_m \varepsilon d_{lm}}{\delta \tau d_o} \tag{1.11}$$

where D_m is the diffusivity of metal ions in the LMs (cm^2/s), d_{lm} is the log–mean diameter (cm), d_o is the outer diameter of the fiber (cm), ε is the porosity of the hollow fiber, τ is the tortuosity of the hollow fiber and δ is the membrane thickness (cm).

The mass transfer coefficient on the shell side can be evaluated by Eq.(1.12):

$$k_o = 1.25 \frac{D_m}{d_h^{0.07}} \left(\frac{d_h v_s}{\vartheta L}\right)^{0.93} \left(\frac{\upsilon}{D_m}\right)^{0.33} \tag{1.12}$$

where v_s is the velocity of stripping solution (cm/s) and υ is the kinematic viscosity (cm^2/s).

The diffusivity of Pd (II) can be calculated by using the empirical equation as proposed by Wilke and Chang [38] as shown below:

$$\mathcal{D}_{Pd} = \frac{7.4x10^{-8}(\emptyset \cdot MW)^{0.5} T}{\eta_w \upsilon_{Pd^{2+}}^{0.6}} \tag{1.13}$$

where Ø is the association factor of water, MW is the molecular weight of water, η_w is the viscosity of water, and υ_{Pd2+} is the molar volume of Pd (II) at normal boiling point.

1.1.7 Flow patterns of HFSLM

The flow patterns in HFSLM operation can be classified as follows:

- *Batch operation*

Batch operation is suitable for the separation of target metal ions from a small volume of aqueous feed solutions and slow extraction and stripping reactions. Both aqueous feed and stripping solutions were circulated along the tube side and shell side, respectively. High efficiency on metal ions separation can be achieved by this type of flow pattern.

- *Continuous operation*

This type of flow pattern is suitable for the separation of target metal ions in a large volume of feed solutions. Continuous operation can be carried out by connecting the module in series or parallel mode. Both aqueous feed and stripping solutions were fed single-pass flow or one-through mode. In the case of a series module continuous operation, a high residence time of both aqueous solutions is needed. This mode is favorable for slow reactions of extraction and stripping. On the other hand, parallel module continuous operation is recommended for fast reaction since a shorter residence time is required compared with series mode.

- *Semi-continuous operation*

The semi-continuous operation provided a continuous process of a large volume of feed solution. It can be operated by fed a single-pass flow of feed solution and circulated flow of stripping solution. Regards this type of flow, a concentrated of metal ions in stripping solution can be achieved up until the equilibrium is reached.

1.1.8 Solvent extraction [39-42]

Solvent extraction (SX) or liquid-liquid extraction (LLE) is widely performed in various processes for recovery and purification of a target species from the solution based on the difference in solubility or distribution coefficient between these two immiscible solvents. From a hydrometallurgical perspective, solvent extraction is exclusively used in the separation and purification of various metal ions. It is an extraction technique applied to liquids, liquid samples, or samples in solution, using a liquid extracting medium. The efficiency of solvent extraction measured in terms of a distribution coefficient which relates the concentrations of the solute in the different phases. A high value of the distribution coefficient indicated good separation. At equilibrium, the distribution coefficient (D) can be defined as shown below:

$$D = \frac{Y_A}{X_A} = \frac{Concentration\ of\ A\ in\ extract\ phase}{Concentration\ of\ A\ in\ raffinate\ phase} \quad (1.14)$$

If solute >1 is present in the solution, the selectivity of the solvent for one (A) over the other (B) is the separation factor (α). The separation factor can be calculated as $\alpha_{AB} = D_A/D_B$. In order to separate A from B, the separation factor (α_{AB}) must be greater than unity.

The solvent extraction procedure uses a given volume of a solvent and a solution that contains the target species, the two liquids being immiscible. The procedure carried out by shaking a solvent and a solution together, after that the two layers of liquid are allowed to separate. The batch extraction provides fast and simple separations specifically when the extraction efficiency of the target species is large. Besides batch extraction, continuous extraction is also applied. The procedure is used typically when the extraction efficiency is relatively small and a large number of batch extractions are necessary to perform a quantitative separation.

จุฬาลงกรณ์มหาวิทยาลัย
Chulalongkorn University

1.1.9 Properties of HFSLM

HFSLM used in this work is a 2.5 x 8 inch Liqui-Cel® Extra-Flow which contains microporous polypropylene hollow fibers. The microporous polypropylene is woven into fabric and wrapped around a central-tube feeder to supply the shell side fluid. Properties of the HF module are shown in **Table 1.3**.

Table 1.3 Properties of the HF module.

Properties	Descriptions
Material	Polypropylene
Module length (cm)	20.3
Module diameter (cm)	6.3
Number of hollow fibers	35,000
Effective length of hollow fiber (cm)	15
Inside diameter of hollow fiber (cm)	0.024
Outside diameter of hollow fiber (cm)	0.03
Effective surface area (cm^2)	$1.4x10^4$
Area per unit volume (cm^2/cm^3)	29.3
Average pore size (cm)	$3x10^{-6}$
Porosity (%)	25
Tortuosity factor	2.6
Operating temperature (K)	273.15-333.15

จุฬาลงกรณ์มหาวิทยาลัย
Chulalongkorn University

1.1.10 Aqueous feed acidity

The acid-base condition in feed solution plays an important role in Pd (II) separation. In order to optimize the suitable acid-base condition, transport mechanisms of metal ions are examined [43-44].

- In the case of coupled facilitated counter-transport: H^+ transport from the stripping phase to the aqueous phase. Therefore, the dissociation equilibrium constant of extractant (pKa) is taken together in order to provide the driving force. The acidity values decrease in the following order: $pH_{feed} > pKa > pH_{stripping}$.

- In the case of coupled facilitated co-transport: in this case, the pH of the stripping phase is higher than in the aqueous feed solution. This type of transport corresponds to the decomposition of acidic molecules in aqueous feed solution and the reaction of metal anion complexes with anions in the stripping phase.

- In the case of simple facilitated transport, the pH of both aqueous solutions does not affect on this type of transport mechanism due to solvating interactions at the interfaces which occurred.

จุฬาลงกรณ์มหาวิทยาลัย
Chulalongkorn University

1.1.11 Carrier concentration

It is evident that the extraction and stripping percentage increases, when the carrier concentration is increased. However, the percentages of extraction decreased owing to high viscosity at higher carrier concentration [45].

1.1.12 Flow rates of both aqueous solutions

Flow rates of both aqueous solutions play an important role on both the stability of LMs and the contacting time of target species and LMs. It has been reported that higher flow rates of both aqueous phases lead to a decrease in contacting

time and degrade the stability of LMs. Additionally, equal flow rates of both aqueous solutions are recommended in order to prevent the pressure drop in the system [46].

1.1.13 Flow patterns of aqueous solutions

Two types of flow patterns fed through HFSLM system are (1) co-current and (2) counter-current. Hence, the counter-current pattern provides a variation in concentrations of metal ions and H^+ in both aqueous phases, which are a driving force in this system. Thus, the separation efficiency increases [47].

1.1.14 Mathematical modelling

Mathematical modelling for Pd (II) transportation across HFSLM system is developed. The mass transfer coefficients are calculated in order to determine the rate controlling step through HFSLM system. Kandwal et. al. [48] developed the mathematical model based on convection and diffusion of cesium ions. Uheida et. al. [49] reported that the transportation of Pd (II) was governed by the diffusion of Pd (II) across HFSLM.

Herein, a mathematical modelling for the transportation of Pd (II) via HFSLM is developed. Axial convection, axial diffusion, radial diffusion and chemical reactions are investigated via mathematical modeling.

จุฬาลงกรณ์มหาวิทยาลัย
Chulalongkorn University

1.1.15 Solubility

The solubility data is an important physicochemical property and a crucial parameter for designing and scaling up in diverse industrial applications viz. separation, purification and crystallization processes. It has been reported that the stability of LMs is considered as the ability to immobilize the LMs in the micropores of the support during the operation proceed. Thus, its solubility data is necessary.

1.2 Objectives of the dissertation

(I) To investigate an influence of operating parameters on the separation of Pd (II) from wastewater of electroless plating process via HFSLM.

(II) To develop a mathematical modelling for Pd (II) extraction and recovery.

1.3 Scope of the dissertation

This study highlights the exploration of an efficient method on a trace level of Pd (II) separation from wastewater of electroless plating process. The scope of this study is shown as follows:

(I) The experiments focused on the separation of Pd (II) from wastewater of electroless plating process.

(II) The investigated parameters were shown as follows:

- Type and concentration of extractants
- Acidity and basicity of feed solution
- Type and concentration of stripping solutions
- Synergistic trippant
- Reaction time
- Flow rate of feed and stripping solutions
- Reaction temperature

(III) The mathematical model was employed to describe the experimental results.

(IV) The model was developed for Pd (II) extraction and stripping based on mass conservation concept. The model was validated by comparison with the experimental results.

จุฬาลงกรณ์มหาวิทยาลัย
Chulalongkorn University

1.4 Expected results

(I) High efficiency of Pd (II) extraction and stripping from wastewater of electroless plating process.

(II) Validation of the mathematical model based on mass conservation (axial convection, axial diffusion and radial diffusion) and chemical reaction.

1.5 Description of the dissertation

This dissertation is divided into 6 chapters. Chapter I provide a brief introduction and rationale of this work. Chapters II presents the published articles regarding the selective separation of Pd (II) from wastewater of electroless plating process via HFSLM. Additionally, SX process is employed in order to investigate the separation of Pd (II) in comparison, as shown in Chapter III and IV. Chapter V reports the measurement of the solubility data of organic acid in the various solvent, which is considered as learning cases for the measurement of the solubility of the extractant in HFSLM system. Chapter VI summarizes the conclusion of this dissertation. Chapters II-V are outlined as follows:

จุฬาลงกรณ์มหาวิทยาลัย
Chulalongkorn University

Chapter II

This chapter aims to investigate the separation of palladium (Pd (II)) from wastewater containing copper (Cu (II)) and nickel (Ni (II)) via hollow fiber supported liquid membrane (HFSLM). The viability to separate Pd (II) is established by controlling the influence of operating conditions. Under optimized conditions viz. 6%(v/v) of Aliquat 336, pH 2 of feed solution, 0.5M of thiourea mixed with 0.1M HCl as a strippant and 100mL/min of flow rate for both aqueous solutions, extraction and stripping of Pd (II) reach >99 % and 87.09 %, respectively. Slope analysis is employed, in order to determine stoichiometric coefficients of extractant. An analysis

of mass transport of Pd (II) across HFSLM is presented. Axial convection, axial diffusion, radial diffusion and chemical reactions are investigated via mathematical modeling. Results indicate that the model proves to be an effective approach for predicting the transportation of Pd (II) across the system. Full details are available in Chapter II and in the published article in the Journal of Environmental Chemical Engineering (2020) 8(5). Article 104234 [50].

Chapter III

This chapter focuses on liquid–liquid extraction of Pd (II) from wastewater of electroless plating process using Aliquat 336 in the presence of cyclohexane as a mobile carrier. Kinetic and thermodynamics analysis showed that Pd (II) extraction was of the first-order reaction: the reaction was an endothermic reaction which was governed by the diffusion region. The influence of temperature was also investigated. Further, the design of an experiment is reported. Response surface methodology was employed to study the five independent variables which have an effect on the percentage of extraction of Pd (II) ions as a dependent variable. Full details are available in Chapter III and in the published article in Chemical Papers (2018) 72: 3129–3139 [51].

จุฬาลงกรณ์มหาวิทยาลัย
Chulalongkorn University

Chapter IV

This chapter highlights the enhancement of the stripping efficiency of the palladium complex with trialkylmethylammonium chloride (Aliquat 336), using synergistic strippants solutions. Results show that synergistic strippants of thiourea and HCl can enhance the palladium stripping efficiency from the loaded Aliquat 336. The extraction of Pd (II) ions is sensitive to the concentration of extractant and chloride medium. Thermodynamics analysis showed that ΔH and ΔS values were obtained at 10.74 kJ/mol and 77.81 J/mol·K, respectively. Full details are available in Chapter IV

and in the published article in SEPARATION SCIENCE AND TECHNOLOGY (2019) 54(17): 2971–2982 [52].

Chapter V

This chapter demonstrates the solubility of 2,2-bis(hydroxymethyl)butyric acid (DMBA) in various organic solvents over the temperature range (298.15 to 353.15) K.

It is evident that the measurement of solubility data exhibits a vital parameter regards the stability of LMs. It has been reported that the stability of LMs is considered as the ability to immobilize the LMs in the micropores of support during the operation proceed [53, 54]. Hence, the extractant should have high solubility values in diluent, but low solubility values in the aqueous phase. Thus, its solubility data is necessary in order to select suitable LMs (extractant dissolved in a solvent) for HFSLM system.

Herein, the solid-liquid equilibrium of 2,2-bis(hydroxymethyl)butyric acid (DMBA) was investigated experimentally in various solvents: namely, ethylacetate, butylacetate, methyl isobutyl ketone, cyclopentyl methyl ether, toluene, gamma-butyrolactone and 1,4-dioxane over the temperature range (298.15 to 353.15) K, as learning cases for the measurement of the solubility of the extractant. The experimental solubility data were correlated with the Apelblat equation, Buchowski–Książczak λh equation and NRTL model. Results showed that the mole fraction solubility of DMBA increased, as temperature increased. The Apelblat equation and NRTL model indicated a good correlation with the experimental solubility data and can be used to describe the solid-liquid equilibrium. Further, the apparent thermodynamic dissolution functions and thermodynamic functions of mixing were evaluated from the solubility data.

Full details are available in Chapter V and in the published article in the Journal of Molecular Liquids. 312 (2020) Article 113370. DOI: https://doi.org/10.1016/ j.molliq.2020.113370 [55].

จุฬาลงกรณ์มหาวิทยาลัย
Chulalongkorn University

CHAPTER II

A numerical and experimental investigation on the selective separation of Pd (II) from wastewater using Aliquat 336 via hollow fiber supported liquid membrane

Vanee Mohdee[a], Prakorn Ramakul[b], Suphot Phatanasri[a] and Ura Pancharoen[a,*]

[a]*Department of Chemical Engineering, Faculty of Engineering, Chulalongkorn University, Bangkok 10330, Thailand*

[b]*Department of Chemical Engineering, Faculty of Engineering and Industrial Technology, Silpakorn University, Nakhon Pathom 73000, Thailand*

จุฬาลงกรณ์มหาวิทยาลัย
CHULALONGKORN UNIVERSITY

This article has been published in Journal: Journal of Environmental Chemical Engineering. Volume: 8. Year: 2020. Article no. 104234. https://doi.org/10.1016/j.jece.2020.104234.

2.1 Graphical Abstract

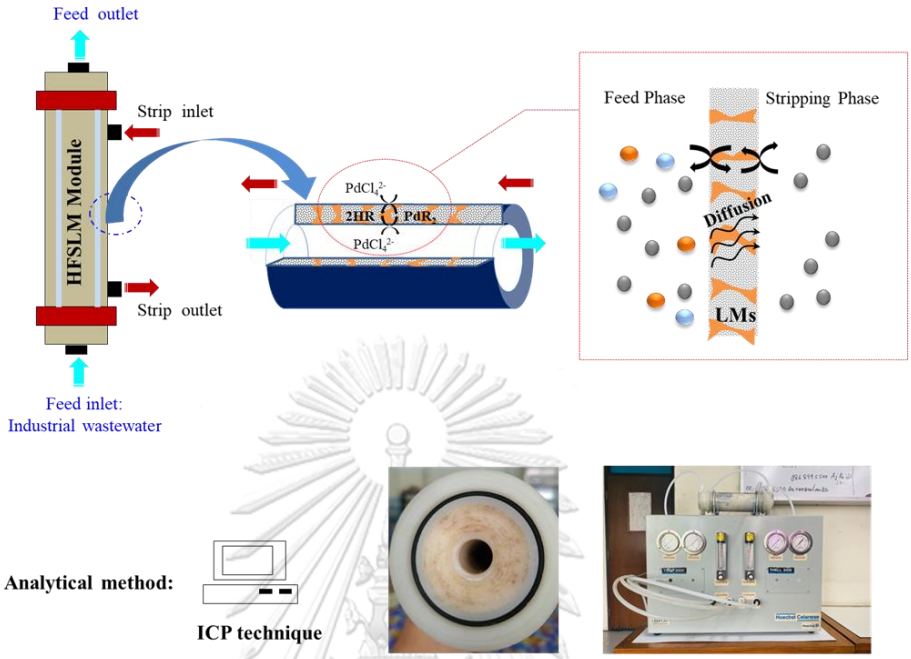

2.2 Abstract

The separation of palladium (Pd (II)) from wastewater containing copper (Cu (II)) and nickel (Ni (II)) is investigated via hollow fiber supported liquid membrane (HFSLM). The viability to separate Pd (II) is established by controlling the influence of operating conditions. Under optimized conditions viz. 6%(v/v) of Aliquat 336, pH 2 of feed solution, 0.5 M of thiourea mixed with 0.1 M HCl as a strippant and 100 mL/min of flow rate for both aqueous solutions, extraction and stripping of Pd (II) reach >99% and 87.09%, respectively. In order to determine stoichiometric coefficients, slope analysis is employed. To study the transport phenomena of Pd (II) across HFSLM, an analysis of mass is presented. Axial convection, axial diffusion, radial diffusion and chemical reactions are investigated via mathematical modeling.

Results indicate that the model proves to be an effective approach for predicting the transportation of Pd (II) across the system.

Keywords: HFSLM; Palladium; Separation; Aliquat 336; Mass transfer

2.3 Introduction

Pd (II) is widely used in diverse processing areas viz. the automotive, jewelry, medical, catalytic and electronic industry; its properties are unique [1-2]. Generally, wastewater generated from industrial processes still contains Pd (II) and other metals at trace level. It is acknowledged that separation of metal ions from industrial wastewater is technologically challenging [3, 4]. Of late, the recovery of Pd (II) from secondary resources has received much attention due to its valuable metal residue, its limited resources and its high demand [5-6]. Conventional methods have been employed for the separation of target metal ions i.e. precipitation, solvent extraction, adsorption and ion exchange [1-2, 4]. Cieszynska and Wieczorek [2] reported that high selectivity of extraction of Pd (II) over Rh (III) was observed using *N*-dodecylpiperidine as an extractant via solvent extraction process. However, such conventional methods have been found to be ineffective at a very low concentration of target metal ions and used a large amount of chemicals [7, 8]. For instance, equal volumes of organic and aqueous phases were employed in the solvent extraction process [1-2]. Thus, high quantities of chemical waste are generated [9].

In recent years, liquid membranes (LMs) have received much attention, involving the separation and removal of target organic and inorganic species [10]. LMs can be classified into two types: flat sheet supported liquid membrane (FSSLM) and hollow fiber supported liquid membrane (HFSLM). Due to the drawbacks of conventional processes, HFSLM is seen as a promising system for processing target

metals ions. HFSLM has high selectivity allowing simultaneous extraction and stripping processes in a single-step. Further, owing to its high surface area of the LMs modules (approximately 104 m^2/m^3), HFSLM can effectively separate trace levels of target metals [11-12]. It can be regarded as a green technology over conventional methods on account of its reusability of LMs and zero discharge of effluent.

HFSLM is a cutting edge system that has been well applied in separation processes. Ni'am et. al. (2020) [9] investigated the simultaneous recovery of rare earth elements from waste permanent magnets (WPMs) via HFSLM. Results showed that HFSLM was successful in recovering the rare earth elements from industrial waste. Scott et. al. (2020) [13] successfully recovered ^{48}V in a very low concentration (part per trillion levels) from aqueous solutions in the presence of Mn, Cr, Ti, B, P, and Ni ions via HFSLM. Extraction efficiency of 71% was reached in 60 min. Hence, HFLSM has been successful in mass separation processes and can be regarded as a promising system for As Low As Reasonably Achievable (ALARA) mass separation. In **Table 2.1**, a summary of previous studies on HFSLM is presented.

Various types of ionic liquids (ILs) have been employed to extract pure metals i.e. amide derivatives [1] and phosphonium group [17]. It has been reported that the extractability of metal complexes increases in the order: quaternary > tertiary > secondary > primary [18]. Thus, Aliquat 336, a cationic liquid of novel quaternary ammonium salts, was selected in order to investigate the performance of Pd (II) extractability via HFSLM. Its structure is given in **Fig. 2.1**.

จุฬาลงกรณ์มหาวิทยาลัย
CHULALONGKORN UNIVERSITY

Table 2.1 Summary of previous research on mass separation via HFSLM.

Feed solution	Extractant	Diluent	Strippant	Separation Efficiency		Year	Ref.
				%Ex	**%St**		
Industrial wastewater	LIX 84-I	Kerosene	HCl	Pd (II)=100%, Sn (IV)=84%	N/A	2015	[7]
Monazite ores in nitrate solutions	DNPPA	n-dodecane	H_2SO_4	Nd (III) 98%	95%	2015	[8]
Waste permanent magnets	D2EHPA	Isopar	HNO_3	Nd 58.62%, Dy 98.46%, Pr 85.59%	Nd 63.13%, Dy 15.21%, Pr 56.29%	2020	[9]
Synthesized feed of levofloxacin	DBTA	1-decanol	HCl	levofloxacin 88.35%	levofloxacin 85.57%	2018	[12]
Beam dump	Aliquat 336	3%dodecanl /dodecane	Ammonia	^{48}V 71%	N/A	2020	[13]
Synthesized feed	Cyanex 272	Kerosene	H_2SO_4	Co (II), Li (I) >99.99%	N/A	2015	[14]
Heavy water board	DNPPA	N/A	H_2SO_4	Y (III)=95%	N/A	2015	[15]
Radioactive waste	CMC	iso-decanol. n-dodecane	N/A	Cs (I)>99%	N/A	2016	[16]

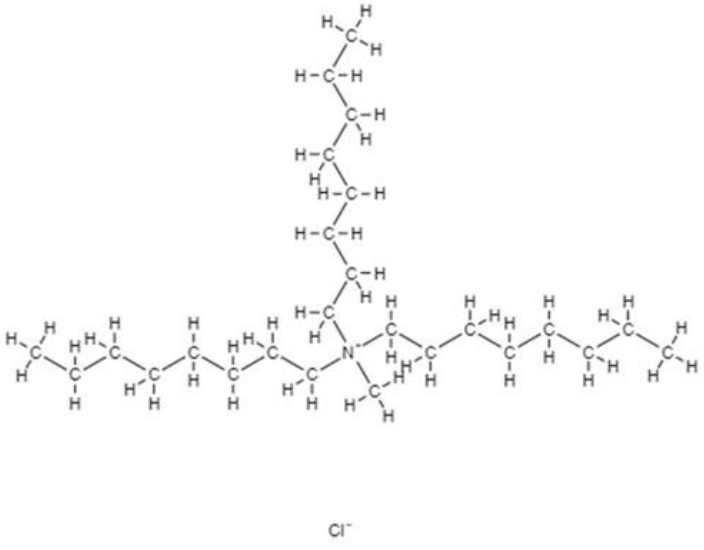

Fig. 2.1. Chemical structure of Aliquat 336.

The aim of this study is to assess the applicability of HFSLM to selectively separate Pd (II) from electronics wastewater containing Cu (II) and Ni (II). Aliquat 336 dissolved in cyclohexane was used as LMs. Nitric acid, hydrochloric acid, sulfuric acid and thiourea were used as strippants. The following parameters were explored: namely, aqueous feed acidity, concentration of extractants, types of strippants and flow rate of aqueous feed and stripping solutions. Further, transportation of Pd (II) across the HFSLM system was determined.

2.4 Theoretical background

HFSLM consists of 3 phases: (i) aqueous feed phase (ii) LMs phase and (iii) stripping phase; in which the LMs are stabilized in the micropores of the polymeric fibers membrane by capillary forces. The aqueous feed solution (electronics wastewater) and stripping solution are in contact with the LMs phase which acts as a barrier to separate these two aqueous solutions [19]. The transference of Pd (II) across HFSLM occurs via the following steps:

Step 1: Palladium chlorocomplex ($PdCl_4^{2-}$) in wastewater is transported to the interface between the feed phase and the LMs phase. At the interface between the feed phase and LMs phase, extraction of $PdCl_4^{2-}$ occurs via ion-exchange. Thereby, it forms an organometallic complex of Pd (II) in the loaded Aliquat 336 ($(R_4N)_2(PdCl_4)$). The extraction mechanism of Pd (II) using Aliquat 336 as an extractant can be written, as shown in Eq. (2.1) [18,20]:

$$2R_4NCl + PdCl_4^{2-} \rightleftharpoons \overline{(R_4N)_2(PdCl_4)} + 2Cl^- \qquad (2.1)$$

Applying mass action law, the chemical equilibrium constant (K_{ex}) can be calculated accordingly, as shown in Eq.(2.2):

$$K_{ex} = \frac{[(R_4N)_2(PdCl_4)][Cl^-]^2}{[R_4NCl]^2[PdCl_4^{2-}]} \quad (2.2)$$

Step 2: An organometallic complex of Pd (II) in the loaded Aliquat 336 is transported across the LMs owing to the concentration gradient to the interface between the LMs phase and stripping phase.

Step 3: Stripping reaction simultaneously occurs at the interface between the LMs phase and stripping phase; Pd (II) is released into the stripping phase. Finally, the extractant as a carrier is regenerated back to the LMs phase. The stripping mechanisms of Pd (II) in the loaded Aliquat 336 using thiourea are shown, as in Eq.(2.3) [21]:

$$2(R_4N)_2(PdCl_4^{2-}) + 2(NH_2)CS \rightleftharpoons PdCl_2.2(NH_2)CS + 2R_4NCl \quad (2.3)$$

The chemical equilibrium constant for the stripping of Pd (II) can be written as:

$$K_{st} = \frac{[PdCl_2 \cdot 2(NH_2)CS][R_4NCl]^2}{[R_4N_2PdCl_4^{2-}]^2[NH_2CS]^2} \quad (2.4)$$

จุฬาลงกรณ์มหาวิทยาลัย
Chulalongkorn University

The schema of Pd (II) separation via HFSLM system is depicted in **Fig. 2.2**.

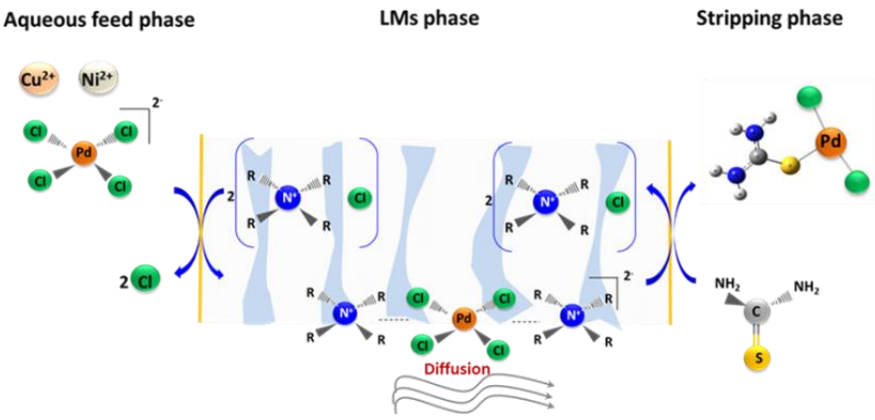

Fig. 2.2. Schematic diagram for separation via HFSLM.

Efficiencies of the HFSLM system are defined in terms of the following Eqs. (2.5) and (2.6):

$$\%Extraction = \frac{C_{f,in} - C_{f,out}}{C_{f,in}} \, x \, 100 \tag{2.5}$$

$$\%Recovery = \frac{C_{s,out}}{C_{f,in}} \, x \, 100 \tag{2.6}$$

where $C_{f,in}$ is the initial concentration of Pd (II) in the feed solution, $C_{f,out}$ is the outlet concentration of Pd (II) in the feed solution and $C_{s,out}$ is the outlet concentration of Pd (II) in the stripping solution.

Distribution ratio (D) can be evaluated as the ratio between concentration of Pd (II) in the organic phase divided by the concentration of Pd (II) in the aqueous phase at equilibrium condition, as shown in Eq.(2.7):

$$D = \frac{[(R_4N)_2(PdCl_4)]}{[PdCl_4^{2-}]} \tag{2.7}$$

The molar flux of Pd (II) across HFSLM can be calculated, as shown below [22]:

จุฬาลงกรณ์มหาวิทยาลัย
Chulalongkorn University

$$J = -V\frac{dC_f}{dt} = Ak_fC_f \tag{2.8}$$

$$ln\frac{C_f}{C_{f0}} = \frac{-k_fAt}{V} \tag{2.9}$$

where J is flux (m^3/m^2s), V is volume (m^3), A is membrane area (m^2) and k_f is mass transfer coefficient in the feed phase (m/s).

2.4.1 Conservation equations of mass

An analysis of mass transfers was carried out to describe the fluid flow and the transport mechanism via HFSLM. The system consists of three sections: tube side, LMs and shell side. **Fig. 2.3** depicts a single fiber module with model domain and its boundaries. The feed solution is fed to the tube side at $z = 0$, whereas the strippant is fed through the shell side at $z = L$. The conservation equations of mass are described, as shown below [23]:

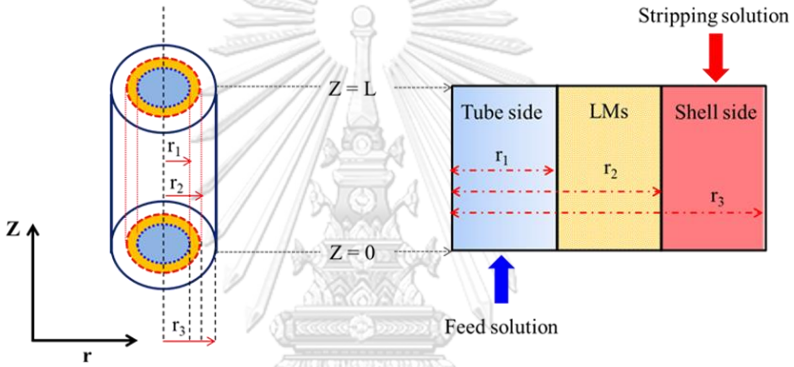

Fig. 2.3. Schematic diagram of a single hollow fiber.

จุฬาลงกรณ์มหาวิทยาลัย
CHULALONGKORN UNIVERSITY

2.4.1.1 *Tube side*

The conception of the model in the tube side is based on the incorporation of chemical reaction and mass transfer, as described in Eq.(2.10):

$$\frac{\partial C_i}{\partial t} = -\nabla \cdot N_i + R_i \qquad (2.10)$$

where C_i is the concentration, N_i is the flux and R_i, is reaction rate of species i.

Using Fick's law, fluxes of species i can be determined as $N_i = -D_i \nabla C_i + C_i V_z$. In which, D_i denotes the diffusion coefficient and V_z denotes axial velocity.

By combining Fick's law diffusion, a mass transfer coefficient is shown as in Eq.(2.11):

$$\frac{\partial C_i}{\partial t} = D_i \nabla^2 C_i - \nabla \cdot C_i V_z + R_i \tag{2.11}$$

Thus, Pd (II) is transported through the tube side based on the consumption of convection and diffusion and can be written as in Eq.(2.12):

$$\frac{\partial C_i}{\partial t} = \mathcal{D}_{i,tube}\left[\frac{\partial^2 C_{i,tube}}{\partial r^2} + \frac{1}{r}\frac{\partial C_{i,tube}}{\partial r} + \frac{\partial^2 C_{i,tube}}{\partial Z^2}\right] - V_{z,tube}\frac{\partial C_{i,tube}}{\partial Z} + R_i \tag{2.12}$$

Velocity distribution in the tube side is tabulated, as in Eq.(2.13) [23]:

$$V_{z,tube} = 2\overline{V}_{tube}[1 - (\frac{r}{r_1})^2] \tag{2.13}$$

where $\overline{V}_{tube}$ is an average flow rate in tube side and r_1 is inner radius of fiber.

The following assumptions are applied, as shown below:

(1) Isothermal operation and constant pressure and volume.

(2) Concentration distribution in radial direction is uniform since the tube of HFSLM is very small.

(3) Extraction reaction is irreversible reaction which occurs at the interface between the feed phase and LMs phase along the length of HFSLM.

The corresponding boundary conditions in the tube side are as follows:

B.C. 1: $Z = 0,\ C = C_{initial}$

B.C. 2: $r = 0,\ \partial C/\partial r = 0$

B.C. 3: $r = r_1,\ C_{tube} = C_{LMs}$

Thus, the generalized mass balance in the tube side under unsteady state condition can be simplified, as in Eq.(2.14):

$$\frac{\partial C_i(z,t)}{\partial t} = \mathcal{D}_{i,tube} \cdot \frac{\partial^2 C_{i,tube}(z,t)}{\partial z^2} - V_{z,tube} \cdot \frac{\partial C_{i,tube}(z,t)}{\partial z} \cdot \left(-\frac{q_f}{A_f}\right) + \varepsilon \cdot \frac{A_p}{A_f} \cdot k_f \cdot C_f^n(z,t) \tag{2.14}$$

A finite difference method was applied to solve the above equation. Both first-order and second-order derivatives, found via the finite difference method, can be expressed as shown in Eqs.(2.15) and (2.16):

$$\left(\frac{\partial C}{\partial Z}\right)_{i,j} = \frac{C_{i,j} - C_{i,j-1}}{h} + O(h) \tag{2.15}$$

$$\left(\frac{\partial^2 C}{\partial Z^2}\right)_{i,j} = \frac{C_{i,j+1} - 2C_{i,j} + C_{i,j-1}}{h^2} + O(h)^2 \tag{2.16}$$

In Eqs.(2.17)-(2.20), the estimated concentration for each term is presented. The estimated concentration of Pd (II) in the outlet feed solution is thus shown, as in Eq.(2.21):

จุฬาลงกรณ์มหาวิทยาลัย
CHULALONGKORN UNIVERSITY

$$\frac{\partial C_i(z,t)}{\partial t} = \frac{C_i(z,t+\Delta t) - C_i(z,t)}{\Delta t} \tag{2.17}$$

$$\mathcal{D}_{i,tube} \cdot \frac{\partial^2 C_{i,tube}(z,t)}{\partial z^2} = \mathcal{D}_{i,tube} \cdot \frac{C_f(z+\Delta z,t) - 2C_f(z,t) - C_f(z-\Delta z,t)}{(\Delta z)^2} \tag{2.18}$$

$$V_{z,tube} \cdot \frac{\partial C_{i,tube}(z,t)}{\partial z} \cdot \left(-\frac{q_f}{A_f}\right) = V_{z,tube} \cdot \frac{C_f(z,t) - C_f(z-\Delta z,t)}{\Delta z} \cdot \left(-\frac{q_f}{A_f}\right) \tag{2.19}$$

$$\frac{C_f(z,t+\Delta t)-C_f(z,t)}{\Delta t} = \mathcal{D}_{i,tube} \cdot \frac{C_f(z+\Delta z,t)-2C_f(z,t)+C_f(z-\Delta z,t)}{(\Delta z)^2} + \left(\frac{q_f}{A_f}\right) \cdot V_{z,tube} \cdot \frac{C_f(z,t)-C_f(z-\Delta z,t)}{\Delta z} + \varepsilon \cdot \frac{A_p}{A_f} k_f (C_f(z,t))^n \quad (2.20)$$

$$C_f(z,t+\Delta t) = C_f(z,t) + \mathcal{D}_{i,tube} \cdot \Delta t \cdot \frac{C_f(z+\Delta z,t)-2C_f(z,t)+C_f(z-\Delta z,t)}{(\Delta z)^2} + \left(\frac{q_f}{A_f}\right) \cdot V_{z,tube} \cdot \Delta t \cdot \frac{C_f(z,t)-C_f(z-\Delta z,t)}{\Delta z} + \varepsilon \cdot \frac{A_p}{A_f} \cdot \Delta t \cdot k_f (C_f(z,t))^n \quad (2.21)$$

2.4.1.2 *LMs side*

The transportation of an organometallic complex of Pd (II) in the loaded Aliquat 336 across the LMs is predominantly due to molecular diffusion. Therefore, the equation of organometallic complex of Pd (II) transported inside the LMs can be shown as follows in Eq.(2.22) [23]:

$$\mathcal{D}_{i,LMs}\left[\frac{\partial^2 C_{i,LMs}}{\partial r^2} + \frac{1}{r}\frac{\partial C_{i,LMs}}{\partial r} + \frac{\partial^2 C_{i,LMs}}{\partial z^2}\right] = 0 \quad (2.22)$$

The following assumptions are applied in the LMs phase as shown below:

(1) The system is examined under a pseudo-steady state condition.

(2) Mass transfer rates in the LMs phase are equal to the concentration flux in both the aqueous feed phase and stripping phase: $J_{LMs} = J_f = J_s$.

(3) The transportation of an organometallic complex of Pd (II) in the loaded Aliquat 336 is in the radial direction and only an organometallic complex can enter the micropore sites.

(4) Only diffusion of mass transport is in this section; no chemical reaction occurs.

(5) There is no interfacial layer between the aqueous phase and the *LMs* phase. Therefore, the flux in the LMs phase can be written as $J_{LMs} = k_m(C_c - C_c)$.

จุฬาลงกรณ์มหาวิทยาลัย
Chulalongkorn University

The corresponding boundary conditions in the LMs are as follows:

B.C. 1: $r = r_1$, $C_{LMs} = C_{tube}$

B.C. 2: $r = r_2$, $C_{LMs} = C_{shell}$

By applying the finite difference method, the flux in the LMs phase is shown below, as in Eq.(2.23):

$$\mathcal{D}_{i,LMs} \cdot \frac{C_i(r+\Delta r,t) - 2C_i(r,t) + C_i(r-\Delta r,t)}{(\Delta r)^2} = 0 \tag{2.23}$$

4.4.1.3 *Shell side*

Pd (II) transported in the shell side is given by Eq.(2.24):

$$\frac{\partial C_i}{\partial t} = \mathcal{D}_{i,shell}\left[\frac{\partial^2 C_{i,shell}}{\partial r^2} + \frac{1}{r}\frac{\partial C_{i,shell}}{\partial r} + \frac{\partial^2 C_{i,shell}}{\partial Z^2}\right] - V_{z,shell}\frac{\partial C_{i,shell}}{\partial Z} + R_i \tag{2.24}$$

จุฬาลงกรณ์มหาวิทยาลัย
Chulalongkorn University

The following assumptions are applied in the shell side:

(1) Isothermal operation and constant pressure and volume.

(2) No radial concentration distribution across the annulus.

(3) The stripping reaction is irreversible reaction and occurs at the interface between the LMs phase and the stripping phase along the length of HFSLM.

The corresponding boundary conditions in the shell side are as follows:

B.C. 1: $r = r_2$, $C_{shell} = C_{LMs}$

B.C. 2: $r = r_3$, $\partial C/\partial r = 0$

B.C. 3: $Z = L$, $C_{shell} = 0$

Having solved Eq.(2.24) by the concept of finite difference, the determining concentration of Pd (II) in the outlet stripping solution is as shown in Eq.(2.25):

$$\frac{C_s(z\prime,t+\Delta t)-C_s(z\prime,t)}{\Delta t} = \mathcal{D}_{i,tube} \cdot \frac{C_s(z\prime+\Delta z,t)-2C_s(z\prime,t)+C_s(z\prime-\Delta z,t)}{(\Delta z)^2} + \left(\frac{q_s}{A_s}\right) \cdot V_{z,tube} \cdot \frac{C_s(z\prime,t)-C_f(z\prime-\Delta z,t)}{\Delta z} + \varepsilon \cdot \frac{A_p}{A_s} k_s (C_s(z',t))^m \quad (2.25)$$

The time depending on mass transfer with chemical reaction in the shell side is obtained, as shown in Eq.(2.26):

$$C_s(z',t+\Delta t) = C_s(z',t) + \mathcal{D}_{i,shell} \cdot \Delta t \cdot \frac{C_s(z\prime+\Delta z,t)-2C_s(z\prime,t)+C_s(z\prime-\Delta z,t)}{(\Delta z)^2} + \left(\frac{q_s}{A_s}\right) \cdot V_{z,shell} \cdot \Delta t \cdot \frac{C_s(z\prime,t)-C_s(z\prime-\Delta z,t)}{\Delta z} + \varepsilon \cdot \frac{A_p}{A_s} \cdot \Delta t \cdot k_s (C_s(z',t))^m \quad (2.26)$$

where the term Z' = L-Z is a correlation between any point of interest in the stripping flow section.

จุฬาลงกรณ์มหาวิทยาลัย
Chulalongkorn University

2.4.2 Mass transportation across HFSLM system

The total mass transfer resistance (R) across HFSLM is the consumption of individual mass–transfer resistances, as expressed in Eq.(2.27) [12, 24]:

$$R = R_f + R_{ex} + R_{LMs} + R_o + R_{st} + R_s \quad (2.27)$$

where R_f, R_{ex}, R_{LMs}, R_o, R_{st} and R_s are the feed-side resistance, the extraction reaction resistance, the liquid membrane resistance, the shell side resistance, the stripping reaction resistance and the strip-side resistance, respectively.

The total mass transfer coefficient can be correlated with the total mass transfer resistances in an empirical relationship, as shown below in Eq.(2.28):

$$\frac{1}{K} = \frac{1}{k_f} + \frac{1}{k_{ex}} + \frac{1}{m_f k_{LMs}} + \frac{1}{m_s k_o} + \frac{1}{m_s k_{st}} + \frac{1}{(m_s/k_s)k_s} \tag{2.28}$$

Since the stripping reaction occurred instantaneously, the mass transfer resistance of the stripping side can be negligible. Thus, the total mass transfer resistances in the system are considered, based on Eq.(2.29):

$$\frac{1}{K} = \frac{1}{k_f} + \frac{1}{k_{ex}} + \frac{1}{m_f k_{LMs}} + \frac{1}{m_s k_o} \tag{2.29}$$

In order to determine the partition coefficient (m_f) of Pd (II), Eq.(2.30) is given:

$$m_f = \frac{[(R_4N)_2PdCl_4]_{org}}{[PdCl_4^{2-}]_f} \tag{2.30}$$

Eqs.(2.31)-(2.33) express the mass transfer coefficients in the feed phase, LMs phase and stripping phase, respectively:

$$k_f = 1.62\frac{D_f}{d_i}\left(\frac{d_i^2 v_f}{LD_f}\right)^{0.33} \tag{2.31}$$

จุฬาลงกรณ์มหาวิทยาลัย
Chulalongkorn University

where D_f is the diffusivity of Pd (II) in feed phase (cm^2/s), v_f is the velocity of feed solution (cm/s) and d_i is the inner diameter of the fiber (cm).

$$k_{LMs} = \frac{D_{LMs}\varepsilon d_{lm}}{\delta\tau d_o} \tag{2.32}$$

where D_{LMs} is the diffusivity of Pd (II) in the LMs (cm^2/s), d_{lm} is the log–mean diameter (cm), d_o is the outer diameter of the fiber (cm), ε is the porosity of the hollow fiber, τ is the tortuosity of the hollow fiber and δ is the membrane thickness (cm).

$$k_o = 1.25\frac{D_{LMs}}{d_h^{0.07}}\left(\frac{d_h v_s}{\vartheta L}\right)^{0.93}\left(\frac{v}{D_{LMs}}\right)^{0.33} \tag{2.33}$$

where v_s is the velocity of stripping solution (cm/s) and υ is the kinematic viscosity (cm^2/s).

2.5 Experimental

2.5.1 Reagents and chemical compounds

Electronics wastewater containing Pd (II), Cu (II) and Ni (II) as feed solution was obtained from Mektec Manufacturing CO., Ltd., Thailand. Aliquat 336 (Acros Organics, USA) was used as an extractant. Cyclohexane (Lobal Chemie, India) was used as diluent. Hydrochloric acid (HCl), nitric acid (HNO_3), and sulfuric acid (H_2SO_4) (Merck, Singapore) and thiourea (QReC, New Zealand) were used as stripping solutions. Commercial palladium chloride ($PdCl_2$) (Sigma-Aldrich, Poland) was used as a standardized solution for analyses. All experiments used deionized water (Millipore, USA). Detailed descriptions of reagents and chemicals used are presented in **Table 2.2**.

จุฬาลงกรณ์มหาวิทยาลัย
Chulalongkorn University

Table 2.2 Detailed information on the materials.*

Chemicals	Molar mass ($g \cdot mol^{-1}$)	Density	CAS No.	Mass fraction Purity	Source
Aliquat 336	404.16	0.88	63393-96-4	0.882-0.906	Acros Organics
Cyclohexane	84.16	0.77	110-82-7	0.995	Lobal Chemie
HCl	36.46	1.18	7647-01-0	0.370	Merck
HNO_3	63.01	1.39	7697-37-2	0.650	Merck
H_2SO_4	98.07	1.84	7664-93-9	0.950-0.970	Merck
Thiourea	76.12	1.40	62-56-6	0.990	QReC

*The physical properties data are from chemical bottle labels.

2.5.2 Experimental apparatus

HFSLM used in this work is a 2.5 x 8 inch Liqui-Cel® Extra-Flow which contains microporous polypropylene hollow fibers. The properties of the HF module are shown in **Table 2.3**.

Table 2.3 Characteristics of the HF module

Properties	**Descriptions**
Inside diameter of hollow fiber	240 μm
Outside diameter of hollow fiber	300 μm
Effective length of hollow fiber (L)	15 cm
Number of hollow fibers (N)	35,000
Average pore size	0.03 μm
Size of pore	0.05 μm
Porosity (ε)	30%
Effective surface area (A)	1.4×10^{4} cm^{2}
Area per unit volume	29.3 cm^{2} cm^{-3}
Module diameter	6.3 cm
Module length	20.3 cm
Contact area	1.4 m^{2}
Tortuosity factor	2.6
Maximum pressure difference	4.2 kg cm^{-2}
Operating temperature	273-333 K

จุฬาลงกรณ์มหาวิทยาลัย
Chulalongkorn University

2.5.3 Experimental procedures

First, Aliquat 336 was dissolved in cyclohexane. Next, the LMs began circulating along the tube and shell sides of the HF simultaneously for 40 min to

ensure that the LMs became enmeshed in the microporous fibers. After that, distilled water was fed through the system to wash out excess LMs. Subsequently, 5 L of the electronics wastewater (as feed solution) and 5 L of stripping solutions were driven counter–currently into the tube and shell sides of the HF, respectively. In **Fig. 2.4**, the HFSLM setup is illustrated. Sampling solutions were collected and characterized for metal ions content using inductively coupled plasma technique (ICP, Optima 2100 DV, Perkin Elmer).

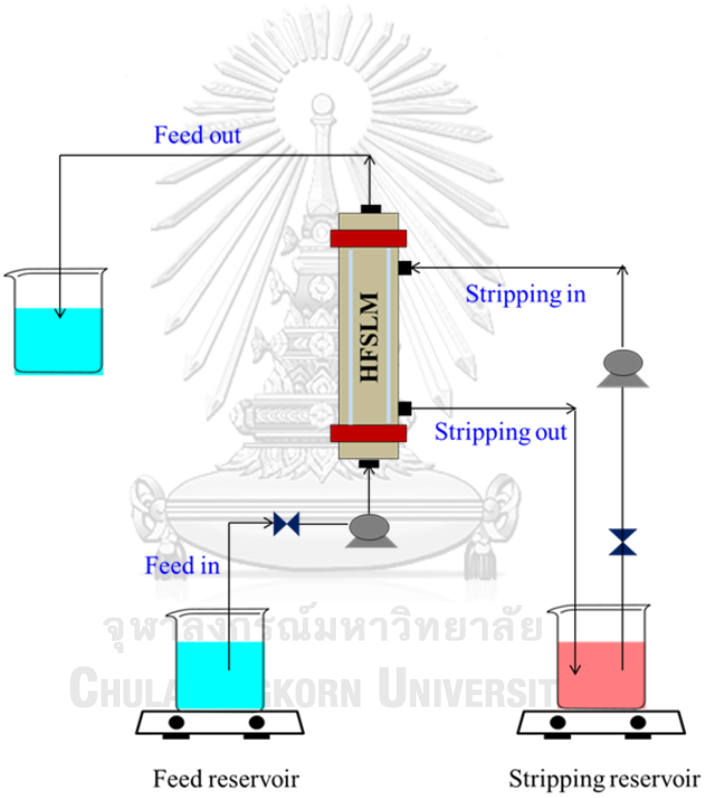

Fig. 2.4. Schematic diagram of the HFSLM system.

2.6 Results and discussion

2.6.1 Effect of aqueous feed acidity

The influence of aqueous feed acidity on the separation of Pd (II) over Cu (II) and Ni (II) was investigated. HCl was used to adjust the acidity of feed solutions in the

range of pH 1-7, as illustrated in **Fig. 2.5**. Results found that the acid-base condition in feed solution plays an important role in Pd (II) extraction. It was observed that extraction of Pd (II) reached maximum at pH 2 which was in good agreement with previous research [25]. Shen and Xue [25] also reported that Pd (II) efficiently separated from Au at pH 2. However, as pH of feed solution increased (pH > 2), extraction of Pd (II) decreased sharply. This decrease in Pd (II) extraction percentages can be explained via the Pourbaix diagram, as depicted in **Fig. 2.6** [26, 27]. The Pourbaix diagram is used to describe metal complex forms and their stability, as a function of pH. The highest stable form of divalent palladium ions in chloride medium was previously reported as $PdCl_4^{2-}$ [2]. As shown in the Pourbaix diagram, this chlorocomplex form is mostly found in the pH range 1-4.

In general, extraction mechanism using Aliquat 336 as an extractant is based on anion exchange of metal chloride species. **Fig. 2.6** reveals that the formation of higher palladium hydroxide complexes at higher pH can lead to a decrease in Pd (II) extraction. This decrease in Pd (II) extraction was also found when concentration of HCl increased [2, 25]. In addition, the change in metal complex forms is considered kinetically inert [28]. As a result, extraction percentage decreased. It is seen that Cu (II) and Ni (II) exhibited low extraction efficiency, owing to the fact that they are mostly found in the form of cationic or neutral species in the investigated pH range [17, 29]. Similar results have been observed, at higher pH, where both Cu (II) and Ni (II) occurred in hydroxide form which led to a decrease in extraction efficiency. Nevertheless, at pH 2, results showed that >79% of Pd (II) can be extracted in the presence of Cu (II) and Ni (II). Thus, pH 2 was selected as the optimum aqueous feed acidity in this experiment.

In **Table 2.4** below, separation factors of Pd (II) over Cu (II) and Ni (II) against feed acidity are reported. The separation factor ($\beta_{Pd/M}$) is defined as the ratio of

distribution of Pd (II) to that of another metal: $\beta_{Pd/M} = D_{Pd}/D_M$. As shown, both $\beta_{Pd/Cu}$ and $\beta_{Pd/Ni}$ reached maximum at pH 2. At pH>2, extraction of Pd (II) was found to decrease sharply resulting in low values of both distribution ratios and separation factors.

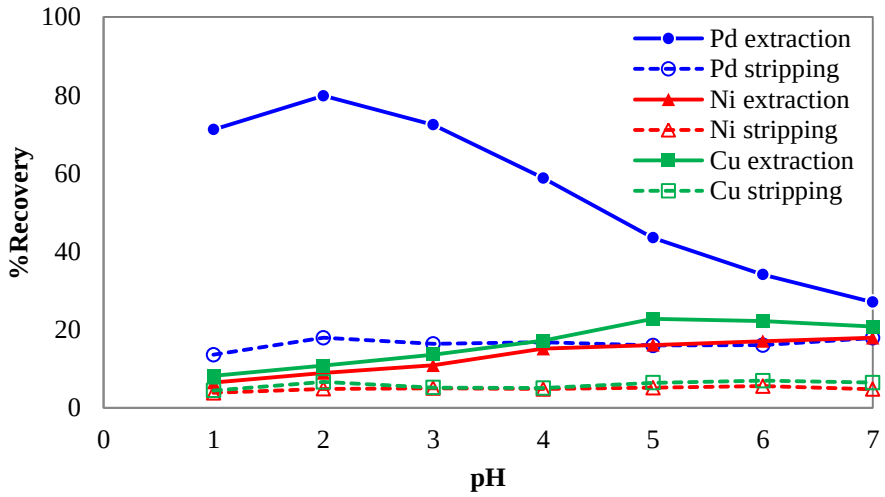

Fig. 2.5. Influence of feed acidity on metal extraction and stripping (Extractant: 2%(v/v) of Aliquat 336, Strippant: 2 M of HNO_3, Flow rate: 100 mL/min for both feed and stripping solutions).

จุฬาลงกรณ์มหาวิทยาลัย
CHULALONGKORN UNIVERSITY

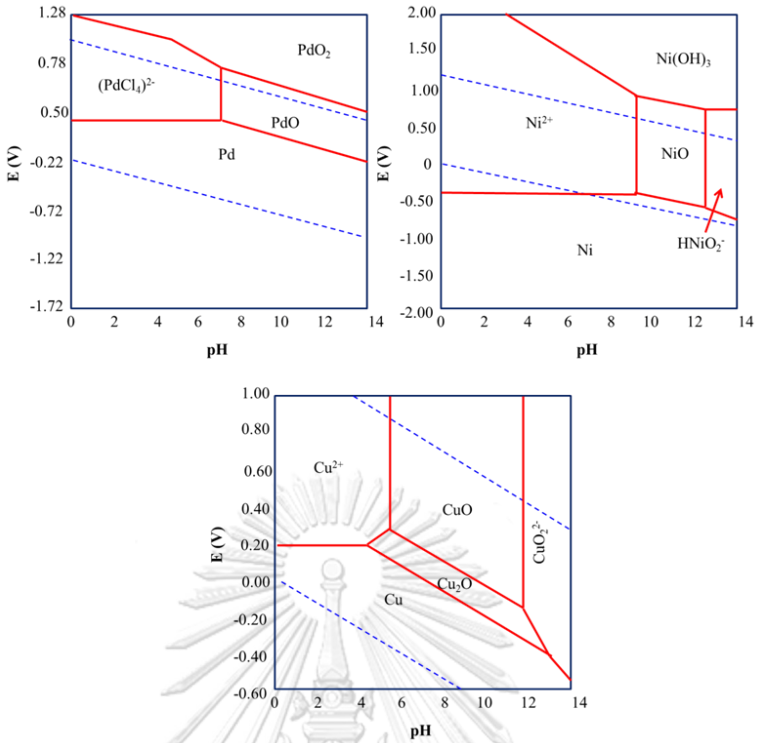

Fig. 2.6. Pourbaix diagram of each metal.

Table 2.4 Separation factor of Pd (II) over Cu (II) and Ni (II) against feed acidity

pH	1	2	3	4	5	6	7
$\beta_{Pd/Cu}$	27.6034	32.7773	16.6674	6.8695	2.6194	1.8155	1.4127
$\beta_{Pd/Ni}$	35.9760	40.4876	21.5752	8.0114	4.0243	2.5192	1.7018

CHULALONGKORN UNIVERSITY

2.6.2 Effect of carrier concentration

As shown in **Fig. 2.7**, the concentration proportion of carrier in the LMs phase was investigated in the range of 2-10 %(v/v) of Aliquat 336. It was observed that when carrier concentration of Aliquat 336 increased to 6%(v/v), extraction percentage of Pd (II) was of a higher tendency and reached 99.21%. Thus, the highest distribution ratios found at 6%(v/v) of carrier concentration indicated that saturation capacity of the LMs phase (for the complex) was reached. When carrier concentration further increased, the percentage of extraction decreased due to high viscosity. Similar results have been

observed previously [8, 30]. Besides, Chakrabarty et. al. [30] reported a decrease in diffusion coefficient and flux, in the presence of an excess amount of carrier concentration. This was also due to the high viscosity during the LMs phase. This phenomena can be explained as follows: when carrier concentration increased from 2-6 %(v/v), chemical reaction at the feed–LMs interface was found to be the controlling step. When a further increase in carrier concentration took place, higher than saturation capacity, mass transfer was found to be the controlling step. Therefore, 6%(v/v) of Aliquat 336 was selected as optimum carrier concentration. In **Table 2.5**, the distribution ratios (*D*) and separation factors are tabulated.

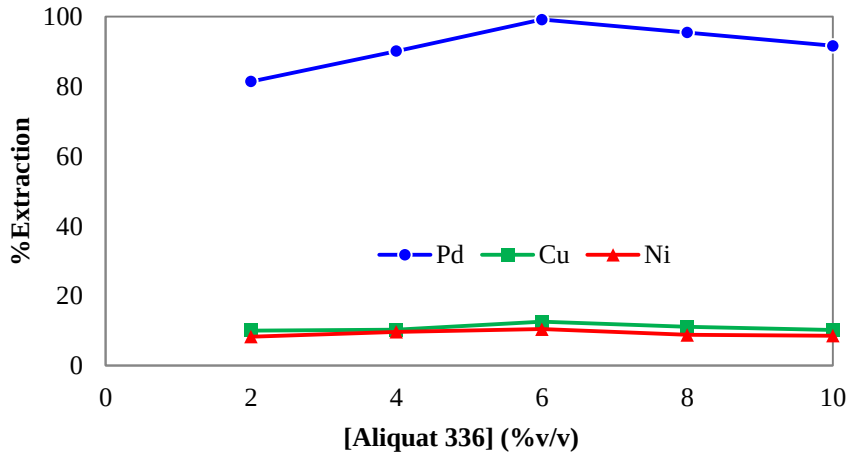

Fig. 2.7. Influence of Aliquat 336 concentration on Pd (II) extraction. (Feed acidity: pH 2, Strippant: 2 M of HNO_3, Flow rate: 100 mL/min for both feed and stripping solutions).

Table 2.5 Distribution ratio against concentration of Aliquat 336

	Aliquat 336				
D	2%(v/v)	4%(v/v)	6%(v/v)	8%(v/v)	10%(v/v)
Pd	4.3937	9.1729	125.5822	21.0555	11.0192
Cu	0.1119	0.1153	0.1440	0.1249	0.1144
Ni	0.0908	0.1075	0.1170	0.0968	0.0940
$\beta_{Pd/Cu}$	39.2382	79.5402	871.8941	168.4635	96.2761
$\beta_{Pd/Ni}$	48.3522	85.2960	1072.7219	217.3994	117.1113

***Note*:** Feed acidity: pH 2, Strippant: 2 M of HNO_3, Flow rate: 100 mL/min for both feed and stripping solutions.

2.6.3 Slope analysis

The stoichiometry of the extraction reaction of Pd (II) with Aliquat 336 was determined by applying slope analysis method. Thus, the distribution ratio of each metal, at different concentrations of Aliquat 336, was investigated. As graphically shown in **Fig. 2.8**, plot of log *D* versus log[Aliquat 336] was conducted depicting a slope of a number of extractant molecules. As log[Aliquat 336] increased, log D of all metals increased. Slope values were found to be 2.83, 0.20 and 0.23 for Pd (II), Cu (II) and Ni (II), respectively. As seen in Eq.(1), the value of 2 was common for the extraction of Pd (II) with Aliquat 336 [18, 20]. Therefore, the value of 2 was selected since the association of two moles of extractant reacts with one mole of metal ion. Previous study also constructed the plot between log *D* vs log[extractant] [2]. Results revealed that the molar ratio of $PdCl_4^{2-}$/extractant was 1:2 which was in good agreement with obtained results. The obtained values for Cu (II) and Ni (II) were found to be very small due to the low extraction efficiency of these two metals, under the investigated conditions.

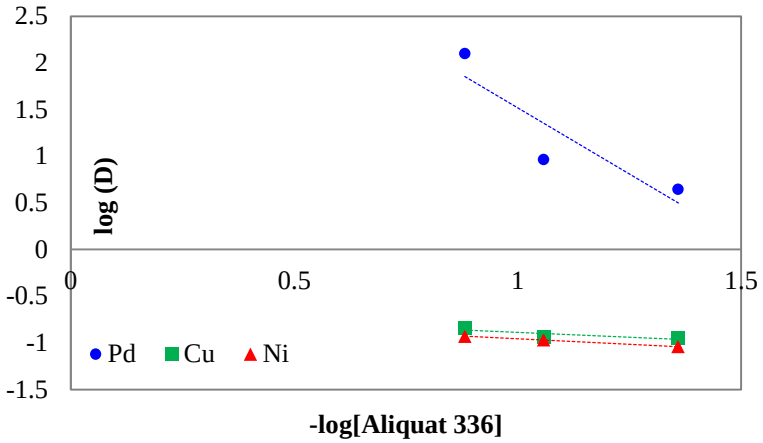

Fig. 2.8. Slope analysis of each metal.

2.6.4 Statistical analysis

Both concentration of the extractant and acidity of the feed solution play an important role in metal extraction. In order to investigate influence of individual variables and their interactive influences, statistical analysis was employed using Minitab. A regression equation was obtained, as shown below in Eq.(2.34):

$$Y = 90.47 + 3.57A - 6.37B - 6.58A^2 - 6.73B^2 + 1.95AB \quad (2.34)$$

จุฬาลงกรณ์มหาวิทยาลัย
Chulalongkorn University

where Y is the %extraction of Pd (II), A and B are %(v/v) of Aliquat 336 and pH of feed solution.

In **Table 2.6**, ANOVA results are presented. Herein, the p-values less than 0.05 indicate a significant factor. The value of the coefficient of determination (R^2) was 0.8121. In **Fig. 2.9**, both the contour plot and surface plot are presented. As shown from the analysis of variance, statistically significant parameters are B, A^2 and B^2. Thereupon, by excluding terms A and AB in Eq.(2.34) (in which the P-values > 0.05), a regression equation can be simplified as shown in Eq.(2.35):

$$Y = 90.47 - 6.37B - 6.58A^2 - 6.73B^2 \quad (2.35)$$

In **Fig. 2.10**, the calculated values of %extraction of Pd (II) based on a regression equation (Eq.(34)), $Y_{cal.,\ regression\ eq.}$, and simplified equation (Eq.(35)), $Y_{cal.,\ simplified\ eq.}$ are presented in comparison to the experimental results, Y_{exp}. As graphically shown, the predicted values, calculated via a regression Eq.(34) and simplified regression Eq.(35) showed good agreement with the experimental results. By excluding terms A and AB in Eq.(34), satisfactory agreement between predicted and experimental values was observed. Hence, the model proved suitable to apply for Pd (II) extraction as a function of conditions of the studied parameters.

Table 2.6 Analysis of variance

Source	DF	Adj SS	Adj MS	F-Value	P-Value
Model	5	987.30	197.459	6.05	0.018
Linear	2	426.65	213.327	6.54	0.025
A	1	101.73	101.732	3.12	0.121
B	1	324.92	324.922	9.96	0.016
Square	2	545.39	272.697	8.36	0.014
A^2	1	301.19	301.192	9.23	0.019
B^2	1	315.32	315.315	9.66	0.017
2-way interaction	1	15.25	15.249	0.47	0.516
A*B	1	15.25	15.249	0.47	0.516
Error	7	228.38	32.626		
Lack-of-fit	3	227.44	75.813	320.90	0.000

จุฬาลงกรณ์มหาวิทยาลัย
CHULALONGKORN UNIVERSITY

Pure error	4	0.95	0.236
Total	12	1215.68	

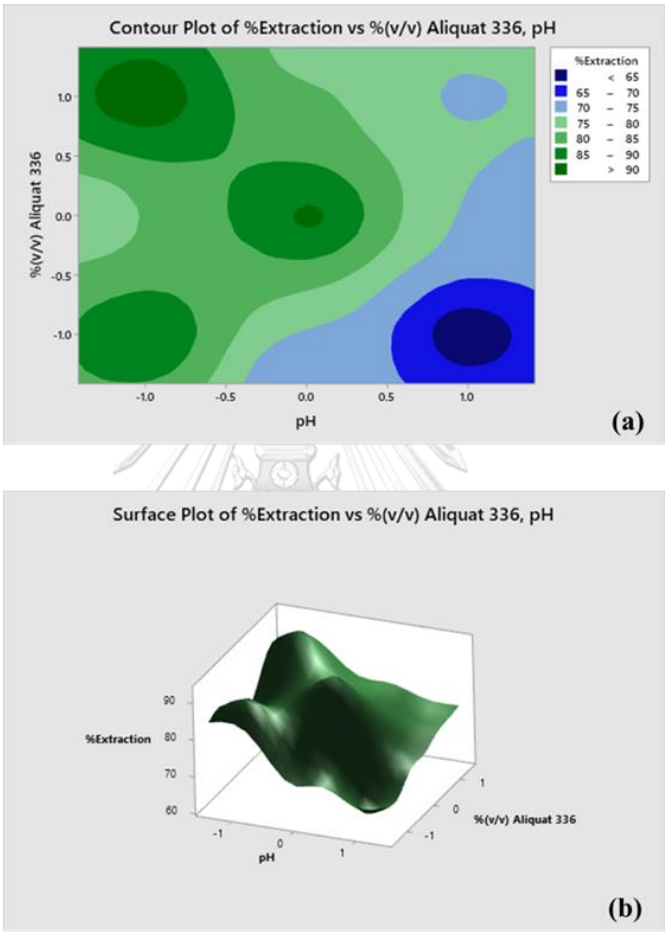

Fig. 2.9. Contour plot and surface plot of %Pd (II) extraction versus concentration of Aliquat 336 and pH of feed solution.

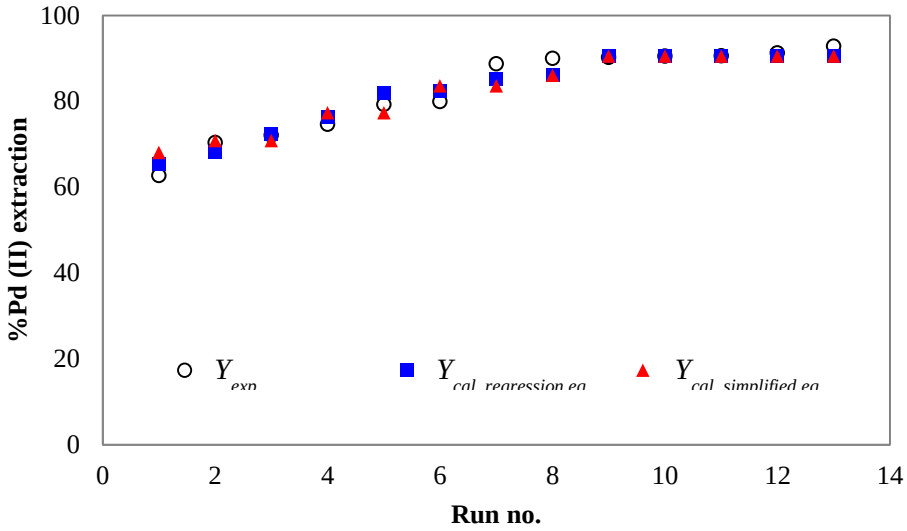

Fig. 2.10. The predicted values of %Pd (II) extraction in comparison to experimental results.

2.6.5 Effect of type of strippants

In the recovery of metal and regeneration of an extractant, stripping reaction is highly significant. Therefore, various types of strippants were employed to investigate the performance of Pd (II) recovery across HFSLM. Stripping reaction is the reverse of extraction reaction. In order to dissociate the ion-pair complex (the organometallic complex of palladium), stripping reaction occurred in basic medium whilst extraction reaction was carried out in an acidic medium [31].

As illustrated in **Fig. 2.11**, 0.5 M thiourea provided the highest efficiency in the stripping of Pd (II) up to 78.74%. Owing to its 2 donor atoms in the molecule and its soft nature, thiourea can effectively trap noble metals in the process of extraction and stripping [32]. Stripping reaction of Pd (II) in the loaded Aliquat 336 along with thiourea occurred via coordination–substitution between $(NH_2)_2CS$ and Cl^- [28]. As stated in Eq.(3): Cl^- in the $(R_4N)_2(PdCl_4)^{2-}$ complex is substituted by $(NH_2)_2CS$. In

contrast, 5 M of HNO_3, H_2SO_4 and HCl exhibited very low Pd (II) stripping efficiencies at 36.66, 20.67 and 14.26%, respectively. Similar results were observed when acid reagents stripped Pd (II) in the loaded Aliquat 336 [21]. Nevertheless, higher acidity was avoided since it impaired the polypropylene hollow fibers [33]. In this work, stripping percentages for Cu (II) and Ni (II) were found to be very low, for all stripping solutions investigated.

It is evident that the synergistic solutions of thiourea mixed with HCl can be used to enhance the stripping efficiency of Pd (II) [2]. Results showed that 87.09% of stripping percentage of Pd (II) was reached using mixed solution of 0.5 M thiourea and 0.1 M HCl. Likewise, Swain et. al. [28] pointed out that synergistic solutions blending thiourea with HCl generated the best stripping solutions for Pd (II).

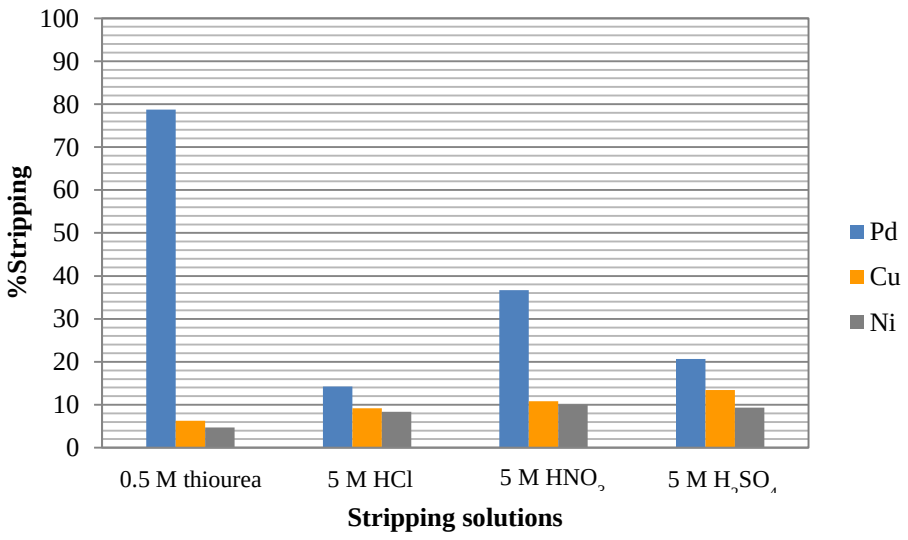

Fig. 2.11. Influence of stripping solutions on metal ions recovery. (Feed acidity: pH 2, Extractant: 6%(v/v) of Aliquat 336, Flow rate: 100 mL/min for both feed and stripping solutions).

2.6.6 Effect of flow rate in Pd (II) transportation

The flow rates of both feed and stripping solutions play a significant role on the transportation of metals ions across HFSLM. Thus, in order to study the transport phenomena in this system, the flow rates of both feed and stripping solutions were adjusted in the range of 50-300 mL/min. Results found that the mass transfer in this system was enhanced when flow rates of both aqueous solutions were increased up to 100 mL/min. However, as flow rates further increased i.e. 150-300 mL/min, efficiency gradually decreased, as shown in **Fig. 2.12**. It is noted that the LMs are found to be decadent at higher flow rates [12, 34]. Moreover, when flow rates of both aqueous solutions increase, the efficiency of Pd (II) separation decreases due to shorter contact time with the LMs which is in agreement with previous studies [12, 34]. Hence, 100 mL/min was selected as the optimum flow rate for both aqueous solutions. In **Table 2.7**, the distribution ratios and separation factors for each metal against flow rate are given.

จุฬาลงกรณ์มหาวิทยาลัย
Chulalongkorn University

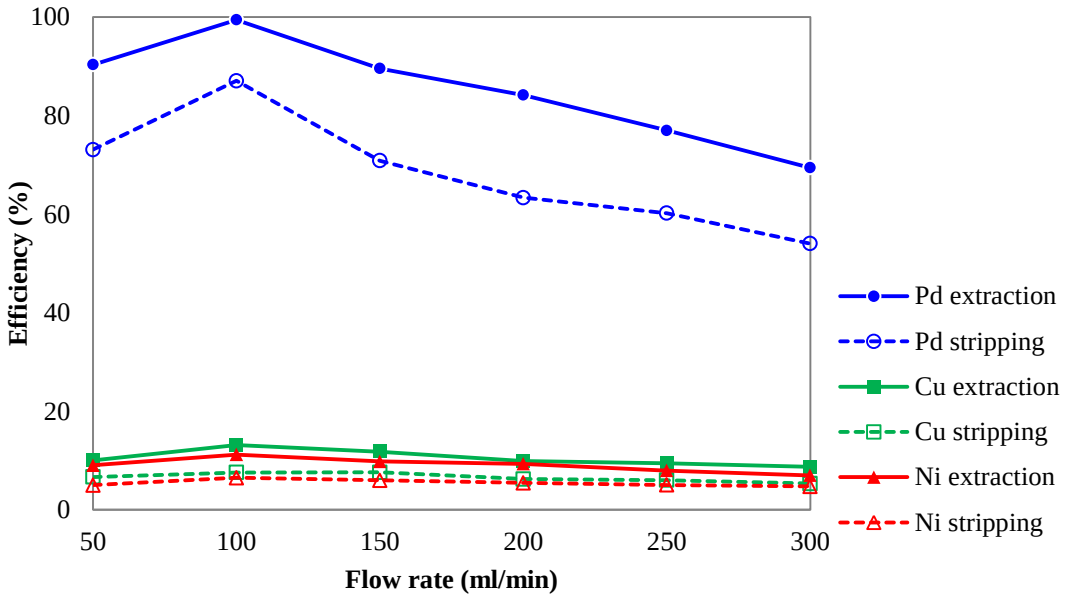

Fig. 2.12. Influence of flow rate on metal ions recovery. (Feed acidity: pH 2, Extractant: 6%(v/v) of Aliquat 336, Strippant: 0.5 M Thiourea mixed with 0.1 M HCl).

Table 2.7 Distribution ratio and separation factor of each metal at various flow rates

Flow rate	D			β	
(mL/min)	Pd	Cu	Ni	$\beta_{Pd/Cu}$	$\beta_{Pd/Ni}$
50	9.3519	0.1114	0.0996	83.8879	93.8706
100	184.1851	0.1516	0.1263	1214.336	1457.394
150	8.5969	0.1336	0.1091	64.3202	78.7702
200	5.3251	0.1101	0.1029	48.3554	51.7500
250	3.3497	0.1041	0.0866	32.1722	38.6793
300	2.2733	0.0951	0.0753	23.8268	30.1563

***Note*:** Feed acidity: pH 2, Extractant: 6%(v/v) of Aliquat 336, Strippant: 0.5 M of Thiourea.

จุฬาลงกรณ์มหาวิทยาลัย
Chulalongkorn University

2.6.7 Numerical solution

In **Fig. 2.13,** the concentration distribution and concentration profile of Pd (II) simulated using the finite difference method (via conservation equation across HFSLM) are graphically shown. In **Fig. 2.13 (a)**, the concentration distribution across HFSLM system is presented. On both tube and shell sides, uniform concentration in radial direction was assumed. A contour plot revealed a change in concentration along the length of the HFSLM system (in z-direction). In the LMs, only diffusion in the radial direction took place. As shown in **Fig. 2.13 (b)**, the concentration profile clearly decreased during the LMs phase, indicating that resistance to Pd (II) transport in the LMs phase is the predominant resistance in the system. In the z-direction, see **Fig. 2.13 (c)**, the aqueous feed solution is fed into the tube side at Z = 0, where the concentration of Pd (II) was highest. It is observed that the model predicts an exponential decrease in concentration of the aqueous feed phase and was found to decrease sharply along the length of the HF module. Similar results regarding axial and radial concentration profile were observed. Eslami et. al. [23] also presented comparable results for the gas phase separation via HFSLM. Besides, Muhammad et. al. [35] described the mathematical modelling for Cu (II) extraction via hollow fiber membrane contactor. Results revealed that diffusion and convection controlled the mass transfer along the system.

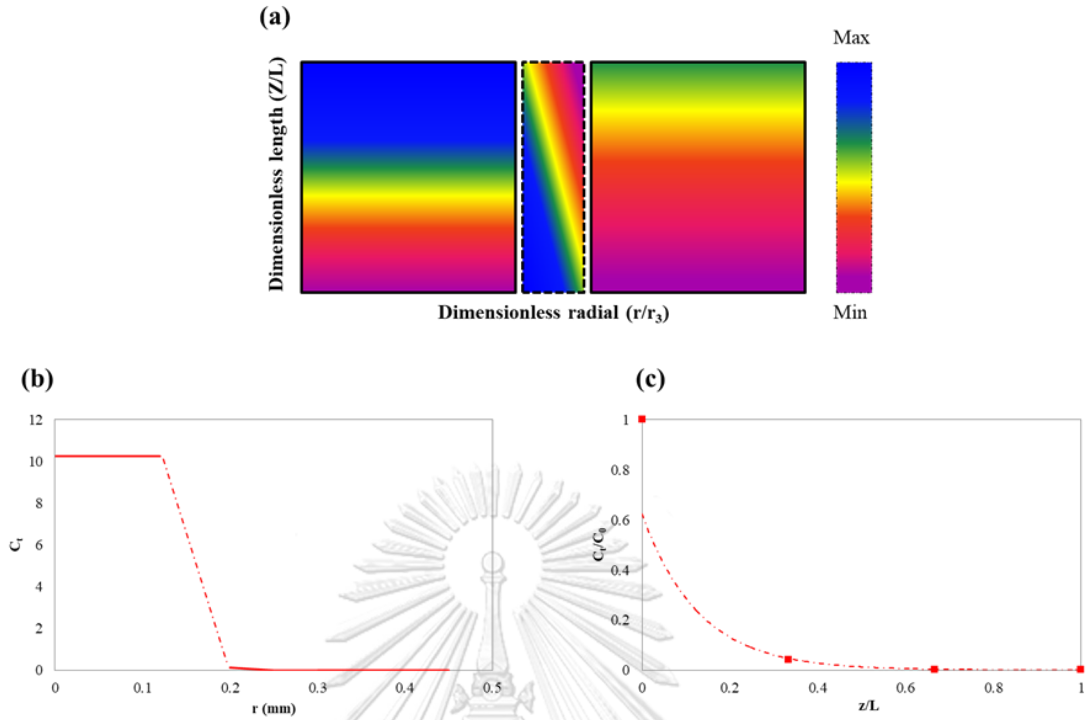

Fig. 2.13. Concentration profile of Pd (II) via finite difference method along the tube, LMs, and shell side via HFSLM system: (a) concentration distribution (b) concentration profile in r-direction and (c) concentration profile in z-direction.

As illustrated in **Fig. 2.14**, experimental results were compared with the findings of the model data. Results found that the numerical prediction showed good agreement with the experimental results, especially in the feed phase. It was noted that within 20 min both extraction and stripping reaction of Pd (II) reached equilibrium; thereafter, it maintained persistently high efficiency under investigated time. As depicted, it can be seen that the transportation of Pd (II) in both aqueous phases correlated to axial convection, axial diffusion as well as the chemical reactions, as stated in the assumptions. Meanwhile in the stripping phase using 0.5 M thiourea as a strippant, the experimental results slightly differed from the model prediction having RMSD equal to 2.15. In **Fig. 2.15**, by using synergistic solutions, the model

predictions showed good correlation with the experimental data having RMSD equal to 0.98.

A numerical method was applied to previous works on Ta [36] and Nd separation [8]. As shown in **Fig. 2.16**, good agreement between the experimental data and the applied numerical method was observed. Thus, it can be stated that the mass transfer of target metal ions via HFSLM depends on the principle of axial convection, axial diffusion, radial diffusion and chemical reaction. Extraction reaction at the interface plays an important role on radial diffusion. Previous works have demonstrated that the mass transfer of metals via HFSLM was based on the above principles [37-39].

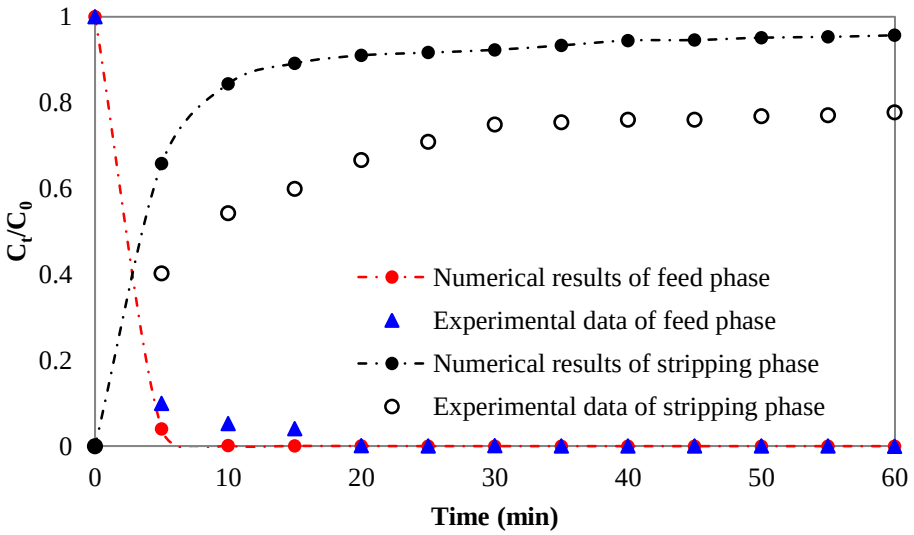

Fig. 2.14. Numerical results compared with experimental results for Pd (II) in both feed and stripping phases (using 0.5 M thiourea as a strippant).

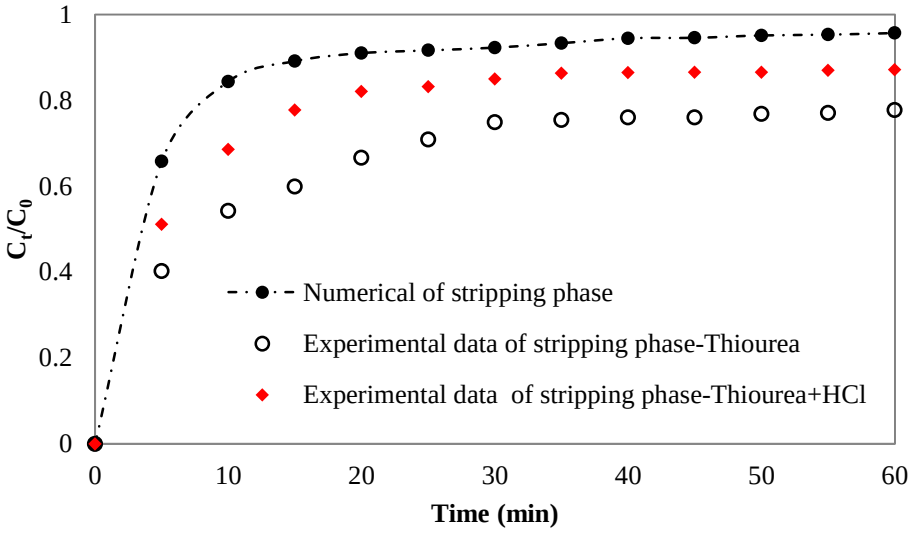

Fig. 2.15. Numerical results compared with experimental results in the stripping phase using thiourea solution and synergistic solutions (0.5 M thiourea mixed with 0.1 M HCl).

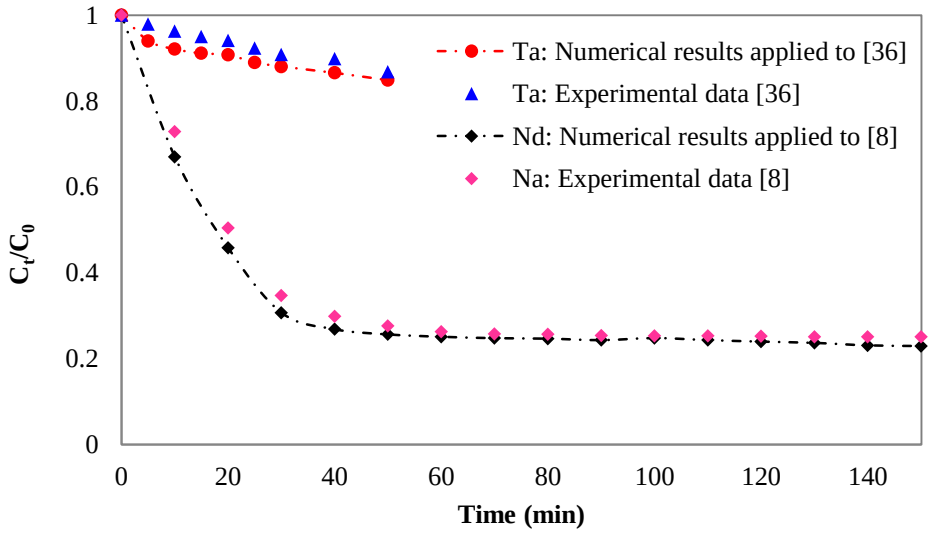

Fig. 2.16. Numerical results compared with experimental results in the feed phase applied to Ta [36] and Nd [8].

2.6.8 Evaluation of mass transfer coefficient

It is acknowledged that the overall permeability coefficient can be correlated with the resistances in an empirical relationship [32]. In **Fig. 2.17,** by plotting $1/P$ and $1/K_d$, the mass transfer coefficient in both feed and LMs phases can be determined. The values of k_f and k_m were found to be 6.96×10^{-4} and 1.02×10^{-5} cm/s, respectively. As obtained, the value of k_m was lower than k_f indicating that the membrane mass transfer coefficient (k_m) was the rate controlling step, in line with previous research [7, 32, 36]. Uheida et. al. [40] also reported that the transportation of Pd (II) was governed by the diffusion of Pd (II) across HFSLM. Yet, the main resistance in this work was found to be in the LMs phase which corresponded with the numerical results, as described in **Fig. 2.13 (b)**.

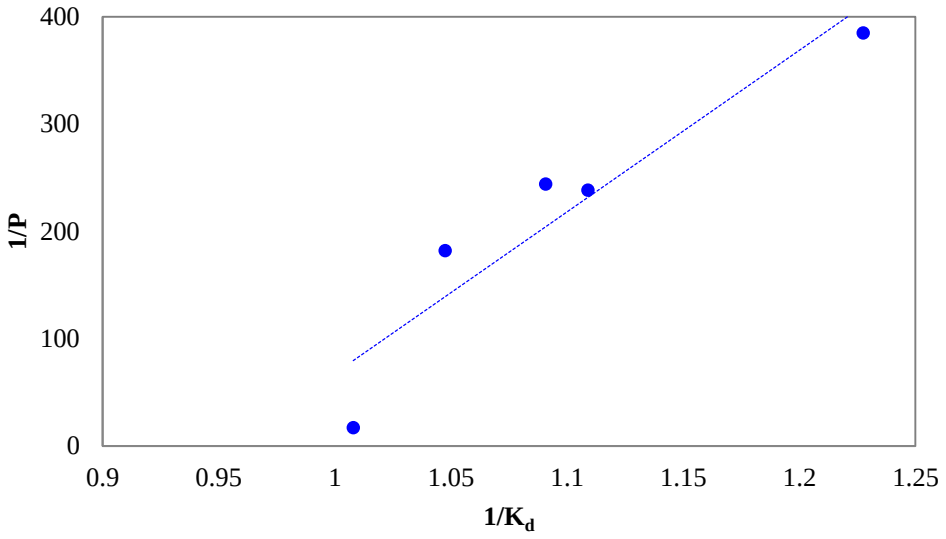

Fig. 2.17. Linear relationship between $1/P$ vs. $1/K_d$ for Pd (II) transportation.

2.7 Conclusion

In this work, it is noted that HFSLM can effectively separate Pd (II) from industrial wastewater containing Cu (II) and Ni (II). Further, Aliquat 336 proved to be

a suitable carrier for the LMs. Under optimum conditions, complete separation of Pd (II) was demonstrated, achieving >99% extraction and 87.09% recovery. Mass transfer in the LMs was found to be the rate controlling step. Results obtained via mathematical modelling found that axial convection, axial diffusion, radial diffusion and the chemical reactions were involved in mass transfer across HFSLM. In the LMs, the predominant mechanism was radial diffusion. In both aqueous phases, axial convection and axial diffusion occurred. Finally, it is significant that model predictions were found to be in good agreement with the obtained experimental data.

2.8 Funding

The authors profoundly appreciate the support from the Thailand Research Fund and Chulalongkorn University under the Research and Researchers for Industries (RRi) Ph.D. Program (Grant No.PHD58I0081). Thanks are also given to the Separation Laboratory, Department of Chemical Engineering, Faculty of Engineering, Chulalongkorn University, for chemical and apparatus support as well as to the Mektec Manufacturing Corporation (Thailand) Ltd, for feed solution.

จุฬาลงกรณ์มหาวิทยาลัย
CHULALONGKORN UNIVERSITY

2.9 Nomenclature

A membrane area (cm^2)

A_f cross sectional area of hollow fiber (cm^2)

A_p cross sectional area of hollow fiber ring (cm^2)

A_s cross sectional area of stripping phase (cm^2)

d_i inner diameter of the hollow fiber (cm)

d_o outer diameter of the hollow fiber (cm)

$\mathcal{D}$ diffusion coefficient of Pd (II)

K_d distribution coefficient

k_f rate constant of extraction reaction ($cm^3 mg^{-1} min^{-1}$)

k_{LMs} mass transfer coefficient in the membrane phase ($cm \cdot min^{-1}$)

k_s rate constant of stripping reaction ($cm^3 mg^{-1} min^{-1}$)

L length of the hollow fiber (cm)

N numbers of hollow fibers in the module

q_f volumetric flow rate of feed solution ($cm^3 min^{-1}$)

q_s volumetric flow rate of stripping solution ($cm^3 min^{-1}$)

r_i inner radius of the hollow fiber (cm)

r_o outter radius of the hollow fiber (cm)

2.10 References

[1] H. Huang, H. Chao, W. Yuxuan, D. Songdong, L. Ning, S. Dongping, L. Tianhao, Extraction of palladium (II) from nitric acid solutions with diglycolthioamide, Hydrometallurgy 156 (2015) 6–11.

[2] A. Cieszynska, D. Wieczorek, Extraction and separation of palladium (II), platinum (IV), gold (III) and rhodium (III) using piperidine-based extractants, Hydrometallurgy 175 (2018) 359–366.

จุฬาลงกรณ์มหาวิทยาลัย
CHULALONGKORN UNIVERSITY

[3] S. Zhang, M. Jian, Q. Zhang, R. Xu, J. Qu, X. Luo, X. Li, J. Hu, R. Liu, X. Zhang, Recyclable Printed Circuit Boards and Alkali Reduction Wastewater: Approach to a Sustainable Copper-Based Metal—Organic Framework, ACS Sustainable Chem. Eng. 8 (2020) 1371—1379.

[4] E. Jean, D. Villemin, M. Hlaibi, L. Lebrun, Heavy metal ions extraction using new supported liquid membranes containing ionic liquid as carrier, Sep. Pur. Tech. 201 (2018) 1–9.

[5] K. Liu, Z. Zhang, F.S. Zhang, Direct extraction of palladium and silver from waste printed circuit boards powder by supercritical fluids oxidation-extraction process, J. Hazard. Materials. 318 (2016) 216–223.

[6] J. Li, X. Zeng, M. Chen, Ogunseitan OA, Stevels A, Control-alt-delete: rebooting solutions for the e-waste problem, Envi. Sci. Technol. 49 (2015) 7095–7108.

[7] K. Wongkaew, N. Sunsandee, U. Pancharoen, K. Nootong, P. Ramakul, Purification of Sn (IV) and recovery of Pd (II) from flexible printed circuit board industry wastewater via HFSLM: Temperature effect investigation, J. Ind. Eng. Chem. 22 (2015) 217–228.

[8] T. Wannachod, V. Mohdee, S. Suren, P. Ramakul, U. Pancharoen, K. Nootong, The separation of Nd (III) from mixed rare earth via hollow fiber supported liquid membrane and mass transfer analysis, J. Ind. Eng. Chem. 26 (2015) 214–217.

[9] A.C. Ni'am, Y.F. Wang, S.W. Chen, G.M. Chang, S.J. You, Simultaneous recovery of rare earth elements from waste permanent magnets (WPMs) leach liquor by solvent extraction and hollow fiber supported liquid membrane, Chem. Eng. Pro.:Pro. Intens. 148 (2020) 107831.

[10] S.K. Vladimir, Chapter 1 - Introduction, General Description, Definitions, and Classification. Overview Liquid Membranes Principles and Applications in Chemical Separations and Wastewater Treatment. 2010, p. 1-15.

[11] K.K. Sirkar, Other new membrane processes. In:W.S.W. Ho, K.K. Sirkar (Eds.), Membrane Handbook, Van Nostrand Reinhold, New York, NY; 1992, p. 904-908.

จุฬาลงกรณ์มหาวิทยาลัย
Chulalongkorn University

[12] N. Sunsandee, S. Phatanasri, P. Ramakul, U. Pancharoen, Thermodynamic parameters and isotherm application on enantiomeric separation of levofloxacin using hollow fiber supported liquid membrane system, Sep. Pur. Tech. 195 (2018) 377–387.

[13] M.D. Scott, J. Schorp, L. Sutherlin, J.D. Robertson, Isotope harvesting with Hollow Fiber Supported Liquid Membrane (HFSLM), Appl. Radiat. Isot. 157 (2020) 109027.

[14] B. Swain, C. Mishra, J. Jeong, J.C. Lee, H.S. Hong, B.D. Pandey, Separation of Co (II) and Li (I) with Cyanex 272 using hollow fiber supported liquid membrane: A comparison with flat sheet supported liquid membrane and dispersive solvent extraction process, Chem. Eng. J. 271 (2015) 61–70.

[15] R. Vijayalakshmi, S. Chaudhury, M. Anitha, D.K. Singh, S.K. Aggarwal, H. Singh, Studies on yttrium permeation through hollow fibre supported liquid membrane from nitrate medium using di-nonyl phenyl phosphoric acid as the carrier phase, Inter. J. Miner. Process 135 (2015) 52–56.

[16] P. Jagasia, S.A. Ansari, D.R. Raut, P.S. Dhami, P.M. Gandhi, A. Kumar, P.K. Mohapatra Hollow fiber supported liquid membrane studies using a process compatible solvent containing calix[4]arene-mono-crown-6 for the recovery of radio-cesium from nuclear waste, Sep. Pur. Tech. 170 (2016) 208-216.

[17] A. Cieszynska, M. Wisniewski, Selective extraction of palladium (II) from hydrochloric acid solutions with phosphonium extractants, Sep. Pur. Tech. 80 (2011) 385–389.

[18] T.H. Nguyen, C.H. Sonu, M.S. Lee, Separation of platinum (IV) and palladium (II) from concentrated hydrochloric acid solutions by mixtures of amines with neutral extractants, J. Ind. Eng. Chem. 32 (2015) 238–245.

[19] D. Pawel, P.W. Piotr, Liquid Membranes: Principles and Applications. In: Chemical Separations and Wastewater Treatment. Van Nostrand Reinhold, New York; 1992, p. 904-908.

[20] M.K. Jha, D. Gupta, J.C. Lee, V. Kumar, J. Jeong, Solvent Extraction of Platinum Using Amine Based Extractants in Different Solutions: A Review, Hydrometallurgy 142 (2014) 60–69.

[21] W. Wei, C.W. Cho, S. Kim, M.H. Song, J.K. Bediako, Y.S. Yun, Selective recovery of Au (III), Pt (IV), and Pd (II) from aqueous solutions by liquid–liquid extraction using ionic liquid Aliquat-336, Mol. Liq. 216 (2016) 18–24.

[22] S.J. Li, H.L. Chen, L. Zhang, Recovery of fumaric acid by hollow-fiber supported liquid membrane with strip dispersion using trialkylamine carrier, Sep. Pur. Tech. 66 (2009) 25–34.

จุฬาลงกรณ์มหาวิทยาลัย
CHULALONGKORN UNIVERSITY

[23] S. Eslami, S.M. Mousavi, S. Danesh, H. Banazadeh, Modeling and simulation of CO_2 removal from power plant flue gas by PG solution in a hollow fiber membrane contactor, Adv. Eng. Software 42 (2011) 612–620.

[24] Y. Tang, W. Liu, J. Wan, Y. Wang, X. Yang, Two-stage recovery of S-adenosylmethionine using supported liquid membranes with strip dispersion, Process Biochem. 48 (2013) 1980-1991.

[25] Y.F. Shen, W.Y. Xue, Recovery palladium, gold and platinum from hydrochloric acid solutionusing 2-hydroxy-4-sec-octanoyl diphenyl-ketoxime, Separ. Purif. Technol. 56 (2007) 278–283.

[26] K. Mech, M. Wróbel, M. Wojnicki, J. Mech-Piskorz, P. Żabiński, R.Kowalik, Electrodeposition of NiPd alloy from aqueous chloride electrolytes, Applied Surface Sci. 388 (B) (2016) 809-816.

[27] H. Nady, M. Negem, Microstructure and Corrosion Behavior of Electrodeposited NiCo, NiZn and NiCu Nanocrystalline Coatings in Alkaline Solution, Inter. J. Research Phys. Chem. Chemphys. (2016). DOI: https://doi.org/10.1515/zpch-2016-0893

[28] B. Swain, J. Jeong, S.K. Kim, J.C. Lee, Separation of platinum and palladium from chloride solution by solvent extraction using Alamine 300, Hydrometallurgy 104 (2010) 1–7.

[29] M. Regel-Rosocka, M. Wisniewski, A. Borowiak-Resterna, A. Cieszynska, A.M. Sastre, Selective extraction of palladium (II) from hydrochloric acid solutions with pyridinecarboxamides and ACORGA®CLX50, Sep. Pur. Tech. 53 (2007) 337–341.

[30] K. Chakrabarty, K.V. Krishna, P. Saha, A.K. Ghoshal, Extraction and recovery of lignosulfonate from its aqueous solution using bulk liquid membrane, J. Membr. Sci. 330 (2009) 135–144.

[31] V.J. Suryavanshi, R.R. Pawar, M.A. Anuse, G.N. Mulik, 2-Octylaminopyridine assisted solvent extraction system for selective separation of palladium (II) ion-pair complex from synthetic mixtures and real samples, Anal. Methods, 2015, 7, 2497–2504.

[32] K.K. Yadav, D.K. Singh, V. Kain, Separation of terbium from aqueous phase employing hollow fibre supported liquid membrane with EHEHPA as carrier, Sep. Sci. Tech. 54 (2019) 1521-1532.

[33] J. Bogojeski, J. Volbeda, M. Freytag, M. Tamm, Ž.D. Bugarčić, Palladium (II) complexes with highly basic imidazolin-2-imines and their reactivity toward small bio-molecules, Dalton Trans. 44 (2015) 17346-17359.

[34] Q. Yang, N.M. Kocherginsky, Copper removal from ammoniacal wastewater through a hollow fiber supported liquid membrane system: modeling and experimental verification, J. Membrane. Sci. 297 (2007) 121–129.

[35] A. Muhammad, M. Younas, S.D. Bocquet, J. Romero, J.S. Marcano, Numerical modelling and simulation of membrane-based extraction of copper (II) using hollow fiber contactors, Desal. Water Treat. 63 (2017) 113–123.

[36] D. Buachuang, P. Ramakul, N. Leepipatpiboon, U. Pancharoen, Mass transfer modeling on the separation of tantalum and niobium from dilute hydrofluoric media through a hollow fiber supported liquid membrane, J. Alloys Compd. 509 (2011) 9549–9557.

[37] V.S. Kislik, Carrier-facilitated coupled transport through liquid membranes: general theoretical considerations and influencing parameters, in: V.S. Kislik (Ed.), Liquid Membranes: Principles and Applications in Chemical Separations and Wastewater Treatment, first ed., Elsevier, The Netherlands, 2010, pp. 17–18.

[38] N. Alizadeh, S. Salimi, A. Jabbari, Transport study of palladium through a bulk liquid membrane using hexadecylpyridinium as carrier, Sep. Purif. Technol. 28 (2002) 173–180.

จุฬาลงกรณ์มหาวิทยาลัย
CHULALONGKORN UNIVERSITY

[39] T. Wongsawa, N. Leepipatpiboon, N. Thamphiphit, U. Pancharoen, A.W. Lothongkum, Fluid-flow models operating on linear algebra for extraction and stripping of silver ions from pharmaceutical wastewater by HFSLM, Chem. Eng. J. 222 (2013) 361–373.

[40] A. Uheida, Y. Zhang, M. Muhammed, Transport of palladium (II) through hollow fiber supported liquid membrane facilitated by nonylthiourea, J. Membrane Sci. 241 (2004) 289–295.

2.11 Recommendations for future research

The development of mathematical modeling on the shell side should be considered in order to yield the best fit with the experimental results. The mass transfer resistance due to chemical reaction should be included in the transport phenomena across the system regading the diffusioanal parameter determining.

จุฬาลงกรณ์มหาวิทยาลัย
CHULALONGKORN UNIVERSITY

CHAPTER III

Optimization of process parameters using response surface methodology for Pd (II) extraction with quaternary ammonium salt from chloride medium: kinetic and thermodynamics study

Vanee Mohdee[1], Kreangkrai Maneeintr[2], Thanaporn Wannachod[1], Suphot Phatanasri[1,*] and Ura Pancharoen[1,**]

[1]*Department of Chemical Engineering, Faculty of Engineering, Chulalongkorn University, Bangkok 10330, Thailand*

[2]*Carbon Capture, Storage and Utilization Research Group, Department of Mining and Petroleum Engineering, Faculty of Engineering, Chulalongkorn University, Bangkok 10330, Thailand*

จุฬาลงกรณ์มหาวิทยาลัย
CHULALONGKORN UNIVERSITY

This article has been published in Journal: Chemical Papers.

Page: 3129–3139. Volume: 72. Year: 2018.

3.1 Abstract

In this study, liquid–liquid extraction with Aliquat 336 in the presence of cyclohexane as a mobile carrier was investigated to purify Pd (II) from industrial wastewater. Kinetic and thermodynamics analysis showed that Pd (II) extraction was of first-order reaction: the reaction was endothermic reaction which was governed by the diffusion region. The influence of temperature on isotherm model was also investigated. With an increase in reaction temperature, all three isotherms Langmuir, Freundlich and Temkin isotherm become inaccurate. Results show that the Langmuir isotherm model was preferred for the study of the Pd (II) ion experimental isotherm. Response surface methodology was employed to study the five independent variables which have an effect on the percentage of extraction of palladium (II) ions as a dependent variable. Optimum extraction conditions for the five independent variables were as follows: Aliquat 336 concentration (0.6 M), pH of feed solution (2.0), stirring speed (600 rpm), reaction time (10 min.) and reaction temperature (318 K).

Keywords: Optimization; CCD; RSM; Pd (II) purification; LLE; Isotherm model

จุฬาลงกรณ์มหาวิทยาลัย
CHULALONGKORN UNIVERSITY

3.2 Graphical Abstract

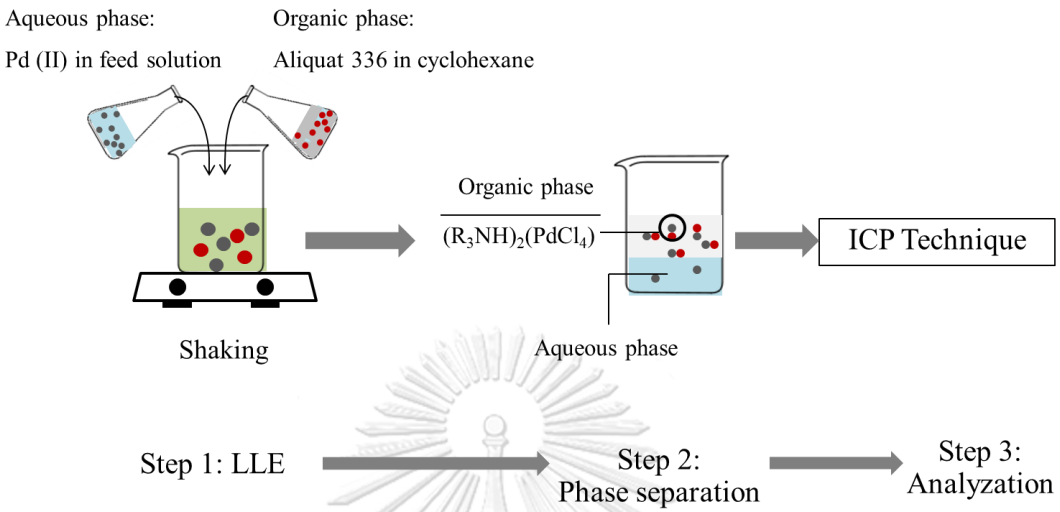

3.3 Introduction

Platinum group metals (PGM) including platinum (Pt), gold (Au), silver (Ag), and palladium (Pd) are widely used in many industries such as the automotive, electronics and chemical process industry owing to their exceptional properties (Patricia 2012; Lu and de Zu 2009; Stefan and Jurgen 2015). However, increasing use of these PGM together with limited resources have led to much endeavour to recycle the PGM from secondary resources (Jonathan 2012; Ana et al. 2016). Industrial wastewater, such as that caused by the flexible printed circuit board process, as a secondary source, contains relatively high concentration of these precious metals. Hence, there is a need to recover and reutilize PGM on account of the cost saving and environmental concern before being discharged (Wei et al. 2016; Jonathan et al. 2014).

Recently, liquid–liquid extraction (LLE) or solvent extraction (SX) has been receiving considerable attention for purification of target metal ions owing to their high efficiency of purifying metal ions, high selectivity, fast extraction rate, and ease of recovery and recycling (Ana et al. 2016; Wei et al. 2016; Anpilogova et al. 2016).

Many researchers have studied the separation and purification of Pd (II) using various extractants. Phosphonium extractants, such as Cyphos®IL 101 and Cyphos®IL 104, have been employed to study the selectivity of Pd (II) over other metals and percentage of Pd (II) extraction (Cieszynska and Wisniewski 2011). LIX 63 has been used to extract Pd (II) from concentrated hydrochloric acid solutions. It has been reported that Pd (II) can be selectively extracted from multi-metal solutions containing Pt (IV), Pd (II), Rh (III) and Ir (IV) using LIX 63 (Thi et al. 2016). Cyanex 923 has also been used to investigate the extraction behavior of Pt (IV), Pd (II) and Rh (III) from real samples (Bina and Indu 2013). Pyridinium-based ionic liquid has been utilized to study Pd (II) extraction mechanism from hydrochloric acid medium (Yu et al. 2014). Further, many studies have highlighted the use of Aliquat 336 for selective extraction and recovery of Pd (II) from multi-metal solutions (Wei et al. 2016; Chen and The-Hua 2014; Giridhar et al. 2006). A summary of previous research on palladium separation is shown in **Table 3.1**.

Table 3.1 Summary of previous research on palladium separation

Extractants	**Diluent**	**Metal**	**%Ex**	**Ref.**
Phosphonium extractants	Toluene	Pd, Ni, Cu, Pb, Fe,Rh, Ru, Pt	>99%	Cieszynska and Wisniewski 2011
LIX 63	Kerosene	Pt, Pd, Rh and Ir	N/A	Thi et al. 2016
Cyanex 923	Toluene	Pt, Pd and Rh	>98%	Bina and Indu 2013
Pyridinium extractants	Chloroform	Pd, Cu, Co, Ni, Fe, Al, Sn	99%	Yu et al. 2014
Aliquat 336	Kerosene	Pd	>99%	Chen and The-Hua 2014

จุฬาลงกรณ์มหาวิทยาลัย
Chulalongkorn University

Response surface methodology (RSM) is an effective statistical technique for investigating the influence of individual parameters and their interactive influences including evaluating the optimum condition of the process (Mehdi et al. 2014; Rajasimman et al. 2009; Long et al. 2012; Chen and Wu 2010; Gabriela et al. 2014).

Central-composite design (CCD) was used to determine the significant parameters to find optimum conditions and to reduce the total number of experiments (Amit et al. 2015; Behzad et al. 2012).

The aim of this work is to investigate the optimum conditions for Pd (II) extraction from industrial wastewater in an aqueous chloride solution. Five experimental variables namely, (A) concentration of Aliquat 336 (M), (B) pH of feed solution, (C) stirring speed (rpm), (D) reaction time (min.) and (E) reaction temperature (K) were optimized using RSM based on CCD technique. The influence of individual parameters and their interaction were also determined.

3.4 Experimental

3.4.1 Reagents and solutions

Aliquat 336 supplied by Acros Organics, USA was used as an extractant. Cyclohexane as a carrier was supplied by Loba Chemie, India. Nitric acid (Merck, Singapore) was used as a stripping solution. The feed solution was supplied by Mektec manufacturing CO., Ltd., Thailand. The initial concentration of Pd (II) in aqueous feed solution is 1.173 mg/L. All materials were of analytical reagent grade and were used as received without any further purification.

จุฬาลงกรณ์มหาวิทยาลัย
Chulalongkorn University

3.4.2 Procedure

LLE was carried out with aqueous/organic phase ratio of 1:1 which was the most effectiveness operating ratio and in agreement with previous studies (Basudev et al. 2010; Pan et al. 2013; Kuixing et al. 2018). Extraction time taken was 60 min. Subsequently, samples were collected after phase separation. The concentration of palladium ions in the sampling solutions were analysed by an inductively coupled plasma spectrometry (Carry 5000, Aligent). The correlation coefficient of standard palladium (II) solutions is 0.995425.

The extraction percentage was expressed as shown in Eq. (3.1):

$$\%\text{Extraction} = \frac{[Pd^{2+}]_{initial} - [Pd^{2+}]_{aq}}{[Pd^{2+}]_{initial}} \quad (3.1)$$

3.5 Design of the experiment

Three levels, (-1, 0, 1), of 5 independent variables was studied in this work as follows: (A) concentration of Aliquat 336 (M); (B) pH of feed solution; (C) stirring speed (rpm); (D) reaction time (min) and (E) reaction temperature (K) as listed in **Table 3.2** where α and $-\alpha$ are axial points. A dependent variable was the extraction percentage of Pd (II) ions. To analyze the optimum condition of the process and investigate influences of individual parameters and their interactive effects, RSM based on CCD was used to optimize the effective parameters. An experiment was randomly run to avoid the effect of confounding which occurs when the standard order test is performed: this helps to justify the assumptions (Yuxiang et al. 2013). Coding of the variables was performed based on Eq. (3.2):

จุฬาลงกรณ์มหาวิทยาลัย
CHULALONGKORN UNIVERSITY

$$x_i = \frac{X_i - X_0}{\Delta x} \quad (3.2)$$

where x_i is the dimensionless value of an independent variable, X_i is the real value of an independent variable, X_0 is the real value of the independent variable at the central point and Δx is the step change value.

The response variable (Y) as an extraction percentage of Pd (II) ions was fitted by a second-order polynomial as shown in Eq. (3.3) (Arrisa and Chayanoot 2013; Ren et al. 2017):

$$Y = \beta_0 + \sum_{i=1}^{k} \beta_i X_i + \sum_{i=1}^{k} \beta_{ii} X_i^2 + \sum_{i=1}^{k-1} \sum_{j=2}^{k} \beta_{ij} X_i X_j + \varepsilon \quad (3.3)$$

where Y is the result of response of the experiment. 0 , i , ii , ij are regression coefficients for the intercept, linear, quadratic and interaction terms. Xi and Xj are independent variables and is a random error.

An ANOVA, the analysis of variance, indicates the significant variable. Generally, p value< 0.05 indicates a significant parameter. A calculated coefficient of determination value (R^2 close to 1.00) better predicts the response (Khattab et al. 2008).

Table 3.2 Five independent variables and levels used for CCD

Independent variable	Unit	Symbol	Variable levels		
			-1	0	1
[Aliquat 336]	M	*A*	0.4	0.6	0.8
pH of feed solution	-	*B*	1	2	3
Stirring speed	Rpm	*C*	450	500	550
Reaction time	min.	*D*	5	10	15
Reaction temperature	K	*E*	308	313	318

จุฬาลงกรณ์มหาวิทยาลัย
Chulalongkorn University

3.6 Statistical analysis

The statistical software program Design-Expert 10.0.6 Trial version (Stat-Ease, Inc., Minneapolis, MN, USA) was utilized for designing the experiment, analysis regression and for plotting 3D response surfaces and 2D contours.

3.7 Thermodynamics study

An investigation of thermodynamic parameters (ΔG, ΔH and ΔS) on Pd (II) extraction can be obtained from the temperature affected on Pd (II) extraction

mechanism. The experiment was investigated in the range (298–318) K with Aliquat 336 as extractant dissolved in cyclohexane as carrier. Three isotherms of chemisorption were applied to describe the experimental isotherms of Pd (II) extraction including Langmuir, Freundlich and Temkin based on the concept of the chemical reaction which occurred between the target metal ions and the extractant at the surface of the extractant. The Langmuir, Freundlich and Temkin models are depicted by the following equations:

Langmuir model (Torab-Mostaedi et al. 2013):

$$\frac{C_e}{q_e} = \frac{C_e}{q_{max}} + \frac{1}{K_L q'_{max}} \tag{3.4}$$

where C_e is equilibrium concentration of Pd (II) (mg/L), q_e is amount of metal ion adsorbed or extracted per weight of carrier (mg/g), q_{max} is maximum adsorbed or extracted capacity and K_L is Langmuir isotherm constant.

Freundlich model (Torab-Mostaedi et al. 2013):

$$\ln q = \ln K_F + \frac{1}{n} lnc_{e'} \tag{3.5}$$

จุฬาลงกรณ์มหาวิทยาลัย
CHULALONGKORN UNIVERSITY

where K_F is Freundlich isotherm constants (mg/g) and $1/n$ is the adsorption intensity.

Temkin model (Li et al. 2017):

$$q_e = BlnK_T + BlnC_{e'} \tag{3.6}$$

where K_T is the Temkin isotherm constant (mg/g) and B is the Temkin constant.

Since the plots between moisture content versus time of the sorption plots have similar semblances as the plots between concentrations versus time of extraction plots, adsorption isotherms can be used to determine experimental data for the extraction process and these plots can be described using mathematical models (Stela et al. 2010). The applicability of adsorption isotherms into the extraction process has previously been investigated (Hitoshi 1985; Darshak et al. 2015; Stela et al. 2010). With regards to chemical reaction occurring and the generation of new bonds, the adsorption process is analogous to the extraction process (Dolapop et al. 2015; Niti et al. 2018). The chemisorption process is a chemical adsorption process which involves the formation of strong bonds between adsorbate molecules and specific surface of adsorbent (Seader et al. 2005). In the extraction process, target metal ions in aqueous feed solution reacted with extractants: subsequently, a new complex species of metal ions was formed. Therefore, three adsorption isotherms were applied in this study. The Langmuir model is based on a homogeneous monolayer sorption to a finite number of surface's sites (María and Katherina 2017; Darshak et al. 2015). The Freundlich model is based on the concept that the adsorbent has a multilayer heterogeneous surface (Bei et al. 2018; Phawinee et al. 2018). The Temkin model is based on account of the adsorbent–adsorbate interactions with non-uniform distribution of sorption heat (Cleide et al. 2018; Mohamed et al. 2015). All three adsorption isotherms show the results between the amount of metal ions adsorbed per weight of extractants and equilibrium concentration of metal ions. The relationship between the adsorption isotherms and extraction process is shown in **Table 3.3** (Dolapop et al. 2015; Niti et al. 2018).

จุฬาลงกรณ์มหาวิทยาลัย
CHULALONGKORN UNIVERSITY

Table 3.3 Relationship between adsorption and extraction process

Parameter	Adsorption	Extraction
C_e	Adsorbate	Target metal ions
	Adsorbent	Extractant
	Equilibrium adsorbate concentration (mg/L)	Equilibrium metal ions concentration (mg/L)
q_e	Amount of adsorbate (mg)/ g of adsorbent	Amount of metal ions (mg)/ g of extractant
q_m	Maximum capacity	Maximum capacity
K_L	Langmiur constant	Langmiur constant
K_F	Freundlich constants	Freundlich constants
1/n	Adsorption intensity	Adsorption intensity
K_T	Temkin constant	Temkin constant

จุฬาลงกรณ์มหาวิทยาลัย
CHULALONGKORN UNIVERSITY

3.8 Kinetic study

Reaction rate of Pd (II) LLE depends on the following factors: concentration of extractant, stirring speed, temperature and interfacial area. The concentration of the extractant is a significant parameter as regards kinetics of metal extraction (Maryam et al. 2017). In this study, an investigation of reaction rate was observed.

3.9 Results and discussion

3.9.1 Influence of Aliquat 336 concentration on Pd (II) extraction

The influence of extractant concentration on Pd (II) extraction was observed by varying Aliquat 336 concentration from (0.2 to 1.0) M. The results are illustrated in **Fig. 3.1**. Thus, it was found that the percentage of extraction increased when concentration of the extractant was increased up to 0.6 M. However, when concentration of Aliquat 336 was increased further, it had no effect on Pd (II) ions extraction. This was because extraction efficiency had almost reached its maximum as can be seen in the range from 0.6 to 1.0 M, whereby the extraction percentage is slightly the same (Wei et al. 2016).

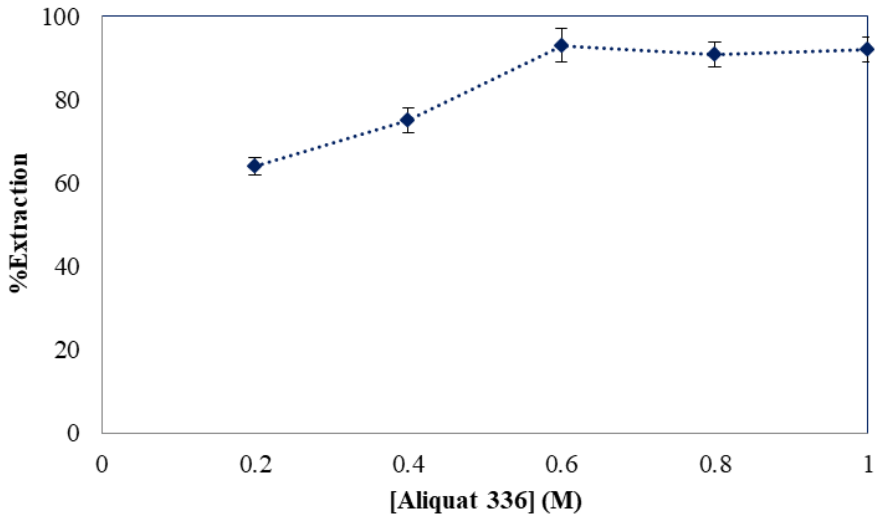

Fig. 3.1 Influence of concentration of Aliquat 336 on Pd (II) extraction.

3.9.2 Influence of pH on Pd (II) extraction

The effect of pH of feed solution on the extraction of Pd (II) using Aliquat 336 in cyclohexane was investigated in the range of pH 1–5 as shown in **Fig. 3.2**. It was

evident that by increasing the pH of feed solution, extraction of Pd (II) increased reaching a maximum value pH 2.0 (Shen and Xue 2007). Thereafter, it decreases. Generally, in chloride media, Pd (II) has 4 chlorocomplexes namely, $[PdCl]^{-}$, $[PdCl_2]$, $[PdCl3]^{-}$ and $[PdCl_4]^{2-}$ of which the latter $[PdCl_4]^{2-}$ is a predominant species (Viet et al. 2016). Equation (3.7) shows the mechanism of target metal ions extracted from chloride medium (Al-Bazi and Chow 1984):

$$MCl_n^{n-}{}_{(aq)} + nR_3NH^+Cl^-{}_{(org)} \longleftrightarrow (R_3NH)_n(MCl_n)_{(org)} + nCl^-{}_{(aq)} \quad (3.7)$$

Thus, Pd (II) ions extracted from chloride solution with ammonium salts as an extractant is shown below (Basudev et al. 2010):

$$PdCl_4^{2-}{}_{(aq)} + 2R_3NH^+Cl^-{}_{(org)} \longleftrightarrow (R_3NH)_2(PdCl_4)_{(org)} + 2Cl^-{}_{(aq)} \quad (3.8)$$

Hence, in a saturated solution of HCl, $[PdCl_4]^{2-}$ as a predominant species will be transformed into $[PdCl_6^{2-}]$. Thus, Pd (II) ions extracted in an excess HCl medium is as shown in Eq. (3.9):

$$2PdCl_6^{2-}{}_{(aq)} + 2R_3NH^+Cl^-{}_{(org)} \longleftrightarrow [(R_3NH)_2(PdCl_5)_2]_{(org)} + 4Cl^-{}_{(aq)} \quad (3.9)$$

จุฬาลงกรณ์มหาวิทยาลัย
Chulalongkorn University

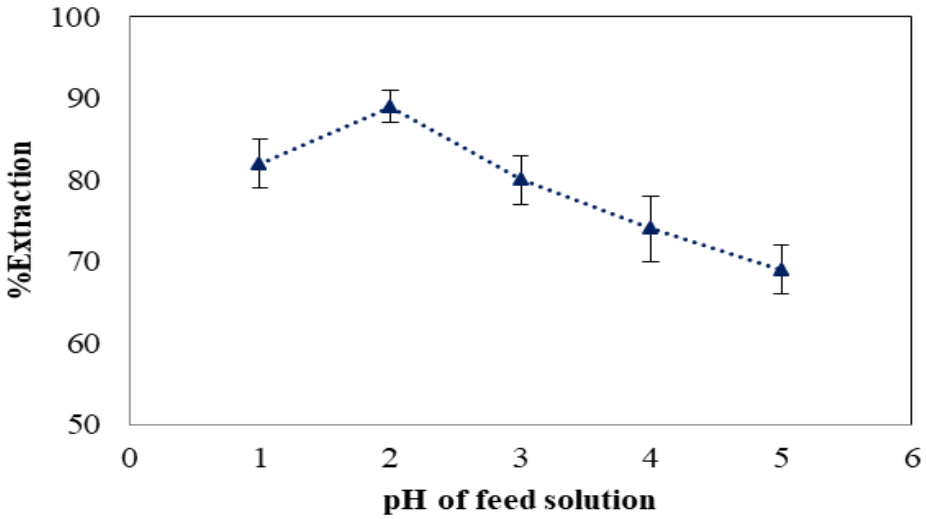

Fig. 3.2 Influence of pH of feed solution on Pd (II) extraction using 0.6 M of Aliquat 336 dissolved in cyclohexane.

3.9.3 Influence of stirring speed on Pd (II) extraction

The impact of speed of the mixture solution on Pd (II) ions extraction was studied by varying stirring speed from 300 to 600 rpm. The change in stirring speed had an effect on the concentration gradient (Peng et al. 2013). Thus, it was found that Pd (II) ions percentage extraction increased when stirring speed increased until it reached a plateau regime at 500–600 rpm. Thereby, it is assumed that the chemical reaction controlled the process and neglected the diffusion (Maryam et al. 2017). The results are illustrated below in **Fig. 3.3**:

จุฬาลงกรณ์มหาวิทยาลัย
CHULALONGKORN UNIVERSITY

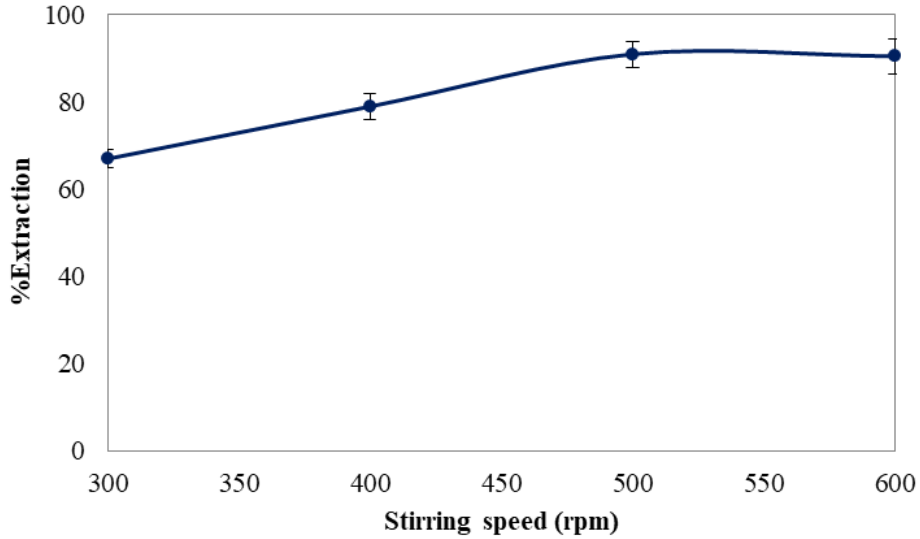

Fig. 3.3 Influence of stirring speed on Pd (II) extraction using 0.6 M of Aliquat 336 dissolved in cyclohexane

3.9.4 Influence of reaction time on Pd (II) extraction

The influence of reaction time on Pd (II) extraction is illustrated as shown in **Fig. 3.4**. Results show that within 5 min. up to 85% of Pd (II) ions were extracted. Moreover, within 10 min. maximum extraction reached 92%. Then, extraction was independent on the reaction time as can be seen in **Fig. 3.4** (Yu et al. 2014). As reaction time increased from 30 min., percentage of Pd (II) extraction remained slightly the same. Therefore, it can be concluded that Pd (II) ions contained in industrial wastewater reacted very fast with the extractant via LLE.

จุฬาลงกรณ์มหาวิทยาลัย
CHULALONGKORN UNIVERSITY

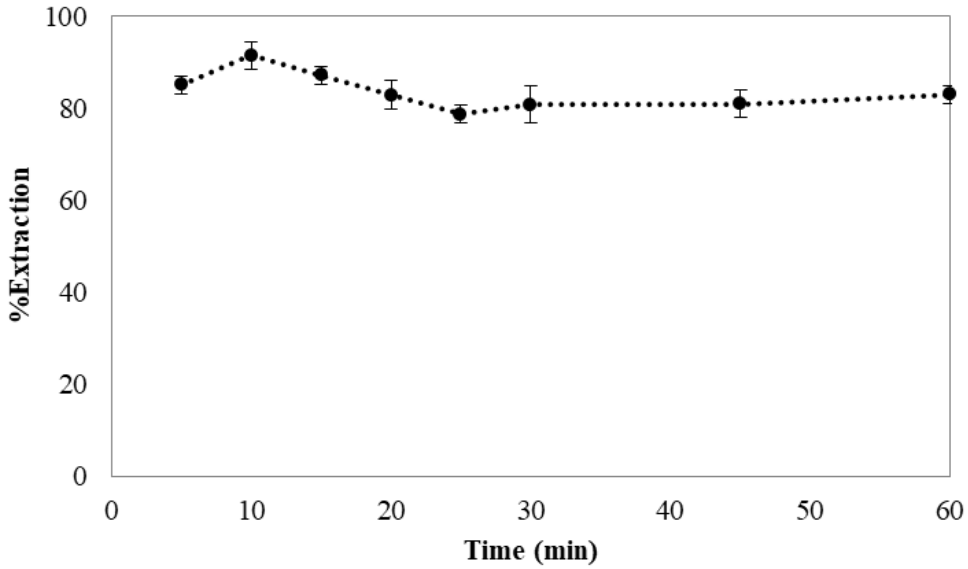

Fig. 3.4 Influence of reaction time on Pd (II) extraction using 0.6 M of Aliquat 336 dissolved in cyclohexane

3.9.5 Thermodynamics study on Pd (II) extraction

The influence of temperature on the extraction of Pd (II) from industrial wastewater was investigated in the range (298–318) K with Aliquat 336 as extractant dissolved in cyclohexane as carrier. Results indicated an increase in percentage extraction when temperature was increased as illustrated in **Fig. 3.5**. The temperature effect on Pd (II) extraction can be evaluated in terms of its thermodynamic parameters (ΔG, ΔH and ΔS). The value of Gibbs free energy (ΔG, kJ/mol) of Pd (II) ions extraction at various studied temperature was calculated as shown in **Table 3.4**. The values of ΔH and ΔS can be calculated from the plot between ln K_{eq} vs $1/T$ as shown in **Fig. 3.6**. From the slope and intercept, the values of ΔH and ΔS obtained are namely, 12.67 and 83.76 J/mol K, respectively. The positive value of the enthalpy change (ΔH) indicated that the extraction process was endothermic and the positive entropy change (ΔS) indicated an increase in the disorder of the process.

จุฬาลงกรณ์มหาวิทยาลัย
Chulalongkorn University

In this study, the activation energy for Pd (II) ions extraction was found to be 12.67 kJ/mol: this indicated that the process was governed by diffusion since the E_a value was found to be less than 20.9 kJ/mol (Naglaa 2007; Javanshir et al. 2011). In the case whereby the E_a value is greater than 40 kJ/mol, the process is controlled by the chemical reaction (González-Centeno et al. 2015). In the case whereby an E_a value is between 20 and 40 kJ/mol, the process is governed by both chemical reaction and diffusion regime (Liliana et al. 2016).

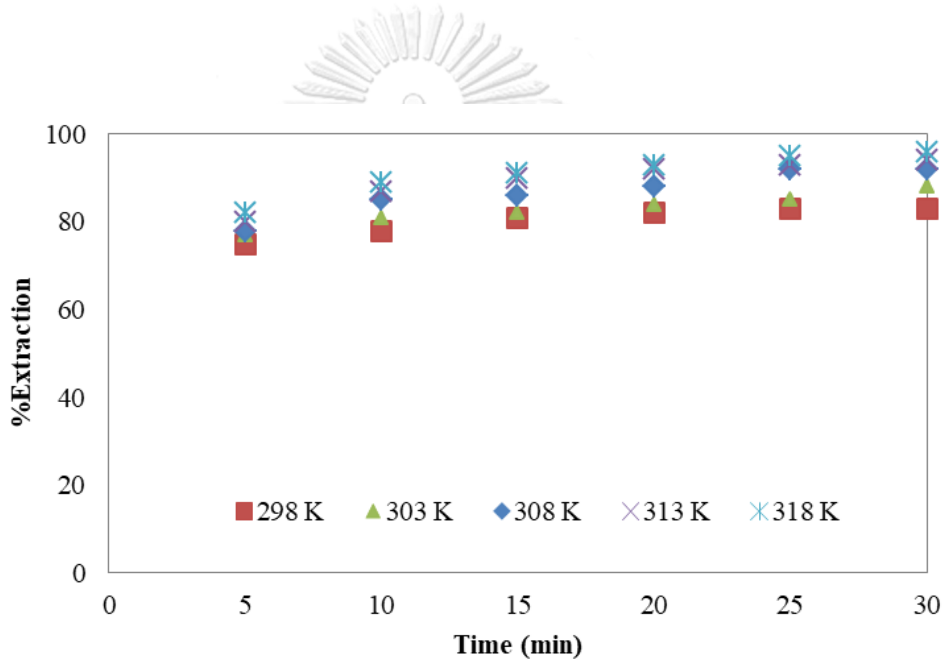

Fig. 3.5 Influence of reaction temperature on Pd (II) extraction using 0.6 M of Aliquat 336 dissolved in cyclohexane

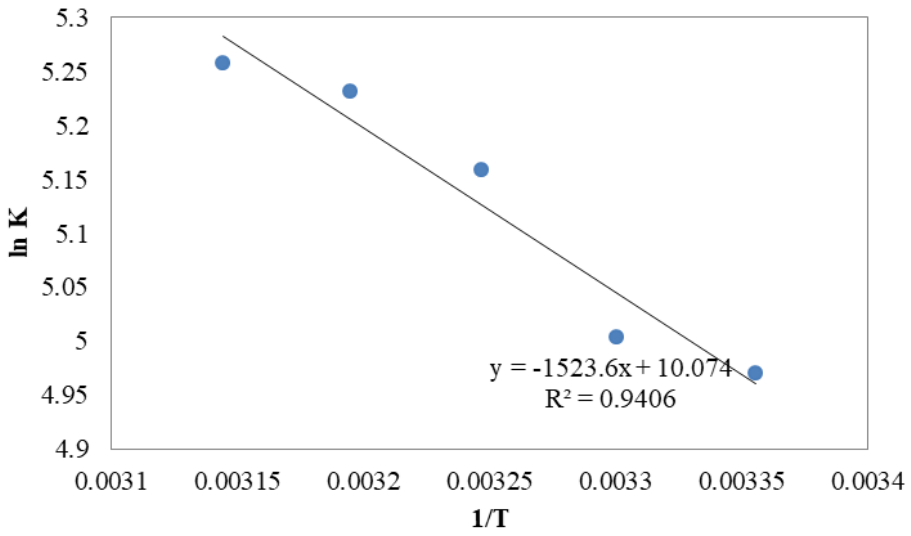

Fig. 3.6 Plot of ln K_{eq} vs $1/T$

Table 3.4 Thermodynamic data for the Pd-Aliquat 336 system

T (K)	ΔG (kJ/mol)
298	-24.96
303	-25.38
308	-25.80
313	-26.22
318	-26.64

จุฬาลงกรณ์มหาวิทยาลัย
Chulalongkorn University

3.9.6 Isotherm model

The experimental data were plotted applying three isotherm models (Langmuir, Freundlich, and Temkin) as shown in **Fig. 3.7**. The constant parameter for each model was calculated by the slope and intercept of the plot as illustrated in **Table 3.5**.

As shown in **Table 3.5**, the R^2 values obtained from the three isotherm models imply that the Langmuir isotherm model was the most preferable for studying the Pd (II) ion experimental isotherms. It is noticed that when reaction temperature is increased, all three isotherms become inaccurate as can be seen by the decrease in R^2 values.

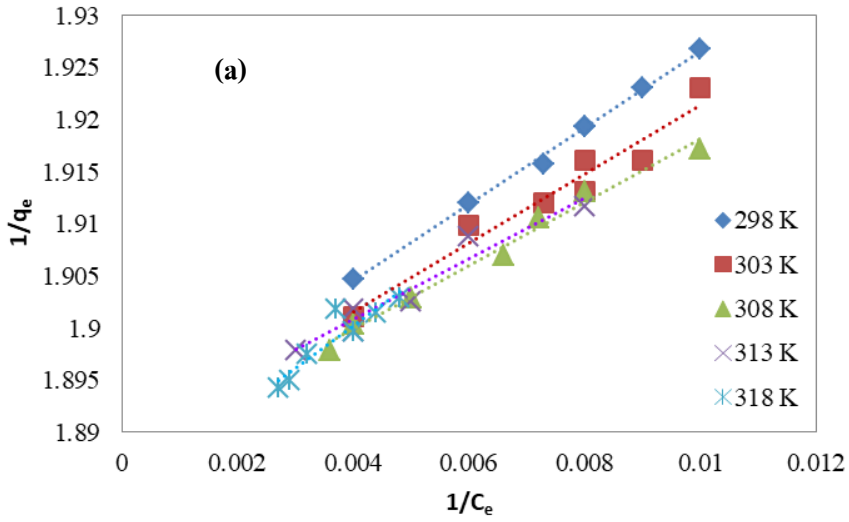

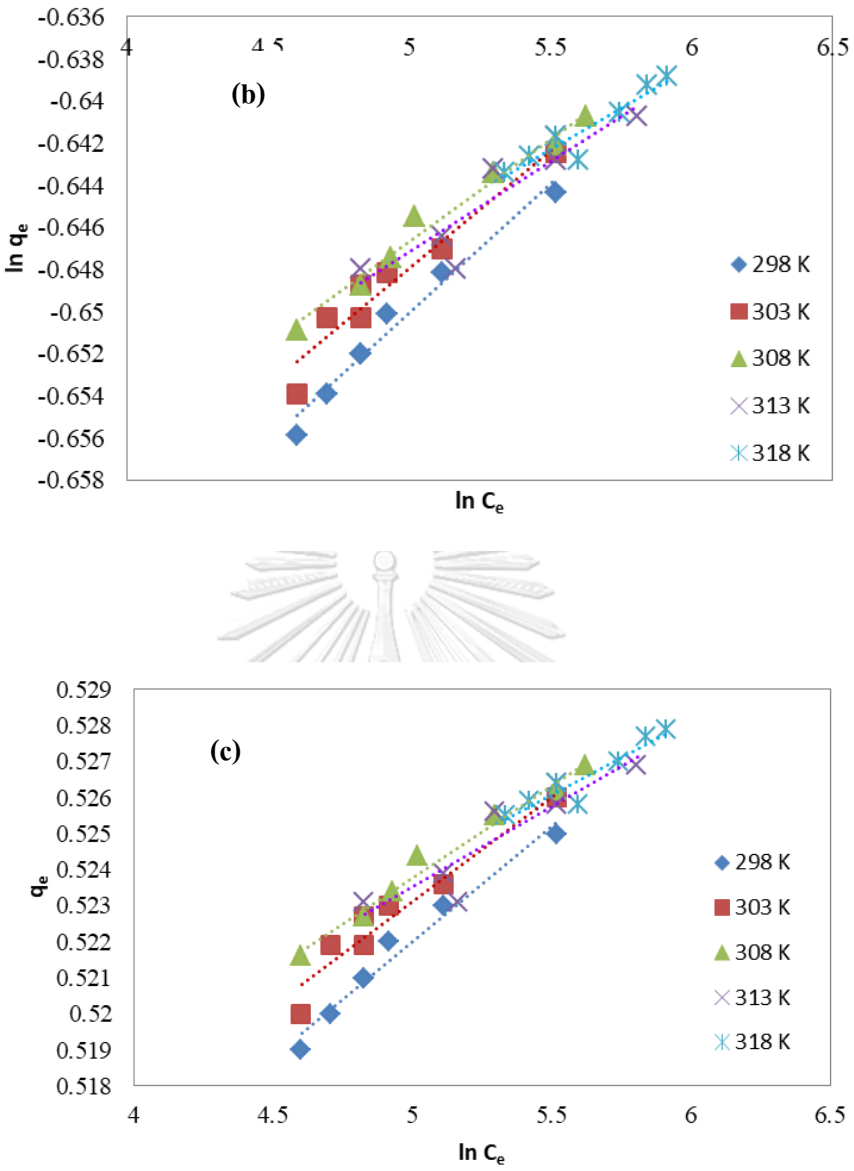

Fig. 3.7 Parameter constants; **(a)** Langmuir model, **(b)** Freundlich model and **(c)** Temkin model

Table 3.5 Comparison of Langmuir, Freundlich and Temkin constants of Pd (II) ions extraction

T (K)	Langmuir		Freundlich		Temkin	
	K_L	R^2	K_F	R^2	K_T	R^2
298	0.514	0.9966	0.490	0.9695	$1.76x10^{33}$	0.9701
303	0.571	0.9469	0.495	0.9275	$9.75x10^{36}$	0.9284
308	0.622	0.9843	0.500	0.9802	$2.71x10^{42}$	0.9804
313	0.650	0.939	0.502	0.8383	$2.30x10^{48}$	0.8386
318	0.463	0.8576	0.504	0.8872	$1.08x10^{52}$	0.8872

3.9.7 Kinetic study on Pd (II) extraction

The order of Pd (II) ions extraction rate is as shown in **Table 3.6**. The results show that the reaction rate order of extraction of Pd (II) ions is first-order reaction. This fits in well with the correlation coefficients as shown in **Fig. 3.8**.

จุฬาลงกรณ์มหาวิทยาลัย
Chulalongkorn University

Table 3.6 The reaction rate order of Pd (II) ions LLE

Reaction order	Equations	R^2
0	$C_{A0} - C_A$ VS Time	0.7914
1	$ln(C_{A0}/C_A)$ VS Time	0.9905
2	$(1/C_A)-(1/C_{A0})$ VS Time	0.7118

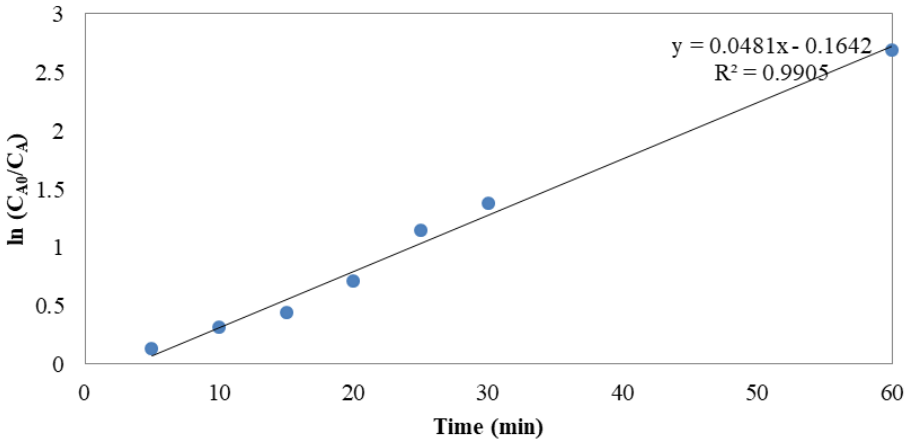

Fig. 3.8 First-order reaction rate plot of Pd (II) LLE

3.9.8 Selection of lower, middle and upper levels for the design variables

In this study, levels of five independent variables were determined based on the preliminary experimental data. Thus, the highest effect of [Aliquat 336] was found to be 0.6 M and decreased thereafter. So, 0.6 M of [Aliquat 336] was chosen for the middle level of the variable and 0.4 and 0.8 M of [Aliquat 336] were chosen to be the lower and upper level.

For pH of feed solution, 1, 2 and 3 were selected as the lower, middle and upper levels of the variable, respectively. A stirring speed at 450, 500 and 550 rpm were chosen as lower, middle and upper level of the variable. Reaction time for the variable optimization namely, 5, 10 and 15 min were chosen as lower, middle, and upper level, respectively. The impact of reaction temperature at 308, 313, and 318 K was selected as lower, middle, and upper level for the optimization of the variable.

3.9.9 ANOVA results and regression model: response surface analysis

A design expert program was used to investigate the influence of three levels for the five selected parameters on the extraction of Pd (II) ions. The empirical model is as given in the following Eq. (3.10):

จุฬาลงกรณ์มหาวิทยาลัย
Chulalongkorn University

$$Y = 88.91 + 4.90A + 0.73B + 1.98C + 1.41D + 1.50E + 1.05AB + 0.15AC - 1.07AD - 0.058AE - 0.24BC - 0.42BD + 0.19BE + 0.35CD + 0.13CE + 0.52DE - 4.74A^2 - 6.30B^2 - 2.67C^2 - 3.00D^2 - 1.77E^2 \quad (3.10)$$

where Y is the percentage of extraction of Pd (II) ions; A, B, C, D and E are concentrations of Aliquat 336 (M), pH of feed solution, stirring speed (rpm), reaction time (min.) and reaction temperature (K).

In Eq. (3.10), the positive and negative coefficients indicate how the responses change according to these variables.

The analysis of variance fitting of quadratic models was investigated. According to Eq. (3), the predicted result for the extraction percentage of Pd (II) ions was obtained. Thus, the model F value (5.50) implies that the model is significant, indicating that the model is fit to explain Pd (II) extraction as a function of conditions of the studied parameters. There is only a 0.01% chance that an F value this large could occur due to noise. Values of "Prob > F" less than 0.0500 indicate model terms are significant. In this study, significant model terms are A, A^2, B^2, C^2, D^2 and E^2. The value of the coefficient of determination (R^2) was 0.8350. The value of R^2 being higher than 0.7 indicated that the model was suitable to apply in the experiment (Hong et al. 2017; Wong et al. 2017). The adjusted determination coefficient (Adj-R^2) was found to be 0.7211 while the coefficient of variation (CV) was 6.50% indicating a very high degree of precision between the actual and predicted experimental value (Mehmet et al. 2015). The Pred-R^2 from the model was found to be 0.2869. The value of adequate precision was 9.481 and was used to measure the signal to noise ratio. A ratio greater than 4 is desirable denoting adequate model discrimination. In this study, the ratio of 9.481 indicates an adequate signal which implies that this model can be used to navigate the design space. The values obtained by the analysis of variance shows that

จุฬาลงกรณ์มหาวิทยาลัย
CHULALONGKORN UNIVERSITY

the model is fit to explain Pd (II) extraction as a function of conditions of the studied parameters.

The value (0.0025) lack of fit implies the lack of fit is significant. The lack of fit p value (< 0.0001) implies that the response surface regression model is valid. There is only a 3.32% chance that a lack of fit this large could occur due to noise. Previous studies have been carried out which have reported significant lack of fit (Xueqin et al. 2018; Guoqiang et al. 2017). A significant lack of fit denotes that adding additional terms to the model such as interaction terms or squared terms should be considered. In the primary item, parameter A was statistically significant. In the quadratic terms (A^2, B^2, C^2, D^2 and E^2) were also statistically significant which allow for curvature in the effect of a control on the response. Due to the significance of the quadratic terms, interaction effect of design parameter was obtained. The 3D response surface plots of two parameters whilst three other parameters are constant at their middle level. The inclusion of the middle levels was applied to check an adequate of the model or to include some quadratic terms to allow for curvature.

3.9.10 Response surface plot

จุฬาลงกรณ์มหาวิทยาลัย
CHULALONGKORN UNIVERSITY

Three dimensional response surface plots were used to characterize the influence of five independent variables on the extraction of Pd (II) ions. The response surface plots and their corresponding contour plots show that two variables were highlighted, while other independent variables were fixed.

The response surface plots and their contour plots are mapped against two parameters whilst three other parameters are constant at their middle level. The maximum percentage of Pd (II) ions extraction is indicated by the surface confined in the smallest curve of the plot.

Results show that the interaction effect of both concentration of Aliquat 336 and pH of feed solution was significant. This was because extraction efficiency increased when concentration of Aliquat 336 was increased. Furthermore, extraction efficiency decreased when pH of feed solution was increased. Maximum yield of Pd (II) was at the centre of the design which corresponded to the middle level of each independent variable. According to Le Chatelier's principle as regards the concentration of extractant, adding reactants shift the reaction towards products. This drives the equilibrium of the reaction towards complex formation and thus improves extraction efficiency of Pd (II): these results are in agreement with several studies (Modise et al. 2012; Thanaporn et al. 2016; Kuixing et al. 2018). As regards the pH of feed solution, results found that Pd (II) extraction attained a maximum value (pH 2.0) which was in agreement with previous studies (Bina et al. 2006; Shen and Xue 2007; Satit et al. 2012). As for the effect of stirring speed, results show that the tendency of extraction increased when stirring speed increased owing to it had an effect on the concentration gradient (Shabani et al. 2012; Maryam et al. 2017). The temperature effect on the LLE of palladium (II) found that the extraction of palladium (II) increased when temperature increased due to the increased in solubility and diffusion coefficients and decreased solvent viscosity as well as the enhanced of mass transfer (Boukraa et al. 2009; Tan et al. 2013; Robinson et al. 2018).

จุฬาลงกรณ์มหาวิทยาลัย
CHULALONGKORN UNIVERSITY

The optimum values of variables in coded units were accordingly, $A = 0.6$, $B = 2.0$, $C = 600$, $D = 10$ and $E = 318$. These correspond to optimum values for the independent variables as follows: [Aliquat 336] (0.6 M), pH of feed solution (2.0), stirring speed (600 rpm), reaction time (10 min.) and reaction temperature (318 K).

A residual plot of the design which described the deviation of experimental values from model predicted values. A random dispersal of the plots indicated that a linear regression model was appropriate. The deviation of each variable from the

optimized values at the center was obtained as a perturbation curve which was used to compare the influence of all studied parameters. Central-composite design for %Pd (II) extraction as the model response, run at lower and upper levels for each parameter, was also provided, the value of the parameter at the center yielded the highest % Pd (II) extraction.

3.10 Conclusion

It was noted that response surface methodology (RSM) with central-composite design (CCD) technique by the design expert program can be used to optimize the extraction of Pd (II) ions from industrial wastewater. Under obtained conditions namely, Aliquat 336 concentration (0.6 M), pH of feed solution (2.0), stirring speed (600 rpm), reaction time (10 min.) and reaction temperature (318 K), maximum percentage of Pd (II) extraction reached 94.68%. Results show that the interaction effect of both concentration of Aliquat 336 and pH of feed solution proved to be significant. The values of thermodynamic parameters (ΔH and ΔS = 75.29 and 83.76 J/mol K, respectively) of Pd (II) extraction indicated that the extraction process was endothermic. The E_a value in this study was found to be 12.67 kJ/mol. This process was in the range of diffusion control. First-order reaction was the model which represented the LLE of palladium ions. The three isotherm models, Langmuir, Freundlich and Temkin isotherms show that when the reaction temperature increased, all three isotherms become inaccurate. Results proved that the Langmuir isotherm model was the most preferable for the study of the Pd (II) ions experimental isotherms.

จุฬาลงกรณ์มหาวิทยาลัย
Chulalongkorn University

3.11 Acknowledgements

The authors profoundly appreciate the support from the Thailand Research Fund and Chulalongkorn University under the Research and Researchers for Industries (RRi) Ph.D. Program (Grant No. PHD58I0081). Thanks are also given to the Separation Laboratory, Department of Chemical Engineering, Faculty of Engineering,

Chulalongkorn University, for chemical and apparatus support as well as to the Mektec Manufacturing Corporation (Thailand) Ltd, for feed solution.

3.12 References

Al-Bazi SJ, Chow A (1984) Platinum metals-solution chemistry and separation methods (ion-exchange and solvent extraction). Talanta 31:815–836. https ://doi.org/10.1016/0039-9140(84)80204 -0

Amit R, Bikash M, Ravindra B (2015) Modeling and response surface analysis of supercritical extraction of watermelon seed oil using carbon dioxide. Sep Purif Technol 141:354–365. https ://doi.org/10.1016/j.seppu r.2014.12.016

Ana A, Ana M, Ana MR, Antonio C, Maria CC (2016) A bridge between liquid–liquid extraction and the use of bacterial communities for palladium and platinum recovery as nanosized metal sulphides. Hydrometallurgy 163:40–48. https ://doi.org/10.1016/j.hydro met.2016.03.012

Anpilogova GR, Khisamutdinov RA, Golubyatnikova LG, Murinov YI (2016) Propiconazole and penconazole as effective extractants for selective recovery and concentration of platinum (IV) and palladium (II) from hydrochloric acid solutions formed in leaching of spent aluminoplatinum and aluminopalladium catalysts. Russ J Appl Chem 89:206–211. https ://doi.org/10.1134/S1070 427216020075

Arrisa R, Chayanoot S (2013) Response surface optimization of enzymatic hydrolysis of narrow-leaf cattail for bioethanol production. Energy Conserv Manag 73:381–388. https ://doi.org/10.1016/j.encon man.2013.05.035

Basudev S, Jinki J, Soo-kyoung K, Jae-chun L (2010) Separation of platinum and palladium from chloride solution by solvent extraction using Alamine 300. Hydrometallugy 104:1–7. https ://doi.org/10.1016/j.hydro met.2010.03.013

จุฬาลงกรณ์มหาวิทยาลัย
Chulalongkorn University

Behzad SB, Manouchehr V, Alemzadeh I (2012) Optimization of diluteacid pretreatment conditions for enhancement sugar recovery and enzymatic hydrolysis of wheat straw. Biosyst Eng 111:166–174. https ://doi.org/10.1016/j.biosy stems eng.2011.11.009

Bei L, Na G, Bangzhu P, Siyi P (2018) Kinetic and isotherm studies on the adsorption of tenuazonic acid from fruit juice using inactivated LAB. J Food Eng 224:45–52. https ://doi.org/10.1016/j.jfood eng.2017.12.027

Bina G, Indu S (2013) Extraction and separation of platinum, palladium and rhodium using Cyanex 923 and their recovery from real samples. Hydrometallurgy 134–135:11–18. https ://doi.org/10.1016/j.hydro met.2013.01.001

Bina S, Ranjan S, Subrahmanyam N (2006) Process intensification of copper extraction using emulsion liquid membranes: experimental search for optimal conditions. Hydrometallurgy 84(1–2):43–53. https ://doi.org/10.1016/j.hydro met.2006.04.002

Boukraa Y, Tayeb A, Benabdellah T, Kameche M (2009) Temperature effect on the solvent extraction of copper (II), cobalt (II) and nickel(II) with salicylideneaniline from sulphate media. J Phys Chem Liq 47(2):133–139. https ://doi.org/10.1080/00319100701594123

Chen YP, The-Hua T (2014) Solvent extraction of palladium (II) from acidic chloride solutions using tri-octyl/decyl ammonium chloride (Aliquat 336). Desal Water Treat 52:1101–1108. https ://doi.org/10.1080/19443 994.2013.826616

Chen H, Wu H (2010) Optimization of volatile fatty acid production with co-substrate of food wastes and dewatered excess sludge using response surface methodology.

จุฬาลงกรณ์มหาวิทยาลัย
Chulalongkorn University

Bioresour Technol 101:5487–5493. https ://doi.org/10.1016/j.biort ech.2010.02.013

Cieszynska A, Wisniewski M (2011) Selective extraction of palladium (II) from hydrochloric acid solutions with phosphonium extractants. Sep Purif Technol 80:385–389. https ://doi.org/10.1016/j.seppu r.2011.05.025

Cleide STA, Ione LSA, Hélen CR, Suzana MLOM, José JLL, Túlio NM (2018) Elucidation of mechanism involved in adsorption of Pb (II) onto lobeira fruit (Solanum lycocarpum) using Langmuir, Freundlich and Temkin isotherms. Microchem J 137:348–354. https ://doi.org/10.1016/j.micro c.2017.11.009

Darshak RB, Kalpana CM, Jigisha KP (2015) Highly efficient micellar extraction of toxic picric acid into novel ionic liquid: effect of parameters, solubilization isotherm, evaluation of thermodynamics and design parameters. J Hazard Mater 300:338–346. https ://doi.org/10.1016/j.jhazm at.2015.07.040

Dolapop S, Niti S, Prakorn R, Ura P, Suphot P (2015) Separation of Cd (II) from industrial wastewater via HFSLM: equilibrium, kinetic and thermodynamic investigation. J Ind Eng Chem 25:22–28. https ://doi.org/10.1016/j.jiec.2014.10.00

Gabriela JS, Sangamithra A, Chandrasekar V (2014) Response surface modeling and process optimization of aqueous extraction of natural pigments from Beta vulgaris using Box–Behnken design of experiments. Dyes Pigm 111:64–74. https ://doi.org/10.1016/j.dyepi g.2014.05.028

Giridhar P, Venkatesan KA, Srinivasan TG, Rao PRV (2006) Extraction of fission palladium by Aliquat 336 and electrochemical studies on direct recovery from ionic liquid phase. Hydrometallurgy 81:30–39. https ://doi.org/10.1016/j.hydro met.2005.10.001

จุฬาลงกรณ์มหาวิทยาลัย
Chulalongkorn University

González-Centeno MR, Comas-Serra F, Femenia A, Rosselló C, Simal S (2015) Effect of power ultrasound application on aqueous extraction of phenolic compounds and antioxidant capacity from grape pomace (Vitis vinifera L.): experimental kinetics and modeling. Ultrason Sonochem 22:506–514. https ://doi.org/10.1016/j.ultsonch.2014.05.027

Guoqiang X, Haochun Z, Quan Z, Yan J (2017) Predicting and analyzing interaction of the thermal cloaking performance through response surface method. Int J Heat Mass Transf 109:746–754. https ://doi.org/10.1016/j.ijheatmasstransfer.2017.02.056

Hitoshi W (1985) Effect of stirring on the ion-association extraction of copper and zinc 4,7-diphenyl-1,10-phenanthroline complexs. Talanta 32(8B):817–820. https ://doi.org/10.1016/0039-9140(85)80189 -2

Hong R, Ting L, Huijie W (2017) Optimization of extraction condition for phytic acid from peanut meal by response surface methodology. Resour Effic Technol 3(3):226–231. https ://doi.org/10.1016/j.reffi t.2017.06.002

Javanshir S, Abdollahy M, Abolghasemi H, Darban AK (2011) Kinetics of Au (III) extraction by DBC from hydrochloric solution using Lewis cell. Int J Miner Process 98:42–47. https ://doi.org/10.1016/j.minpr o.2010.10.002

Jonathan B (2012) Platinum 2012 interim review. Johnson Matthey Plc, Royston Jonathan C, María TC, Agustín F, Patricio ND, Ana MS (2014) Cu (II) extraction using quaternary ammonium and quaternary phosphonium based ionic liquid. Hydrometallurgy 141:89–96. https ://doi.org/10.1016/j.hydro met.2013.11.001

จุฬาลงกรณ์มหาวิทยาลัย
Chulalongkorn University

Khattab IS, Al-Saidan SM, Aly HN, Abdelazim AZ (2008) Using factorial design to improve the solubility and in vitro dissolution of nimesulide hydrophilic polymer binary systems. Drug Discov Ther 2(2):122–127

Kuixing D, Yunqing L, Jia T, Youchen Z, Xiaohui L, Jiugang H (2018) Efficiently enriching zinc(II) from and into ammonium chloride media with species regulation and Aliquat 336. Sep Purif Technol 190:100–107. https://doi.org/10.1016/j.seppur.2017.08.057

Li X, Wang Z, Liang H, Ning J, Li G, Zhou Z (2017) Chitosan modification persimmon tannin bioadsorbent for highly efficient removal of Pb (II) from aqueous environment: the adsorption equilibrium, kinetics and thermodynamics. Environ Technol. https://doi.org/10.1080/09593 330.2017.1380712

Liliana L, Adina IT, Irina V, Valentin IP (2016) Kinetic modeling of the ultrasound-assisted extraction of polyphenols from Picea abies bark. Ultrason Sonochem 32:191–197. https ://doi.org/10.1016/j.ultso nch.2016.03.009

Long W, Kit-lun Y, Sun-pui N, Joanne Y (2012) Application of the Box–Behnken design to the optimization of process parameters in foam cup molding. Exp Syst Appl 39:8059–8065. https ://doi.org/10.1016/j.eswa.2012.01.137

Lu P, de Zu Z (2009) Solvent extraction and separation of palladium (II) and platinum (IV) from hydrochloric acid medium with dibutyl sulfoxide. Miner Eng 22:1271–1276. https ://doi.org/10.1016/j.minen g.2009.07.006

María SP, Katherina F (2017) Modelling the hydrophilic extraction of the bark of Eucalyptus nitens and Eucalyptus globulus: adsorption isotherm and thermodynamic studies. Ind Crops Prod 109:558–569. https ://doi.org/10.1016/j.indcr op.2017.08.059

จุฬาลงกรณ์มหาวิทยาลัย
Chulalongkorn University

Maryam K, Hossein B, Mohammad AM (2017) A kinetic study on solvent extraction of copper from sulfate solution with Cupromex-3302 using Lewis cell. J Environ Chem Eng 5:3044–3050. https ://doi.org/10.1016/j.jece.2017.06.013

Mehdi A, Hamed T, Meisam TM, Ghaffar H, Alireza H (2014) Response surface methodology based on central composite design as a chemometric tool for optimization of dispersive-solidification liquid–liquid microextraction for speciation of inorganic arsenic in environmental water samples. Talanta 123:25–31. https://doi.org/10.1016/j.talan ta.2013.11.071

Mehmet KA, Kubilay T, Mehmet A, Selhan K (2015) Sage oil extraction and optimization by response surface methodology. Ind Crops Prod 76:829–835. https://doi.org/10.1016/j.indcr op.2015.08.005

Modise R, Godfred D, Nelson T (2012) Optimal synthesis of a Ni (II)-dimethylglyoxime ion-imprinted polymer for the enrichment of Ni (II) ions in water, soil and mine tailing samples. Water SA 38(2):261–268. https ://doi.org/10.4314/wsa.v38i2.12

Mohamed E, Fatima AT, Ragwan M, Khadija A (2015) Isotherm, kinetic and thermodynamic studies for the sorption of mercury (II) onto activated carbon from Rosmarinus officinalis leaves. AJAC 6:1–10. https ://doi.org/10.4236/ajac.2015.61001

Naglaa EEH (2007) Kinetics and mechanism of extraction and stripping of neodymium using a Lewis cell. Chem Eng Process 46:623–629. https ://doi.org/10.1016/j.cep.2006.08.007

Niti S, Suphot P, Prakorn R, Ura P (2018) Thermodynamic parameters and isotherm application on enantiomeric separation of levofloxacin using hollow fiber

จุฬาลงกรณ์มหาวิทยาลัย
Chulalongkorn University

supported liquid membrane system. Sep Purif Technol 195:377–387. https ://doi.org/10.1016/j.seppur.2017.12.034

Pan L, Bao X, Gu G (2013) Solvent extraction of palladium (II) and effective separation of palladium (II) and platinum (IV) with synthetic sulfoxide MSO. J Min Metall B Metall 49(1):57–63. https://doi.org/10.2298/jmmb1 20117 037p

Patricia JL (2012) Minerals yearbook—platinum-group metals. Science for a Changing World, 2013, pp 57.1–57.12

Peng X, Cheng-yan W, Sheng-ming X, Zhong-jun J (2013) Kinetics of cobalt (II) extraction from sulfate aqueous solution by sodium salt of di-decylphosphonic acid (DDPA). Trans Nonferrous Met Soc China 23:517–523. https ://doi.org/10.1016/S1003 -6326(13)62493-0

Phawinee N, Kittiwut K, Wanwisa S (2018) Isotherm and kinetic modeling on superparamagnetic nanoparticles adsorption of polysaccharide. J Environ Chem Eng 6:794–802. https ://doi.org/10.1016/j.jece.2017.12.063

Rajasimman M, Sangeetha R, Karthik P (2009) Statistical optimization of process parameters for the extraction of chromium (VI) from pharmaceutical wastewater by emulsion liquid membrane. Chem Eng J 150:275–279. https ://doi.org/10.1016/j.cej.2008.12.026

Ren H, Li T, Wan H (2017) Optimization of extraction condition for phytic acid from peanut meal by response surface methodology. Res Effic Technol 3:226–231. https ://doi.org/10.1016/j.reffit.2017.06.002

Robinson T, Brenda SB, Gretchen TL (2018) Effect of temperature on copper, iron and lead leaching from e-waste using citrate solutions. Waste Manag 71:420–425. https ://doi.org/10.1016/j.wasman.2017.10.029

จุฬาลงกรณ์มหาวิทยาลัย
CHULALONGKORN UNIVERSITY

Satit P, Korbratna K, Supawan T (2012) Extraction of palladium from acidic chloride media into emulsion liquid membranes using LIX 984N-C®. Int J Nonferrous Metall 1:13–22. https ://doi.org/10.4236/ijnm.2012.12003

Seader JD, Henley EJ, Roper DK (2005) Separation process principles: chemical and biochemical operation, 3rd edn. Wiley, New York

Shabani MA, Irannajad M, Azadmehr AR (2012) Investigation on leaching of malachite by citric acid. Int J Miner Metall Mater 19(9):782–786. https ://doi.org/10.1007/s1261 3-012-0628-9

Shen YF, Xue WY (2007) Recovery palladium, gold and platinum from hydrochloric acid solution using 2-hydroxy-4-sec-octanoyldiphenyl-ketoxime. Sep Purif Technol 56:278–283. https ://doi.org/10.1016/j.seppu r.2007.02.001

Stefan S, Jurgen A (2015) Potential of a hydrometallurgical recycling process for catalysts to cover the demand for critical metals, like PGMs and cerium. JOM 67:406–411. https ://doi.org/10.1007/s1183 7-014-1263-x

Stela J, Veliḉ Darko, Mate B, Ana BK, Mirela P, Sreḉko T (2010) Modelling of the process of solid-liquid extraction of total polyphenols from soybeans. Czech J Food Sci 28(3):206–212

Tan MC, Tan CP, Ho CW (2013) Effects of extraction solvent system, time and temperature on total phenolic content of henna (*Lawsonia inermis*) stems. Int Food Res J 20(6):3117–3123

Thanaporn W, Thidarat W, Prakorn R, Ura P, Soorathep K (2016) The synergistic extraction of uranium ions from monazite leach solution via HFSLM and its mass transfer. J Ind Eng Chem 33:246–254. https ://doi.org/10.1016/j.jiec.2015.10.006

จุฬาลงกรณ์มหาวิทยาลัย
CHULALONGKORN UNIVERSITY

Thi HN, Chong HS, Man SL (2016) Separation of Pt (IV), Pd (II), Rh (III) and Ir (IV) from concentrated hydrochloric acid solutions by solvent extraction. Hydrometallurgy 164:71–77. https ://doi.org/10.1016/j.hydro met.2016.05.014

Torab-Mostaedi M, Asadollahzadeh M, Hemmati A, Khosravi A (2013) Equilibrium kinetic and thermodynamic studies for biosorption of cadmium and nickel on grapefruit peel. J Taiwan Inst Chem Eng 44:295–302. https ://doi.org/10.1016/j.jtice .2012.11.001

Viet TN, Jae-chun L, Alexandre C, Min-seuk K, Jinki J, Gérard C (2016) Highly selective separation of individual platinum group metals (Pd, Pt, Rh) from acidic chloride media using phosphonium-based ionic liquid in aromatic diluent. RSC Adv 6:62717–62728. https ://doi.org/10.1039/C6RA0 9328K

Wei W, Chul-Woong C, Sok K, Myung-Hee S, Yeoung-Sang Y (2016) Selective recovery of Au (III), Pt (IV), and Pd (II) from aqueous solutions by liquid–liquid extraction using ionic liquid Aliquat-336. J Mol Liq 216:18–24. https ://doi.org/10.1016/j.molliq.2016.01.016

Wong KH, Li GQ, Li KM, Valentina RN, Chan K (2017) Optimisation of Pueraria isoflavonoids by response surface methodology using ultrasonic-assisted extraction. Food Chem 231(15):231–237. https://doi.org/10.1016/j.foodc hem.2017.03.068

Xueqin L, Tingzhou L, Zhiwei W, Xiangyu L, Mingyu W, Miao Y, Gaofeng C, Xiaofeng H, Haiyan X, Qian G, Zijie L (2018) Catalytic pyrolysis of corn straw with magnetic solid acid catalyst to prepare levulinic acid by response surface methodology. Ind Crops Prod 116:73–80. https ://doi.org/10.1016/j.indcr op.2018.02.049

จุฬาลงกรณ์มหาวิทยาลัย
Chulalongkorn University

Yu T, Chen W, Jing L, Yanzhao Y (2014) Extraction mechanism, behavior and stripping of Pd (II) by pyridinium-based ionic liquid from hydrochloric acid medium. Hydrometallurgy 147–148:164–169. https ://doi.org/10.1016/j.hydrometallurgy.2014.05.016

Yuxiang T, Wei L, Jiangling W, Yuanxin W, Xiangliang Y (2013) Two stage recovery of S-adenosylmethionine using supported liquid membranes with strip dispersion. Process Biochem 48:1980–1991. https ://doi.org/10.1016/j.procb io.2013.09.006

จุฬาลงกรณ์มหาวิทยาลัย
Chulalongkorn University

CHAPTER IV

Synergistic strippants of Pd (II) ions in the presence of chloride medium from wastewater of electroless plating process via solvating system: Kinetics and thermodynamics study

Vanee Mohdee[a], Kreangkrai Maneeintr[b], Suphot Phatanasri[a,*] and Ura Pancharoen[a,**]

[a]*Department of Chemical Engineering, Faculty of Engineering, Chulalongkorn University, Bangkok, Thailand*

[b]*Carbon Capture, Storage and Utilization Research Group, Department of Mining and Petroleum Engineering, Faculty of Engineering, Chulalongkorn University, Bangkok, Thailand*

จุฬาลงกรณ์มหาวิทยาลัย
CHULALONGKORN UNIVERSITY

This article has been published in Journal: Separation Science ans Technology.

Page: 2971–2982. Volume: 54 (17). Year: 2019.

4.1 Abstract

Synergistic strippants of palladium complex with Trialkylmethylammonium chloride (Aliquat 336) has been investigated. Results show that synergistic strippants of thiourea and HCl can enhance the palladium stripping efficiency from the loaded Aliquat 336. Extraction of Pd (II) ions is sensitive to the concentration of extractant and chloride medium. The partition coefficient ascertained from the model was fitted with an experimental value. Thermodynamics analysis showed that ΔH and ΔS values were obtained at 10.74 kJ/mol and 77.81 J/molK, respectively.

Keywords: Synergistic strippants; solvating system; Aliquat 336; Pd (II) separation; stripping kinetic

4.2 Introduction

Recently, global environmental issues have become serious problems that urgently need action. Trace organics (from both manufactured and natural compounds) and heavy metals generated from industrial manufacturing processes are recognized as environmental contaminants. The growing awareness of the effects of heavy metals has resulted in an increasing number of studies in order to investigate their impact in the environment such as an accumulation in soil and water. Thus, these heavy metal contaminants need to be treated and solved before being discharged into the environment.[1–6] Industrial wastewater is one of the most serious problems that must be put right. Heavy metals, e.g. Fe, Ni, and Cu, toxic metals, e.g. As,Hg, and Pb, as well as precious metals, e.g. Au, Pt, and Pd, that remain in the industrial wastewater cause harm to human beings and all other living beings. Owing to their unique properties, precious metals such as above have been widely used in industry.[7] Due to their limited resources and increasing use, these precious metals, which pollute industrial wastewater, have received much attention of late as secondary resources. The latter needs to be recovered and then recycled in order to save processing costs and to be

จุฬาลงกรณ์มหาวิทยาลัย
Chulalongkorn University

environmentally friendly.[8–11] There are several techniques which have been highlighted in the process of treating industrial wastewater. Conventional methods like solvent extraction (SX) or solvating extractants are widely used. They have become important techniques for application in hydrometallurgical recovery owing to their high efficiency of target species purification, simple operation, and good adaptability.[9,11–14] Previous researches on Pd (II) ions separation using SX are shown in **Table 4.1**.

Table 4.1 Summary of previous research on SX of Pd (II) ions.

Extractants	Strippants	Diluent	Metal	%Ex	%St	Ref.
Cyanex 923	$HCl+HClO_4$	Toluene	Pd	98.2%	N/A	[15]
TOA+Aliquat 336	HNO_3	Benzene	Pd	99%	99%	[16]
DDPB	NH_4SCN	Benzene	Pd	>98%	>96%	[17]
Dihexyl sulfide	-	Toluene	Pd	N/A	-	[18]
DMDOT DMA	CH_4N_2S	75%n-dodecane + 25 %n-octanol (%v/v)	Pd	>90%	N/A	[19]
di-TODGTA	Thiourea	Kerosene	Pd	99%	100%	[20]
Cyanex 471X	Thiosulfate	Kerosene	Pd	72%	75%	[21]

จุฬาลงกรณ์มหาวิทยาลัย
Chulalongkorn University

Many researchers have attempted to separate and purify Pd (II) ions using various extractants and strippants. They have also been involved in creating and improving novel extractants. Meanwhile, few studies have investigated the enhancement of stripping efficiency. Herein, the present work focuses on the enhancement of stripping efficiency of Pd (II) ions using synergistic strippants. Optimum conditions for Pd (II) ions recovery via solvating extractants are likewise investigated. Theoretical phenomena, such as thermodynamics and kinetics of Pd (II)

ions solvent extraction and stripping processes, are again emphasized. Moreover, a review of the literature shows that the following three extractants have not been used in real wastewater samples before, namely, Aliquat 336, TBP, and D2EHPA.[22] Therefore, this study has employed the above three extractants to recover Pd (II) ions from real samples of wastewater.

4.3 Experimental

4.3.1 Reagents and solutions

Feed solution was supplied by Mektec manufacturing CO., Ltd., Thailand. All materials were of analytical reagent grade and were used as received without any further purification. Sources and %purity of materials used are listed in **Table 4.2**.

Table 4.2 Sources and %purity of materials used.

Material name	Source	%Purity
Aliquat 336	Acros Organics (USA)	90.6
Cyclohexane	Lobal Chemie (India)	99.5
D2EHPA	Cognis (USA)	99.8
Hydrochloric acid	Merck (Singapore)	37.0
Nitric acid	Merck (Singapore)	99.8
Sulfuric acid	Merck (Singapore)	95-97
TBP	Cytec (Canada)	99.8
Thiourea	QReC (New Zealand)	AR Grade

จุฬาลงกรณ์มหาวิทยาลัย
Chulalongkorn University

4.3.2 Procedure

The hydrometallurgical process includes two steps. The first step is the extraction reaction and the second step is the stripping reaction.[22]

Step 1: Extraction rxn.

Target metal ions in the aqueous phase contacts with the selective extractant dissolved in solvent (organic phase) and forms a complex species between the target metal ions and selective extractant by solvation system.

Step 2: Stripping rxn.

The complex species of target metal ions (organic phase) react with the strippant solution (aqueous phase) and release aqueous target metal ions into the solution.

The two solutions (aqueous phase and organic phase) with a ratio 1:1 (v/v) were shaken at 600 rpm at ambient condition. After the phase separation, stripping reaction was performed which followed the same procedure as the extraction step. The concentrations of Pd (II) ions in the sampling solutions were analyzed by an Inductively Coupled Plasma Spectrometry (Carry 5000, Aligent, Santa Clara, CA, USA).

4.3.3 Thermodynamics study

In this study, thermodynamics phenomena for the extraction of Pd (II) using Aliquat 336 as an extractant can be investigated via the following equation[23]:

$$\Delta G = -RT\ lnK_{ex} \tag{4.1}$$

where R is gas constant, T is temperature, and K_{ex} is the equilibrium constant.

Regard to Gibbs–Helmholtz Equation:

$$\Delta G^0 = \Delta H^0 - T\Delta S^0 \quad (4.2)$$

At equilibrium, ΔG^o was calculated based on the relation with K_{ex} as shown in Eq. (4.1). Thus, Gibbs–Helmholtz Equation above in Eq. (2), replaces Eq. (1). Then, an equation was derived as shown in Eq. (4.3)[24–28]:

$$\ln K_{ex} = -\frac{\Delta H^0}{RT} + \frac{\Delta S^0}{R} \quad (4.3)$$

4.3.4 Kinetics study

A solvating system of Pd (II) ions extraction using 6%(v/v) of Aliquat 336 dissolved in cyclohexane was carried out to determine the extraction order as a function of time (t) from 5 to 60 min at 600 rpm, at ambient condition. According to graphical methods, with regard to concentration of reactant, the graph that is most linear shows the order of the reaction in that reactant. Experimental results were expressed by plotting the concentration of the reactant as a function of time (t). Zero order, first order, and second order were employed to test the extraction rate data. The differential rate law is depicted as follows:

จุฬาลงกรณ์มหาวิทยาลัย
Chulalongkorn University

Zero order:

$$\frac{-d[A]}{dt} = k \quad (4.4)$$

First order:

$$\frac{-d[A]}{dt} = k[A] \quad (4.5)$$

Second order:

$$\frac{-d[A]}{dt} = k[A]^2 \tag{4.6}$$

4.4 Results and discussion

4.4.1 Influence of types of solvating extractant

In this research, Aliquat 336, D2EHPA, and TBP were used as extractants. Results show that Aliquat 336 yielded the highest extraction of Pd (II) owing to its partially decreased interfacial tension.[29,30] The extractability of palladium ions followed: Aliquat 336 > D2EHPA > TBP as shown in **Fig. 4.1**. In chloride medium, Pd (II) has four chlorocomplexes species: $[PdCl]^+$, $[PdCl_2]$, $[PdCl_3]^-$, and $[PdCl_4]^{2-}$. The predominant species is $[PdCl_4]^{2-}$.[31–35] The stability constant of each species was presented in **Table 4.3**.[35] Meanwhile, TBP can extract $[PdCl_3]^-$[36] giving the lowest extraction efficiency in this study. Therefore, Aliquat 336 was selected in order to study other variable factors. The extraction mechanism using Aliquat 336 is shown below [32,37–39]:

จุฬาลงกรณ์มหาวิทยาลัย
CHULALONGKORN UNIVERSITY

$$\overline{2R_3N^+CH_3Cl^-} + PdCl_4^{2-} \longrightarrow \overline{2R_3NCH_3PdCl_4} + 2Cl^- \tag{4.7}$$

The equilibrium constant of Pd (II) ions extraction using Aliquat 336 can be expressed as shown in Eq. (4.8):

$$K_{ex} = \frac{[R_3NCH_3PdCl_4]^2[Cl^-]^2}{[R_3N^+CH_3Cl^-]^2[PdCl_4^{2-}]} \tag{4.8}$$

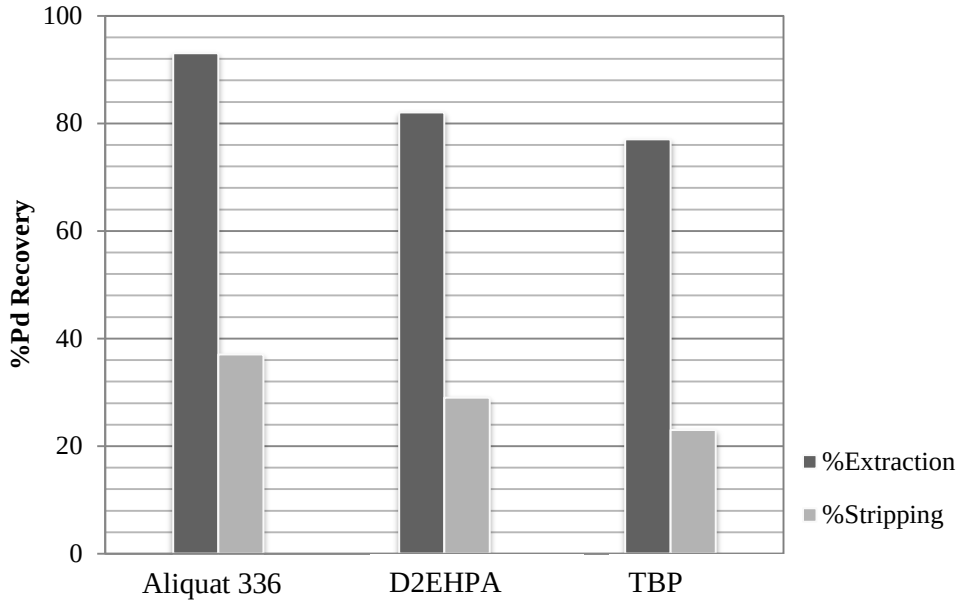

Figure 4.1. Influence of extractants on Pd (II) ions solvating system using 2%v/v of extractant.

Table 4.3 Palladium chlorocomplexes's stability constant.

Chlorocomplex form	Stability constant (β)
$PdCl^+$	$10^{4.5}$
$PdCl_2$	$10^{7.8}$
$PdCl_3^-$	$10^{10.2}$
$PdCl_4^{2-}$	$10^{11.5}$

จุฬาลงกรณ์มหาวิทยาลัย
Chulalongkorn University

4.4.2 Influence of Aliquat 336 concentration

The concentration of an extractant has a huge impact on the efficiency of target metal ions extraction. Moreover, in the study of theoretical phenomena, the concentration of extractant is one of the most significant factors which have an effect on the extraction process. In this study, Aliquat 336 was chosen to investigate the

extraction of Pd (II) ions from real wastewater samples in the concentration range 2–10% (v/v). Results show that as the concentration of Aliquat 336 increased, extraction efficiency increased up to 99% at 6% (v/v) as illustrated in **Fig. 4.2**. Thus, when concentration of Aliquat 336 was increased further from 6% (v/v) to 10% (v/v), extraction efficiency reached almost to the maximum. It can be seen that the percentages of extraction are slightly the same.[11]

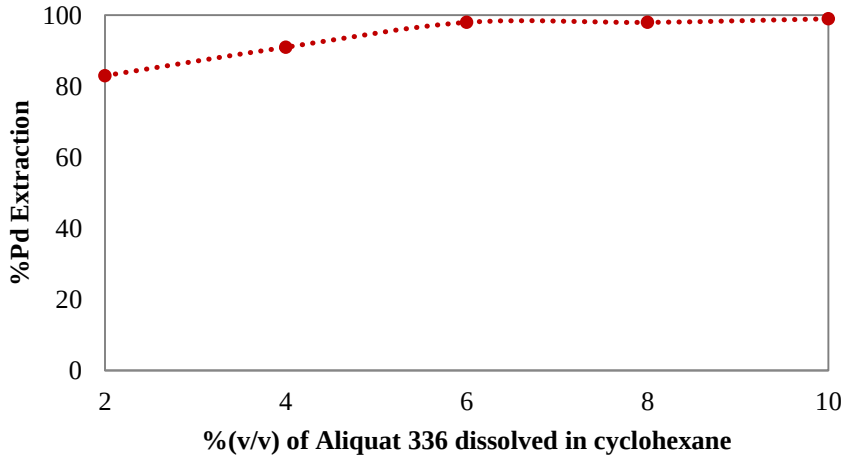

Figure 4.2. Influence of concentration of Aliquat 336 on Pd (II) ions solvating system.

จุฬาลงกรณ์มหาวิทยาลัย
CHULALONGKORN UNIVERSITY

4.4.3 Influence of HCl concentration

Chloride medium provides the most effective operating medium for the separation of platinum group metals.[40] In this work, in order to investigate the impact of HCl concentration on Pd (II) ions solvating system, the concentration of HCl varied from 1 to 8 M. Herein, the concentration of Aliquat 336 was fixed at 6% (v/v). **Figure 4.3** shows that the extraction of Pd (II) using Aliquat 336 dissolved in cyclohexane strongly depends on the concentration of chloride medium. Thus, as the concentration of chloride medium increased from 4 to 8 M, due to the solvating system of Pd (II)

ions and Aliquat 336, extraction of Pd (II) decreased sharply.[41,42] In the presence of excess chloride medium condition, a backward reaction occurred as illustrated in Eq. (4.9).[32]

$$PdCl_4^{2-}{}_{(aq)} + 2R_3N^+CH_3Cl^-{}_{(org)} \longleftrightarrow [(R_3NCH_3)_2(PdCl_4)_2]_{(org)} + 2Cl^-{}_{(aq)} \quad (4.9)$$

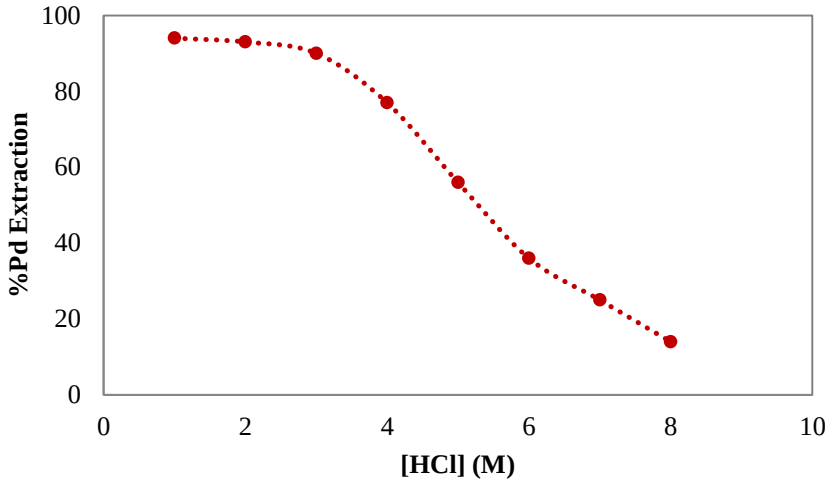

จุฬาลงกรณ์มหาวิทยาลัย
Chulalongkorn University

Figure 4.3. Influence of chloride medium concentration on Pd (II) ions extracted via solvating system.

4.4.4 Influence of types of strippants

Various types of strippants were used to investigate the stripping efficiency of Pd (II) via the solvating system from the Pd (II)-loaded Aliquat 336. Stripping percentages of Pd (II) ions from the loaded Aliquat 336 with various strippants are shown below in **Table 4.4**.

Table 4.4. Stripping efficiency of Pd (II) ions solvating system using various strippants.

Strippants	%Stripping
2 M HCl	24.57
2 M HNO_3	37.81
2 M H_2SO_4	10.23
0.5 M Thiourea	58.90

Results show that 0.5 M thiourea yielded the maximum stripping percentage compared with other strippants (HCl, HNO_3, and H_2SO_4). It can be seen that the stripping of Pd (II) using HCl, HNO_3, and H_2SO_4 from the loaded Aliquat 336 was very low. Likewise, previous works exhibited the low efficiency of Pd (II) stripping from the loaded organic phase using these acid solutions.[37] It has been reported that solutions containing thiourea could quantitatively strip Pd (II) from the loaded organic phase. The results obtained in this study were in agreement with previous research.[41,43] Stripping mechanisms using thiourea are shown below[11]:

จุฬาลงกรณ์มหาวิทยาลัย
CHULALONGKORN UNIVERSITY

$$2R_3NCH_3PdCl_4^{2-} + 2(NH_2)CS \longrightarrow PdCl_2 2(NH_2)CS + 2R_3N^+CH_3Cl^- \quad (4.10)$$

The equilibrium constant for stripping of Pd (II) ions (K_{st}) from the loaded Aliquat 336 using thiourea can be written as shown in Eq. (4.11):

$$K_{st} = \frac{[PdCl_2 \cdot 2(NH_2)CS][R_3N^+CH_3Cl^-]^2}{[R_3NCH_3PdCl_4^{2-}]^2[(NH_2)CS]^2} \quad (4.11)$$

Due to the low stripping efficiency of Pd (II) ions using the single stripping solution, synergistic strippants were carried out to evaluate the stripping efficiency of Pd (II) ions as shown in **Fig. 4.4** and **Table 4.5**. Synergistic solution is a mixture of two solutions to enhance the separating efficiency of separation processes, instead of using a single solution. Generally, synergistic solution is proposed to improve the efficiency as well as selectivity of the processes of separation. The synergistic coefficient (R) is defined as follows [43–46]:

$$R = \frac{D_{AB}}{D_A + D_B}$$

where D_{AB} denoted the distribution ratio of Pd (II) by the mixture of A and B. D_A and D_B denoted the distribution ratio of Pd (II) by the single A and B, respectively.

In the case of thiourea and HCl solution as illustrated in **Table 4.4**, it is found that the stripping of Pd (II) from the loaded organic phase was very low. Meanwhile, the synergistic solution between thiourea mixed with HCl yielded a higher percentage of Pd (II) stripping than when thiourea and HCl were used singly.[47] Results show that synergistic strippants of 0.5 M of thiourea mixed with 0.1 M of HCl were most effective in the stripping of Pd (II) ions[47,48] from the loaded Aliquat 336 reaching 86.27%. As the ratio of HCl concentration increased from 0.1 to 0.3 M, the stripping percentage of Pd (II) ions using synergistic solution decreased. This is owing to the increase in concentration of HCl in the synergistic solution; the activity of thiourea during the stripping of Pd (II) decreased.[43,49] Thus, the stripping mechanism of Pd (II) using the synergistic solution can be described based on a coordination–substitution reaction between thiourea and Cl^-.[32] For synergistic strippants of thiourea mixed with HNO_3 and H_2SO_4, it is noted that when the concentration of an acid in solution increased, stripping percentage increased. In **Table 4.5**, the synergistic coefficient (R)

is shown. The value of R > 1 indicated the occurrence of synergism, whereas the value of R < 1 shows antagonism.

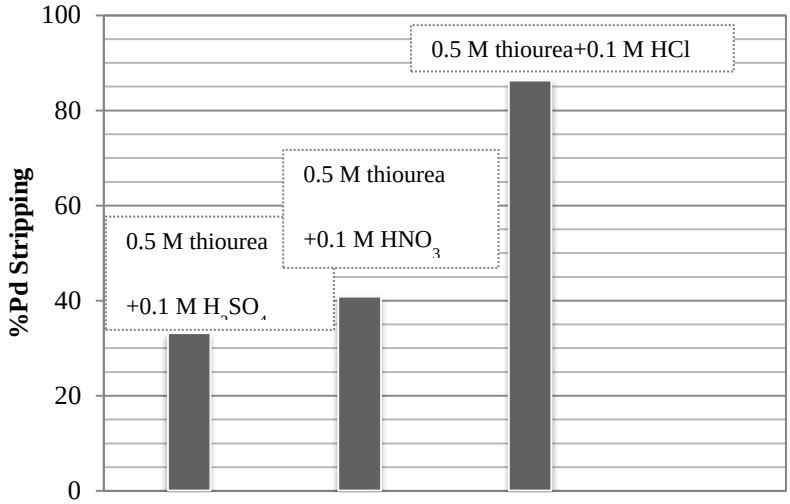

Figure 4.4. Influence of synergistic strippants on Pd (II) ions solvating system.

Table 4.5. Stripping efficiency of Pd (II) ions solvating system using various synergistic strippants.

Strippants	Concentration ratio(M)	%Stripping	R
Thiourea+HCl	0.5:0.1	86.27	10.62
	0.5:0.2	66.37	3.13
	0.5:0.3	50.86	1.68
Thiourea+HNO_3	0.5:0.1	40.81	0.86
	0.5:0.2	45.20	1.00
	0.5:0.3	49.58	1.16
Thiourea+H_2SO_4	0.5:0.1	33.11	1.59
	0.5:0.2	37.05	1.91
	0.5:0.3	42.90	2.41

4.4.5 Thermodynamics study on Pd (II) ions solvating system

As illustrated in **Fig. 4.5**, results indicate that when temperature is increased, percentage extraction and stripping of Pd (II) ions increased. This is due to an increase in solubility and diffusion coefficients and a decrease in solvent viscosity, as well as an enhanced of mass transfer via the solvating system.[50–52] Le Châtelier's principle states that a change in temperature is a stress on the process at the equilibrium. Thus, an equilibrium shift can occur enabling the development of a faster process. An increase in temperature during separation processes can enhance the rate of reaction, especially the rate of the endothermic reaction.[53]

As shown in **Fig. 4.6**, the thermodynamics parameters ($\Delta G°$, $\Delta H°$, and $\Delta S°$) can be calculated from the plot between ln K_{ex} and $1/T$. As shown in **Table 4.6**, the value of Gibbs free energy (ΔG) of Pd (II) ions extraction was calculated. The positive value of the enthalpy change (ΔH) obtained at 10.74 kJ/mol indicated that the extraction process was endothermic and the positive entropy change (ΔS) obtained at 77.81 J/molK indicated an increase in the disorder of the process.

จุฬาลงกรณ์มหาวิทยาลัย
Chulalongkorn University

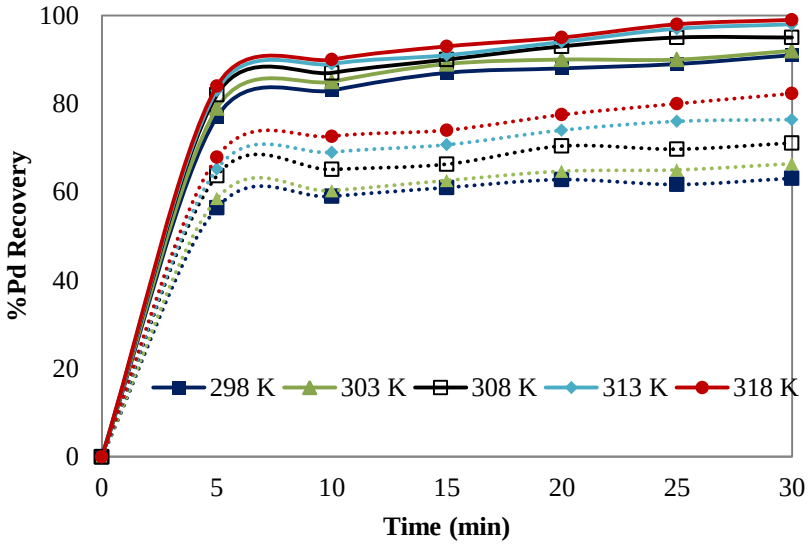

Figure 4.5. Influence of reaction temperature on Pd (II) ions solvating system. (Solid line: %Pd extraction and dash line: %Pd stripping).

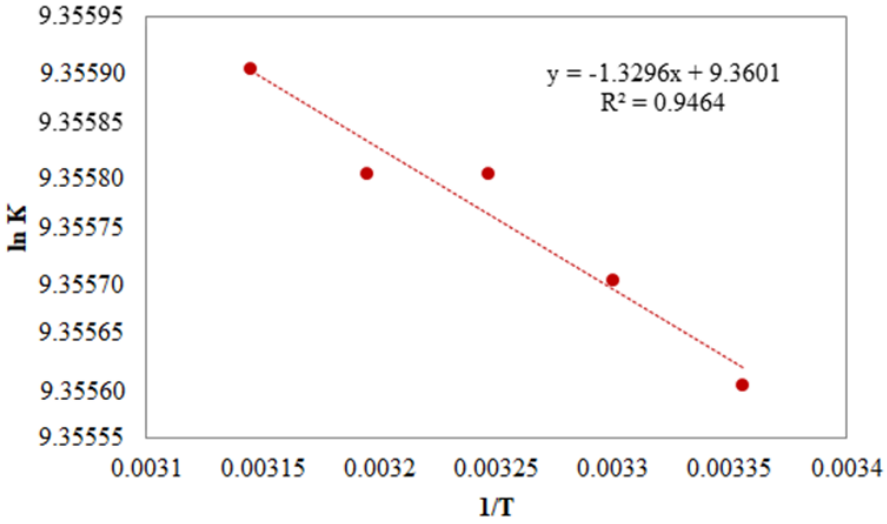

Figure 4.6. Plot of ln K_{eq} versus 1/T.

Table 4.6. Thermodynamic data for the Pd-Aliquat 336 system.

T (K)	Δ*G* (kJ/mol)
298	-23.18
303	-23.57
308	-23.96
313	-24.34
318	-24.73

4.4.6 Kinetics study on Pd (II) ions solvating system

An investigation of kinetics phenomena on Pd (II) ions solvating system is shown in **Table 4.7**. Results show that first-order equation provided a good fit with the experimental data for Pd (II) extraction using Aliquat 336 dissolved in cyclohexane as shown in **Fig. 4.7(a)**. In **Fig. 4.7(b)**, as regard the kinetics of the stripping of Pd (II) using synergistic solutions, a pseudo-first-order equation provided a good fit with the data. The reaction rate indicated that concentration of one reactant was controlled and assumed to be the concentration of thiourea. The values of reaction rate constants for Pd (II) extraction and stripping in this study were found to be -0.0473 s^{-1} and 0.0488 min^{-1}, respectively. These values, as stated, can verify that the stripping reaction rate was the determining step in the Pd (II) separation process.

จุฬาลงกรณ์มหาวิทยาลัย
CHULALONGKORN UNIVERSITY

Table 4.7. The reaction rate order of Pd (II) ions solvating system.

Reaction order	Equations	R^2
0	$C_{A0} - C_A$ VS Time	0.7963
1	$ln(C_{A0}/C_A)$ VS Time	0.9938
2	$(1/C_A)-(1/C_{A0})$ VS Time	0.7421

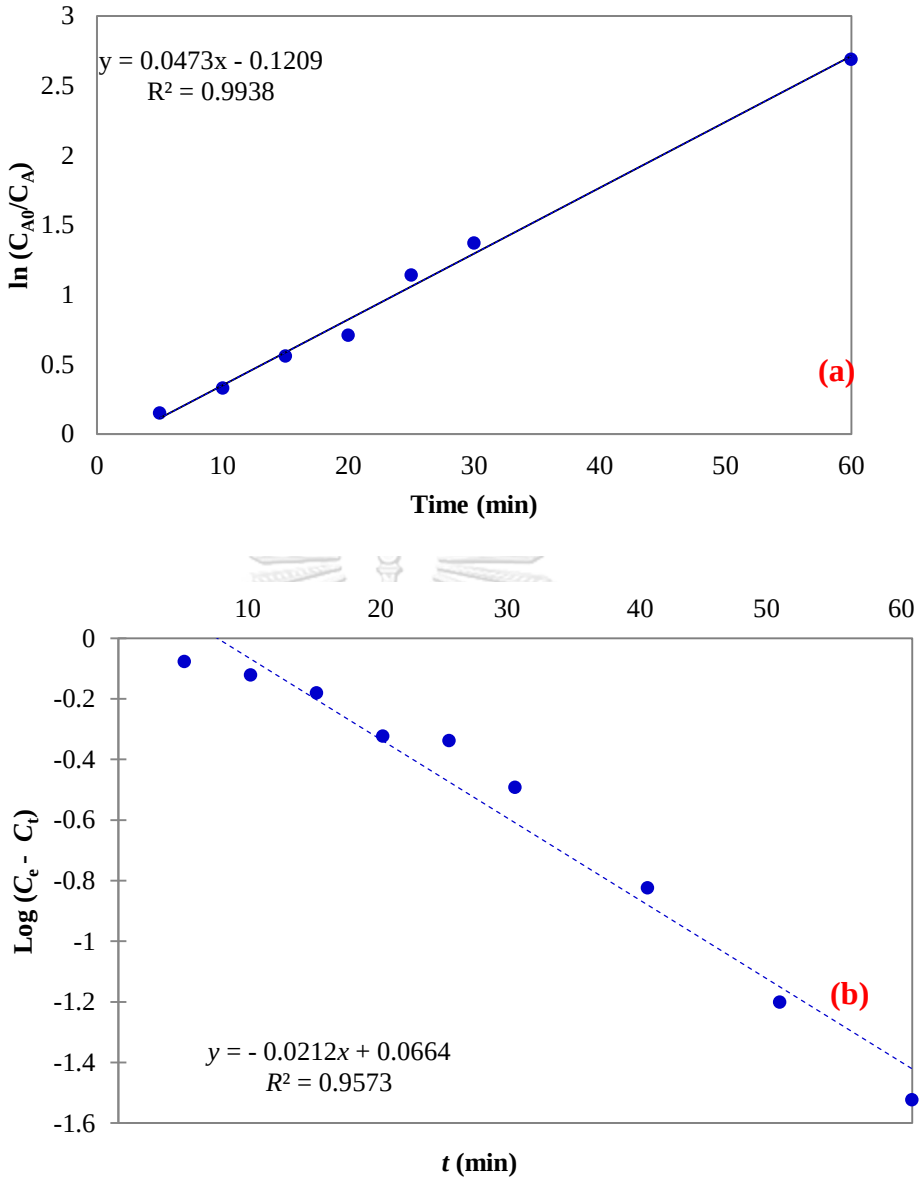

Figure 4.7. Graphical plot of kinetics study on Pd (II) ions solvating system (a) Pd (II) extraction reaction and (b) Pd (II) stripping reaction.

4.4.7 Mechanism and model

The mechanism of the organic phase of Pd (II) ions from the loaded Aliquat 336 ($2R_3NCH_3PdCl_4^{2-}$) and the aqueous phase of synergistic strippants solution of

thiourea mixed with hydrochloric acid occurred at the interface between the two-phase systems (**Fig. 4.8**).

Firstly, the protonated HCl reacts with the amide group (NH_2) in thiourea. Thereafter, ammoniumyl (NH_3^+) as an intermediate are formed (**Fig. 4.9**).[54]

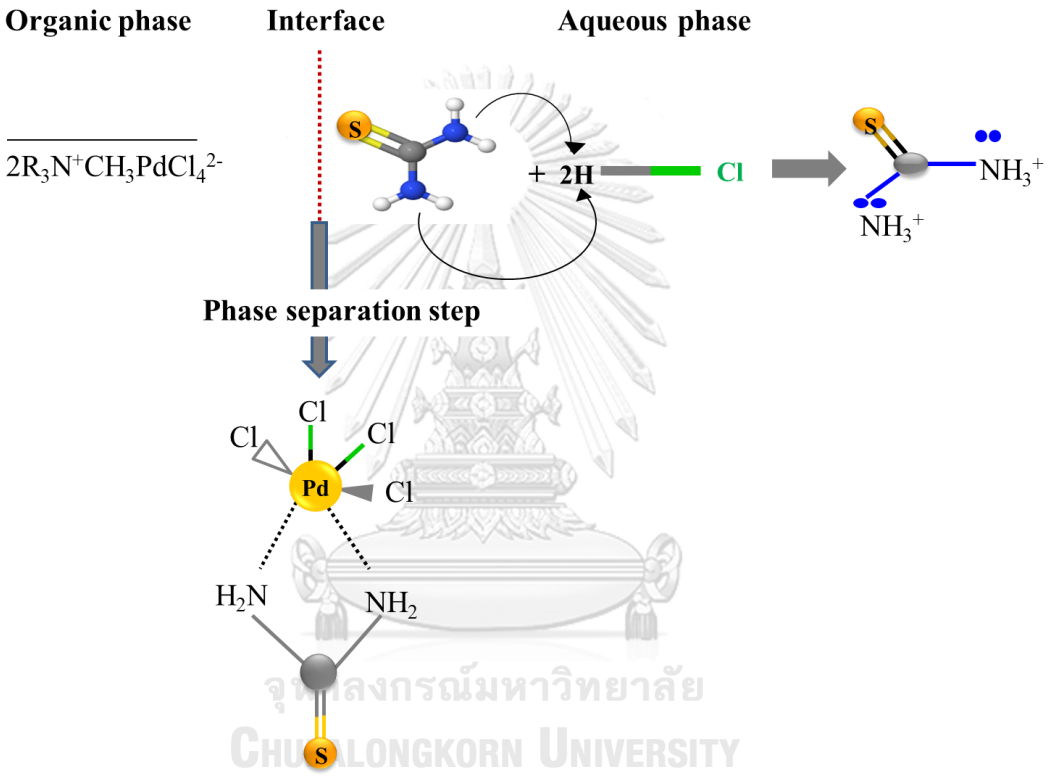

จุฬาลงกรณ์มหาวิทยาลัย
CHULALONGKORN UNIVERSITY

Figure 4.8. Mechanism of Pd (II) ions stripping in an aqueous/organic two-phase system.

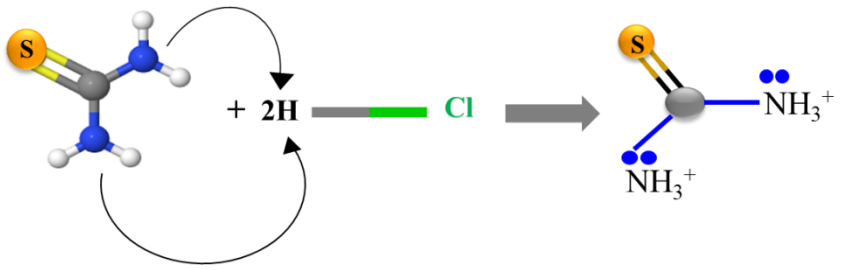

Figure 4.9. Mechanism of synergistic strippants solution, thiourea + HCl.

Thus, ammonia ions acts like a strong Lewis base due to their strong tendency to donate a lone pair nitrogen electron to a deficient species.[55] Then, protonated thiourea ($CS(NH_3^+)_2$) reacts with Pd-loaded Aliquat 336 ($2R_3NCH_3PdCl_4^{2-}$). Consequently, $PdCl_4(NH_2)_2CS$ is released into the solution.[55]

Aqueous phase

$$HCl \longleftrightarrow H^+ + Cl^- \tag{4.12}$$

The dissociation constant of HCl is demonstrated as in Eq.(4.13):

$$K_a = \frac{[H^+][Cl^-]}{[HCl]} \tag{4.13}$$

The mechanism of synergistic strippants of thiourea mixed with HCl is shown below:

$$(NH_2)_2CS + 2HCl \underset{K'_1}{\overset{K_1}{\rightleftharpoons}} (NH_3^+)_2CS + 2Cl^- \tag{4.14}$$

The reaction rate constant of thiourea mixed with HCl is shown in Eq. (4.15):

$$K_1 = \frac{[(NH_3^+)_2CS][Cl^-]^2}{[(NH_2)_2CS][HCl]^2} \tag{4.15}$$

Interface

The reaction between the aqueous/organic two-phase systems is shown as follows:

$$2Cl^- + 2R_3NCH_3PdCl_4^{2-} + (NH_3^+)_2CS \underset{K'_I}{\overset{K_I}{\rightleftharpoons}} PdCl_4(NH_2)_2CS + 2R_3N^+CH_3Cl^- \quad (4.16)$$

The reaction rate constant at the interface can be described as follows:

$$K_I = \frac{[PdCl_4(NH_2)_2CS][R_3N^+CH_3Cl^-]^2}{[R_3NCH_3PdCl_4^{2-}]^2\left[(NH_3^+)_2CS\right][Cl^-]^2} \quad (4.17)$$

Thus, the intermediate $CS(NH_3^+)_2$ formed in this step is very small and very difficult to quantify. Then, the intermediate $CS(NH_3^+)_2$ reacts with the palladiumchlorocomplex at the interface between the two phase systems. The physical partition coefficient of Pd (II) is defined below as in Eq. (4.18):

$$P_0 = \frac{[PdCl_4(NH_2)_2CS]_{aq}}{[R_3NCH_3PdCl_4^{2-}]^2_{org}} \quad (4.18)$$

The apparent physical partition coefficient (P_{app}) can be simplified according to Eq.(4.19) below[39]:

$$P_{app} = (1 - \frac{1}{1+ 10^{pH-pK_a}}) \cdot P_0 \quad (4.19)$$

An influence of pH on calculated Papp is shown in **Fig. 4.10**. As can be seen, the experimental value was fitted with the P_{app} model. It is evident that Pd (II) ions extraction efficiency increased when pH of feed solution increased, attaining amaximumvalue at pH 2.0. However, when pH of feed solution increased further, Pd (II) ions extraction efficiency sharply decreased.[56] Results indicate that pH of feed solution plays an important role on Pd (II) ions recovery via the solvating system. This

จุฬาลงกรณ์มหาวิทยาลัย CHULALONGKORN UNIVERSITY

is due to the increase or decrease in the pH condition which results in the diversity of Pd (II) ions yielded.

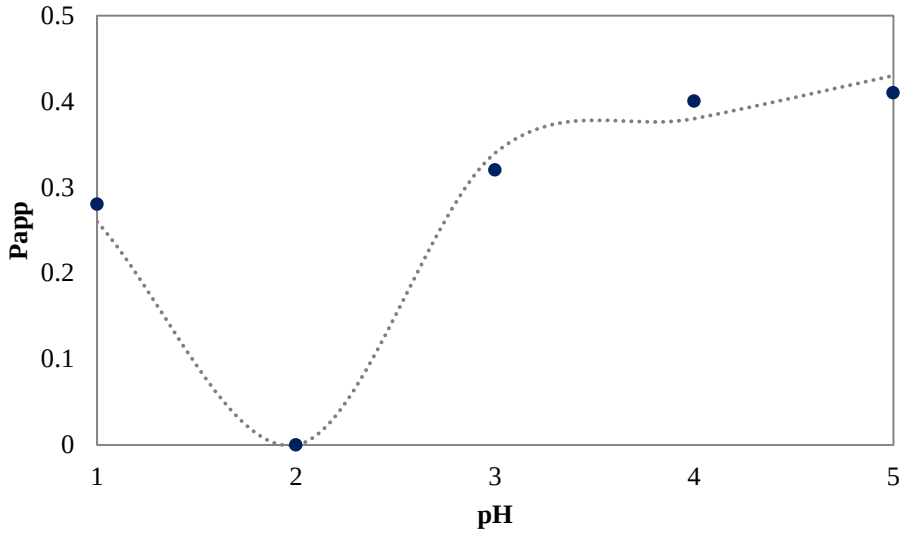

Figure 4.10. Influence of pH on P_{app}. (Symbols: experimental value and line: calculated value.).

The distribution coefficient (K_D), defined as the ratio of the concentrations of the compound in the organic phase to the concentrations of the compound in the aqueous phase at equilibrium, is as shown in Eq. (4.20):

$$K_D = \frac{[Pd\ (II)]_{org}}{[Pd(II)]_{aq}} \tag{4.20}$$

The influence of reaction temperature on the distribution of Pd (II) ions in an aqueous/organic two-phase system was investigated in the range of (298–318) K. Results are shown in **Fig. 4.11**. Thus, it was found that when reaction temperature

increased, distribution ratio also increased. The linear plot between ln D and $1/T$ indicated a good correlation coefficient ($R^2 = 0.9861$).

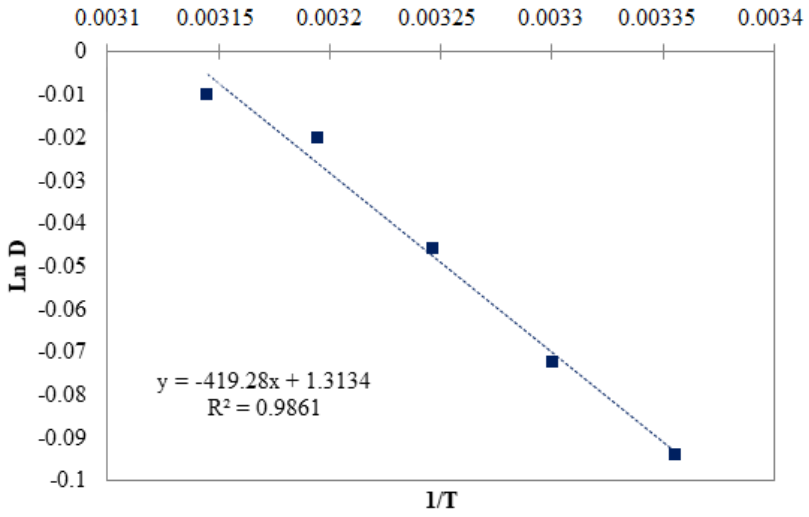

Figure 4.11. Influence of reaction temperature on Pd (II) ions distribution ratio.

4.5 Conclusion

Aliquat 336 both as an extractant and concentration of chloride medium plays an important role as regard the Pd (II) ions solvating system. By increasing the chloride medium from 4 to 8 M, extraction of Pd (II) decreased sharply in extraction efficiency. The thermodynamics parameters indicated that the extraction process was endothermic and the process was in disorder. The kinetics study showed the solvating system to be of first-order reaction. Synergistic strippants enhanced the stripping efficiency of Pd (II) ions up to 86.27%. At optimum condition, 6%(v/v) of Aliquat 336 dissolved in cyclohexane, 0.1 M of chloride medium, synergistic strippants of 0.5 M thiourea, and 0.1 HCl with a stirring speed 600 rpm at ambient condition, extraction efficiency of Pd (II) reached 99%. The partition coefficient ascertained from the model

was fitted with an experimental value. Finally, results showed that when reaction temperature increased, the distribution ratio also increased.

4.6 Acknowledgments

Thanks are also given to the Separation Laboratory, Department of Chemical Engineering, Faculty of Engineering, Chulalongkorn University, for chemical and apparatus support, as well as to the Mektec Manufacturing Corporation (Thailand) Ltd, for feed solution.

4.7 Funding

The authors profoundly appreciate the support from the Thailand Research Fund and Chulalongkorn University under the Research and Researchers for Industries (RRi) PhD Program (Grant No. PHD58I0081).

4.8 References

[1] Ho, Y.C.; Show, K.Y.; Guo, X.X.; Norli, I.; Abbas, F.M.A.; Morad, N. (2012) Industrial discharge and their effect to the environment. Show, K.-Y., editor. Industrial waste, InTech. doi:10.5772/38830

[2] Naidoo, S.; Olaniran, A.O. (2014) Treated wastewater effluent as a source of microbial pollution of surface water resources. International Journal of Environmental Research and Public Health, 11 (1): 249–270. doi:10.3390/ijerph110909256

[3] Focazio, M.J.; Kolpin, D.W.; Barnes, K.K.; Furlong, E.T.; Meyer, M.T.; Zaugg, S.D.; Barber, L.B.; Thurman, M.E. (2008) A national reconnaissance for pharmaceuticals and other organic wastewater contaminants in the United States — II) untreated drinking water sources. Science of the Total Environment, 402 (2–3): 201–216. doi:10.1016/j.scitotenv.2008.02.021

จุฬาลงกรณ์มหาวิทยาลัย
Chulalongkorn University

[4] Kelepertzis, E.;. (2014) Investigating the sources and potential health risks of environmental contaminants in the soils and drinking waters from the rural clusters in Thiva area (Greece). Ecotoxicology and Environmental Safety, 100: 258–265. doi:10.1016/j.ecoenv.2013.09.030

[5] Lapworth, D.J.; Baran, N.; Stuart, M.E.; Ward, R.S. (2012) Emerging organic contaminants in groundwater: a review of sources, fate and occurrence. Environmental Pollution, 163: 287–303. doi:10.1016/j.envpol.2011.12.034

[6] Oostdam, J.V.; Gilman, A.; Dewailly, E.; Usher, P.; Wheatley, B.; Kuhnlein, H.; Neve, S.; Walker, J.; Tracy, B.; Feeley, M.; Jerome, V.; Kwavnick, B. (1999) Human health implications of environmental contaminants in Arctic Canada: a review. Science of the Total Environment, 230 (1–3): 1–82. doi:10.1016/S0048-9697(99)00036-4

[7] Matthey, J.;. (2017) Precious Metals Management, Johnson Matthey's technology review. Johnson Matthey Plc: Royston, UK.

[8] Butler, J.;. (2012) Platinum 2012 Interim Review, Johnson Matthey's technology review. Johnson Matthey Plc: Royston, UK.

จุฬาลงกรณ์มหาวิทยาลัย
Chulalongkorn University

[9] Assunção, A.; Matos, A.; Costa, A.M.R.; Candeias, A.; Costa, M.C. (2016) A bridge between liquid–liquid extraction and the use of bacterial communities for palladium and platinum recovery as nanosized metal sulphides. Hydrometallurgy, 163: 40–48. doi:10.1016/j.hydromet.2016.03.012

[10] Castillo, J.; Coll, M.T.; Fortuny, A.; Donoso, P.N.; Sepúlveda, R.; Sastre, A.M. (2014) Cu (II) extraction using quaternary ammonium and quaternary phosphonium based ionic liquid. Hydrometallurgy, 141: 89–96. doi:10.1016/j.hydromet.2013.11.001

[11] Wei, W.; Cho, C.W.; Kim, S.; Song, M.H.; Bediako, J.K.; Yun, Y.S. (2016) Selective recovery of Au (III), Pt (IV), and Pd (II) from aqueous solutions by liquid–liquid extraction using ionic liquid Aliquat-336. Journal of Molecular Liquids, 216: 18–24. doi:10.1016/j.molliq.2016.01.016

[12] Anpilogova, G.R.; Khisamutdinov, R.A.; Golubyatnikova, L.G.; Murinov, Y.I. (2016) Propiconazole and penconazole as effective extractants for selective recovery and concentration of platinum (IV) and palladium (II) from hydrochloric acid solutions formed in leaching of spent aluminoplatinum and aluminopalladium. Catalysts Russian Russian Journal of Applied Chemistry, 89: 206–211. doi:10.1134/S1070427216020075

[13] Kumar, V.; Sahu, S.K.; Pandey, B.D. (2010) Prospects for solvent extraction processes in the Indian context for the recovery of base metals. A review. Hydrometallurgy, 103: 45–53. doi:10.1016/j.hydromet.2010.02.016

[14] Rotuska, K.; Chmielewski, T. (2008) Growing role of solvent extraction in copper ores processing. Physicochemical Problems of Mineral Processing, 42: 29–36.

[15] Devendra, V.C.; Purushottam, M.D. (2003) Extraction and separation of platinum (IV), and palladium (II) with cyanex 923 in chloride media – a possible recovery from spent autocatalysts. Journal of Scientific and Industrial Research, 62: 834–837.

[16] Mezhov, E.A.; Druzhenkov, V.V.; Sirotinin, A.N. (2002) Study of extraction of palladium from nitric acid solutions with nitrogen-containing compounds, as applied to recovery of fission palladium from spent nuclear fuel of nuclear power plants: 3. optimization of extraction process for palladium recovery and refining. Radiochemistry, 44: 146–150.

จุฬาลงกรณ์มหาวิทยาลัย
Chulalongkorn University

[17] Liu, Y.; Huang, Z.; Li, J.; Chen, J. (2016) Solvent extraction of palladium (II) from alkaline cyanide solution by the dodecyl dimethyl-2-phenoxyethyl ammonium bromide. Journal of the Chilean Chemical Society, 61(2): 2864–2869. doi:10.4067/S0717-97072016000200004

[18] Yoshinari, B.; Toshiya, E.; Katsutoshi, I. (1986) Sovent extraction of palladium with dihexyl sulfide. Journal of Chemical Engineering of Japan, 19: 361–366. doi:10.1252/jcej.19.361

[19] Mowafy, E.A.; Mohamed, D. (2017) Recovery of palladium from concentrated nitrate solutions with N,N 2-dimethyl-N,N 2-dioctyltetradecy Imaionamide as new extractant. Oriental Journal of Chemistry, 33 (5): 2377–2385. doi:10.13005/ojc/330530

[20] Huang,H.;Chao,H.; Songdong,D.;Ning, L.;Dongping, S.; Tianhao, L. (2015) Extraction of palladium (II) from nitric acid solutions with diglycothioamide. Hydrometallurgy, 156: 6–11. doi:10.1016/j.hydromet.2015.05.002

[21] Ahmed, I.M.; Nayl, A.A.; Daoud, J.A. (2011) Extraction of palladium from nitrate solution by Cyanex 471X. International Journal of Mineral Processing, 101: 89–93. doi:10.1016/j.minpro.2011.07.009

[22] Paiva, A.P.;. (2017) Recycling of palladium from spent catalysts using solvent extraction-some critical points. Metals, 7 (11): 505. doi:10.3390/met7110505

[23] Westland, A.D.; Out, E.O. (1991) The thermodynamics of extraction of some lanthanide and other ions by 2-ethylhexylhydrogen-p-phenylphosphonate. Solvent Extraction and Ion Exchange, 9: 607–621. doi:10.1080/07366299108918073

[24] Greiner, W.; Neise, L.; Stöcker, H. (1995) Thermodynamics and Statistical Mechanics, Springer-Verlag: Berlin and Heidelberg.

จุฬาลงกรณ์มหาวิทยาลัย
Chulalongkorn University

[25] Ramakul, P.; Yanachawakul, Y.; Leepipatpiboon, N.; Sunsandee, N. (2012) Biosorption of palladium(II) and platinum(IV) from aqueous solution using tannin from Indian almond (Terminalia catappa L.) leaf biomass: kinetic and equilibrium studies. Chemical Engineering Journal, 193–194: 102–111. doi:10.1016/j.cej.2012.04.035

[26] Aksu, Z.;. (2002) Determination of the equilibrium, kinetic and thermodynamic parameters of the batch biosorption of nickel (II) ions onto Chlorella vulgaris. Pharmacology Biochemistry, 38 (1): 89–99. doi:10.1016/S0032-9592(02)00051-1

[27] Handayani, A.D.; Indraswati, N.; Ismadji, S. (2008) Extraction of astaxanthin from giant tiger (Panaeus monodon) shrimp waste using palm oil: studies of extraction kinetics and thermodynamic. Biotechnology,99 (10): 4414–4419. doi:10.1016/j.biortech.2007.08.028

[28] Ajmal, M.; Rao, R.A.K.; Ahmad, R.; Ahmad, J. (2000) Adsorption studies on Citrus reticulata (fruit peel of orange): removal and recovery of Ni(II) from electroplating wastewater. Journal of Hazardous Materials, B79: 117–131. doi:10.1016/S0304-3894(00)00234-X

[29] Oliveira, B.D.; Bertazzoli, R. (2007) On the role of the surfactant Aliquat 336 on the kinetics of oxygen reduction and on the rate of hydrogen peroxide electrosynthesis. Journal of Electroanalytical Chemistry, 611: 126–132. doi:10.1016/j.jelechem.2007.08.010

[30] Yu, Y.J.; Su, G.Y.; Lam, M.H.W.; Lam, P.K.S.; Yu, H.X. (2009) Cloud point extraction of bisphenol A from water utilizing cationic surfactant aliquat 336. Chinese Journal of Analytical Chemistry, 37: 1717–1721. doi:10.1016/S1872-2040(08)60148-6

จุฬาลงกรณ์มหาวิทยาลัย
Chulalongkorn University

[31] Nguyen, V.T.; Lee, J.C.; Chagnes, A.; Kim, M.S.; Jeong, J.; Cote, G. (2016) Highly selective separation of individual platinum group metals (Pd, Pt, Rh) from acidic chloride media using phosphonium-based ionic liquid in aromatic diluent. RSC Advances, 6: 62717–62728. doi:10.1039/C6RA09328K

[32] Nguyen, T.H.; Sonu, C.H.; Lee, M.S. (2015) Separation of platinum (IV) and palladium (II) from concentrated hydrochloric acid solutions by mixtures of amines with neutral extractants. Journal of Industrial and Engineering Chemistry, 32: 238–245. doi:10.1016/j.jiec.2015.08.022

[33] Bernardis, F.L.; Grant, R.A.; Sherrington, D.C. (2005) A review of methods of separation of the platinum-group metals through their chloro-complexes. Reactive and Functional Polymers, 65: 205–217. doi:10.1016/j.reactfunctpolym.2005.05.011

[34] Nikoloski,A.N.;Ang,K.L. (2014) Review of the application of ion exchange resins for the recovery of platinum-group metals from hydrochloric acid solution. Mineral Processing and Extractive Metallurgy Review, 35: 369–389. doi:10.1080/08827508.2013.764875

[35] Cieszynska, A.; Wieczorek, D. (2018) Extraction and separation of palladium (II), platinum (IV), gold (III) and rhodium (III) using piperidine-based extractants. Hydrometallurgy, 175: 359–366. doi:10.1016/j.hydromet.2017.12.019

[36] Sadeghi, N.; Alamdari, E.K. (2015) Solvent extraction of palladium from chloride media by TBP. MCET —2018 IEEE International Multidisciplinary Conference on Engineering Technology, 623–626.

[37] Truong, H.T.; Lee, M.S. (2018) Separation of Pd (II) and Pt (IV) from hydrochloric acid solutions by solvent extraction with Cyanex 301 and LIX 63. Minerals Engineering, 115: 13–20. doi:10.1016/j.mineng.2017.10.001

จุฬาลงกรณ์มหาวิทยาลัย
Chulalongkorn University

[38] Al-Bazi, S.J.; Chow, A. (1984) Platinum metals-solution chemistry and separation methods (ion-exchange and solvent extraction). Talanta, 31: 815–836. doi:10.1016/0039-9140(84)80204-0

[39] Zhang, P.; Wang, S.; Xu, W.; Tang, K. (2017) Modeling multiple chemical equilibrium in single-stage extraction of Atenolol enantiomers with tartrate and boric acid as chiral selector. Journal of Chemical & Engineering Data, 62 (12): 4344–4355. doi:10.1021/acs.jced.7b00698

[40] Charlesworth, P. (1981) Separating the platinum group metals by liquid-liquid extraction. Platinum Metals Review, 25 (3): 106–112.

[41] Nguyen, T.H.; Sonu, C.H.; Lee, M.S. (2016) Separation of Pt (IV), Pd (II), Rh (III) and Ir (IV) from concentrated hydrochloric acid solutions by solvent extraction. Hydrometallurgy, 164: 71–77. doi:10.1016/j.hydromet.2016.05.014

[42] El-Hefny, N.E.; Daoud, J.A. (2013) Solvent extraction of palladium (II) from aqueous chloride medium by triphenylphosphine, triphenylphosphine oxide or triphenylphosphine sulphide in Benzene. Journal of Physical Science, 24 (2): 35–47.

จุฬาลงกรณ์มหาวิทยาลัย
CHULALONGKORN UNIVERSITY

[43] Truong, H.T.; Lee, M.S.; Son, S.H. (2017) Extraction of palladium (II) from hydrochloric acid solutions by solvent extraction with mixtures containing either cyanex 301 or LIX 63. Metals, 7: 541. doi:10.3390/met7120541

[44] Kuang, S.; Zhang, Z.; Li, Y.; Wei, H.; Liao, W. (2017) Synergistic extraction and separation of rare earths from chloride medium by the mixture of HEHAPP and D2EHPA. Hydrometallurgy, 174: 78–83. doi:10.1016/j.hydromet.2017.09.011

[45] Zhao, Z.; Lyu, H.; Guo, X.; Dong, Y.; Wang, Y.; Sun, X. (2017) The synergistic extraction by combined ammonium and phosphonium type ionic liquids for rare

earth elements separation. Hydrometallurgy, 174: 234–247. doi:10.1016/j.hydromet.2017.05.020

[46] Rahman, H.A.; Jusoh, N.; Othman, N.; Rosly, M.B.; Sulaiman, R.N.R.; Noah, N.F.M. (2019) Green formulation for synthetic dye extraction using synergistic mixture of acid-base extractant. Separation and Purification Technology, 209: 293–300. doi:10.1016/j.seppur.2018.07.053

[47] Swain, B.; Jeong, J.; Kim, S.K.; Lee, J.C. (2010) Separation of platinum and palladium from chloride solution by solvent extraction using Alamine 300. Hydrometallurgy, 104: 1–7. doi:10.1016/j.hydromet.2010.03.013

[48] Peng, C.Y.; Tsai, T.H. (2014) Solvent extraction of palladium (II) from acidic chloride solutions using trioctyl/decyl ammonium chloride (Aliquat 336). Desalination and Water Treatment, 52: 1101–1121. doi:10.1080/19443994.2013.826616

[49] Paiva, A.P.; Carvalho, G.I.; Costa, M.C.; Costa, A.M.R.; Nogueira, C. (2014) Recovery of platinum and palladium from chloride solutions by a thiodiglycolamide derivative. Solar Extract Ion Exchange, 32: 78–94. doi:10.1080/07366299.2013.810969

[50] Torres, R.; Bailón, B.S.; Lapidus, G.T. (2018) Effect of temperature on copper, iron and lead leaching from e-waste using citrate solutions. Waste Management, 71: 420–425. doi:10.1016/j.wasman.2017.10.029

[51] Tan, M.C.; Tan, C.P.; Wai, H.C. (2013) Effects of extraction solvent system, time and temperature on total phenolic content of henna (Lawsonia inermis) stems. International Food Research Journal, 20 (6): 3117–3123.

จุฬาลงกรณ์มหาวิทยาลัย
Chulalongkorn University

[52] Boukraa, Y.; Tayeb, A.; Benabdellah, T.; Kameche, M. (2009) Temperature effect on the solvent extraction of copper (II), cobalt (II) and nickel (II) with salicylideneaniline from sulphate media. J. Physics and Chemistry of Liquids, 47 (2): 133–139. doi:10.1080/00319100701594123

[53] Kay, J.J. (2000) Application of the second law of thermodynamics and Le Chatelier's principle to the developing ecosystem. Muller, F., editor. Handbook of Ecosystem Theories and Management; CRC Press-Lewis Publishers: New York, NY, pp. 135–160.

[54] Cyganowski, P.; Leśniewicz, A.; Polowczyk, I.; Chęcmanowski, J.; Koźlecki, T.; Pohl, P.; Bartkowiak, D.J. (2018) Surface-activated anion exchange resins for synthesis and immobilization of gold and palladium nano- and microstructures. Reactive and Functional Polymers, 124: 90–103. doi:10.1016/j.reactfunctpolym.2018.01.013

[55] Gandhi, M.R.; Yamada, M.; Kondo, Y.; Shibayama, A.; Hamada, F. (2016) Rapid and selective extraction of Pd (II) ions using the SCS type pincer ligand 1,3-bis(dimethylthiocarbamoyloxy)benzene, and its Pd (II) extraction mechanism. RSC Advances, 6: 1243–1252. doi:10.1039/C5RA23146A

[56] Shen, Y.F.; Xue,W.Y. (2007) Recovery palladium, gold and platinum from hydrochloric acid solution using 2-hydroxy-4-sec-octanoyl diphenyl-ketoxime. Separation and Purification Technology, 56: 278–283. doi:10.1016/j.seppur.2007.02.001

CHAPTER V

Solubility modelling and solvent effect on solid-liquid equilibrium of 2,2-bis(hydroxymethyl)butyric acid at different temperatures

Vanee Mohdee[a,b], Katarína Fulajtárová[b], Tomáš Soták[b], Suphot Phatanasri[a], Milan Hronec[b,c,*], Ura Pancharoen[a,**]

[a]*Department of Chemical Engineering, Faculty of Engineering, Chulalongkorn University, Bangkok 10330, Thailand*

[b]*Department of Organic Technology, Faculty of Chemical and Food Technology, Slovak University of Technology in Bratislava, Radlinského 9, 81237 Bratislava, Slovak Republic*

[c] VUP a.s., Prievidza, Slovak Republic

จุฬาลงกรณ์มหาวิทยาลัย
Chulalongkorn University

This article has been published in Journal: Journal of Molecular Liquids. 312 (2020) 113370. Year: 2020. DOI: https://doi.org/10.1016/j.molliq.2020.113370

5.1 Graphical abstract

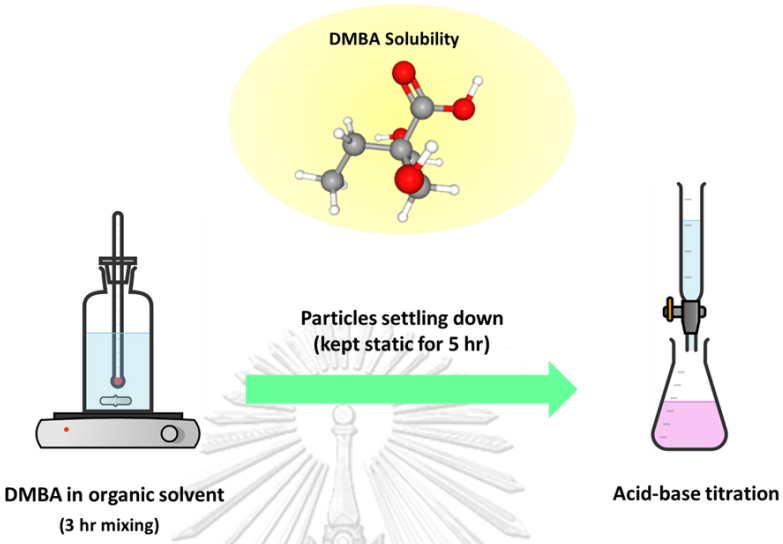

5.2 Abstract

In this work, the solid-liquid equilibrium of 2,2-bis(hydroxymethyl)butyric acid (DMBA) was investigated experimentally in various solvents: namely, ethylacetate, butylacetate, methyl isobutyl ketone, cyclopentyl methyl ether, toluene, gamma-butyrolactone and 1,4-dioxane over the temperature range (298.15 to 353.15) K. The experimental solubility data were correlated with the Apelblat equation, Buchowski–Książczak λh equation and NRTL model. Results showed that the mole fraction solubility of DMBA increased, as temperature increased. The Apelblat equation and NRTL model indicated a good correlation with the experimental solubility data and can be used to describe the solid-liquid equilibrium. Further, the apparent thermodynamic dissolution functions and thermodynamic functions of mixing were evaluated from the solubility data.

จุฬาลงกรณ์มหาวิทยาลัย
Chulalongkorn University

Keywords: 2,2-Bis(hydroxymethyl)butyric acid**;** Dimethylolbutyric acid**;** Solubility**;** Solid-liquid equilibrium**;** Apelblat model**;** λh model**;** NRTL model

5.3 Introduction

2,2-Bis(hydroxymethyl)butyric acid, otherwise known as dimethylolbutyric acid (DMBA), is a consequential building block and has good crosslinking in the polymer industry. DMBA consists of carboxylic acid and two hydroxyl groups which are well-known, as desirable functional groups in the polymeric industry. In **Fig. 5.1**, its structure is given [1]. DMBA has been used commercially in diverse areas such as elastomers, coatings, adhesives, thermoplastics, thermosets and foams [2–4]. In addition, DMBA is considered to be a new kind of environment-friendly substitute for 2,2-bis(hydroxymethyl)propionic acid (DMPA).

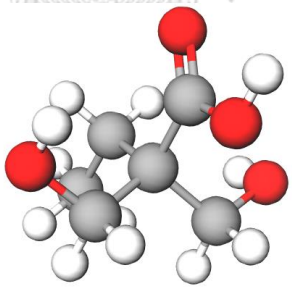

Fig. 5.1. The chemical structure of 2,2-Bis(hydroxymethyl)butyric acid.[1]

Crystallization is one of the most important methods in the process of separation and purification of a solid compound from solution. The equilibrium conditions for crystallization are controlled, based on thermodynamics principles. Thus, its solubility data is necessary [5]. The solubility of solid in liquid is an important physicochemical property in order to understand the solid-liquid equilibrium of a crystallization process. Moreover, the measurement of solubility data is a crucial

parameter for designing and scaling up in industrial applications [6,7]. Especially in the coatings industry, solubility data have shown their greatest use regarding the solvents selected [8]. A suitable solvent is essential in order to yield adequate solubility [9]. Thermodynamics modelling of experimental solubility data were applied to describe mathematical aspects of solubility as well as to reduce the time consumption of the experiment [8].

As yet, the solubility of DMBA in different solvents has not been studied. In consideration of the above, the solubility data of DMBA were measured using various solvents: viz. ethylacetate, butylacetate, methyl isobutyl ketone, cyclopentyl methyl ether, toluene, gamma-butyrolactone and 1,4-dioxane, in the temperature range (298.15 to 353.15) K. The Apelblat equation, Buchowski–Książczak λh equation and NRTL model were applied to correlate the solubility data of DMBA. Models were verified by comparing the calculated solubility data with the experimental solubility data. Further, the values of the apparent thermodynamic parameters were calculated from the experimental solubility data using the Van't Hoff equation. The thermodynamic properties of DMBA were calculated based on the NRTL model.

จุฬาลงกรณ์มหาวิทยาลัย
Chulalongkorn University

5.4 Solubility modelling

In this work, the Apelblat, Buchowski–Książczak and NRTL models are manipulated to describe the experimental solubility data, as shown below.

5.4.1 The Apelblat equation

The Apelblat equation has been widely used to describe the solid solubility in liquid, as a function of temperature. This model is suitable for polar and nonpolar system. The Apelblat equation is expressed, as shown in Eq.(5.1): [10,11]

$$\ln x = A + \frac{B}{T} + C\ln(T) \tag{5.1}$$

where x is the mole fraction solubility of solute in solvent, T is the absolute temperature and A, B and C are the empirical parameters.

5.4.2 Buchowski–Książczak λh equation

The λh equation was originally proposed by Buchowski. It is widely employed to describe solubility behavior and the correlation between solubility as well as activity, as a function of temperature. Two parameters in this equation (λ and h) provide adjustability in fitting experimental solubility data for many systems. The parameter λ is related to the non-ideality of solution, which is considered as the association number of solute molecules in the system, and h is related to excess enthalpy of solution. The Buchowski–Książczak λh equation is shown below [12]:

$$\ln\left[1 + \frac{\lambda(1-x)}{x}\right] = \lambda h\left(\frac{1}{T} - \frac{1}{T_m}\right) \tag{5.2}$$

จุฬาลงกรณ์มหาวิทยาลัย
Chulalongkorn University

where λ and h are the empirical parameters, T_m is the melting temperature of solute and x is the mole fraction of a solute compound in a solvent.

5.4.3 NRTL model

The NRTL model has been widely used in order to evaluate the activity coefficient of solute in the solution based on the local composition concept. The equation can be written as follows: [12]

$$ln\gamma_1 = x_2^2\left[\frac{\tau_{21}G_{21}^2}{(x_1+G_{21}x_2)^2} + \frac{\tau_{12}G_{12}^2}{(x_2+G_{12}x_1)^2}\right] \quad (5.3)$$

where G_{12}, G_{21}, τ_{12}, τ_{21} are parameters of this model which can be expressed as:

$$G_{ij} = \exp(-\alpha_{ij}\tau_{ij}) \quad (5.4)$$

$$\tau_{ij} = (g_{ij} - g_{jj})/RT \quad (5.5)$$

where i, j = 1 and 2, g_{12} and g_{21} are equation parameters which refer to cross interaction energies. α_{ij} is the solution nonrandomness and was considered to be 0.47 [13].

When the solid-liquid equilibrium system is achieved, the fugacity of the component in liquid state and solid state is equal and can be expressed as follows: [14]

จุฬาลงกรณ์มหาวิทยาลัย
Chulalongkorn University

$$f_i^L(T, P, x^L) = f_i^S(T, P) \quad (5.6)$$

Thus, NRTL model can be described, as shown in Eq.(5.7):

$$ln\ x_i = \frac{\Delta_{fus}H}{R}\left(\frac{1}{T_m} - \frac{1}{T}\right) - ln\ \gamma_i \quad (5.7)$$

where $\Delta_{fus}H$ is the fusion enthalpy of DMBA, T_m is the melting point of DMBA and γ_i is the activity coefficient of the component i in the saturated solution.

5.4.4 The apparent thermodynamic parameters for DMBA dissolution

In order to understand the dissolution process of DMBA in selected solvents, an investigation in terms of dissolution enthalpy ($\Delta_{sol}H$) and dissolution entropy

($\Delta_{sol}S$) was carried out. The dissolution process which is a pseudo chemical reaction of solid (S) in liquid (L) can be written as: S+L = SL. The equation of the dissolution equilibrium constants can be expressed in terms of activities of solid in liquid, as shown in Eq.(5.8): [15-16]

$$K_{\mathrm{i}} = \frac{a_i}{a_S a_L} \tag{5.8}$$

where a_i is the activity of DMBA in the solution and as and a_L are the activities of pure solid and pure liquid, respectively.

At standard states, the values of a_s and a_L are considered to be constant. Therefore, the dissolution equilibrium constants can be written as in Eq. (5.9):

$$K_i = \frac{\gamma_i x_i}{a_S a_L} \tag{5.9}$$

where, γ_i is the activity coefficient of DMBA (i) in the solution and x_i is the mole fraction solubility of DMBA (i) in the solvent.

จุฬาลงกรณ์มหาวิทยาลัย
Chulalongkorn University

At a certain temperature range, the activity coefficient is considered as an invariable. Thus, by taking the logarithm of Eq.(5.7) and with regards to an inferential process for the Apelblat equation, Eq.(5.10) is given: [17]

$$\ln K_i = \ln x_i + J \tag{5.10}$$

where J is a temperature-independent constant and equal to $\ln\gamma_i - \ln a_s a_L$.

According to Gibbs-Helmholtz equation together with the modified Van't Hoff equation, the equation for calculating the molar enthalpies of dissolution is as shown in Eq.(5.11):

$$\Delta_{\mathrm{sol}}H = -R\frac{\mathrm{d}\ln K_{\mathrm{i}}}{\mathrm{d}T^{-1}} \tag{5.11}$$

By substituting the differential of Eq.(5.10) into Eq.(5.11), the molar enthalpies of dissolution equation are as follows:

$$\Delta_{\mathrm{sol}}H = -R\frac{\mathrm{d}\ln x_{\mathrm{i}}}{\mathrm{d}T^{-1}} \tag{5.12}$$

The parameters *A, B* and *C* from the Apelblat equation were employed to determine the values of $\Delta_{sol}H$ and $\Delta_{sol}S$ by substituting into Eq.(10). The equations for $\Delta_{sol}H$ and $\Delta_{sol}S$ are written accordingly, as in Eqs. (5.13)-(5.14):

$$\Delta_{\mathrm{sol}}H = RT(C - \frac{B}{T}) \tag{5.13}$$

$$\Delta_{sol}S = R(C - \frac{B}{T}) \tag{5.14}$$

จุฬาลงกรณ์มหาวิทยาลัย
CHULALONGKORN UNIVERSITY

5.5 Experimental

5.5.1 Materials

2,2-Bis(hydroxymethyl)butyric acid was supplied by VUP a.s., Slovakia. Ethylacetate, Butylacetate and Cyclopentyl methyl ether (CPME) were purchased from Sigma-Aldrich. Methyl isobutyl ketone (MIBK) was obtained from Mikrochem®. Toluene and 1,4-dioxane were received from centralchem®. Gamma-butyrolactone

(GBL) was purchased from Acros organics. All chemicals are of analytical grade and used without further purification. In **Table 5.1** and **5.2**, the detailed description of DMBA and the solvents are presented. Information as regards materials used was provided by the supplier.

Table 5.1 Detailed information on DMBA.

Properties*	
Molecular formula	$C_6H_{12}O_4$
Molar mass ($g \cdot mol^{-1}$)	148.15
Melting point (K)	382.15-385.15
Boiling point (K)	633.15 (at 760 mmHg)
Acid value (mg KOH/g)	374
Hydroxyl value (mg KOH/g)	743
Form	white crystalline powder
CAS No.	10097-02-6
Purity	99%
Source	VUP a.s., Slovak republic

*Properties and purity are as stated by supplier (VUP a.s., Slovak republic)

จุฬาลงกรณ์มหาวิทยาลัย
Chulalongkorn University

Table 5.2 Detailed information on the solvents.*

Chemicals	Molecular formula	Molar mass ($g \cdot mol^{-1}$)	Density (g·mL)	Boiling point (K)	CAS No.	Mass fraction purity	Analytical method	Source
Ethylacetate	$C_4H_8O_2$	88.11	0.90	350.15	141-78-6	≥0.999	GC	Sigma-Aldrich
Butylacetate	$C_6H_{12}O_2$	116.16	0.88	398.15	123-86-4	≥0.990	GC	Sigma-Aldrich
Toluene	C_7H_8	92.14	0.86	383.75	108-88-3	0.990	HPLC	Centralchem®
MIBK	$C_6H_{12}O$	100.16	0.80	390.15	108-10-1	0.995	GC	Mikrochem®
CPME	$C_6H_{12}O$	100.16	0.86	379.15	5614-37-9	≥0.999	GC	Sigma-Aldrich
1,4-dioxane	$C_4H_8O_2$	88.11	1.03	374.25	123-91-1	0.990	GC	Centralchem®
GBL	$C_4H_6O_2$	86.09	1.12	477.15	96-48-0	0.990	GC	Acros organics

*The physical properties data are from chemical bottle labels.

GC = Gas chromatography

HPLC = High Performance Liquid Chromatography

Note: MIBK, CPME and GBL are methyl isobutyl ketone, cyclopentyl methyl ether and gamma-butyrolactone, respectively.

5.5.2 Characterization of DMBA

The properties of the DMBA solid samples were characterized by differential scanning calorimetry (DSC) and high-performance liquid chromatography (HPLC) techniques. DSC (Perkin Elmer) was performed in order to investigate the thermal behaviour and the crystallization and polymorphic state of the solid sample. The stability and purity of DMBA after solubility determination was analysed by HPLC (Shimadzu). The conditions of HPLC were as follows viz. column: C18 (5 μm, 250 mm), column temperature: 45 ºC, mobile phase: acetonitrile: water (1:1 by vol.), flow rate: 0.8 ml/min and detector: PDA.

5.5.3 Measurement of DMBA solubility

The solubility of DMBA in various solvents was measured over the temperature range (298.15 to 353.15) K under atmospheric pressure, using a solid-liquid equilibrium method [18]. Firstly, an excess amount of DMBA was added to a capped glass vial containing 5 g of pure solvent. The mixture was shaken continuously using a mechanical shaker. Subsequently, the system was kept static to allow the suspended particles to settle down. In order to optimize the optimal time of the solubility measurement, preliminary studies were performed every 1, 2, 3, 4, and 5 hr. for mixing and 3, 4, 5, 6 and 24 hr. for the phase settling down. Results showed that after 3 hr. of mixing and 5 hr. of the phase settling down, changes were found to be negligible. Therefore, in this work, 3 hr. of mixing and 5 hr. of the phase settling down were selected. In order to determine the amount of DMBA solubility in the solution,

จุฬาลงกรณ์มหาวิทยาลัย
Chulalongkorn University

acid-base titration was carried out. To eliminate the solidification of the acid after cooling the sample inside the syringe, a ca. 1 ml of solution was withdrawn using a syringe where ca. 0.5 ml of methanol was present. After weighing the amount of the sample inside the syringe, it was quantitatively transferred into ca. 20 ml of methanol. Titration of the formed homogeneous solution with 0.1 M methanolic solution of sodium hydroxide was performed, using phenolphthalein as an indicator. All experiments were done in duplicate and repeated three times. To control the obtained results, the solubility of DMBA was checked accordingly: the mixture of DMBA and a solvent corresponding to the solubility, at a given temperature, was prepared and heated in a thermostatic bath. The experimental mole fraction solubility (x_e) of DMBA in the various solvents was calculated, as shown in Eq. (5.15):

$$x_{\mathrm{e}} = \frac{\mathrm{m_1}/\mathrm{M_1}}{\frac{\mathrm{m_1}}{\mathrm{M_1}}+\frac{\mathrm{m_2}}{\mathrm{M_2}}} \tag{5.15}$$

where m_1 and m_2 are the masses of DMBA and solvent, respectively. M_1 and M_2 are the molar masses of DMBA and solvent, respectively.

จุฬาลงกรณ์มหาวิทยาลัย
Chulalongkorn University

In order to evaluate the accuracy of the model, the root mean square deviation (RMSD) was applied, as in Eq.(5.16):

$$\mathrm{RMSD} = \left(\sum_{\mathrm{i}=1}^{\mathrm{n}}(x_c - x_e)^2/\mathrm{n}\right)^{1/2} \tag{5.16}$$

where n is the total experimental points and x_e and x_c are the experimental and calculated molar fraction of solubility, respectively.

5.6 Results and discussion

5.6.1 Solid phase properties of DMBA

In order to investigate the polymorphic state of DMBA before and after recrystallization, the solid samples were analysed via DSC. In **Fig. 5.2**, the results of DSC analysis are displayed; 2A is before recrystallization and 2B is after recrystallization. As shown, the large endothermic peaks with onset at 98.9 °C (2A) and 98.4 °C (2B) corresponded to the transition temperatures of DMBA. It was noticed that DMBA underwent solid form transformation at around 98 ºC. Moreover, for the small peak at 112.5 °C (2A) and at 113.9 °C (2B), melting points were duly observed. The standard uncertainty for the solid-to-solid phase transition temperature was found to be 3.8 °C. As for 2B, however, a slightly higher melting point and sharper melting peak was probably due to purification brought about by the process of recrystallization. Results revealed that the obtained peak before recrystallization showed the same pattern as after recrystallization, indicating that no polymorph transformation took place during the mutual solubility determination. Further, after the measurements of solubility, HPLC was applied to check the stability and purity of the DMBA solid samples. Thus, it was found that no change of DMBA was observed, demonstrating that there was no solvate formation throughout the experimental investigations.

จุฬาลงกรณ์มหาวิทยาลัย
Chulalongkorn University

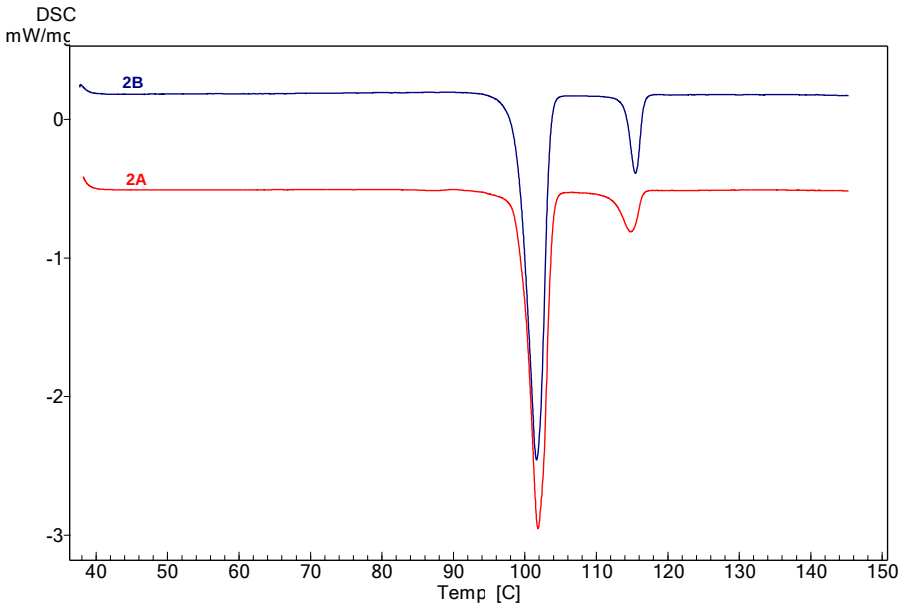

Fig. 5.2. Thermal analysis (DSC) of DMBA (2A – before recrystallization and 2B – after recrystallization).

5.6.2 Solubility data

In **Fig. 5.3**, the measured mole fraction solubility of DMBA in the various solvents i.e. ethylacetate, butylacetate, MIBK, CPME, toluene, GBL and 1,4-dioxane over the temperature range (298.15 to 353.15) K are graphically shown. In **Table 5.3**, the requisite values are presented. Thus, it can be seen that the solubility of DMBA is a function of temperature. Consequently, for all investigated solvents, as temperature increased, the equilibrium solubility of DMBA increased. Results found that DMBA yielded the highest solubility in 1,4-dioxane and the lowest solubility in toluene. The mole fraction of DMBA solubility in these solvents from, high to low, was in the order: 1,4-dioxane > GBL > MIBK > ethylacetate > butylacetate > CPME > toluene. As shown, over all the investigated temperature ranges, toluene gave the poorest solubility.

จุฬาลงกรณ์มหาวิทยาลัย
Chulalongkorn University

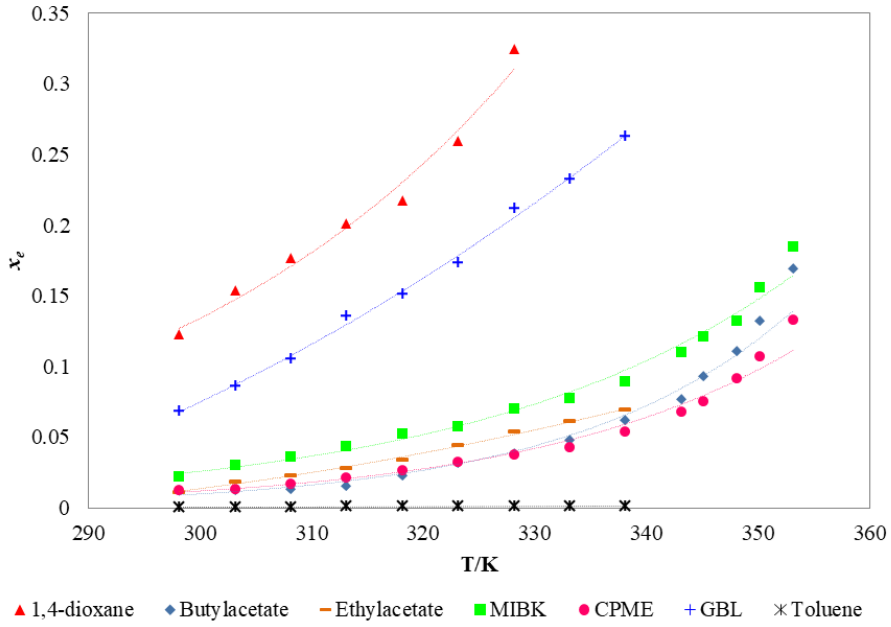

Fig. 5.3. Mole fraction solubility (x_e) of DMBA in various solvents, as a function of temperature.

จุฬาลงกรณ์มหาวิทยาลัย
CHULALONGKORN UNIVERSITY

Table 5.3 Experimental mole fraction solubility (x_e) of DMBA in different solvents at elevated temperature range from T = (298.15 to 353.15) K at atmospheric pressure (101.325 kPa).

T/K	$100x_e$						
	1,4-dioxane	GBL	Toluene	Ethyl-acetate	CPME	MIBK	Buthyl-acetate
298.15	12.25	6.879	0.039	1.108	1.210	2.179	1.187
303.15	15.35	8.589	0.056	1.842	1.299	2.975	1.250
308.15	17.64	10.55	0.073	2.276	1.683	3.624	1.290
313.15	20.07	13.57	0.080	2.812	2.075	4.333	1.527
318.15	21.72	15.10	0.087	3.376	2.663	5.232	2.280
323.15	25.93	17.32	0.093	4.429	3.198	5.751	3.171
328.15	32.43	21.20	0.093	5.388	3.743	7.001	3.794
333.15	-	23.24	0.099	6.120	4.249	7.696	4.773
338.15	-	26.32	0.105	6.899	5.402	8.909	6.187
343.15	-	-	-	-	6.741	10.97	7.677
345.15	-	-	-	-	7.486	12.13	9.303
348.15	-	-	-	-	9.174	13.21	11.06
350.15	-	-	-	-	10.68	15.56	13.17
353.15	-	-	-	-	13.27	18.43	16.92

Note: Standard uncertainties u are u(T) = 0.10 K and u(x) = 0.008. MIBK, CPME and GBL are methyl isobutyl ketone, cyclopentyl methyl ether and gamma-butyrolactone, respectively.

จุฬาลงกรณ์มหาวิทยาลัย
Chulalongkorn University

5.6.3 Solvent selection

In order to enhance a production yield or avoid a side reaction or a formation of any by-products, solvent selection was one of the choices that was employed. The selection of an effective solvent can be performed based on experimental solubility data. In the present work, various solvents were chosen to study the solubility of DMBA. Regarding the carboxylic acid groups in the DMBA structure, the use of alcohol was avoided to ensure that an esterification reaction did not occur. In the presence of carboxylic acid and alcohol, Fischer esterification will occur. At higher

temperatures, DMBA was found to be unstable. Therefore, the experiment was carried out over the temperature range (298.15 to 353.15) K. DMBA is a strong polar compound owing to its having two polar groups: hydroxyl and carbonyl groups. Therefore, it tended to dissolve in a polar solvent. 1,4-dioxane had the highest polarity index compared with other solvents, resulting in the highest solubility of DMBA. At the same time, toluene being a non-polar solvent was found to have the poorest solubility.

In **Table 5.4**, the polarity indexes of solvents used are shown. In larger alkyl groups, the solubility decreased and the hydrophobic effect was increased [19]. Meanwhile, the O-H group of DMBA possessed strong proton donor ability. Nevertheless, the selected solvents, excluding toluene, had the character of strong proton acceptors. Thus, DMBA can form strong hydrogen bonds with these six solvents. It is noted that the formation between solute and solvents often occurred via H-bonding which has a significant influence on the solubility of solutes [12, 20]. For instance, functional groups i.e. those groups that are capable of forming hydrogen bonds can enhance the solubility [21]. However, solubility behavior should be considered based on many factors such as polarity, molecular shapes and sizes, the interactions between solute-solvent and self-interactions of solvent and solute [12].

จุฬาลงกรณ์มหาวิทยาลัย
Chulalongkorn University

Table 5.4 The polarity index of different solvents.

Polarity index						
Ethylacetate[22, 23]	Butylacetate[22, 23]	CPME	MIBK[22, 23]	GBL	1,4-dioxane	Toluene[22, 23]
4.4	4.0	N/A	4.2	N/A	4.8	2.4

*solubility of CPME in water at 23 °c = 1.1 (g/100 g)[24]

*solubility of 1,4-dioxane in water at 23 °c = infinite[24]

*solubility of GBL in water = very soluble[25]

5.6.4 Effect of solvent properties

In this work, solvent properties: namely, polarity, hydrogen bond donor propensity, hydrogen bond acceptor propensity and cohesive energy density of solvents were studied. This was done in the interest of further understanding the solid-liquid equilibrium of DMBA in selected solvents. In molecular interactions, the cohesive energy density represents the self-interactions of solvent. Thus, a higher value of cohesive energy density indicates stronger self-interactions of solvent molecules. In **Table 5.5**, the physicochemical properties of the selected solvents are listed. As displayed in **Fig. 5.4**, the relationship between the solubility of DMBA and these physicochemical properties (at 298.15 K) were plotted. As can be seen, the solubility of DMBA depended on 3 factors: namely, polarity, hydrogen bond acceptor propensity and cohesive energy density. 1,4-Dioxane was found to have high polarity, the highest hydrogen bond acceptor propensity and cohesive energy density, exhibiting great solubility among the investigated solvents. Herein, the higher values of cohesive energy density, resulting in the higher amount of solubility of DMBA, demonstrated the strength of solute-solvent interaction and played an important role in the solid-liquid equilibrium [26].

จุฬาลงกรณ์มหาวิทยาลัย
Chulalongkorn University

Table 5.5 Physicochemical properties of selected solvents.[27]

Solvents	π^a	$\sum\alpha^b$	$\sum\beta^c$	Cohesive energy density[d]
Ethylacetate	0.55	0.00	0.45	300.64
Butylacetate	0.46	0.00	0.45	256.96
Toluene	0.54	0.00	0.14	289.05
MIBK	0.65	0.00	0.51	253.06
CPME	N/A	N/A	N/A	N/A
1,4-dioxane	0.51	0.00	0.64	372.17
GBL	N/A	N/A	N/A	N/A

Note: MIBK, CPME and GBL are methyl isobutyl ketone, cyclopentyl methyl ether and gamma-butyrolactone, respectively.

[a]Polarity of solvents.

[b]Summation of the hydrogen bond donor propensities of the solvent.

[c]Summation of the hydrogen bond acceptor propensities of the solvent.

[d]Cohesive energy density in the unit of $J \cdot mol^{-1} \cdot mL^{-1}$.

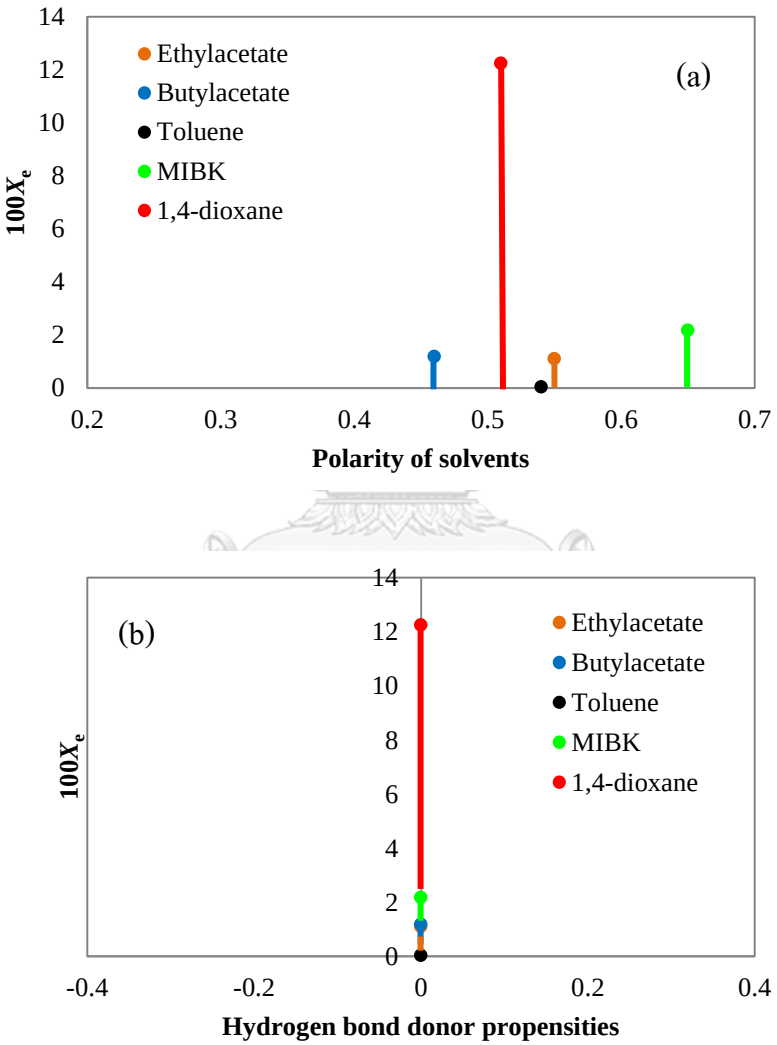

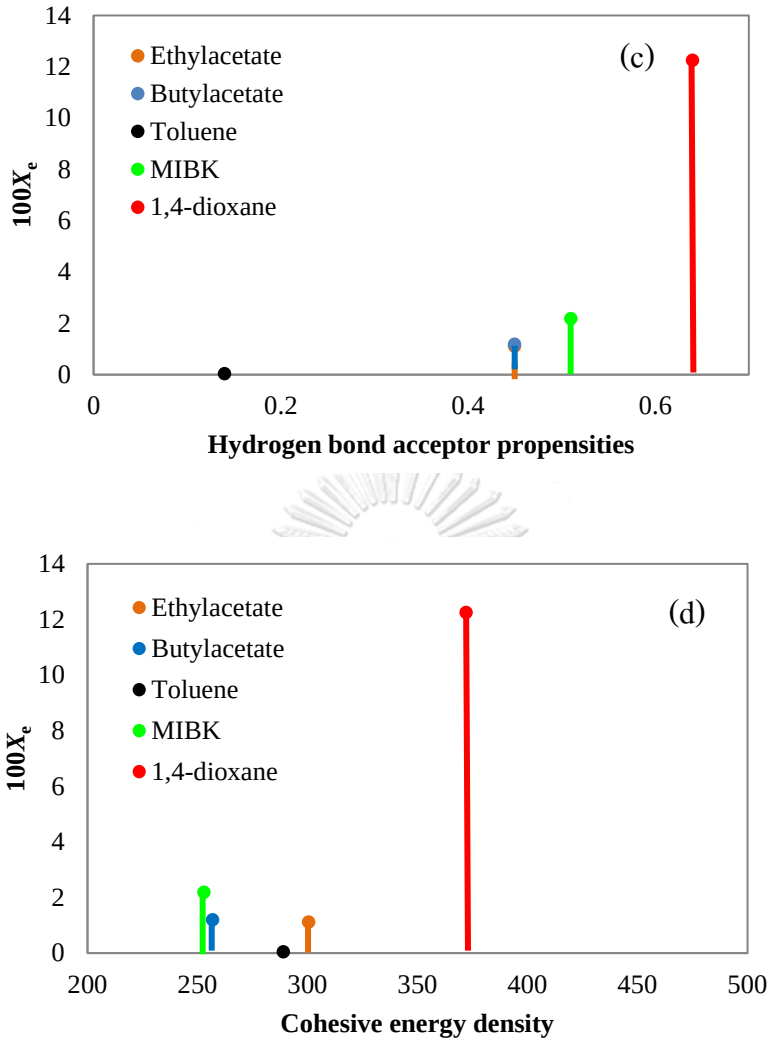

จุฬาลงกรณ์มหาวิทยาลัย
Chulalongkorn University

Fig. 5.4. Solubility spectra of DMBA in selected solvents at 298.15 K as a function of (a) solvent polarity, (b) hydrogen bond donor propensity, (c) hydrogen bond acceptor propensity and (d) cohesive energy density.

5.6.5 Correlation of DMBA solubility

Experimental mole fraction solubility of DMBA in selected solvents was correlated with thermodynamic models as described below.

5.6.5.1 The Apelblat equation

The values of *A* and *B* stand for the variation of activity coefficient in real solution; *C* reflects the effect of temperature on fusion enthalpy [28]. In **Table 5.6**, the values of the model parameters are shown. Thus, results showed good agreement between the calculated molar fraction of solubility and the experimental values using the Apelblat equation, considering the values of R^2 and RMSD for all investigated solvents with the largest R^2 and the smallest RMSD.

Table 5.6 Apelblat equation parameters for DMBA in various solvents.

Solvents	***A***	***B***	***C***	**R^2**	**RMSD**
Ethylacetate	619.7245	-33,017	-90.1106	0.9920	$8.57x10^{-6}$
Butylacetate	-762.434	31,876	114.2589	0.9924	$1.07x10^{-5}$
Toluene	1017.2	-49,930	-150.5038	0.9669	$9.92x10^{-10}$
MIBK	-143.878	3,613.4	22.4721	0.9892	$2.40x10^{-5}$
CPME	-438.6233	17,059	66.1666	0.9929	$1.57x10^{-5}$
1,4-dioxane	-151.2376	4,450.2	23.5628	0.9836	$3.57x10^{-5}$
GBL	325.2706	-18,231	-46.8267	0.9971	$7.01x10^{-6}$

Note: MIBK, CPME and GBL are methyl isobutyl ketone, cyclopentyl methyl ether and gamma-butyrolactone, respectively.

จุฬาลงกรณ์มหาวิทยาลัย
Chulalongkorn University

5.6.5.2 Buchowski–Książczak λh equation

In **Table 5.7**, the regression results of the solubility of DMBA in selected organic solvents and the values of the parameters λ and *h* are presented. Regarding the values of R^2 and RMSD, the λh equation was found to be suitable for six solvents only; toluene was the exception since toluene is a non-polar molecule whilst the λh equation deals with a strong polarity molecule. Further, the values of λ, in investigated solvents, were found to be very small showing that during the dissolution process of DMBA,

there was no association number of DMBA molecules in solvent. Positive values of *h* denoted that there were no repulsive interactions between DMBA and solvent molecules [29].

Table 5.7 The λh equation parameters for DMBA in various solvents.

Solvents	λ	***H***	R^2	**RMSD**
Ethylacetate	0.1522	19,858	0.9759	0.000828
Butylacetate	0.6375	9020.7	0.9897	0.003573
Toluene	-0.00014767	2,731,900	0.7885	8.7×10^{-7}
MIBK	0.1277	18,133	0.9916	0.000744
CPME	0.2137	19,233	0.9872	0.001391
1,4-dioxane	0.778	2,603.1	0.9838	0.014235
GBL	0.343	5614.1	0.9795	0.004845

Note: MIBK, CPME and GBL are methyl isobutyl ketone, cyclopentyl methyl ether and gamma-butyrolactone, respectively.

5.6.5.3 NRTL model

NRTL models were applied to correlate the solubility of DMBA in selected solvents, under temperature range. In **Table 5.8**, the values of the model parameter (g_{12} and g_{21}) are shown. As illustrated in **Fig. 5.5**, the comparison between the experimental mole fraction solubility and the calculated mole fraction solubility obtained via NRTL is plotted. The accuracy of the model was determined via RMSD, as addressed in Eq.(16). The obtained values of RMSD are: 0.00034, 0.00014, 0.00033, 8.4626×10^{-5}, 8.4319×10^{-5}, 1.5420×10^{-5} and 0.0024 for butylacetate, cyclopentyl methyl ether, methyl isobutyl ketone, ethylacetate, gamma-butyrolactone, toluene and 1,4-dioxane, respectively.

จุฬาลงกรณ์มหาวิทยาลัย
CHULALONGKORN UNIVERSITY

Table 5.8 NRTL parameters for DMBA in various solvents.

	Solvents							
***T*/K**	Butylacetate		CPME		MIBK		1,4-dioxane	
	g_{12}	g_{21}	g_{12}	g_{21}	g_{12}	g_{21}	g_{12}	g_{21}
298.15	1880.25	4930.14	2783.16	4817.12	534.66	3981.14	-1911.49	4351.73
303.15	2468.13	5287.64	3273.22	5222.34	342.36	3896.97	-2041.24	4917.09
308.15	2736.37	5751.95	4391.89	5220.44	369.74	3924.21	-2073.52	5647.81
313.15	3049.52	5882.84	4389.32	5226.17	347.12	4053.45	-2091.29	6292.14
318.15	3684.91	5454.11	4521.11	5154.25	323.51	4174.86	-1934.85	6207.62
323.15	3981.46	5187.06	4404.77	5271.46	322.26	4556.74	-1948.22	6646.75
328.15	2861.67	5234.53	4328.65	5367.92	303.53	4722.49	-2090.19	7292.44
333.15	2674.13	5326.74	3917.51	5591.02	386.57	5119.06	-	-
338.15	2399.93	5228.29	3912.94	5598.59	517.22	5373.48	-	-
343.15	2564.65	5329.38	3531.22	5677.71	614.58	5622.31	-	-
345.15	2101.17	5233.39	3303.03	5694.67	703.43	5758.14	-	-
348.15	2109.24	5271.67	2601.45	5697.33	836.32	5999.09	-	-
350.15	2058.76	5256.58	2413.66	5728.91	864.71	6134.16	-	-
353.15	1986.72	5198.45	2360.01	5818.13	1088.21	6596.67	-	-

	Solvents					
***T*/K**	Ethylacetate		GBL		Toluene	
	g_{12}	g_{21}	g_{12}	g_{21}	g_{12}	g_{21}
298.15	2290.05	5075.13	-1546.73	4951.19	2597.81	13183.59
303.15	1645.67	4434.89	-1582.58	5132.34	2783.81	12968.25
308.15	1638.33	4413.16	-1604.71	5378.25	2244.57	13007.03
313.15	1622.44	4447.81	-1623.94	5391.18	1950.30	13270.99
318.15	1620.78	4546.03	-1541.99	5662.47	1696.13	13800.56
323.15	1327.27	4527.89	-1467.61	6048.74	1525.66	14286.21
328.15	1235.06	4661.46	-1421.62	6497.84	1314.38	15008.02
333.15	1216.84	4988.90	-1226.06	6578.29	1304.33	15494.67
338.15	1202.63	5411.21	-1036.17	6495.94	1332.71	15851.02

จุฬาลงกรณ์มหาวิทยาลัย
CHULALONGKORN UNIVERSITY

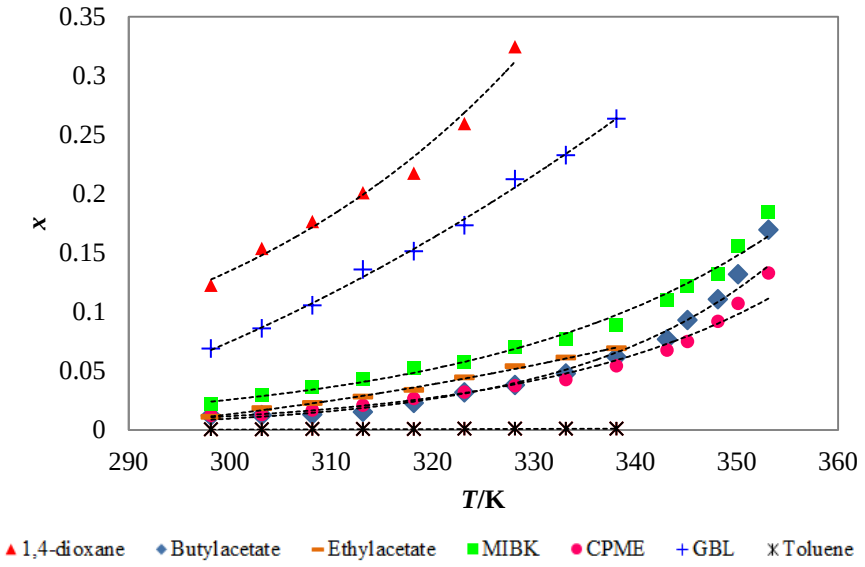

Fig. 5.5. Experimental mole fraction solubility (x_e) and the calculated mole fraction solubility ($x_{c,\ NRTL}$) of DMBA in various solvents, as a function of temperature.

5.6.6 Model comparison

Fig. 5.6 depicts the experimental mole fraction solubility data of DMBA compared with the calculated mole fraction solubility obtained from the Apelblat and λh equations. As shown graphically, it is obvious that the Apelblat equation is more suitable for describing the DMBA solid–liquid equilibrium than the λh equation. In Table 5.9, the values of the experimental mole fraction solubility (x_e) and correlated solubility (x_c) of DMBA in different solvents, at an elevated temperature range, are tabulated. It was found that the NRTL and Apelblat models proved to be in good agreement with the calculated molar fraction of solubility and the experimental values. Thus, the NRTL model provided the highest accuracy on solid-liquid equilibrium of DMBA in selected solvents.

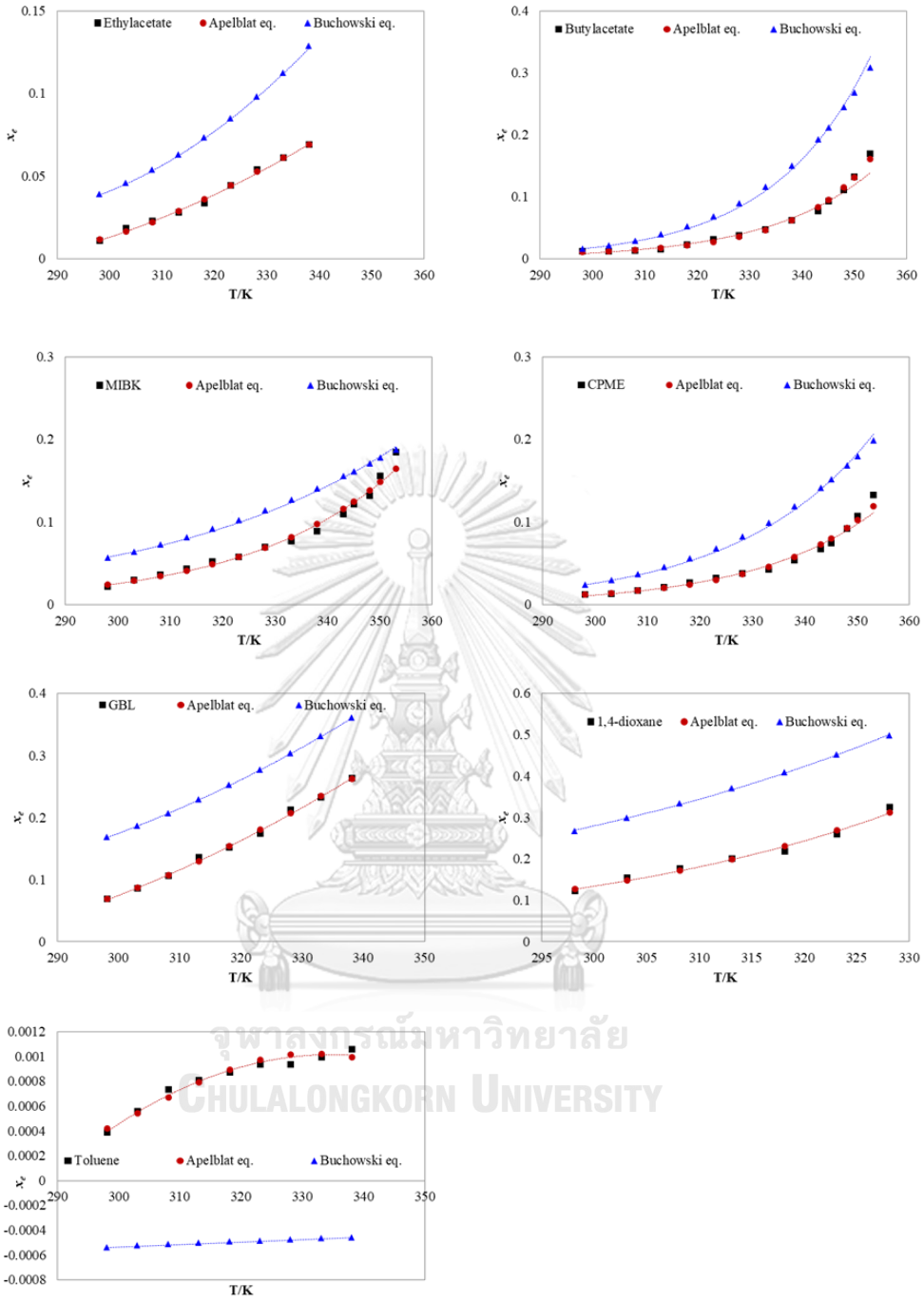

จุฬาลงกรณ์มหาวิทยาลัย
Chulalongkorn University

Fig. 5.6. Experimental mole fraction solubility (x_e) and the calculated mole fraction solubility of DMBA in various solvents, as a function of temperature.

Table 5.9 Experimental mole fraction solubility (x_e) and correlated solubility (x_c) of DMBA in different solvents at elevated temperature range from T = (298.15 to 353.15) K at atmospheric pressure (101.325 kPa)

T/K	$100x_e$	$100x_{c,\ Apelblat}$	$100x_{c,\ \lambda_h}$	$100x_{c,\ NRTL}$
		Butylacetate		
298.15	1.187	1.089	1.525	1.188
303.15	1.250	1.248	2.096	1.251
308.15	1.290	1.469	2.852	1.290
313.15	1.527	1.772	3.842	1.527
318.15	2.280	2.187	5.127	2.280
323.15	3.171	2.757	6.782	3.171
328.15	3.794	3.545	8.894	3.788
333.15	4.773	4.643	11.57	4.676
338.15	6.187	6.189	14.93	6.185
343.15	7.677	8.384	19.13	7.693
345.15	9.303	9.508	21.08	9.309
348.15	11.06	11.53	24.34	11.08
350.15	13.17	13.15	26.75	13.11
353.15	16.92	16.09	30.75	16.95
		Cyclopentyl methyl ether		
298.15	1.210	1.207	2.312	1.215
303.15	1.299	1.412	2.902	1.294
308.15	1.683	1.673	3.616	1.684
313.15	2.075	2.005	4.474	2.078
318.15	2.663	2.429	5.500	2.663
323.15	3.198	2.974	6.717	3.155
328.15	3.743	3.674	8.153	3.753
333.15	4.249	4.580	9.839	4.257
338.15	5.402	5.756	11.80	5.406

จุฬาลงกรณ์มหาวิทยาลัย
CHULALONGKORN UNIVERSITY

T/K	$100x_e$	$100x_{c,\ Apelblat}$	$100x_{c,\ \lambda_h}$	$100x_{c,\ NRTL}$
343.15	6.741	7.290	14.09	6.741
345.15	7.486	8.028	15.11	7.481
348.15	9.174	9.297	16.74	9.171
350.15	10.68	10.26	17.91	10.66
353.15	13.27	11.93	19.78	13.28
		Methyl isobutyl ketone		
298.15	2.179	2.419	5.583	2.175
303.15	2.975	2.879	6.346	2.976
308.15	3.624	3.427	7.183	3.627
313.15	4.333	4.080	8.099	4.338
318.15	5.232	4.859	9.097	5.236
323.15	5.751	5.786	10.18	5.760
328.15	7.001	6.891	11.35	7.006
333.15	7.696	8.205	12.62	7.690
338.15	8.909	9.768	13.99	8.908
343.15	10.97	11.62	15.45	10.97
345.15	12.13	12.46	16.07	12.00
348.15	13.21	13.83	17.03	13.22
350.15	15.56	14.82	17.69	15.57
353.15	18.43	16.45	18.71	18.42
		Ethylacetate		
298.15	1.108	1.192	3.867	1.100
303.15	1.842	1.655	4.571	1.838
308.15	2.276	2.219	5.374	2.297
313.15	2.812	2.879	6.285	2.818
318.15	3.376	3.622	7.315	3.374
323.15	4.429	4.427	8.473	4.421
328.15	5.388	5.264	9.771	5.385
333.15	6.120	6.100	11.21	6.122

จุฬาลงกรณ์มหาวิทยาลัย
CHULALONGKORN UNIVERSITY

T/K	$100x_e$	$100x_{c,\ Apelblat}$	$100x_{c,\ \lambda_h}$	$100x_{c,\ NRTL}$
338.15	6.899	6.899	12.83	6.892
		GBL		
298.15	6.879	6.882	16.78	6.867
303.15	8.589	8.660	18.67	8.587
308.15	10.55	10.68	20.70	10.54
313.15	13.57	12.92	22.87	13.57
318.15	15.10	15.37	25.19	15.10
323.15	17.32	17.97	27.66	17.32
328.15	21.20	20.69	30.29	21.20
333.15	23.24	23.46	33.08	23.24
338.15	26.32	26.23	36.03	26.34
		Toluene		
298.15	0.039	0.041	-0.054	0.038
303.15	0.056	0.054	-0.052	0.054
308.15	0.073	0.067	-0.051	0.070
313.15	0.080	0.079	-0.050	0.081
318.15	0.087	0.089	-0.049	0.086
323.15	0.093	0.096	-0.048	0.093
328.15	0.093	0.101	-0.047	0.093
333.15	0.099	0.102	-0.046	0.098
338.15	0.105	0.099	-0.046	0.109
		1,4-dioxane		
298.15	12.25	12.74	26.72	12.25
303.15	15.35	14.74	29.89	15.35
308.15	17.64	17.08	33.31	17.69
313.15	20.07	19.81	37.00	20.71
318.15	21.72	23.02	40.95	21.69
323.15	25.93	26.77	45.19	25.93
328.15	32.43	31.16	49.72	32.48

จุฬาลงกรณ์มหาวิทยาลัย
Chulalongkorn University

5.6.7 Apparent thermodynamic parameters for DMBA dissolution

As regards Eqs.(5.13)-(5.14), apparent thermodynamic parameters for the dissolution of DMBA in selected solvents were calculated. Results are listed in **Table 5.10**. As shown, the values of $\Delta_{sol}H$ and $\Delta_{sol}S$ are positive except for toluene at higher temperature (333.15- 338.15) K. The positive values of $\Delta_{sol}H$ indicated that the dissolution of DMBA in all investigated solvents was an endothermic process, in the experimental temperature range. These values revealed that the molecular interactions between DMBA and the selected solvent molecules were stronger than the self-interactions between solvent-solvent molecules and DMBA-DMBA molecules. Thus, the energy of the bond formation between the DMBA-solvent was not strong enough to overcome the energy needed for breaking the self-interaction bonds of solute and solvent [30]. Further, the high values of $\Delta_{sol}H$ showed that in order to overcome the cohesive forces of DMBA-selected solvents, more energy was required [28, 31]. Meanwhile, the negative values of $\Delta_{sol}H$ and $\Delta_{sol}S$, at the higher temperature (333.15-338.15) K in toluene, indicated that the dissolution of DMBA was an exothermic process. The exothermic dissolution process of toluene implies that more heat energy is released during the formation of DMBA-solvent than is used in breaking up the solute and solvent interaction. The positive values of $\Delta_{sol}S$ proved that the dissolution process of DMBA was an entropy-driven process [32]. This was due to the differences in molecular structures and space conformations between DMBA and solvents, resulting in various interactions such as dipole–dipole, hydrogen bonding, hydrophobic interactions, and stereoscopic effects. These interactions distorted the solvent molecules, therefore entropy increased. As temperature increased, more disorder was found to be in the system [15]. The values of $\Delta_{sol}H$ were found to be higher than $\Delta_{sol}S$ which meant that more energy was required to overcome the force between DMBA and solvent molecules [5,33-34]. As for butylacetate, CPME, MIBK and 1,4-dioxane,

as temperature increased, the values of $\Delta_{sol}H$ and $\Delta_{sol}S$ increased, indicating an increase in molecular interactions between DMBA-solvent molecules. Thus, more energy was required to break the bonds of solute and solvent to insert one of the molecules into solution. As for ethylacetate, toluene and GBL, however, as temperature increased, the values of $\Delta_{sol}H$ and $\Delta_{sol}S$ decreased. Several studies [15,20] also reported the decrease in $\Delta_{sol}H$, as temperature increased. The decrease in $\Delta_{sol}H$ can be caused by the endothermic effect due to the breaking of self-interaction bonds. This effect is compensated by the exothermic formation of new bonds. The reason for the increase in the values of $\Delta_{sol}S$, as temperature increased, could be due to disruption of DMBA molecules with molecules of solvent. Thus, during the dissolution process, the degree of the order of the system was reduced. The decrease in $\Delta_{sol}S$ indicated that the system was more ordered. Thus, interactions between DMBA and solvent molecules were stronger. Results confirmed that the solubility of DMBA was a function of temperature. At 298.15 K, enthalpies of dissolution increased in the range: butylacetate < 1,4-dioxane < CPME < MIBK < GBL < toluene < ethylacetate. This implied that the interaction between DMBA-ethylacetate could be stronger than that in other solvents. The interaction between DMBA-solvents, from low to high, was in the order: butylacetate < 1,4-dioxane < CPME < MIBK < GBL < toluene < ethylacetate.

จุฬาลงกรณ์มหาวิทยาลัย
CHULALONGKORN UNIVERSITY

Table 5.10 Thermodynamic parameters $\Delta_{sol}H$ (kJ·mol^{-1}) and $\Delta_{sol}S$ (J·mol^{-1}·K^{-1}) for DMBA in various solvents at different temperatures and at atmospheric pressure (101.325 kPa).

	Solvents							
***T*/K**	Butylacetate		CPME		MIBK		1,4-dioxane	
	$\Delta_{sol}H$	$\Delta_{sol}S$	$\Delta_{sol}H$	$\Delta_{sol}S$	$\Delta_{sol}H$	$\Delta_{sol}S$	$\Delta_{sol}H$	$\Delta_{sol}S$
298.15	18.21	61.07	22.18	74.41	25.66	86.07	21.41	71.80
303.15	22.96	75.73	24.93	82.25	26.59	87.73	22.38	73.85
308.15	27.701	89.92	27.68	89.85	27.53	89.34	23.36	75.83
313.15	32.45	103.6	30.43	97.20	28.46	90.90	24.34	77.75
318.15	37.20	116.9	33.18	104.3	29.40	92.40	25.32	79.60
323.15	41.95	129.8	35.93	111.2	30.33	93.86	26.30	81.40
328.15	46.70	142.3	38.69	117.9	31.26	95.28	27.28	83.15
333.15	51.45	154.4	41.44	124.3	32.20	96.65	-	-
338.15	56.20	166.2	44.19	130.6	33.13	97.99	-	-
343.15	60.95	177.6	46.94	136.8	34.07	99.28	-	-
345.15	62.85	182.1	48.04	139.1	34.44	99.79	-	-
348.15	65.70	188.7	46.69	142.7	35.00	100.5	-	-
350.15	67.70	193.0	50.79	145.0	35.37	101.0	-	-
353.15	70.45	199.5	52.44	148.5	35.93	101.7	-	-

จุฬาลงกรณ์มหาวิทยาลัย
Chulalongkorn University

	Solvents					
***T*/K**	Ethylacetate		GBL		Toluene	
	$\Delta_{sol}H$	$\Delta_{sol}S$	$\Delta_{sol}H$	$\Delta_{sol}S$	$\Delta_{sol}H$	$\Delta_{sol}S$
298.15	51.13	171.50	35.49	119.0	42.04	141.0
303.15	47.39	156.32	33.55	110.6	35.79	118.0
308.15	43.64	141.63	31.60	102.5	29.53	95.84
313.15	39.89	127.40	29.65	94.70	23.27	74.33
318.15	36.15	113.63	27.71	87.10	17.02	53.49
323.15	32.40	100.28	25.76	79.73	10.76	33.31
328.15	28.66	87.33	23.81	72.58	4.507	13.73
333.15	24.91	74.78	21.87	65.65	-1.748	-5.249
338.15	21.16	62.60	19.92	58.92	-8.005	-23.67

5.6.8 Thermodynamic functions of mixing

Based on the Lewis Randall rule, thermodynamic functions of mixing of real solution can be derived as following: [26]

$$\Delta_{mix}G = \Delta_{mix}G^{id} + G^{E} \quad (5.17)$$

$$\Delta_{mix}H = \Delta_{mix}H^{id} + H^{E} \quad (5.18)$$

$$\Delta_{mix}S = \Delta_{mix}S^{id} + S^{E} \quad (5.19)$$

where G^E, H^E, and S^E are the excess properties, which can be determined as shown below:

$$G^{E} = RT\sum_{i}^{N} x_i \ln \gamma_i \quad (5.20)$$

$$H^{E} = -RT^{2}\sum_{i}^{N} x_i \left(\frac{\partial \ln \gamma_i}{\partial T}\right)_{p,x} \quad (5.21)$$

$$S^{E} = \frac{H^{E}-G^{E}}{T} \quad (5.22)$$

จุฬาลงกรณ์มหาวิทยาลัย
CHULALONGKORN UNIVERSITY

where γ_i is the activity coefficient of component i in real system and can be calculated from the NRTL model.

The Gibbs free energy of mixing of DMBA in selected solvents are listed as shown in **Table 5.11**. The values of mixing Gibbs free energy in all solvents are negative and decrease as temperature increased, indicating a spontaneous and favorable mixing process of DMBA.

Table 5.11 Gibbs free energy of mixing ($\Delta_{mix}G$) of DMBA in selected solvents.

T/K	$\Delta_{mix}G$ (J·mol^{-1})						
	1,4-dioxane	GBL	Toluene	Ethyl-acetate	CPME	MIBK	Buthyl-acetate
298.15	-955.29	-532.75	-3.07	-86.92	-94.85	-170.02	-93.09
303.15	-1154.72	-638.85	-4.27	-138.80	-98.16	-223.08	-94.54
308.15	-1273.33	-751.63	-5.38	-164.73	-122.19	-260.68	-93.92
313.15	-1390.41	-924.72	-5.73	-194.92	-144.48	-298.29	-106.72
318.15	-1426.42	-978.81	-5.94	-223.63	-177.16	-343.50	-152.06
323.15	-1625.94	-1063.94	-6.11	-278.84	-202.85	-359.72	-201.20
328.15	-1956.6	-1230.04	-5.86	-321.55	-225.80	-414.30	-228.78
333.15	-	-1262.78	-5.98	-345.39	-242.99	-430.33	-271.75
338.15	-	-1330.44	-6.06	-366.48	-290.27	-467.25	-330.41
343.15	-	-	-	-	-338.07	-533.70	-382.13
345.15	-	-	-	-	-363.92	-569.63	-445.75
348.15	-	-	-	-	-422.65	-590.44	-501.95
350.15	-	-	-	-	-472.50	-664.15	-571.12
353.15	-	-	-	-	-548.51	-733.46	-680.48

จุฬาลงกรณ์มหาวิทยาลัย
Chulalongkorn University

5.7 Conclusion

The solubility of 2,2-Bis(hydroxymethyl)butyric acid (DMBA) was carried out employing various pure solvents: namely, ethylacetate, butylacetate, MIBK, CPME, toluene, GBL and 1,4-dioxane from (298.15- 353.15) K, under atmospheric pressure using a solid-liquid equilibrium method. Results found that the solubility of DMBA depended on the temperature. As temperature increased, the mole fraction solubility of DMBA in the selected solvents increased. Of all the investigated solvents, the solubility of DMBA in 1,4-dioxane was found to be the highest. In contrast, toluene was found to be the least soluble. The mole fraction of DMBA solubility in these solvents, from high to low, was in the order: 1,4 dioxane > GBL > MIBK >

ethylacetate > butylacetate > CPME > toluene. The experimental data correlated well with the Apelblat equation and NRTL model regarding the values of R^2 and RMSD. Thus, it was significant that the NRTL model and the Apelblat equation provided a better prediction for the solute than the Buchowski–Książczak λh equation. Further, the apparent thermodynamic parameters for DMBA dissolution were estimated using Van't Hoff equation. The values of $\Delta_{sol}H$ and $\Delta_{sol}S$ indicated that the dissolution process was endothermic and entropy-driven process.

5.8 Declaration of competing interest

The authors would like to inform that there is “no conflict of interest” on this article.

5.9 Acknowledgement

The authors profoundly appreciate the support from the Thailand Research Fund and Chulalongkorn University under the Research and Researchers for Industries (RRi) Ph.D. Program (Grant No. PHD58I0081) and the Slovak grant APVV-15-0482. Thanks are also given to the Laboratory of Catalyzed Processes, Department of Organic Technology, Faculty of Chemical and Food Technology, Slovak University of Technology in Bratislava, Slovak Republic, for supplying chemical compounds and instruments for analysis and measurement.

5.10 Reference

[1] http://molview.org/ (01/01/2020)

[2] M. Sayed, T. Dishisha, W.F. Sayed, W.M. Salem, H.A. Temerk, S.H. Pyo, Selective oxidation of trimethylolpropane to2,2-bis(hydroxymethyl)butyric acid using growing cells of Coryne bacterium sp. ATCC 21245, J. Biotech. 221 (2016) 62–69.

[3] S.H. Pyo, P. Persson, M.A. Mollaahmad, K. Sörensen, S. Lundmark, R.H. Kaul, Cyclic carbonates as monomers for phosgene and isocyanate-free polyurethanes and polycarbonates, Pure Appl. Chem. 84(3) (2012) 637–661.

[4] K. Hill, Fats and oils as oleochemical raw materials. Pure Appl. Chem. 72(7) (2000) 1255–1264.

[5] L. Wang, C. Xing, L. Zhao, L. Xu, G. Liu, Measurement and correlation of solubility of 2-chloro-3-(trifluoromethyl)pyridine in pure solvents and ethanol + n-propanol mixtures, J. Mol. Liq. 238 (2017) 470-477.

[6] A.G. Carr, J.W. Tester, Prediction of the solubility of quartz in salt solutions from 25 °C to 900 °C using the 3-parameter Non-Random Two-Liquid (NRTL) model, Fluid Phase Equi. 337 (2013) 288-297.

[7] P. Jain, K. Sepassi, S.H. Yalkowsky, Comparison of aqueous solubility estimation from AQUAFAC and the GSE, Inter. J. Pharma. 360(1–2) (2008) 122-147.

[8] E.K. Goharshadi, M. Hesabi, Estimation of solubility parameter using equations of state, J. Mol. Liq. 113(1–3) (2004) 125-132.

จุฬาลงกรณ์มหาวิทยาลัย
CHULALONGKORN UNIVERSITY

[9] S. Suren, N. Sunsandee, M. Stolcova, M. Hronec, N. Leepipatpiboon, U. Pancharoen, S. Kheawhom, Measurement on the solubility of adipic acid in various solvents at high temperature and its thermodynamics parameters, Fluid Phase Equi. 360 (2013) 332– 337.

[10] E. Manzurola, A. Apelblat, Solubilities of L-glutamic acid, 3-nitrobenzoic acid, p-toluic acid, calcium-L-lactate, calcium gluconate, magnesium-DL-aspartate, and magnesium-L-lactate in water, J. Chem. Thermodyn. 34 (2002) 1127–1136.

[11] A. Apelblat, E. Manzurola, Solubilities of manganese, cadmium, mercury andleadacetates in water from T=278.15 K to T=340.15 K, J. Chem. Thermodyn. 33 (2001) 147–153.

[12] M. Zheng, J. Chen, G. Chen, A. Farajtabar, H. Zhao, Solubility modelling and solvent effect for domperidone in twelve green solvents, J. Mol. Liq. 261 (2018) 50–56.

[13] H. Renon, J.M. Prausnitz, Local Compositions in Thermodynamic Excess Functions for Liquid Mixtures, AlChE Journal 14(1) (1968) 135-144.

[14] J. Ouyang, L. Zhou, Z. Liu, S. Xiao, X. Huang, J.Y.Y. Heng, Solubility determination and modelling of benzamide in organic solvents at temperatures from 283.15 K and 323.15 K, and ternary phase diagrams of benzamide-benzoic acid cocrystals in ethanol at 298.15 K, J. Mol. Liq. 286 (2019)110885.

[15] C.L. Zhang, F. Zhao, Y. Wang, Thermodynamics of the solubility of sulfamethazine in methanol, ethanol, 1-propanol, acetone, and chloroform from 293.15 to 333.15 K, J. Mol. Liq. 159 (2011) 170–172.

จุฬาลงกรณ์มหาวิทยาลัย
Chulalongkorn University

[16] C.L. Zhang, B.Y. Li, Y. Wang, Solubilities of Norfloxacin in Ethanol, 1-Propanol, Acetone, and Chloroform from 294.15 to 318.15 K, Can. J. Chem. Eng. 88 (2010) 63-66.

[17] F.A. Wang, L.C. Wang, J.C. Song, L. Wang, H.S. Chen, Solubilities of Bis(2,2,6,6-tetramethyl-4-piperidinyl) Maleate in Hexane, Heptane, Octane, m-Xylene, and Tetrahydrofuran from (253.15 to 310.15) K, J. Chem. Eng. Data, 49(6) (2004) 1539-1541.

[18] E.S. Ha, Y.R. Lee, M.S. Kim, Solubility of dronedarone hydrochloride in six pure solvents at the range of 298.15 to 323.15 K, J. Mol. Liq. 216 (2016) 360-363.

[19] G.L. Patrick, Chapter 14: Drug design: optimizing access to the target, An Introduction to Medicinal Chemistry, Fifth Edition, Great Clarendon Street, Oxford, OX2 6DP, United Kingdom, 2013.

[20] M.A. Varfolomeev, M.A. Stolov, R.N. Nagrimanov, I.T. Rakipov, Jr., W.E. Acree, M.H. Abraham, Analysis of solute-pyridine intermolecular interactions based on experimental enthalpies of solution and enthalpies of solvation of solutes dissolved in pyridine, Thermochimica Acta 660 (2018) 11–17.

[21] M.W. Harrold, and R.M. Zavod, Chapter 2: Functional Group Characteristics and Roles, Basic Concepts in Medicinal Chemistry, American Society of Health-System Pharmacists®, Bethesda, Maryland, 2013.

[22] M. Kleiman, K.A. Ryu, A.P. Esser-Kahn, Determination of Factors Influencing the Wet Etching of Polydimethylsiloxane Using Tetra-n-butylammonium Fluoride, Macromol. Chem. Phys. 217 (2016) 284—291.

จุฬาลงกรณ์มหาวิทยาลัย
CHULALONGKORN UNIVERSITY

[23] L.R. Snyder, J.J. Kirkland, J.L. Glajch, PROPERTIES OF SOLVENTS USED IN HPLC, Practical HPLC Method Development, Second Edition, 1997 John Wiley & Sons, Inc.

[24] K. Watanabe, N. Yamagiwa, Y. Torisawa, Cyclopentyl Methyl Ether as a New and Alternative Process Solvent, Organic Pro. Research&Develop. 11 (2007) 251—258.

[25] Gamma-butyrolactone (GBL), Critical Review Report Agenda item 4.3, Expert Committee on Drug Dependence, Thirty-sixth Meeting, WHO Secretariat, Essential

Medicines and Health Products, Policy Access and Rational Use Unit Geneva, 16-20 June 2014.

[26] S. Zhao, Y. Ma, J. Gong, B. Hou, W. Tang, Solid-liquid phase equilibrium and thermodynamic analysis of griseofulvin in twelve mono-solvents, J. Mol. Liq. 296 (2019) 111861.

[27] C.H. Gu, H. Li, R.B. Gandhi, K. Raghavan, Grouping solvents by statistical analysis of solvent property parameters: implication to polymorph screening, Int. J. Pharm. 283 (2004) 117-125.

[28] B. Tao, X. Li, M. Yan, W. Luo, Solubility of dibenzothiophene in nine organic solvents: Experimental measurement and thermodynamic modelling. J. Chem. Thermodyn. 129 (2019) 73–82.

[29] R. Xu, J. Wang, S. Han, C. Du, L. Meng, H. Zhao, Solubility modelling and thermodynamic dissolution functions of phthalimide in ten organic solvents, J. Chem. Thermodyn. 94 (2016) 160–168.

จุฬาลงกรณ์มหาวิทยาลัย
Chulalongkorn University

[30] K.D. Bhesaniya, K.V. Chavda, C.H. Sadhu, S. Baluja, Thermodynamic characteristics of solutions of ornidazole in different organic solvents at different temperatures, J. Mol. Liq. 191 (2014) 124–127.

[31] E.S. Ha, D.H. Kuk, D.H. Ha, W.Y. Sim, I.H. Baek, J.S. Kim, M.S. Kim, Determination and correlation of solubility of sarpogrelate hydrochloride in eight solvents at different temperatures, J.Mol. Liq. 237 (2017) 141–145.

[32] F. Shakeel, M. Iqbal, E. Ezzeldin, N. Haq, Thermodynamics of solubility of ibrutinib in ethanol + water cosolvent mixtures at different temperatures, J. Mol. Liq. 209 (2015) 461–464.

[33] Z.H. Yang, Z.X. Zeng, L. Sun, W.L. Xue, N. Chen, Determination and correlation of solubilities of lauric acid in eight alcohols, J. Chem. Eng. Data 59 (2014) 2725–2731.

[34] K. Wang, Y.H. Hu, W. Yang, S. Guo, Y. Shi, Measurement and correlation of the solubility of 2,3,4,5-tetrabromothiophene in different solvents, J. Chem. Thermodyn. 55 (2012) 50–55.

5.11 Notation

The corrigendum to this paper, regards the Buchowski-Ksiazcak λh equation has been revised in order to yield the best fit curve to the experimental data. Please find our corrigendum to the aforementioned paper as published in [56].

จุฬาลงกรณ์มหาวิทยาลัย
Chulalongkorn University

CHAPTER VI

CONCLUSION

6.1 Conclusion

HFSLM is a cutting edge system that has been well applied in separation processes and can be regarded as a promising system for As Low As Reasonably Achievable (ALARA) mass separation. In this work, it is evidented that HFSLM can effectively separate Pd (II) from wastewater of electroless plating process containing Cu (II) and Ni (II). Ionic liquids, Aliquat 336, successfully demonstrated to be a suitable carrier for the HFSLM system. The viability to separate Pd (II) is established by controlling the influence of operating conditions. Under optimum conditions, a complete separation of Pd (II) was achieved; > 99 % extraction and 87.09 % recovery. The optimized conditions viz. 6 %(v/v) of Aliquat 336, pH 2 of the feed solution, synergistic solutions of 0.5 M thiourea mixed with 0.1 M HCl as a strippant and 100 mL/min of flow rate for both aqueous solutions.

The overall contents of this dissertation cover the following studies:

จุฬาลงกรณ์มหาวิทยาลัย
Chulalongkorn University

The superior extraction of Pd (II) over Cu (II) and Ni (II) from industrial wastewater was investigated via both solvent extraction and HFSLM systems. Aliquat 336, D2EHPA, and TBP were employed as extractants. Results show that Aliquat 336 yielded the highest extraction of Pd (II). The extractability of Pd (II) followed: Aliquat 336 > D2EHPA > TBP. It was observed that within 10 min., the extraction percentages of Pd (II) acheived 92% and 96.62% via a solvent extraction and HFSLM, respectively. The extraction reaction of Pd (II) reached equilibrium at 20 and 30 min. via HFSLM and SX, respectively. The metal complex forms and their stability is a function of pH. The predominant species (the highest stable form) of divalent Pd (II) was found to be $PdCl_4^{2-}$, mostly found at pH 1-4. Thus, at pH 2, >79 % of Pd (II) can

be extracted in the presence of Cu (II) and Ni (II) owing to both Cu (II) and Ni (II) are mostly found in the form of cationic in an investigated pH range.

Herein, the enhancement of stripping efficiency was investigated. Results showed that the synergistic strippants of 0.5 M of thiourea mixed with 0.1 M of HCl were most effective in the stripping of Pd (II) ions from the loaded Aliquat 336. A higher percentage of Pd (II) stripping was obtained than when thiourea and HCl were used singly. Further, a study on temperature effect was as followed: the separation efficiency of Pd (II) increased when the temperature is increased due to an increase in solubility and diffusion coefficients and a decrease in solvent viscosity, as well as an enhanced of mass transfer via the solvating system.

Kinetics and thermodynamics study were evaluated in order to explain a phenomena on Pd (II) separation via solvent extraction process. Results demonstrated that the order of reactions were found to be first order and pseudo-first order for extraction and stripping pf Pd (II), respectively. Thermodynamics analysis found that the separation process of Pd (II) was spontaneous and endothermic process.

An evaluation of mass transfer coefficient was examined. The values of k_f and k_m were found to be 6.96×10^{-4} and 1.02×10^{-5} cm/s, respectively. As obtained, the value of k_m was lower than k_f indicating that the membrane mass transfer coefficient (k_m) was the rate controlling step.

Besides, a mathematical model was developed on the basis of the conservation of mass. Axial convection, axial diffusion, radial diffusion as well as chemical reactions are considered via mathematical modeling. The mathematical model was presented to predict the concentration of Pd (II) in both aqueous solutions. Results indicate that the model proves to be an effective approach for predicting the transportation of Pd (II) across the HFSLM system. In the LMs, only the diffusion in

the radial direction took place. The resistance to Pd (II) transport in the LMs phase is the predominant resistance in the system. Thus, axial convection, axial diffusion, radial diffusion and the chemical reactions were involved in mass transfer across HFSLM and considered as an important concept for accurate prediction in the unsteady state model. This robust model with its high accuracy provides a greater understanding of the transport mechanisms across the HFSLM system. A design scale-up for industrial application could prove useful.

Additionally, learning cases for the measurement of the solubility of extractant was investigated. The solid-liquid equilibrium of 2,2-bis(hydroxymethyl)butyric acid (DMBA) was performed experimentally in various solvents. Results showed that the mole fraction solubility of DMBA increased, as temperature increased. The Apelblat equation and NRTL model indicated a good correlation with the experimental solubility data and can be used to describe the solid-liquid equilibrium. The mole fraction of DMBA solubility in these solvents, from high to low, was in the order: 1,4 dioxane > GBL > MIBK > ethylacetate > butylacetate > CPME > toluene. The dissolution process was found to be an endothermic and entropy-driven process.

จุฬาลงกรณ์มหาวิทยาลัย
CHULALONGKORN UNIVERSITY

6.2 Limitation

A major concern regarding HFSLM is the stability of LMs in terms of long time performance. This is mainly due to the loss of carrier and/or solvent from the membrane support which has an influence on both the flux and selectivity of the membrane. In consideration of this, further study on the stability of the LMs should be considered for scaling up for industrial applications.

6.3 Recommendations for future research

The advantages of HFSLM over conventional methods viz. less chemical used, high selectivity as well as low operating cost. HFSLM shows to be ease to scalability

by operating in parallel or in series mode in order to yield higher capacity. Regards, simultaneous extraction and stripping of target species contribute unit very compact with less operating time and energy consumption. Following are recommendations for future research:

(1) Pretreatment of wastewater must be performed in order to prevent the fouling in the system.

(2) A high concentration of acid and high temperature should be avoided since it impaired the polypropylene hollow fiber.

(3) Measurement of the solubility of extractant in aqueous solutions should be investigated.

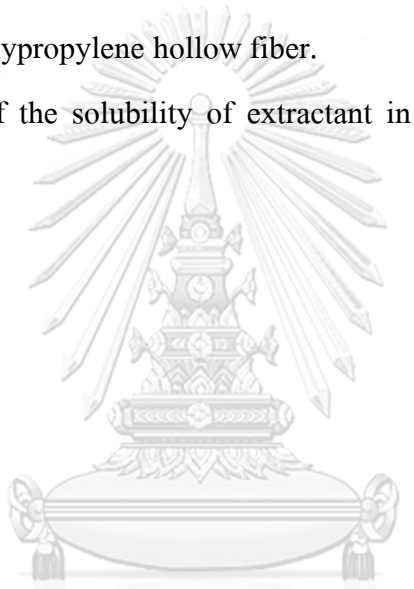

จุฬาลงกรณ์มหาวิทยาลัย
Chulalongkorn University

APPENDICES

จุฬาลงกรณ์มหาวิทยาลัย
Chulalongkorn University

APPENDIX A

List of publications

[1] Vanee Mohdee, Kreangkrai Maneeintr, Thanaporn Wannachod, Suphot Phatanasri, Ura Pancharoen, Optimization of process parameters using response surface methodology for Pd(II) extraction with quaternary ammonium salt from chloride medium: kinetic and thermodynamics study, Chemical Papers 72 (2018) 3129–3139.

[2] Vanee Mohdee, Kreangkrai Maneeintr, Suphot Phatanasri, Ura Pancharoen, Synergistic strippants of Pd (II) ions in the presence of chloride medium from wastewater of electroless plating process via solvating system: Kinetics and thermodynamics study, Separation Science and Technology 54 (17) (2019) 2971-2982.

[3] Vanee Mohdee, Katarína Fulajtárová, Tomáš Soták, Suphot Phatanasri, Milan Hronec, Ura Pancharoen, Solubility modelling and solvent effect on solid-liquid equilibrium of 2,2-bis(hydroxymethyl)butyric acid at different temperatures, Journal of Molecular Liquids. 312 (2020) Article 113370. DOi: https://doi.org/10.1016/j.molliq.2020.113370.

จุฬาลงกรณ์มหาวิทยาลัย
Chulalongkorn University

[4] Vanee Mohdee, Prakorn Ramakul, Suphot Phatanasri, Ura Pancharoen, A numerical and experimental investigation on the selective separation of Pd (II) from wastewater using Aliquat 336 via hollow fiber supported liquid membrane, Journal of Environmental Chemical Engineering. 8 (2020) Article 104234. Doi: https://doi.org/10.1016/j.jece.2020.104234

[5] Thanaporn Wannachod, Vanee Mohdee, Sira Suren, Prakorn Ramakul, Ura Pancharoen, Kasidit Nootong, The separation of Nd (III) from mixed rare earth via

hollow fiber supported liquid membrane and mass transfer analysis, Journal of Industrial and Engineering Chemistry 26 (2015) 214-217.

[6] Thanaporn Wannachod, Phupairum Phuphaibul, Vanee Mohdee, Ura Pancharoen, Suphot Phatanasri, Optimization of synergistic extraction of neodymium ions from monazite leach solution treatment via HFSLM using response surface methodology, Minerals Engineering 77 (2015) 1-9.

[7] Srestha Chaturabul, Thanaporn Wannachod, Vanee Mohdee, Ura Pancharoen, Suphot Phatanasri, An investigation of Calix[4]arene nitrile for mercury (II) treatment in HFSLM application, Chemical Engineering and Processing: Process Intensification 89 (2015) 35-40.

[8] Krirkratthawit Wongkaew, Thanaporn Wannachod, Vanee Mohdee, Ura Pancharoen, Amornchai Arpornwichanop, Anchaleeporn W.Lothongkum, Mass transfer resistance and response surface methodology for separation of platinum (IV) across hollow fiber supported liquid membrane, Journal of Industrial and Engineering Chemistry 42 (2016) 23-35.

[9] Krirkratthawit Wongkaew, Katarína Fulajtárova, Milan Hronec, Vanee Mohdee, Ura Pancharoen, Kasidit Nootong, Measurement of the solubility of the salt of 2-mercaptobenzothiazole with cyclohexylamine and tert-butylamine in various solvents at low temperatures: Models and thermodynamic parameters, Fluid Phase Equilibria 434 (2017) 141-151.

[10] Krirkratthawit Wongkaew, Vanee Mohdee, Ura Pancharoen, Amornchai Arpornwichanop, Anchaleeporn W.Lothongkum, Separation of platinum (IV) across hollow fiber supported liquid membrane using non-toxic diluents: Mass transfer and thermodynamics, Journal of Industrial and Engineering Chemistry 54 (2017) 278-289.

จุฬาลงกรณ์มหาวิทยาลัย
Chulalongkorn University

APPENDIX B

Effect of Temperature on the Equilibrium Solubility of Dimethylolpropionic Acid: Measurement, Correlation, Thermodynamic analysis and Solvent selection

Vanee Mohdee[a,b], Katarína Fulajtárová[b], Tomáš Soták[b], Suphot Phatanasri[a], Milan Hronec[b,c,*], Ura Pancharoen[a,**]

[a]*Department of Chemical Engineering, Faculty of Engineering, Chulalongkorn University, Bangkok 10330, Thailand*

[b]*Department of Organic Technology, Faculty of Chemical and Food Technology, Slovak University of Technology in Bratislava, Radlinského 9, 81237 Bratislava, Slovak Republic*

[c] VUP a.s., Prievidza, Slovak Republic

จุฬาลงกรณ์มหาวิทยาลัย
CHULALONGKORN UNIVERSITY

This article has been submitted in Journal: Journal of Molecular Liquids. *In press*.

B.1 Graphical abstract

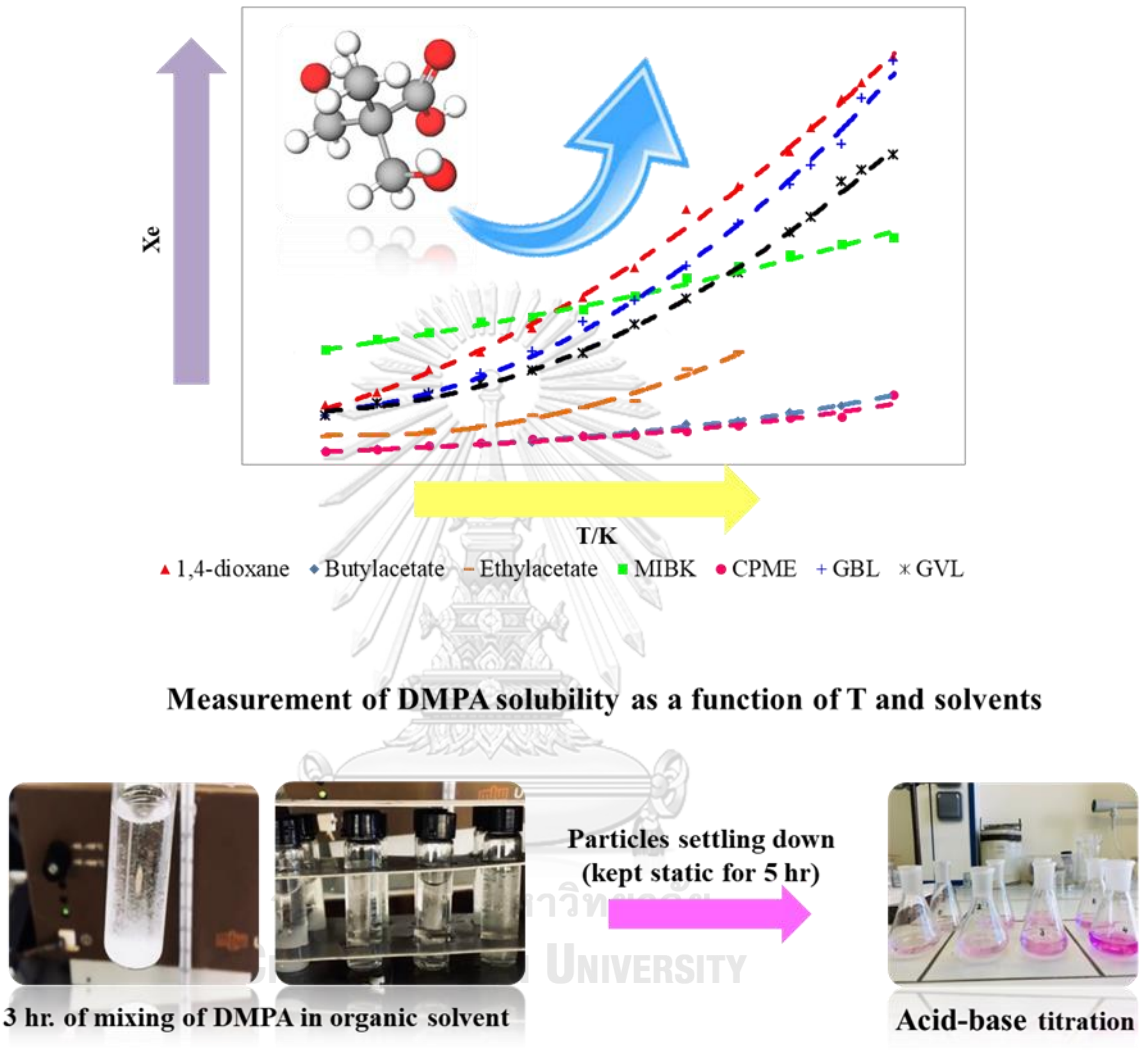

B.2 Abstract

This work highlights the effect of temperature on the equilibrium solubility of dimethylolpropionic acid (DMPA). Results demonstrate that the solubility of DMPA is a function of temperature. It is seen that when temperature increases, molecular interactions between DMPA and solvent molecules are promoted; thereby enhancing the solubility of DMPA. Mole fraction solubility of DMPA in mono solvents from high to low is in the order: 1,4-dioxane > gamma-butyrolactone (GBL) > gamma-valerolactone (GVL) > methyl isobutyl ketone (MIBK) > ethylacetate > butylacetate > cyclopentyl methyl ether (CPME). The experimental solubility data are reported and found to correlate with the Apelblat equation, Buchowski–Książczak λh equation and NRTL model. Additionally, thermodynamic properties of DMPA are analyzed.

Keywords: Dimethylolpropionic acid; 2,2-Bis(hydroxymethyl)propionic acid ; solubility; Apelblat model; λh model; NRTL model.

B.3 Introduction

In recent years, hyperbranched polymers have received much attention. They have been widely applied in diverse areas such as: coatings, additives, drug delivery, adhesives and resins; their structures, chemical and physical properties are unique [1]. In the synthesis of hyperbranched polymers, one feasible, consequential monomer is DMPA, which is also known as 2,2-bis(hydroxymethyl)propionic acid [2-5]. Its structure is shown in **Fig. B.1**. DMPA is a trifunctional compound which consists of one carboxylic group (COOH) and two hydroxyl groups (OH). Its structure has captured the interest of researchers into investigating many polymer reactions. DMPA can be used in pharmaceutical and biotechnology processes since it is a nontoxic solid crystalline hydroxyl acid. DMPA can also be used to provide a carboxylate functional

จุฬาลงกรณ์มหาวิทยาลัย
Chulalongkorn University

group for polyurethane polymers. Moreover, it can be utilized as an intermediate in the synthesis of perfumes and dyes. [6]

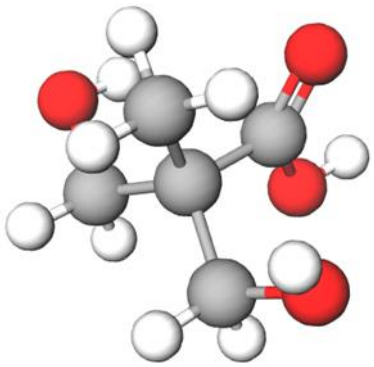

Fig. B.1 The chemical structure of DMPA.

Solubility's dependence on temperature data provides vital information regards the optimization of various processes i.e. purification, crystallization as well as extraction processes. Thus, an investigation on the solubility of a solute in solvents contributes significantly to the design and development of these processes. The solubility of a solute in a solvent depends upon three fundamental factors: namely, temperature, pressure, and the polymorphic property of a solute [7-9]. The viability of equilibrium solubility is based on thermodynamics. Generally, thermodynamic solubility is considered as the concentration of a solute dissolved in a saturated solvent. Hence, the molecular interactions between solute and solvent including their self-interactions can have a significant effect on solubility [7]. Various types of solvents with unique physicochemical properties have been employed in an attempt to enhance solubility. Therefore, the selection of a suitable solvent should provide high solubility.

As yet, an investigation on the effect of temperature and solvents on equilibrium solubility of DMPA has not been reported. In consideration of this, the equilibrium solubility of DMPA is measured at T = (298.15 to 353.15) K, under atmospheric

pressure (101.32 kPa). Various types of mono solvents are employed i.e. ethylacetate, butylacetate, MIBK, CPME, 1,4-dioxane, GBL and GVL. In addition, the effects of solvent properties are examined. However, experimental solubility is time consuming and expensive. Consequently, thermodynamic models are conducted to correlate the equilibrium solubility of DMPA, as a function of temperature. Hence, the Apelblat equation, Buchowski–Książczak λh equation and NRTL model are employed. The accuracy of the models have been elucidated using the root mean square deviation (RMSD). Further, thermodynamic analyses of solubility's dependence on temperature have been evaluated.

B.4 Experimental

B.4.1 Materials

In **Table B.1 and B.2**, the detailed descriptions of DMPA and selected solvents are presented. All information regarding the materials has been provided by the supplier. Distilled water was used in the experiments. All chemicals have been used without further purification.

Table B.1 Detailed information of DMPA. [10]

Properties	
Molecular formula	$C_5H_{10}O_4$
Molar mass ($g \cdot mol^{-1}$)	134.13
Melting point (K)	463.15[b]
Acid value (mg KOH/g)[a]	415.8
Hydroxyl value (mg KOH/g)[a]	831.1
Purity (% wt.)[a]	98.5
Form	white crystalline powder
CAS no.	4767-03-7
Source	VUP a.s., Slovak republic

จุฬาลงกรณ์มหาวิทยาลัย
Chulalongkorn University

Note: No further purification of the studied compounds was conducted.

[a]As stated by supplier (VUP a.s., Slovak republic)

[b]http://www.chemspider.com/Chemical-Structure.70865.html (09/01/2020)

Table B.2 Detailed information of materials used.

Chemicals	Molecular formula	Molar mass* (g·mol^{-1})	Density* (g·mL)	Boiling pt.[c,*] (K)	CAS No.	Mass fraction Purity*	Analytical method	Source
Ethylacetate	$C_4H_8O_2$	88.11	0.90[a]	350.15	141-78-6	≥0.999	GC	Sigma-Aldrich
Butylacetate	$C_6H_{12}O_2$	116.16	0.88[b]	398.15	123-86-4	≥0.990	GC	Sigma-Aldrich
MIBK	$C_6H_{12}O$	100.16	0.80[b]	390.15	108-10-1	0.995	GC	Mikrochem®
CPME	$C_6H_{12}O$	100.16	0.86[a]	379.15	5614-37-9	≥0.999	GC	Sigma-Aldrich
1,4-dioxane	$C_4H_8O_2$	88.11	1.03[a]	374.25	123-91-1	0.990	GC	Centralchem®
GBL	$C_4H_6O_2$	86.09	1.12[a]	477.15	96-48-0	0.990	GC	Acros organics
GVL	$C_5H_8O_2$	100.12	1.05[b]	480.15	108-29-2	0.980	GC	Acros organics

Note: No further purification of the studied compounds was conducted.

*The physical properties data are from chemical bottle labels.

[a]Measured at 298.15 K

[b]Measured at 293.15 K

[c]Measured at 101.32 kPa (atmospheric boiling point)

MIBK, CPME, GBL and GVL are methyl isobutyl ketone, cyclopentyl methyl ether, gamma-butyrolactone and gamma-valerolactone, respectively.

GC = Gas chromatography

จุฬาลงกรณ์มหาวิทยาลัย
Chulalongkorn University

B.4.2 Measurement of equilibrium solubility of DMPA as a function of temperature

The effect of temperature on the equilibrium solubility of DMPA in the selected mono solvents was investigated using a solid-liquid equilibrium method [11]. The experimental procedures followed on from previous work [12]. All experiments were performed in duplicate and repeated three times. Further, a non-aqueous system was introduced since many organic compounds cannot be performed via direct titration in an aqueous system.

The non-aqueous system was studied by employing alcohol in the system. This was done in the interest of the verification of phenolphthalein which in methanolic solutions works adequately in the presence of selected solvents. In addition, titration in methanol solutions using phenolphthalein as an indicator was checked by benzoic acid as standard. Results showed that phenolphthalein could work quite adequately in the studied solvents in the presence of methanol solution. Similarly, Folin et. al. reported that acid compounds can be titrated accurately in organic solvents with basic solution in the presence of alcohol, using phenolphthalein as an indicator [13]. Many works have been performed via titration in non-aqueous systems [14-17].

B.5 Results and discussion

B.5.1 Effect of temperature on the equilibrium solubility of DMPA

In this work, the mole fraction solubility of DMPA with respect to temperature is reported. The experimental solubility mole fraction of a solute (x_e) in various solvents was calculated, as illustrated in our previous work [12]. Results show that the solubility of DMPA is a function of temperature. As temperature increased, the equilibrium solubility of DMPA increased for all investigated solvents. **Fig. B.2** shows DMPA solubility's dependence on temperature in the various solvents, at constant pressure (101.32 kPa).

In **Table B.3**, the experimental values of equilibrium solubility, as a variation of temperature, are listed. The highest solubility of DMPA was found to be in 1,4-dioxane and the lowest solubility was found to be in CPME. The mole fraction of DMPA solubility in these solvents from high to low was in the order: 1,4-dioxane > GBL > GVL > MIBK > ethylacetate > butylacetate > CPME. Thus, at the lower temperature from (298.15 – 318.15) K, MIBK exhibited greater DMPA solubility than

จุฬาลงกรณ์มหาวิทยาลัย
Chulalongkorn University

1,4-dioxane, GBL and GVL. However, when T > 320 K, the solubility of DMPA in MIBK was found to be lower than the latter three solvents.

After the measurement of DMPA solubility, high-performance liquid chromatography technique (HPLC) was employed in order to check the stability and purity of DMPA. It was found that no change of DMPA was observed, indicating that no polymorphic transformations or solvate formations during the experiment proceeded.

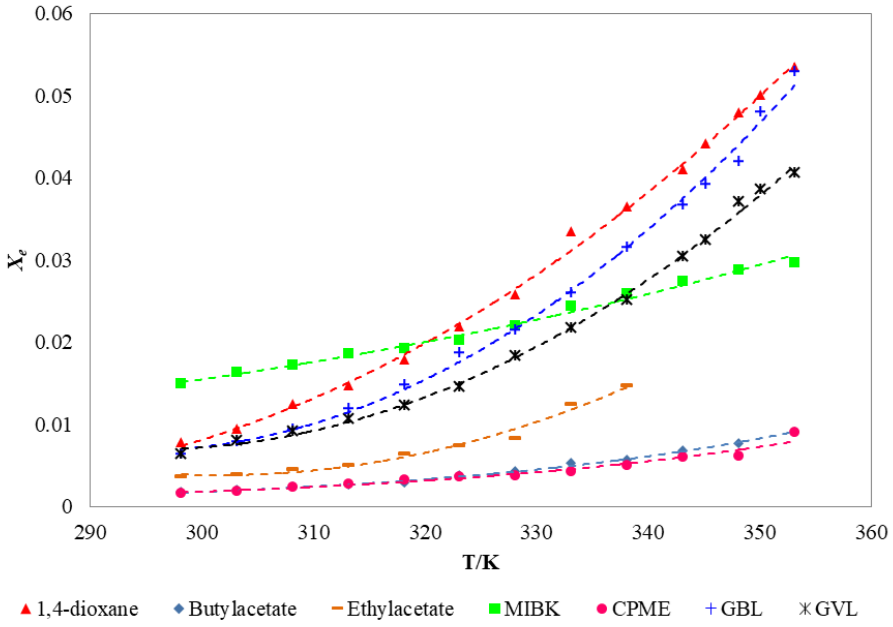

Fig. B.2 Mole fraction solubility (x_e) of DMPA in different solvents, as a function of temperature.

Table B.3 Experimental mole fraction solubility of DMPA in different solvents at temperature range from T = (298.15 to 353.15) K and 101.32 kPa.

T/K	$100x_e$						
	1,4-dioxane	GBL	GVL	Buthyl-acetate	CPME	MIBK	Ethyl-acetate
298.15	0.778	0.637	0.643	0.173	0.164	1.493	0.368
303.15	0.937	0.793	0.800	0.199	0.194	1.637	0.388
308.15	1.243	0.942	0.913	0.234	0.239	1.720	0.447
313.15	1.469	1.195	1.071	0.268	0.276	1.856	0.507
318.15	1.783	1.482	1.236	0.294	0.329	1.924	0.646
323.15	2.192	1.867	1.455	0.381	0.366	2.022	0.745
328.15	2.583	2.143	1.832	0.433	0.381	2.196	0.824
333.15	3.341	2.604	2.180	0.528	0.433	2.439	1.243
338.15	3.648	3.154	2.514	0.572	0.501	2.591	1.469
343.15	4.099	3.668	3.046	0.685	0.598	2.736	-
345.15	4.415	3.922	3.237	-	-	-	-
348.15	4.787	4.204	3.703	0.763	0.621	2.880	-
350.15	5.008	4.804	3.856	-	-	-	-
353.15	5.348	5.292	4.063	0.902	0.906	2.964	-

Note: Standard uncertainties u are u(T) = 0.10 K, u(P) = 0.45 kPa and u(x) = 0.001.

B.5.2 Correlation of DMPA solubility as a variation of temperature

The experimental mole fraction solubility of DMPA, as a function of temperature (constant pressure), in the different mono solvents, was correlated using thermodynamics modelling as follows:

B.5.2.1 The Apelblat equation

The Apelblat equation represents the relationship between the mole fraction solubility of DMPA as a function of temperature. The equation is expressed, as shown in Eq.(B.1) [18]:

$$\ln x = \mathrm{A} + \frac{\mathrm{B}}{T} + \mathrm{Cln}(T) \qquad \text{(B.1)}$$

where x is the mole fraction solubility of DMPA in solvent, T is the absolute temperature and A, B and C are the empirical parameters. Here, a nonlinear regression analysis of experimental mole fraction solubility is applied to solve the empirical parameters.

Table B.4 presents the values for the model parameters A, B and C via the Apelblat equation as well as R^2 and RMSD values. Results show good agreement between the experimental solubility values (x_e) and the calculated molar fraction of DMPA solubility values (x_c). It is noted that the Apelblat equation proved suitable to correlate the solubility of DMPA, over the investigated temperature range, since the largest R^2 and the smallest RMSD values were achieved.

Table B.4 The Apelblat equation parameters for DMPA in various solvents.

Solvents	***A***	***B***	*C*	$\mathbf{R^2}$	**RMSD**
Ethylacetate	-795.127	34,058	118.5202	0.9895	9.7793×10^{-8}
Butylacetate	-101.7342	1,871.1	15.6354	0.9966	8.5324×10^{-9}
MIBK	-36.1942	394.1836	5.3837	0.9925	1.0252×10^{-7}
CPME	-93.0168	1,697.3	14.2101	0.9805	8.9782×10^{-8}
1,4-dioxane	183.8008	-12,171	-25.9512	0.9982	2.7384×10^{-7}
GBL	2.5455	-3,747.5	0.8703	0.9989	2.6357×10^{-7}
GVL	-166.1313	4,683.1	25.5183	0.9983	2.3092×10^{-7}

จุฬาลงกรณ์มหาวิทยาลัย
CHULALONGKORN UNIVERSITY

B.5.2.2 Buchowski–Książczak λh equation

The λh equation is as shown in Eq.(B.2). [18]:

$$\ln\left[1 + \frac{\lambda(1-x)}{x}\right] = \lambda h\left(\frac{1}{T} - \frac{1}{T_m}\right) \quad \text{(B.2)}$$

where λ and h are the empirical parameters, T_m is the melting temperature of DMPA and x is the mole fraction of the DMPA compound in a solvent.

In **Table B.5**, the values of the model parameters and the regression results of the solubility of DMPA in the different solvents are illustrated. The obtained values of λ were found to be very small, confirming that an association of DMPA in solvents was not found during the dissolution process. However, positive values of h indicated that no repulsive interactions between DMPA and the solvents occurred [19]. As shown, the correlated solubility of DMPA had the largest R^2 and the smallest RMSD values.

Table B.5 The λh equation parameters for DMPA in various investigated solvents.

Solvents	λ	h	R^2	**RMSD**
Ethylacetate	0.4442	9,918.4	0.9989	0.0009
Butylacetate	0.1057	33,612	0.9792	0.0007
MIBK	0.0101	40,917	0.9805	0.0005
CPME	0.1231	31,053	0.9985	0.0009
1,4-dioxane	1.0122	4,042.9	0.9980	0.0046
GBL	2.7552	1,990	0.9976	0.0062
GVL	0.8786	5,193.9	0.9981	0.0025

จุฬาลงกรณ์มหาวิทยาลัย
Chulalongkorn University

B.5.2.3 NRTL model

The NRTL model can be described accordingly, as in Eq.(B.3):

$$ln\ x_i = \frac{\Delta_{fus}H}{R}\left(\frac{1}{T_m} - \frac{1}{T}\right) - ln\ \gamma_i \quad \text{(B.3)}$$

where $\Delta_{fus}H$ is the fusion enthalpy of DMPA, T_m is the melting point of DMPA and γ_i is the activity coefficient of the component i in the saturated solution.

The activity coefficient, the parameters of the *NRTL* model (G_{12}, G_{21}) and the dimensionless interaction parameters (τ_{12}, τ_{21}) can be calculated via equations as previously reported [20].

In **Table** B.6, the values of g_{12} and g_{21} (the model parameters) are tabulated. RMSD was calculated to evaluate the accuracy of the model. Thus, the RMSD values were found to be: 3.7438×10^{-6}, 4.1194×10^{-6}, 5.0150×10^{-6}, 3.5594×10^{-6}, 0.0027, 0.0010 and 0.0032 for ethylacetate, butylacetate, CPME, MIBK, GBL, GVL and 1,4-dioxane, respectively. As shown in **Table B.6**, the NRTL model can be applied to correlate the experimental solubility of DMPA regarding the smallest RMSD values.

Table B.6 NRTL parameters for DMPA in various solvents.

T/K	Solvents							
	1-4,-dioxane		GBL		GVL		Ethylacetate	
	g_{12}	g_{21}	g_{12}	g_{21}	g_{12}	g_{21}	g_{12}	g_{21}
298.15	937.73	21399.56	5.34	21580.90	6.17	21527.82	-1.24	24669.33
303.15	1005.23	20685.06	63.87	20650.78	416.33	21066.19	3.91	24717.89
308.15	1241.14	19476.34	171.26	20001.01	551.29	20688.41	67.22	24303.58
313.15	1302.55	18740.49	453.55	19144.48	680.74	20099.09	98.06	23917.54
318.15	1311.66	17736.44	520.92	18002.76	888.88	19634.29	554.86	23254.69
323.15	1303.02	16500.20	671.89	16721.44	1210.51	19076.74	970.37	22999.41
328.15	1889.77	15899.33	735.32	15729.01	3001.62	18366.11	1399.72	22901.01
333.15	2134.81	14029.11	1131.78	14801.75	3217.23	17386.19	2971.11	20961.45
338.15	2474.09	12892.88	1638.99	13102.31	3301.03	16500.88	6491.83	19356.64
343.15	3100.21	12290.16	3111.19	12820.66	3330.51	14994.59	-	-
345.15	3150.77	12130.34	3119.57	12611.12	3390.86	14315.67	-	-
348.15	3206.99	11932.22	3228.79	12370.23	3412.12	12909.59	-	-
350.15	3278.11	11843.25	3226.03	11988.11	3087.71	12793.38	-	-
353.15	3210.02	11593.03	3281.92	11686.34	3195.80	12794.90	-	-

T/K	Solvents					
	Butylacetate		CPME		MIBK	
	g_{12}	g_{21}	g_{12}	g_{21}	g_{12}	g_{21}
298.15	-88.95	28727.36	-139.34	28965.16	3112.47	18396.55
303.15	139.46	28598.21	-44.55	28559.05	3126.28	18113.03
308.15	155.84	28114.57	21.89	27861.66	3144.70	18032.61
313.15	171.22	27736.87	90.17	27492.41	3165.39	17781.11
318.15	191.27	27583.91	159.03	26897.99	3190.34	17736.83
323.15	1120.03	27055.35	171.26	26611.08	3217.58	17591.85
328.15	1584.34	26817.09	183.42	26711.13	3344.23	17201.92
333.15	1894.74	26044.72	195.77	26246.22	3433.45	16609.06
338.15	1986.29	25896.44	204.80	25630.03	3560.78	16244.59
343.15	2267.56	25133.11	282.66	24822.47	3677.93	15848.69
348.15	2506.31	24763.57	351.29	24923.06	3752.48	15360.19
353.15	3013.88	23977.92	390.81	22473.62	3839.35	14880.76

Note: The tunable parameter; α_{ij}, is the solution non-randomness and was considered to be 0.47 [21].

จุฬาลงกรณ์มหาวิทยาลัย
Chulalongkorn University

B.5.3 Model comparison

In **Fig.B.3**, the calculated mole fraction solubility data of DMPA obtained for all 3 models are used for comparison with the experimental mole fraction solubility data. As graphically shown, as temperature increased, the calculated mole fraction solubility of DMPA, obtained via λh equation, slightly differed from the experimental results.

In **Table B.7**, the values of the experimental mole fraction solubility (x_e) as well as the correlated solubility (x_c) of DMPA in different solvents, at an elevated temperature range, are presented.

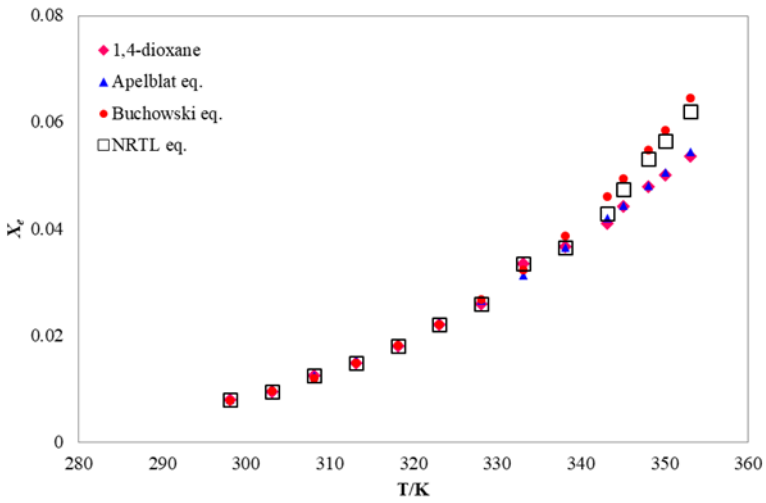

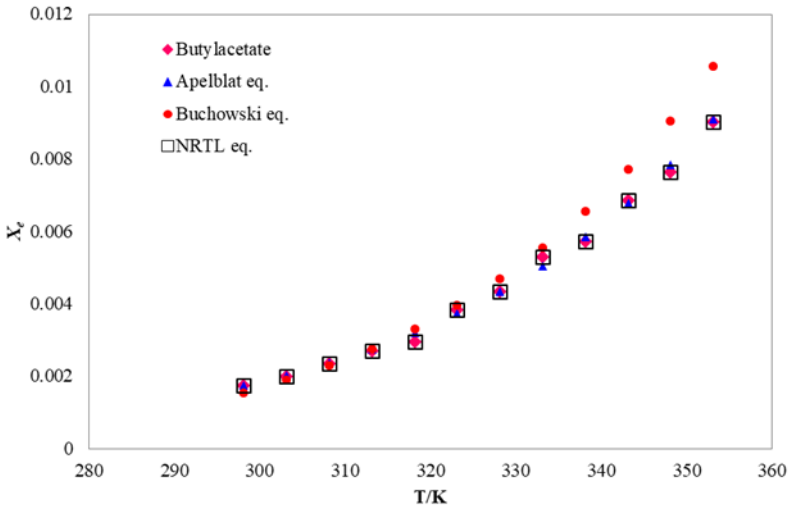
0.012
0.01
0.008
0.006
0.004
0.002
0
X_e
Butylacetate
Apelblat eq.
Buchowski eq.
NRTL eq.
280
290
300
310
320
330
340
350
360
T/K

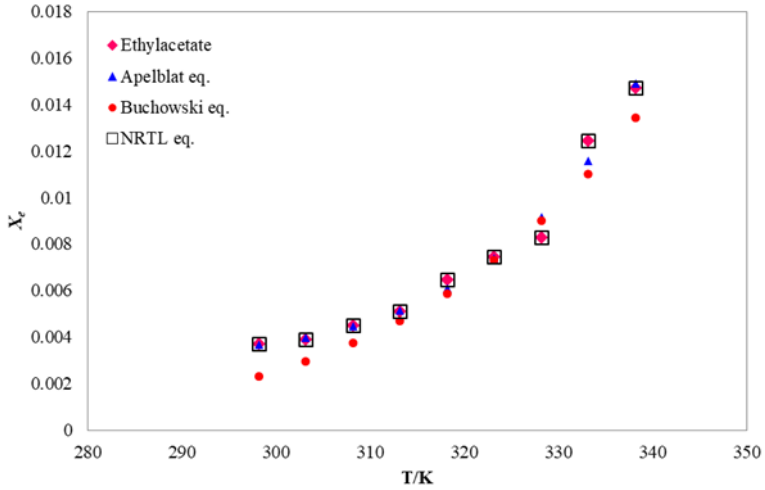
0.018
0.016
0.014
0.012
0.01
0.008
0.006
0.004
0.002
0
X_e
Ethylacetate
Apelblat eq.
Buchowski eq.
NRTL eq.
280
290
300
310
320
330
340
350
T/K

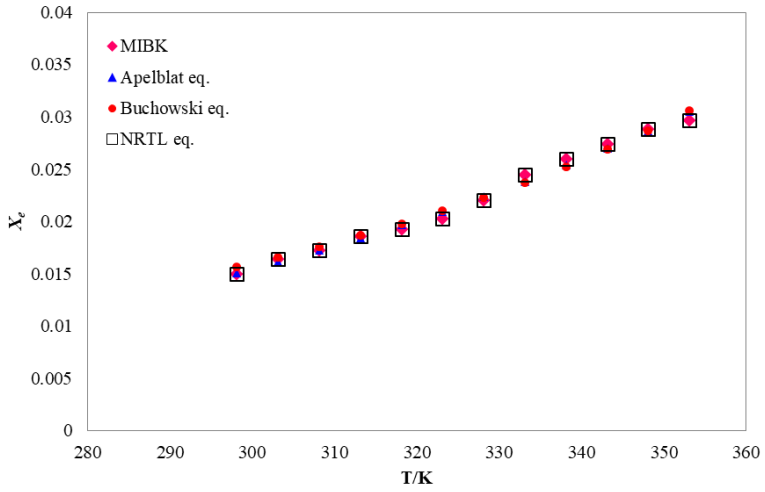
0.04
0.035
0.03
0.025
0.02
0.015
0.01
0.005
0
x_e
MIBK
Apelblat eq.
Buchowski eq.
NRTL eq.
280
290
300
310
320
330
340
350
360
T/K

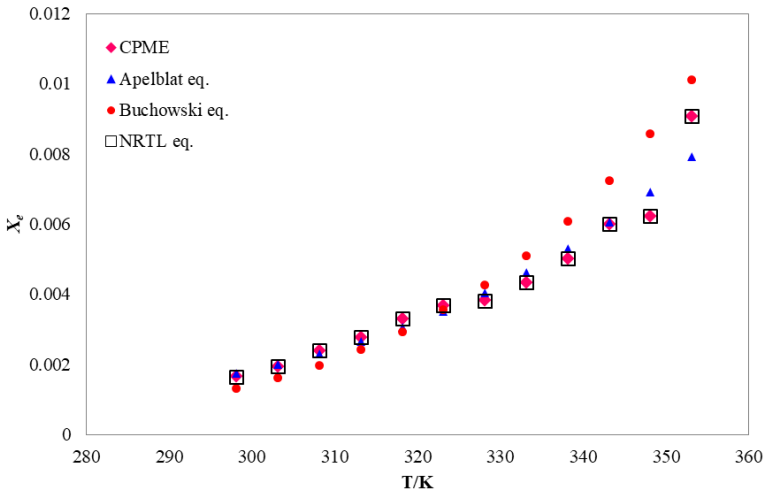
0.012
0.01
0.008
0.006
0.004
0.002
0
x_e
CPME
Apelblat eq.
Buchowski eq.
NRTL eq.
280
290
300
310
320
330
340
350
360
T/K

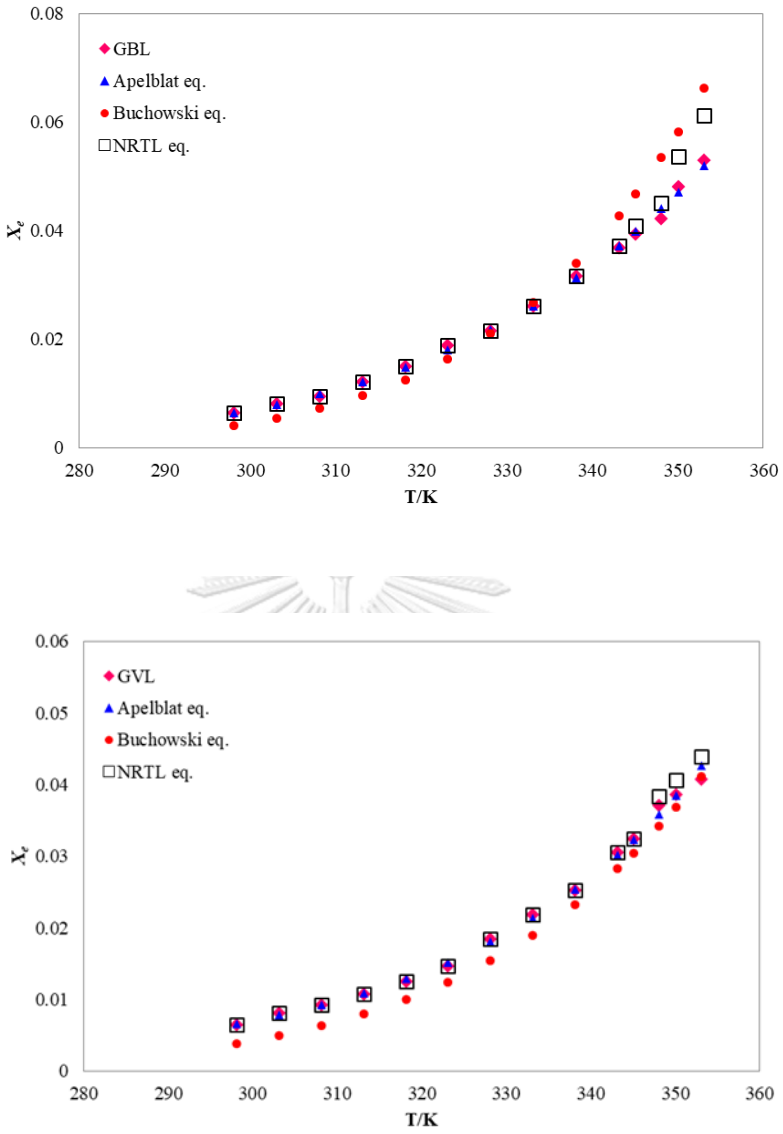

Fig. B.3 Experimental mole fraction solubility (x_e) and the calculated mole fraction solubility of DMPA in different solvents, as a function of temperature.

Table B.7 Experimental mole fraction solubility (x_e) and correlated solubility (x_c) of DMPA in different solvents at temperature range from T = (298.15 to 353.15) K and atmospheric pressure (101.325 kPa)

T/K	$100x_e$	$100x_{c,\ Apelblat}$	$100x_{c,\ \lambda h}$	$100x_{c,\ NRTL}$
		1,4-dioxane		
298.15	0.7782	0.7593	0.7614	0.7779
303.15	0.9373	0.9670	0.9549	0.9373
308.15	1.2430	1.2133	1.1886	1.2430
313.15	1.4695	1.5012	1.4693	1.4699
318.15	1.7835	1.8331	1.8042	1.7840
323.15	2.1926	2.2106	2.2014	2.1934
328.15	2.5831	2.6345	2.6698	2.5829
333.15	3.3418	3.1047	3.2191	3.3417
338.15	3.6483	3.6202	3.8600	3.6478
343.15	4.0996	4.1789	4.6039	4.2777
345.15	4.4153	4.4139	4.9331	4.7354
348.15	4.7873	4.7781	5.4634	5.2994
350.15	5.0084	5.0282	5.8425	5.6464
353.15	5.3479	5.4138	6.4519	6.1870
		gamma-butyrolactone		
298.15	0.6377	0.6313	0.3925	0.6376
303.15	0.7929	0.7881	0.5311	0.7930
308.15	0.9420	0.9769	0.7114	0.9416
313.15	1.1953	1.2031	0.9437	1.1947
318.15	1.4820	1.4722	1.2403	1.4820
323.15	1.8677	1.7906	1.6154	1.8676
328.15	2.1434	2.1655	2.0857	2.1426
333.15	2.6046	2.6044	2.6700	2.6047
338.15	3.1546	3.1158	3.3897	3.1550

จุฬาลงกรณ์มหาวิทยาลัย
CHULALONGKORN UNIVERSITY

T/K	$100x_e$	$100x_{c,\ Apelblat}$	$100x_{c,\ \lambda_h}$	$100x_{c,\ NRTL}$
343.15	3.6678	3.7089	4.2685	3.7054
345.15	3.9222	3.9712	4.6703	4.0704
348.15	4.2041	4.3937	5.3321	4.4974
350.15	4.8044	4.6957	5.8154	5.3604
353.15	5.2930	5.1809	6.6079	6.1084
		gamma-valerolactone		
298.15	0.6433	0.6531	0.3766	0.6426
303.15	0.8008	0.7705	0.4849	0.8012
308.15	0.9134	0.9104	0.6191	0.9132
313.15	1.0712	1.0770	0.7845	1.0709
318.15	1.2368	1.2756	0.9867	1.2373
323.15	1.4552	1.5122	1.2322	1.4554
328.15	1.8326	1.7943	1.5287	1.8326
333.15	2.1807	2.1304	1.8844	2.1806
338.15	2.5144	2.5309	2.3090	2.5144
343.15	3.0468	3.0082	2.8124	3.0467
345.15	3.2374	3.2239	3.0387	3.2372
348.15	3.7035	3.5769	3.4071	3.8243
350.15	3.8567	3.8338	3.6733	4.0543
353.15	4.0637	4.2543	4.1058	4.3811
		Butylacetate		
298.15	0.1732	0.1704	0.1535	0.1726
303.15	0.1992	0.1993	0.1873	0.1993
308.15	0.2339	0.2329	0.2273	0.2335
313.15	0.2686	0.2719	0.2743	0.2691
318.15	0.2945	0.3171	0.3294	0.2945
323.15	0.3812	0.3694	0.3936	0.3813
328.15	0.4333	0.4300	0.4682	0.4329

จุฬาลงกรณ์มหาวิทยาลัย
Chulalongkorn University

T/K	$100x_e$	$100x_{c,\ Apelblat}$	$100x_{c,\ \lambda_h}$	$100x_{c,\ NRTL}$
333.15	0.5287	0.5001	0.5546	0.5292
338.15	0.5720	0.5809	0.6546	0.5721
343.15	0.6849	0.6742	0.7700	0.6854
348.15	0.7630	0.7816	0.9028	0.7634
353.15	0.9019	0.9052	1.0557	0.9023
		Cyclopentyl methyl ether		
298.15	0.1643	0.1728	0.1290	0.1637
303.15	0.1942	0.1993	0.1597	0.1935
308.15	0.2391	0.2296	0.1965	0.2386
313.15	0.2765	0.2643	0.2402	0.2774
318.15	0.3289	0.3040	0.2921	0.3288
323.15	0.3663	0.3493	0.3533	0.3662
328.15	0.3813	0.4011	0.4252	0.3805
333.15	0.4337	0.4601	0.5094	0.4335
338.15	0.5011	0.5273	0.6076	0.5013
343.15	0.5986	0.6038	0.7220	0.5987
348.15	0.6211	0.6907	0.8549	0.6205
353.15	0.9063	0.7895	1.0090	0.9062
		Methyl isobutyl ketone		
298.15	1.4935	1.5026	1.5571	1.4939
303.15	1.6369	1.6079	1.6514	1.6372
308.15	1.7200	1.7193	1.7518	1.7201
313.15	1.8560	1.8370	1.8587	1.8558
318.15	1.9241	1.9614	1.9730	1.9238
323.15	2.0225	2.0926	2.0953	2.0225
328.15	2.1967	2.2311	2.2265	2.1966
333.15	2.4394	2.3771	2.3676	2.4385
338.15	2.5913	2.5309	2.5197	2.5910

จุฬาลงกรณ์มหาวิทยาลัย
Chulalongkorn University

T/K	$100x_e$	$100x_{c,\ Apelblat}$	$100x_{c,\ \lambda h}$	$100x_{c,\ NRTL}$
343.15	2.7358	2.6929	2.6840	2.7357
348.15	2.8804	2.8634	2.8622	2.8798
353.15	2.9641	3.0427	3.0560	2.9641
		Ethylacetate		
298.15	0.3685	0.3640	0.2304	0.3687
303.15	0.3883	0.3972	0.2943	0.3881
308.15	0.4477	0.4460	0.3729	0.4477
313.15	0.5071	0.5145	0.4691	0.5074
318.15	0.6459	0.6088	0.5860	0.6458
323.15	0.7452	0.7374	0.7273	0.7447
328.15	0.8246	0.9133	0.8971	0.8253
333.15	1.2430	1.1548	1.1001	1.2426
338.15	1.4695	1.4887	1.3417	1.4699

B.5.4 Characterization of DMPA via DSC analysis

Differential scanning calorimetry (DSC) is a practical technique to analyze the thermal behavior and crystallization of a solid compound. In this work, DSC (Perkin Elmer) was carried out to evaluate the polymorphic transitions of DMPA in the various solvents. In order to achieve high accurate results, calibration of DSC was conducted. A calibration for the calorimeter was determined by constructing a curve of the transition/fusion temperatures of reference materials. In this work, the temperature scale of the calorimeter was calibrated to the fusion point of Indium and Zinc. The enthalpy scale was calibrated to the enthalpy of fusion of Indium.

As shown in **Fig. B.4**, the transition temperatures of DMPA before recrystallization (1A) were found to be 425.65 K, 455.65 K and 463.15 K. **Fig. B.4** also depicts the transition temperatures of DMPA after recrystallization (1B) i.e. 423.95 K, 457.15 K and 466.15 K. Thus, when T>463.15 K, before recrystallization

(1A), and when T>466.15 K, after recrystallization (1B), the DMPA sample melts through decomposition/evaporation. In **Fig. B.4-(1A)**, when T > 475.65 K, the DMPA sample begins to decompose. The uncertainty for the solid-to-solid phase transition temperature was found to be 4.34 K. It is acknowledged that onset temperature can have wide uncertainty values [22].

The temperature of solid-solid transition of DMPA has been reported previously. Murrill and Breed [23] pointed out that the transition temperature and fusion temperature/melting of DMPA occurred at (425.15-428.15) K and (467.15-470.15) K, respectively. Meanwhile, Haillot et. al. [24] showed that DMPA began to melt at 470.15 K. It is noted that the melting point value of DMPA obtained in this work (T_m = 463.15 K) is in line with various research findings, as regards the experimental melting point of DMPA. Many works have demonstrated the melting point of DMPA to be in the range (455.15 – 464.15) K [10]. Riemschneider's work, for instance, recorded a melting temperature of 456.15 K [25]. Thus, it is recognized that the different sources of DMPA, different testing devices and methods of measurement can lead to deviations in the transition temperature and fusion temperature/melting temperature.

The value of fusion enthalpy was calculated from the DSC curve. Herein, the experimental enthalpy of fusion of DMPA was found to be 3.54 kJ·mol^{-1} which is much closer to the value of fusion enthalpy as stated previously. Murrill and Breed also recorded the value of fusion enthalpy as 3.59 kJ·mol^{-1} [23]. Hence, the obtained value of fusion enthalpy was used to calculate the excess enthalpy of solutions. The enthalpy of the phase transition was also determined from the DSC curve by consolidating the area under the endothermic peaks [26]. The experimental enthalpy of the phase transition of DMPA was 37.79 kJ·mol^{-1}. Waschull et. al. [27] summarized the transition enthalpy of DMPA in the range (35.28-38.90) kJ·mol^{-1} at (425.15-426.15) K, which was found to be in agreement with the results obtained in this work. The

จุฬาลงกรณ์มหาวิทยาลัย
CHULALONGKORN UNIVERSITY

standard uncertainties for the measured enthalpy of transition and fusion were ±0.13 and ±0.50 kJ·mol^{-1}, respectively.

In **Fig. B.5**, the results of DSC analysis of DMPA before and after solubility experiments are given. Results, obtained from the DSC curve, revealed that during the experiment no change of DMPA was observed, indicating no polymorphic transformations of DMPA in the solvents took place.

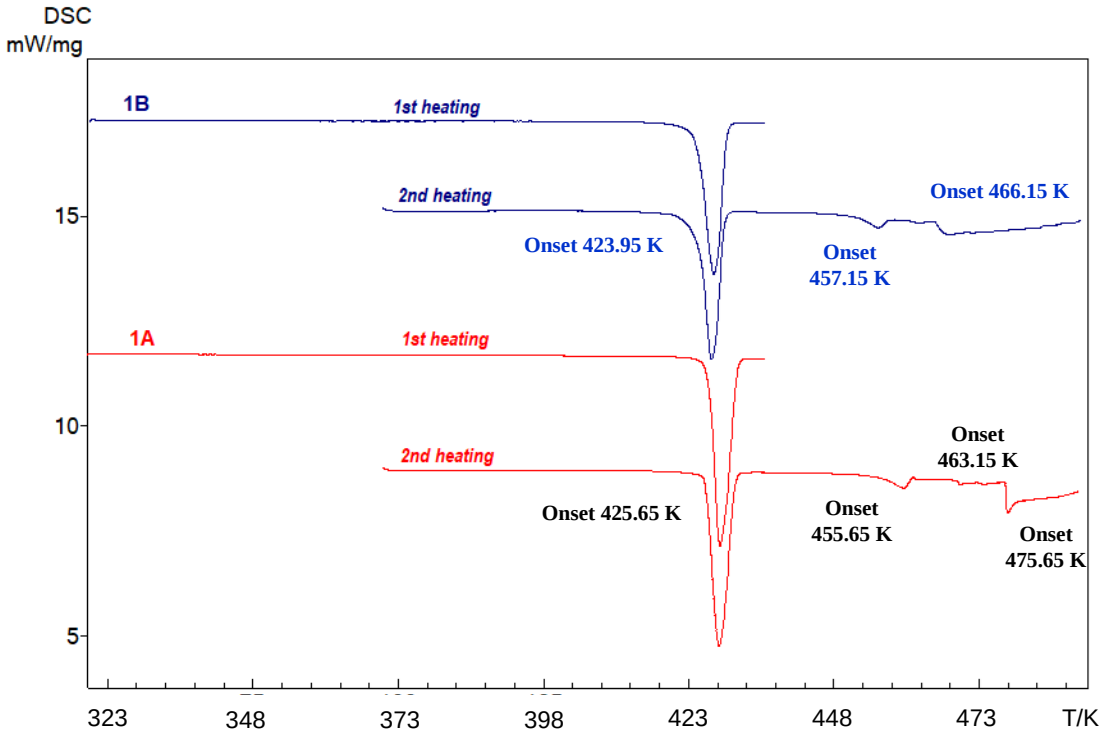

Fig. B.4. DSC thermograms of DMPA: Before recrystallization (1A) and after recrystallization (1B).

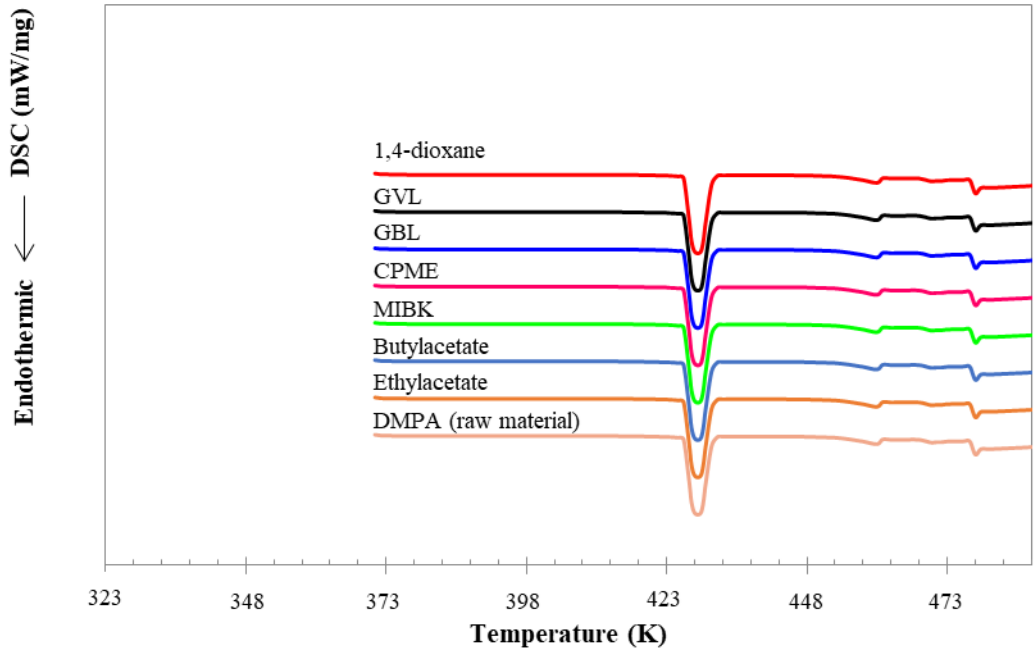

Fig. B.5. DSC thermograms of DMPA: Original sample and equilibrium bottom solid phases in different solvents.

B.5.5 Characterization of DMPA via DSC analysis

The values of dissolution enthalpy ($\Delta_{sol}H$) and dissolution entropy ($\Delta_{sol}S$) of DMPA were evaluated using Van't Hoff equation along with the parameters from the Apelblat equation. The equations have been reported elsewhere by several researchers [28, 29]. On the basis of such assumptions, the numerical values of $\Delta_{sol}G$ were found to be zero, indicating $\Delta_{sol}G$ is independent of temperature and the system is at equilibrium.

In **Table B.8**, both temperature and types of solvent had an effect on the dissolution process of DMPA. Positive values of $\Delta_{sol}H$ indicated that the dissolution of DMPA in selected solvents is an endothermic process. Besides, the $\Delta_{sol}H$ values revealed that the molecular interactions between DMPA and solvent molecules are stronger than the self-interactions between solvent-solvent and DMPA-DMPA

molecules. Thus, more energy is required in order to overcome the cohesive forces of DMPA and solvent molecules [30-32]. Likewise, the values of $\Delta_{sol}S$ were also found to be positive which proved that the dissolution process of DMPA is an entropy-driven process [33]. Results showed that the dissolution of DMPA in selected solvents favored the entropy process [33, 34].

In **Fig. B.6**, the dissolution properties of DMPA in the various mono solvents, as a function of temperature, are graphically shown. The effect of temperature on the apparent thermodynamics of dissolution functions is described as follows. As temperature increased, the system was found to be in more disorder. Consequently, the values of $\Delta_{sol}S$ increased; thereby demonstrating that DMPA distorted the solvent molecules [35]. However, the values of $\Delta_{sol}S$ were found to be lower than the values of $\Delta_{sol}H$. Similar results have previously been described [36, 37]. Further, it was noted that the values of $\Delta_{sol}H$ for the six mono solvents were seen to increase, as temperature increased, except for 1,4-dioxane. The values of $\Delta_{sol}S$ for the selected solvents were also seen to increase, except for 1,4-dioxane and GBL. The increase in dissolution entropy caused by the solute molecules distorted the alignment of the solvent molecules. Thus, different molecular structures resulted in various kinds of interactions between the solute and solvent molecules such as dipole–dipole, hydrogen bond formation, hydrophobic interactions, and stereoscopic effects [38]. When T = 298.15 K, enthalpies of dissolution from low to high were in the range of: MIBK < ethylacetate < CPME < butylacetate < GVL < GBL < 1,4-dioxane. This implied that the interaction between DMPA and 1,4-dioxane was stronger than that in other solvents.

จุฬาลงกรณ์มหาวิทยาลัย
CHULALONGKORN UNIVERSITY

Table B.8 Apparent thermodynamic parameters: molar enthalpy, $\Delta_{sol}H$ (kJ·mol^{-1}), and molar entropy, $\Delta_{sol}S$ (J·mol^{-}1·K^{-1}), for DMPA in various solvents at different temperatures and 101.32 kPa.

	Solvents							
***T*/K**	1,4-dioxane		GBL		GVL		Ethylacetate	
	$\Delta_{sol}H$	$\Delta_{sol}S$	$\Delta_{sol}H$	$\Delta_{sol}S$	$\Delta_{sol}H$	$\Delta_{sol}S$	$\Delta_{sol}H$	$\Delta_{sol}S$
298.15	36.86	123.6	33.31	111.7	24.32	81.57	10.63	35.66
303.15	35.78	118.0	33.35	110.0	25.38	83.72	15.55	51.32
308.15	34.70	112.6	33.38	108.3	26.44	85.80	20.48	66.48
313.15	33.62	107.3	33.42	106.7	27.50	87.82	25.41	81.15
318.15	32.54	102.3	33.45	105.1	28.56	89.78	30.33	95.36
323.15	31.46	97.37	33.49	103.6	29.62	91.67	35.26	109.1
328.15	30.39	92.60	33.53	102.2	30.68	93.50	40.19	122.4
333.15	29.30	87.98	33.56	100.7	31.74	95.29	45.12	135.4
338.15	28.23	83.48	33.60	99.37	32.80	97.01	50.04	148.0
343.15	27.15	79.12	33.64	98.03	33.86	98.69	-	-
345.15	26.72	77.41	33.65	97.50	34.29	99.35	-	-
348.15	26.07	74.89	33.67	96.73	34.92	100.3	-	-
350.15	25.64	73.23	33.69	96.21	35.35	100.9	-	-
353.15	24.99	70.77	33.71	95.46	35.99	101.9	-	-

	Solvents					
***T*/K**	Buthylacetate		CPME		MIBK	
	$\Delta_{sol}H$	$\Delta_{sol}S$	$\Delta_{sol}H$	$\Delta_{sol}S$	$\Delta_{sol}H$	$\Delta_{sol}S$
298.15	23.20	77.81	21.11	70.81	10.07	33.76
303.15	23.85	78.67	21.70	71.59	10.29	33.95
308.15	24.50	79.51	22.29	72.35	10.51	34.12
313.15	25.15	80.31	22.88	73.08	10.74	34.29
318.15	25.80	81.09	23.47	73.78	10.96	34.45
323.15	26.45	81.85	24.06	74.47	11.18	34.61
328.15	27.10	82.58	24.65	75.14	11.41	34.77
333.15	27.75	83.29	25.24	75.78	11.63	34.92
338.15	28.40	83.99	25.84	76.41	11.85	35.06
343.15	29.05	84.66	26.43	77.02	12.08	35.21
348.15	29.70	85.31	27.02	77.61	12.30	35.34
353.15	30.35	85.94	27.61	78.18	12.53	35.48

จุฬาลงกรณ์มหาวิทยาลัย
Chulalongkorn University

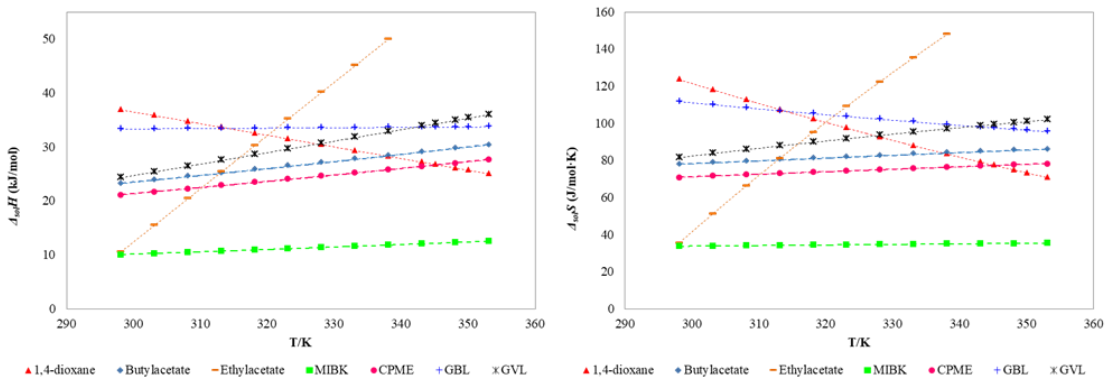

Fig. B.6. Dissolution properties of DMPA as a function of temperature, in various mono solvent.

B.5.6 Excess enthalpy of solutions

The excess enthalpy of solutions (H^E) can be exploited to provide a better understanding of solution behavior. Using Buchowski et al.'s equation [39], the general formula based on an implicit function of temperature is shown below, as in Eq.(B.4):

$$\left(\frac{\partial \ln(1-a_B)}{\partial T^{-1}}\right)_y = \left(\frac{\partial \ln(1-a_B)}{\partial \ln a_A}\right)_T \left(\frac{\partial \ln a_A}{\partial T^{-1}}\right)_y + \left(\frac{\partial \ln(1-a_B)}{\partial T^{-1}}\right)_{a_A} \quad \text{(B.4)}$$

จุฬาลงกรณ์มหาวิทยาลัย
CHULALONGKORN UNIVERSITY

Together with the Gibbs-Duhem equation, λ can be expressed, as in Eq.(B.5):

$$\lambda = \frac{a_B}{1-a_B}\frac{x_A}{x_B} = \left(\frac{\partial \ln(1-a_B)}{\partial \ln a_A}\right)_T \quad \text{(B.5)}$$

Therefore, the enthalpy of fusion of A and the enthalpy of mixing, as a function of temperature, are obtained, as shown in Eqs.(B.6) and (B.7), respectively:

$$-\frac{\mathrm{d}\ln a_A^{sat}}{\mathrm{d}T^{-1}} = \frac{\Delta_m H_A^f}{R} \quad \text{(B.6)}$$

$$\frac{H^E}{R} = \left(\frac{\partial(G^M/RT)}{\partial T^{-1}}\right)_{x_A} = \left(\frac{\partial(x_A \ln a_A + x_B \ln a_B)}{\partial T^{-1}}\right)_{x_A} \quad \text{(B.7)}$$

Finally, Eq.(B.8) was obtained:

$$\lambda h = -\frac{d \ln(1-a_B)_{sat}}{dT^{-1}} \quad \text{(B.8)}$$

Thus, the equation of H^E derived from Buchowski equation is given [39, 40]:

$$hR = \Delta_{fus}H + H^E/x \quad \text{(B.9)}$$

where $\Delta_{fus}H$ is the fusion enthalpy of DMPA. In this work, the experimental value of fusion enthalpy, obtained via DSC, was applied to calculate the excess enthalpy of solutions.

In **Table B.9**, the calculated H^E is presented. As temperature increased, the values of H^E were found to increase for all solvents, as depicted in **Fig. B.7**. Positive values of H^E indicated that dissolution is an endothermic process with various kinds of interactions in solution [40]. Further, the values of excess enthalpy, using the value of fusion enthalpy from literature [23], were calculated and then compared with the values obtained in this work. Excess enthalpy values followed the same pattern.

Table B.9 Excess enthalpy of DMPA in selected solvents at various temperatures and 101.32 kPa.

T/K	H^E/kJ·mol^{-1}											
	1,4-dioxane			GBL			GVL			Ethylacetate		
	This work	Literature (cal.)	%S.D.	This work	Literature (cal.)	%S.D.	This work	Literature (cal.)	%S.D.	This work	Literature (cal.)	%S.D.
298.15	0.234	0.233	0.427	0.083	0.083	0.000	0.255	0.254	0.392	0.291	0.290	0.343
303.15	0.282	0.281	0.356	0.103	0.103	0.000	0.317	0.317	0.000	0.306	0.306	0.000
308.15	0.374	0.373	0.267	0.122	0.122	0.000	0.362	0.361	0.276	0.353	0.353	0.000
313.15	0.442	0.441	0.226	0.155	0.155	0.000	0.425	0.424	0.235	0.400	0.400	0.000
318.15	0.536	0.535	0.187	0.193	0.192	0.518	0.490	0.490	0.000	0.510	0.509	0.196
323.15	0.659	0.658	0.152	0.243	0.242	0.411	0.577	0.576	0.173	0.588	0.588	0.000
328.15	0.777	0.775	0.257	0.279	0.277	0.712	0.727	0.725	0.275	0.651	0.650	0.153
333.15	1.005	1.003	0.199	0.339	0.337	0.590	0.864	0.863	0.115	0.981	0.980	0.102
338.15	1.097	1.095	0.182	0.410	0.408	0.488	0.997	0.995	0.200	1.160	1.159	0.086
343.15	1.233	1.230	0.243	0.477	0.475	0.419	1.208	1.206	0.165	-	-	-
345.15	1.328	1.325	0.226	0.510	0.508	0.392	1.283	1.281	0.156	-	-	-
348.15	1.440	1.437	0.208	0.547	0.544	0.548	1.468	1.466	0.136	-	-	-
350.15	1.506	1.503	0.199	0.625	0.622	0.480	1.529	1.527	0.130	-	-	-
353.15	1.608	1.605	0.186	0.688	0.685	0.436	1.611	1.609	0.124	-	-	-

T/K	H^E/kJ·mol^{-1}								
	Buthylacetate			CPME			MIBK		
	This work	Literature (cal.)	%S.D	This work	Literature (cal.)	%S.D.	This work	Literature (cal.)	%S.D.
298.15	0.478	0.478	0.000	0.418	0.418	0.000	5.028	5.027	0.020
303.15	0.550	0.550	0.000	0.495	0.494	0.202	5.510	5.510	0.000
308.15	0.645	0.645	0.000	0.609	0.609	0.000	5.790	5.789	0.017
313.15	0.741	0.741	0.000	0.704	0.704	0.000	6.248	6.247	0.016
318.15	0.813	0.812	0.123	0.837	0.837	0.000	6.477	6.476	0.015
323.15	1.052	1.052	0.000	0.933	0.932	0.107	6.808	6.807	0.014
328.15	1.195	1.195	0.000	0.971	0.971	0.000	7.395	7.394	0.013
333.15	1.459	1.458	0.068	1.104	1.104	0.000	8.212	8.211	0.012
338.15	1.578	1.578	0.000	1.276	1.276	0.000	8.723	8.722	0.011
343.15	1.890	1.889	0.053	1.524	1.523	0.065	9.210	9.208	0.021
348.15	2.105	2.104	0.047	1.581	1.581	0.000	9.697	9.695	0.020
353.15	2.488	2.488	0.000	2.308	2.307	0.043	9.979	9.977	0.020

Note: The experimental value of fusion enthalpy was applied to calculate the excess enthalpy of solutions compared with the calculated excess enthalpy using fusion enthalpy value from literature [23].

จุฬาลงกรณ์มหาวิทยาลัย
Chulalongkorn University

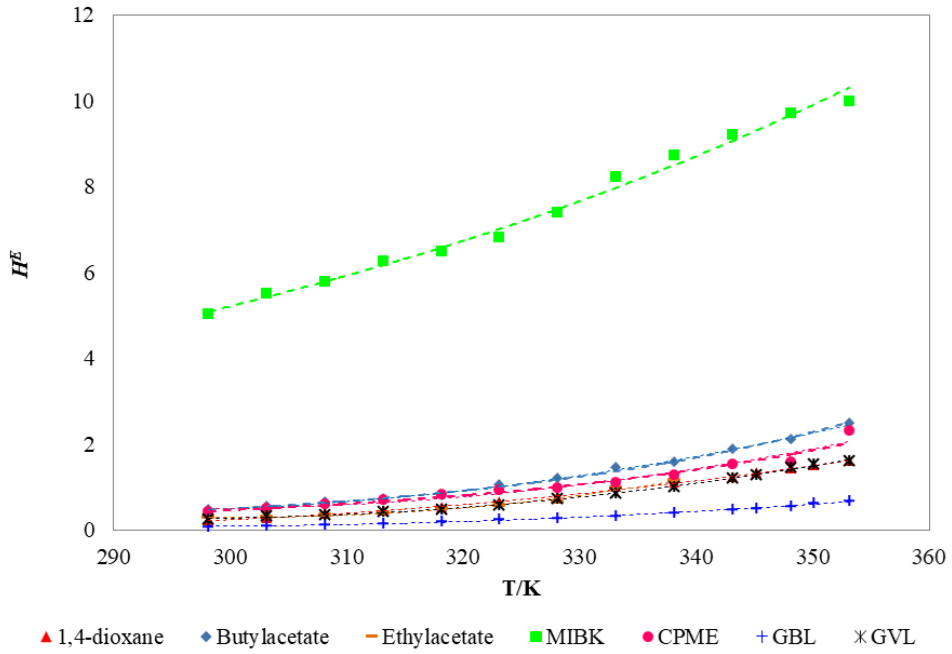

Fig. B.7. Excess enthalpy of solutions as a function of temperature.

B.5.7 Gibbs free energy of mixing

Gibbs free energy of mixing of real solution can be determined, as shown below: [41]

$$\Delta_{mix}G = \Delta_{mix}G^{id} + G^{E} \qquad \text{(B.10)}$$

where $G^E = RT\sum_i^N x_i \ln \gamma_i$

In **Table B.10**, the values of Gibbs free energy of mixing of DMPA in solvents are evaluated. In **Fig. B.8,** the relationship between the Gibbs free energy of mixing and temperature is represented. As shown, the values of $\Delta_{mix}G$ in all solvents are negative and decrease as temperature increased, indicating a spontaneous and favorable mixing process of DMPA.

Table B.10 Gibbs free energy of mixing ($\Delta_{mix}G$) of DMPA in selected solvents.

T/K	$\Delta_{mix}G$ (J·mol^{-1})						
	1,4-dioxane	GBL	GVL	Buthyl-acetate	CPME	MIBK	Ethyl-acetate
298.15	-28.37	-23.33	-23.54	-6.432	-6.104	-53.50	-13.59
303.15	-34.04	-28.90	-29.19	-7.395	-7.212	-58.44	-14.32
308.15	-44.80	-34.21	-33.20	-8.678	-8.870	-61.28	-16.49
313.15	-52.67	-43.13	-38.78	-9.959	-10.25	-65.91	-18.66
318.15	-63.43	-53.09	-44.59	-10.92	-12.17	-68.20	-23.67
323.15	-77.20	-66.27	-52.17	-14.10	-13.55	-71.49	-27.24
328.15	-90.08	-75.52	-65.06	-16.00	-14.11	-77.30	-30.08
333.15	-114.4	-90.73	-76.73	-19.47	-16.03	-85.30	-44.81
338.15	-123.9	-108.4	-87.72	-21.05	-18.49	-90.23	-52.65
343.15	-137.9	-124.4	-104.8	-25.12	-22.02	-94.87	-
345.15	-147.6	-132.4	-110.8	-	-	-	-
348.15	-158.9	-141.1	-125.5	-27.93	-22.84	-99.45	-
350.15	-165.5	-159.3	-130.2	-	-	-	-
353.15	-175.5	-173.9	-136.6	-32.88	-33.03	-102.0	-

จุฬาลงกรณ์มหาวิทยาลัย
CHULALONGKORN UNIVERSITY

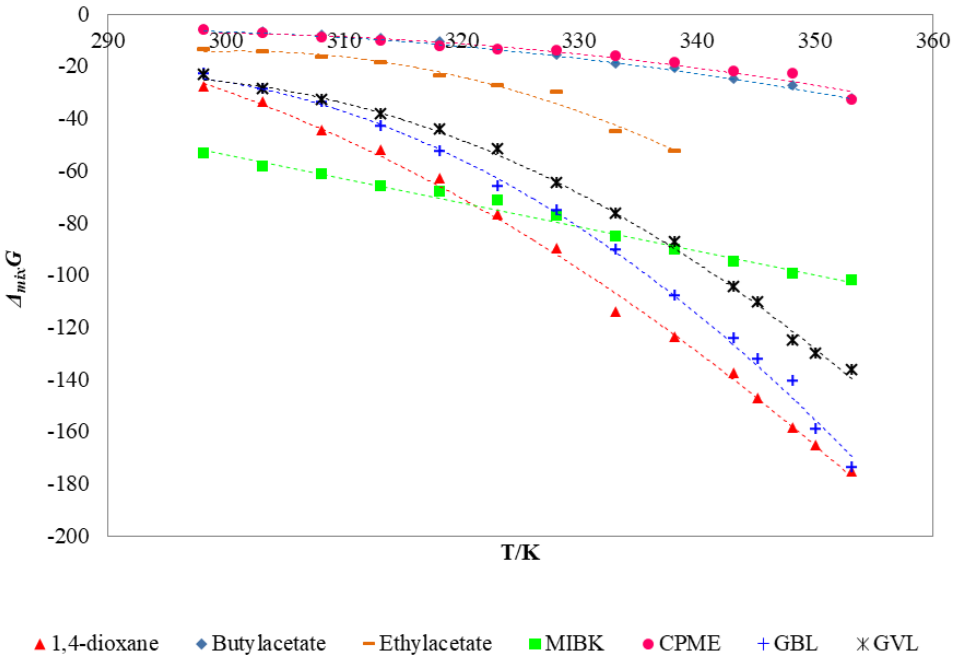

Fig. B.8. Gibbs free energy of mixing as a function of temperature.

B.5.8 Effect of solvent properties

DMPA is a strong polar compound so it is favored to dissolve in polar solvents. Moreover, it has been reported that the larger alkyl groups increased the hydrophobic effect, resulting in a decrease in solubility [42]. Besides, the O-H group of DMPA possesses strong proton donor ability, whereas the selected solvents are strong proton acceptors. DMPA, therefore, formed a strong hydrogen bond with these solvents. Hence, the solute-solvent interactions often occurred via H-bonds. These newly formed H-bonds between solute-solvent have a great effect on the solubility of a solute [20, 43]. Consequently, it was found that the functional groups that are capable of forming hydrogen bonds can enhance solubility [44]. However, the solubility behavior of a solute dissolved in a solvent is affected by various factors, such as polarity, molecular shapes and sizes, as well as the interactions between solute-solvent and self-interactions of solvent and solute [20]. In **Table B.11**, the polarity indexes of solvents used are presented.

Table B.11 The polarity index of solvents used. [45, 46]

Polarity index						
Ethylacetate	Butylacetate	CPME	MIBK	GBL	1,4-dioxane	GVL
4.4	4.0	N/A	4.2	N/A	4.8	N/A

*solubility of CPME in water at 296.15 K = 1.1 (g/100 g) [47]

*solubility of 1,4-dioxane in water at 296.15 K = infinite [47]

*solubility of GBL in water = very soluble [48]

*solubility of GBL in water at 285.93 K = greater than or equal to 100 (mg/mL) [49]

*solubility of GVL in water at 295.37 K = greater than or equal to 100 (mg/mL) [49]

In **Table B.12**, the physicochemical properties of the selected solvents are listed in order to further understand the solid-liquid equilibrium of DMPA. As graphically shown in **Fig. B.9**, the relationship between the solubility of DMPA (at 298.15 K) and the physicochemical properties are depicted. Results reveal that the solubility of DMPA depends on polarity, hydrogen bond acceptor propensity and cohesive energy density. A higher value of cohesive energy density indicates the strength of solute-solvent interaction and plays a vital role in the solid-liquid equilibrium [41]. Thus, the higher values of cohesive energy density result in the higher amount of solubility of DMPA. Of all solvents investigated, 1,4-dioxane exhibited the highest solubility owing to its high polarity, its highest hydrogen bond acceptor propensity and its cohesive energy density.

Table B.12 Physicochemical properties of selected solvents.[50]

Solvents	**π^a**	**$\sum\alpha^b$**	**$\sum\beta^c$**	**Cohesive energy density[d]**
Ethylacetate	0.55	0.00	0.45	300.64
Butylacetate	0.46	0.00	0.45	256.96
MIBK	0.65	0.00	0.51	253.06
1,4-dioxane	0.51	0.00	0.64	372.17
GBL	N/A	N/A	N/A	N/A
GVL	N/A	N/A	N/A	N/A
CPME	N/A	N/A	N/A	N/A

Note: MIBK, GBL, GVL and CPME, are methyl isobutyl ketone, gamma-butyrolactone, gamma-valerolactone and cyclopentyl methyl ether, respectively.

[a]Polarity of solvents.

[b]Summation of the hydrogen bond donor propensities of the solvent.

[c]Summation of the hydrogen bond acceptor propensities of the solvent.

[d]Cohesive energy density in the unit of $J \cdot mol^{-1} \cdot mL^{-1}$.

จุฬาลงกรณ์มหาวิทยาลัย
Chulalongkorn University

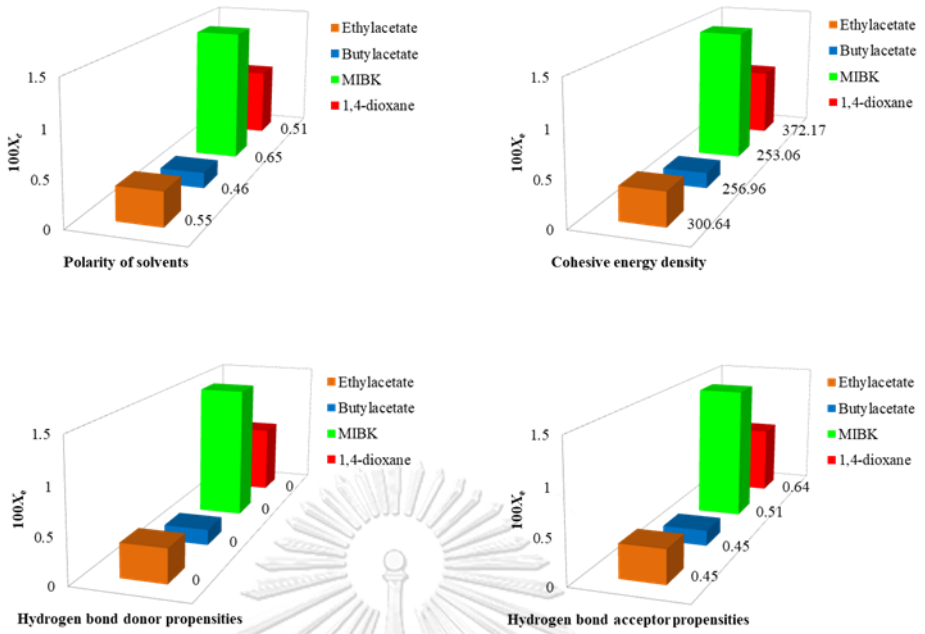

Fig. B.9. Solubility spectra of DMPA in selected solvents at 298.15 K as a function of solvent polarity, hydrogen bond donor propensity, hydrogen bond acceptor propensity and cohesive energy density.

Solvent selection was carried out in order to enhance production yield. When aliphatic alcohols were employed, partial esterification of DMPA was observed. For this reason, alcohol as a solvent for the measurement of DMPA solubility was not used to prevent esterification reaction. Esterification reaction can occur in the presence of carboxylic acid and alcohol. Further, DMPA is unstable at higher temperatures; therefore, the experiment has been conducted at low temperature range.

B.6 Conclusion

Herein, it is evident that the solubility of DMPA is dependent on temperature. As temperature increased, the mole fraction solubility of DMPA in the selected solvents

increased. Moreover, effective solvent selection can be achieved using experimental solubility data. It is noted that all three thermodynamic models proved to be suitable for the solubility correlation of DMPA regarding the solvents considered. Positive values of H^E indicated that dissolution was an endothermic process. Besides, the values of $\Delta_{sol}H$ and $\Delta_{sol}S$ demonstrated that the dissolution process was both an endothermic and entropy-driven process.

B.7 Acknowledgement

The authors profoundly appreciate the support from the Thailand Research Fund and Chulalongkorn University under the Research and Researchers for Industries (RRi) Ph.D. Program (Grant No. PHD58I0081) and the Slovak grant APVV-15-0482. Thanks are also given to the Laboratory of Catalyzed Processes, Department of Organic Technology, Faculty of Chemical and Food Technology, Slovak University of Technology in Bratislava, Slovak Republic, for supplying chemical compounds and instruments for analysis and measurement.

B.8 Nomenclature

a_i	activity of DMPA
a_s	activities of solid
a_w	activities of liquid
A, B and C	empirical parameters (the Apelblat equation)
CPME	cyclopentyl methyl ether
DMPA	dimethylolpropionic acid or 2,2-bis(hydroxymethyl)propanoic acid
GBL	gamma-butyrolactone
GVL	gamma-valerolactone
g_{12} and g_{21}	equation parameters (NRTL model)

จุฬาลงกรณ์มหาวิทยาลัย
Chulalongkorn University

H^E	excess enthalpy of solutions ($kJmol^{-1}$)
K_i	dissolution equilibrium constants
MIBK	methyl isobutyl ketone
M_1	molar masses of DMPA
M_2	molar masses of solvent
m_1	mass of DMPA
m_2	mass of solvent
n	total experimental points
R	gas constant
T	the absolute temperature (K)
T_m	melting temperature (K)
x	mole fraction solubility of solute in solvent
x_c	the calculated molar fraction of solubility
x_e	the experimental molar fraction of solubility
λ and h	empirical parameters (Buchowski–Ksiązczak λh equation)
$\Delta_{fus}H$	fusion enthalpy of DMPA ($kJ \cdot mol^{-1}$)
$\Delta_{sol}H$	molar enthalpy of dissolutions ($kJ \cdot mol^{-1}$)
$\Delta_{sol}S$	molar entropy of dissolutions ($J \cdot mol^{-1} \cdot K^{-1}$)
α_{ij}	the solution non-randomness

จุฬาลงกรณ์มหาวิทยาลัย
CHULALONGKORN UNIVERSITY

B.9 References

[1] C. Gao, D. Yan, Hyperbranched polymers: from synthesis to applications, Prog. Polym. Sci. 29 (2004) 183–275.

[2] L. Chikh, M. Tessier, A. Fradet, NMR and MALDI-TOF MS study of side reactions in hyperbranched polyesters based on 2,2-bis(hydroxymethyl)propanoic acid, Polymer 48 (2007) 1884-1892.

[3] E. Zagar, M. Zigon, Aliphatic hyperbranched polyesters based on 2,2-bis(methylol)propionic acid—Determination of structure, solution and bulk properties, Prog. Polym. Sci. 36 (2011) 53–88.

[4] A. Burgath, A. Sunder, H. Frey, Role of cyclization in the synthesis of hyperbranched aliphatic polyesters, Macromol. Chem. Phys. 201 (2000) 782–791.

[5] E. Zagar, M. Zigon, S. Podzimek, Characterization of commercial aliphatic hyperbranched polyesters, Polymer 47 (2006) 166-175.

[6] T.S. Demina, T.A. Akopova, L.V. Vladimirov, A.N. Shchegolikhin, A.S. Kechek'yan, N.S. Perov, A.O. Chernyshenko, A.N. Zelenetskii, The Study of the Interaction between Chitosan and 2,2Bis(hydroxymethyl)propionic Acid during SolidPhase Synthesis, Polymer Sci., Ser.B. 53(5–6) (2011) 358–370.

จุฬาลงกรณ์มหาวิทยาลัย
Chulalongkorn University

[7] J. Taskinen, U. Norinder (2007) ADME-Tox Approaches, Vol. 5 (eds. in Comprehensive Medicinal Chemistry II (series eds D. Triggle and J. Taylor), Elsevier, Oxford, pp. 627–648.

[8] R. Sulaiman, M.K. Hadj-Kali, S.W. Hasan, S. Mulyono, I.M. Alnashef, Investigating the solubility of chlorophenols in hydrophobic ionic liquids, J. Chem. Thermodyn. 135 (2019) 97–106.

[9] R. Gillet, A. Fierro, L.M. Valenzuela, J.R. Perez-Correa, Using molecular dynamics simulations to predict the effect of temperature on aqueous solubility for aromatic compounds, Fluid Phase Equilib. 472 (2018) 85-93.

[10] http://www.chemspider.com/Chemical-Structure.70865.html(09/01/2020)

[11] E.S. Ha, Y.R. Lee, M.S. Kim, Solubility of dronedarone hydrochloride in six pure solvents at the range of 298.15 to 323.15 K, J. Mol. Liq. 216 (2016) 360-363.

[12] V. Mohdee, K. Fulajtárová, T. Soták, S. Phatanasri, M. Hronec, U. Pancharoen, Solubility modelling and solvent effect on solid-liquid equilibrium of2,2-bis(hydroxymethyl)butyric acid at different temperatures, J. Mol. Liq. 312 (2020) 113370.

[13] O. Folin, F.F. Flanders, Is ionization, as indicated by conductivity, A necessary prerequisite for the combination of acids with bases, J. Am. Chem. Soc. 34 (1912) 774-779.

[14] J.S. Fritz, N.M. Lisicki, Titration of Acids in Nonaqueous Solvents, Anal. Chem. 23(4) (1951) 589-591.

[15] T. Gundiiz, N. Giindiiz, E. Killc, F. Koseoglu, S.G.Oztas, Titrations in Non-aqueous Media: Part X.* Potentiometric and Conductimetric Titrations of Amino Acids with Tetrabutylammonium Hydroxide in Pyridine and Acetonitrile Solvents, Analyst, 113 (1988) 715-719.

[16] L. Wu, X. Hu, D. Mourant, Y. Wang, C. Kelly, M. Garcia-Perez, M. He, C.Z. Li, Quantification of strong and weak acidities in bio-oil via non-aqueous potentiometric titration, Fuel, 115 (2014) 652–657.

[17] J.A. Riddick, Acid-Base titrations in non-aqueous solvents, Anal. Chem. 24(1) (1952) 41-46.

จุฬาลงกรณ์มหาวิทยาลัย
Chulalongkorn University

[18] X. Zhang, Y. Wang, X. Huang, X. Meng, L. Luo, X. Li, B. Sakoth, H. Hao, Solubility and thermodynamic properties of azlocillin in pure and binary solvent systems, J. Mol. Liq. 286 (2019) 110897.

[19] R. Xu, J. Wang, S. Han, C. Du, L. Meng, H. Zhao, Solubility modelling and thermodynamic dissolution functions of phthalimide in ten organic solvents, J. Chem. Thermodyn. 94 (2016) 160–168.

[20] M. Zheng, J. Chen, G. Chen, A. Farajtabar, H. Zhao, Solubility modelling and solvent effect for domperidone in twelve green solvents, J. Mol. Liq. 261 (2018) 50–56.

[21] H. Renon, J.M. Prausnitz, Local Compositions in Thermodynamic Excess Functions for Liquid Mixtures, AlChE Journal 14(1) (1968) 135-144.

[22] M.J. Richardson and E.L. Charsley, Chapter 13: Calibration and standardization in DSC, in: Handbook of Thermal Analysis and Calorimetry: Principles and Practice, Vol.1, Elsevier, Amsterdam, 1998, pp.547-575.

จุฬาลงกรณ์มหาวิทยาลัย
CHULALONGKORN UNIVERSITY

[23] E. Murrill, L. Breed, Solid-solid phase transitions determined by differential scanning calorimetry: Part 1 Tetrahedral substances, Thermochim. Acta, 1 (1970) 239-246.

[24] D. Haillot, T. Bauer, U. Kröner, R. Tamme, Thermal analysis of phase change materials in the temperature range 120–150 °C, Thermochimica Acta, 513 (2011) 49–59.

[25] R. Riemschneider, K. Schneider, S. Brennecke, H.D. Otto, O. Matzer, Cinnamic acid ester of dihydroxypivalic acid, Monatsh. Chem. 88 (1957) 1099-1104.

[26] S.S. Moreno, S. Doppiu, G.A. Lopez, N. Marinova, Á. Serrano, E. Silveira, E.P. Del Barrio, Study of the Phase Transitions in the Binary System NPG-TRIS for Thermal Energy Storage Applications, Materials, 13 (2020) 1162.

[27] J. Waschull, R. Müller, S. Römer, Investigation of phase change materials for elevated temperatures, in: Proceeding of Effstock Conference 2009, 14–17 June, Stockholm, Sweden, 2009.

[28] S. Kandi, A.L. Charles, Measurement, correlation, and thermodynamic properties for solubilities of bioactive compound (−)-epicatechin in different pure solvents at 298.15 K to 338.15 K, J. Mol. Liq. 264 (2018) 269–274.

[29] C.L. Zhang, F. Zhao, Y. Wang, Thermodynamics of the solubility of sulfamethazine in methanol, ethanol,1-propanol, acetone, and chloroform from 293.15 to 333.15 K, J. Mol. Liq. 159 (2011) 170-172.

[30] E.S. Ha, S.K. Lee, J.S. Jeong, W.Y. Sim, J.I. Yang, J.S. Kim, M.S. Kim, Solvent effect and solubility modeling of rebamipide in twelve solvents at different temperatures, J. Mol. Liq. 288 (2019) 111041.

[31] K.D. Bhesaniya, K.V. Chavda, C.H. Sadhu, S. Baluja, Thermodynamic characteristics of solutions of ornidazole in different organic solvents at different temperatures, J. Mol. Liq. 191 (2014) 124–127.

[32] F. Shakeel, M. Iqbal, E. Ezzeldin, N. Haq, Thermodynamics of solubility of ibrutinib in ethanol + water cosolvent mixtures at different temperatures, J. Mol. Liq. 209 (2015) 461–464.

จุฬาลงกรณ์มหาวิทยาลัย
Chulalongkorn University

[33] E.S. Ha, D.H. Kuk, D.H. Ha, W.Y. Sim, I.H. Baek, J.S. Kim, M.S. Kim, Determination and correlation of solubility of sarpogrelate hydrochloride in eight solvents at different temperatures, J. Mol. Liq. 237 (2017) 141–145.

[34] M.K. Anwer, R. Al-Shdefat, S. Jamil, P. Alam, M.S. Abdel-Kader, F. Shakeel, Solubility of bioactive compound hesperidin in six pure solvents at (298.15 to 333.15) K, J. Chem. Eng. Data 59 (2014) 2065–2069.

[35] C.L. Zhang, F. Zhao, Y. Wang, Thermodynamics of the solubility of sulfamethazine in methanol, ethanol, 1-propanol, acetone, and chloroform from 293.15 to 333.15 K, J. Mol. Liq. 159 (2011) 170–172.

[36] K. Wang, Y.H. Hu, W. Yang, S. Guo, Y. Shi, Measurement and correlation of the solubility of 2,3,4,5-tetrabromothiophene in different solvents, J. Chem. Thermodyn. 55 (2012) 50–55.

[37] Z.H. Yang, Z.X. Zeng, L. Sun,W.L. Xue, N. Chen, Determination and correlation of solubilities of lauric acid in eight alcohols, J. Chem. Eng. Data 59 (2014) 2725–2731.

จุฬาลงกรณ์มหาวิทยาลัย
CHULALONGKORN UNIVERSITY

[38] K.D. Bhesaniya, K.V. Chavda, C.H. Sadhu, S. Baluja, Thermodynamic characteristics of solutions of ornidazole in different organic solvents at different temperatures, J. Mol. Liq. 191 (2014) 124–127.

[39] H. Buchowski, A. Ksiazczak, S. Pietrzyk, Solvent Activity along a Saturation Line and Solubility of Hydrogen-Bonding Solids, J. Phys. Chem. 84 (1980) 975-979.

[40] R. Xu, J. Wang, S. Han, C. Du, L. Meng, H. Zhao, Solubility modelling and thermodynamic dissolution functions of phthalimide in ten organic solvents, J. Chem. Thermodyn. 94 (2016) 160–168.

[41] S. Zhao, Y. Ma, J. Gong, B. Hou, W. Tang, Solid-liquid phase equilibrium and thermodynamic analysis of griseofulvin in twelve mono-solvents, J. Mol. Liq. 296 (2019) 111861.

[42] G.L. Patrick, Chapter 14: Drug design: optimizing access to the target, An Introduction to Medicinal Chemistry, Fifth Edition, Great Clarendon Street, Oxford, United Kingdom, 2013.

[43] M.A. Varfolomeev, M.A. Stolov, R.N. Nagrimanov, I.T. Rakipov, W.E. Acree Jr., M.H. Abraham, Analysis of solute-pyridine intermolecular interactions based on experimental enthalpies of solution and enthalpies of solvation of solutes dissolved in pyridine, Thermochimica Acta 660 (2018) 11–17.

[44] M.W. Harrold and R.M. Zavod, Chapter 2: Functional Group Characteristics and Roles, Basic Concepts in Medicinal Chemistry, American Society of Health-System Pharmacists®, Bethesda, Maryland, 2013.

[45] M. Kleiman, K.A. Ryu, A.P. Esser-Kahn, Determination of Factors Influencing the Wet Etching of Polydimethylsiloxane Using Tetra-n-butylammonium Fluoride, Macromol. Chem. Phys. 217 (2016) 284—291.

[46] L.R. Snyder, J.J. Kirkland, J.L. Glajch, Practical HPLC Method Development, Second Edition, John Wiley & Sons, Inc. 1997,

[47] K. Watanabe, N. Yamagiwa, Y. Torisawa, Cyclopentyl Methyl Ether as a New and Alternative Process Solvent, Organic Pro. Research&Develop. 11 (2007) 251—258.

CHULALONGKORN UNIVERSITY

[48] Gamma-butyrolactone (GBL), Critical Review Report Agenda item 4.3, Expert Committee on Drug Dependence, Thirty-sixth Meeting, WHO Secretariat, Essential Medicines and Health Products, Policy Access and Rational Use Unit Geneva, 2014.

[49] National Toxicology Program, Institute of Environmental Health Sciences, National Institutes of Health (NTP). 1992.

[50] C.H. Gu, H. Li, R.B. Gandhi, K. Raghavan, Grouping solvents by statistical analysis of solvent property parameters: implication to polymorph screening, Int. J. Pharm. 283 (2004) 117-125.

จุฬาลงกรณ์มหาวิทยาลัย
CHULALONGKORN UNIVERSITY

References

1 Huang, H., Huang, C., Wu, Y., Ding, S., Liu, N., Su, D., Lv., T. *Extraction of palladium (II) from nitric acid solutions with diglycolthioamide*. Hydrometallurgy, 2015. **156**: p.6–11.

2 Cieszynska, A. and Wieczorek, D. *Extraction and separation of palladium (II), platinum (IV), gold (III) and rhodium (III) using piperidine-based extractants.* Hydrometallurgy, 2018. **175**: p.359–366.

3 Liu, K., Zhang, Z., Zhang, F.S. *Direct extraction of palladium and silver from waste printed circuit boards powder by supercritical fluids oxidation-extraction process*. Journal of Hazardous Materials, 2016. **318**: p. 216–223.

4 Li, J., Lu, H., Guo, J., Xu, Z., Zhou, Y. *Recycle technology for recovering resources and products from waste printed circuit boards*. Environmental Science & Technology, 2007. **411**: p.995–2000.

5. Dabrowski, X., Hubicki, Z., Podkóscielny, P., Robens, E. *Selective removal of the heavy metal ions from waters and industrial wastewaters by ion-exchange method*. Chemosphere, 2004. **56**: p.91–106.

6. Aziz, A., Jan, S., Waqar, F., Mohammad, B., Hakim, M., Yawar, W. *Selective ion exchange separation of uranium from concomitant impurities in uranium materials and subsequent determination of the impurities by ICP-OES*. Journal of Radioanalytical and Nuclear Chemistry, 2010. **284**: p.117-121.

7. Malhotra, R.K. and Satyanarayana, K. *Estimation of trace impurities in reactor-grade uranium using ICP-AES*. Talanta, 1999. **50**: p.601-608.

8. Assunção, A., Matos, A., Costa, A.M.R., Candeias, A., Costa, M.C. *A bridge between liquid–liquid extraction and the use of bacterial communities for palladium and platinum recovery as nanosized metal sulphides*. Hydrometallurgy, 2016. **163**: p.40–48.

9. Wannachod, T., Mohdee, V., Suren, Sira., Ramakul, P., Pancharoen, U., Nootong, K. *The separation of Nd (III) from mixed rare earth via hollow fiber supported liquid membrane and mass transfer analysis*. Journal of Industrial and Engineering Chemistry, 2015. **26**: p.214–217.

10. Vladimir, S.K. Chapter 1: Introduction, General Description, Definitions, and Classification. Liquid Membranes Principles and Applications in Chemical Separations and Wastewater Treatment. 2010, p.1-15.

11. Sirkar, K.K. Other new membrane processes. In:W.S.W. Ho, K.K. Sirkar (Eds.), Membrane Handbook, Van Nostrand Reinhold, New York, NY; 1992, p.904-908.

12. Coelhoso, I.M., Cardoso, M.M., Viegas, R.M.C., Crespo, J.P.S.G. *Transport mechanisms and modelling in liquid membrane contactors*. Separation and Purification Technology, 2000. **19**: p.183-197.

13. Rout, P.C. and Sarangi, K. *A comparative study on extraction of Mo (VI) using both solvent extraction and hollow fiber membrane technique*. Hydrometallurgy, 2013. **133**: p.149-155.

14. Uheida, A., Zhang, Y., Muhammed, M. *Transport of palladium (II) through hollow fiber supported liquid membrane facilitated by nonylthiourea*. Journal of Membrane Science, 2004. **241**: p.289–295

จุฬาลงกรณ์มหาวิทยาลัย
Chulalongkorn University

15. Wongkaew, K., Sunsandee, N., Pancharoen, U., Nootong, K., Ramakul, P. *Purification of Sn (IV) and recovery of Pd (II) from flexible printed circuit board industry wastewater via HFSLM: Temperature effect investigation*. Journal of Industrial and Engineering Chemistry, 2015. **22**: p.217–228.

16. Swain, B., Jeong, J., Kim, S.K., Lee, J.C. *Separation of platinum and palladium from chloride solution by solvent extraction using Alamine 300*. Hydrometallurgy, 2010. **104**: p.1–7.

17. Ahmed, I.M., Nayl, A.A., Daoud, J.A. *Extraction of palladium from nitrate solution by CYANEX 471X*. International Journal of Mineral Processing, 2011. **101(1–4)**: P.89-93.

18. Wei, W., Cho, C.W., Kim, S., Song, M.H., Bediako, J.K., Yun, Y.S. *Selective recovery of Au (III), Pt (IV), and Pd (II) fromaqueous solutions by liquid–liquid extraction using ionic liquid Aliquat-336*. Journal of Molecular Liquids, 2016. **216**: p.18–24.

19. Cieszynska, A., and Wisniewski, M. *Selective extraction of palladium (II) from hydrochloric acid solutions with phosphonium extractants*. Separation and Purification Technology, 2011. **80**: p.385–389

20. Scott, M.D., Schorp, J., Sutherlin, L., Robertson, J.D. *Isotope harvesting with Hollow Fiber Supported Liquid Membrane (HFSLM)*. Applied Radiation and Isotopes, 2020. **157**: 109027.

21. Ni'am, A.C., Wang, Y.F., Chen, S.W., Chang, G.M., You, S.J. *Simultaneous recovery of rare earth elements from waste permanent magnets (WPMs) leach liquor by solvent extraction and hollow fiber supported liquid membrane*. Chemical Engineering and Processing - Process Intensification, 2020. **148**: 107831.

จุฬาลงกรณ์มหาวิทยาลัย
Chulalongkorn University

22. Sunsandee, N., Phatanasri, S., Ramakul, P., Pancharoen, U. *Thermodynamic parameters and isotherm application on enantiomeric separation of levofloxacin using hollow fiber supported liquid membrane system*. Separation and Purification Technology, 2018. **195**: p. 377–387.

23. Swain, B., Mishra, C., Jeong, J., Lee, J.C., Hong, H.S., Pandey, B.D., *Separation of Co (II) and Li (I) with Cyanex 272 using hollow fiber supported liquid membrane: A comparison with flat sheet supported liquid membrane and dispersive solvent extraction process*. Chemical Engineering Journal, 2015. **271**: p.61–70.

24. Jagasia, P., Ansari, S.A., Raut, D.R., Dhami, P.S., Gandhi, P.M., Kumar, A., Mohapatra, P.K. *Hollow fiber supported liquid membrane studies using a process compatible solvent containing calix[4]arene-mono-crown-6 for the recovery of radio-cesium from nuclear waste*. Separation and Purification Technology, 2016. **170**: p.208-216.

25. Kandwal, P., Ansari, S.A., Mohapatra, P.K. *Transport of cesium using hollow fiber supported liquid membrane containing calix[4]arene-bis(2,3-naphtho)crown-6 as the carrier extractant: Part II. Recovery from simulated high level waste and mass transfer modeling*. Journal of Membrane Science, 2011. **384**: p.37-43.

26. Liu, Y., Shi, B. *Hollow fiber supported liquid membrane for extraction of ethylbenzene and nitrobenzene from aqueous solution: A Hansen Solubility Parameter approach*. Separation and Purification Technology, 2009. **65(3)**: P.233-242.

27. Sun, H., Yao, J., Li, D., Liu, B., Liu, S., Cong, H., Agtmaal, S.V., Feng, C. *Removal of phenols from coal gasificationwastewater through polypropylene*

จุฬาลงกรณ์มหาวิทยาลัย
Chulalongkorn University

hollow fibersupported liquid membrane. Chemical Engineering Research and Design, 2017. **123**: p.277–283.

28. Kocherginsky, N.M., Yang, Q., Seelam, L. *Recent advances in supported liquid membrane technology*. Separation and Purification Technology, 2007. **53**: p.171–177

29. Kislik, V.S. Chapter 2: Carrier-facilitated coupled transport through liquid membranes: General theoretical considerations and influencing parameters. Liquid Membranes: Principles and Applications in Chemical Separations and Wastewater Treatment. p.17-71.

30. Parhi, P.K. *Supported liquid membrane principle and its practices: A short review*. Journal of Chemistry, 2013. **2013**: p.1-11. http://dx.doi.org/10.1155/2013/618236.

31. Chitra, K.R., Gaikwad, A.G., Surender, G.D., Damodaran, A.D. *Studies on ion transport of some rare earth elements through solvating extractants immobilised on supported liquid membrane*. Journal of Membrane Science, 1997. **125(2)**: p.257–268.

32. Aamrani, F.Z., Kumar, A., Beyer, L., Florido, A., Sastre, A.M. *Mechanistic study of active transport of silver (I) using sulfur containing novel carriers across a liquid membrane*. Journal of Membrane Science, 1999. **152(2)**: p.263–275.

33. Sastre, A.M., Madi, A., Alguacil, F.J. *Solvent extraction of* $Au(CN)^{-2}$ *and application to facilitated supported liquid membrane transport*. Hydrometallurgy, 2000. **54(2)**: p.171–184.

จุฬาลงกรณ์มหาวิทยาลัย
CHULALONGKORN UNIVERSITY

34. Parhi, P.K. and Sarangi, K. *Separation of copper, zinc, cobalt and nickel ions by supported liquid membrane technique using LIX 84I, TOPS-99 and Cyanex 272*. Separation and Purification Technology, 2008. **59(2)**: p.169–174.

35. Eljaddi, T., Lebrun, L., Hlaibi, M. *Review on Mechanism of Facilitated Transport on Liquid Membranes*. Journal of Membrane Science and Research, 2017. **3**: p.199-208.

36. Kocherginsky, N.M., Yang, Q., Seelam, L. *Recent advances in supported liquid membrane technology*. Separation and Purification Technology, 2007. **53**: p.171–177

37. Tang, Y., Liu, W., Wan, J., Wang, Y., Yang, X. *Two-stage recovery of S-adenosylmethionine using supported liquid membranes with strip dispersion*. Process Biochemistry, 2013. **48(12)**: p.1980-1991.

38. Wilke, C.R. and Chang, P. *Correlation of diffusion coefficients in dilute solutions*. AIChE J. (1955). **1**: p.264–270.

39. Moldoveanu, S. and David V. Chapter 6. Solvent extraction. In: Modern Sample Preparation for Chromatography. 2015. p.131-189.

40. Todd D.B. Chapter 11 – Solvent extraction. In: Fermentation and Biochemical Engineering Handbook (Third Edition), 2014. p.225-238.

41. Chen, H. and Wang L. Chapter 8 - Posttreatment Strategies for Biomass Conversion. Technologies for Biochemical Conversion of Biomass. 2017, p.197-217.

42. Clarke K.G. Chapter 11 - Downstream processing. Bioprocess Engineering An Introductory Engineering and Life Science Approach. 2013, P.209-234.

43. Pei, L., Wang, L., Yu, G. *Separation of Eu (III) with supported dispersion liquid membrane system containing D2EHPA as carrier and HNO_3 solution as stripping solution*. Journal of Rare Earths, 2011. **29**: p.7-14.

44. Bhatluri, K.K., Manna, M.S., Saha, P., Ghoshal, A.K. *Supported liquid membrane based simultaneous separation of cadmium and lead from wastewater*. Journal of Membrane Science, 2014. **459**: p.256-263.

45. Wannachod, T., Mohdee, V., Suren, S., Ramakul, P., Pancharoen, U., Nootong, K. *The separation of Nd (III) from mixed rare earth via hollow fiber supported liquid membrane and mass transfer analysis*. Journal of Industrial and Engineering Chemistry, 2015. **26**: p.214–217.

46. Rout, P.C., Sarangi, K. *Separation of vanadium using both hollow fiber membrane and solvent extraction technique – a comparative study*. Separation and Purification Technology, 2014. **122**: p.270-277.

47. Kumar, A., Haddad, R., Alguacil, F.J., Sastre, A.M. *Comparative performance of non-dispersive solvent extraction using a single module and the integrated membrane process with two hollow fiber contactors*. Journal of Membrane Science, 2005. **248**: p.1-14.

48. Kandwal, P., Dixit, S., Mukhopadhyay, S., Mohapatra, P.K. *Mass transport modelling of Cs (I) through hollow fiber supported liquid membrane containing calix-[4]-bis(2,3-naptho)-crown-6 as the mobile carrier*. Chemical Engineering Journal, 2011. **174**: p.110-116.

49. A. Uheida, Y. Zhang, M. Muhammed, Transport of palladium (II) through hollow fiber supported liquid membrane facilitated by nonylthiourea, J. Membrane Sci. 241 (2004) 289–295.

จุฬาลงกรณ์มหาวิทยาลัย
Chulalongkorn University

50. Mohdee, V., Ramakul, P., Phatanasri, S., Pancharoen, U. *A numerical and experimental investigation on the selective separation of Pd (II) from wastewater using Aliquat 336 via hollow fiber supported liquid membrane*. Journal of Environmental Chemical Engineering, 2020. **8** Article 104234. Doi: https://doi.org/10.1016/j.jece.2020.104234.

51. Mohdee, V., Maneeintr, K., Wannachod, T., Phatanasri, S., Pancharoen, U. *Optimization of process parameters using response surface methodology for Pd (II) extraction with quaternary ammonium salt from chloride medium: kinetic and thermodynamics study*. Chemical Papers, 2018. **72**: p.3129–3139.

52. Mohdee, V., Maneeintr, K., Phatanasri, S., Pancharoen, U. *Synergistic strippants of Pd (II) ions in the presence of chloride medium from wastewater of electroless plating process via solvating system: Kinetics and thermodynamics study*. Separation Science and Technology, 2019. **54(17)**: p.2971–2982.

53. Manna, M.S., Saha, P., Ghoshal, A.K. *Studies on the stability of a supported liquid membrane and its cleaning protocol*. RSC Adv. 2015. **5**: p.71999–72008

54. Koonsang, T., Aunnankat, K., Maneeintr, K., Pancharoen, U., Wongsawa, T. *The mutual solubility of organic-liquid membrane and aqueous phases atdifferent water pH for the stability of SLM using Aliquat 336 as anionic-liquid extractant*. Journal of Molecular Liquids, 2019. **292** Article 111363. Doi: https://doi.org/10.1016/j.molliq.2019.111363.

55. Mohdee, V., Fulajtárová, K., Soták, S., Phatanasri, S., Hronec, M., Pancharoen, U. *Solubility modelling and solvent effect on solid-liquid equilibrium of 2,2-bis(hydroxymethyl)butyric acid at different temperatures*. Journal of Molecular

Chulalongkorn University

Liquids, 2020. **312** Article 113370. Doi: https://doi.org/10.1016/j.molliq.2020.113370.

56. Mohdee, V., Fulajtárová, K., Soták, S., Phatanasri, S., Hronec, M., Pancharoen, U. *Corrigendum to "Solubility modelling and solvent effect on solid-liquid equilibrium of 2,2-bis(hydroxymethyl)butyric acid at different temperatures" [J. Mol. Liq. 312 (2020) 113370]*. Journal of Molecular Liquids, 2020. Article 113752. Doi: https://doi.org/10.1016/j.molliq.2020.113752.

จุฬาลงกรณ์มหาวิทยาลัย
CHULALONGKORN UNIVERSITY

REFERENCES

จุฬาลงกรณ์มหาวิทยาลัย
Chulalongkorn University

จุฬาลงกรณ์มหาวิทยาลัย
Chulalongkorn University

VITA

NAME Vanee Mohdee

DATE OF BIRTH 21 May 1986

PLACE OF BIRTH Udonthani

INSTITUTIONS ATTENDED 2009 - 2012 M.Sc.(Chemical Technology)
Chulalongkorn University
2004 - 2008 B.Sc.(CHEMISTRY)
Khon Kaen University

HOME ADDRESS 1356/309 Mansion 107, Baring 12
Sukhumvit road Samrong Nua
Muang, Samutprakarn, 10270

PUBLICATION

[1] Vanee Mohdee, Kreangkrai Maneeintr, Thanaporn Wannachod, Suphot Phatanasri, Ura Pancharoen, Optimization of process parameters using response surface methodology for Pd(II) extraction with quaternary ammonium salt from chloride medium: kinetic and thermodynamics study, Chemical Papers 72 (2018) 3129–3139.

จุฬาลงกรณ์มหาวิทยาลัย
CHULALONGKORN UNIVERSITY

[2] Vanee Mohdee, Kreangkrai Maneeintr, Suphot Phatanasri, Ura Pancharoen, Synergistic strippants of Pd (II) ions in the presence of chloride medium from wastewater of electroless plating process via solvating system: Kinetics and thermodynamics study, Separation Science and Technology 54 (17) (2019) 2971-2982.

[3] Vanee Mohdee, Katarína Fulajtárová, Tomáš Soták, Suphot Phatanasri, Milan Hronec, Ura Pancharoen, Solubility modelling and solvent effect on solid-liquid equilibrium of 2,2-bis(hydroxymethyl)butyric acid at different temperatures, Journal of Molecular Liquids. 312 (2020) Article 113370. DOi: https://doi.org/10.1016/j.molliq.2020.113370.

[4] Vanee Mohdee, Prakorn Ramakul, Suphot Phatanasri, Ura Pancharoen, A numerical and experimental investigation on the selective separation of Pd (II) from wastewater using Aliquat 336 via hollow fiber supported liquid membrane, Journal of Environmental Chemical Engineering. 8 (2020) Article 104234. Doi: https://doi.org/10.1016/j.jece.2020.104234

[5] Thanaporn Wannachod, Vanee Mohdee, Sira Suren, Prakorn Ramakul, Ura Pancharoen, Kasidit Nootong, The separation of Nd (III) from mixed rare earth via hollow fiber supported liquid membrane and mass transfer analysis, Journal of Industrial and Engineering Chemistry 26 (2015) 214-217.

[6] Thanaporn Wannachod, Phupairum Phuphaibul, Vanee Mohdee, Ura Pancharoen, Suphot Phatanasri, Optimization of synergistic extraction of neodymium ions from monazite leach solution treatment via HFSLM using response surface methodology, Minerals Engineering 77 (2015) 1-9.

[7] Srestha Chaturabul, Thanaporn Wannachod, Vanee Mohdee, Ura Pancharoen, Suphot Phatanasri, An investigation of Calix[4]arene nitrile for mercury (II) treatment in HFSLM application, Chemical Engineering and Processing: Process Intensification 89 (2015) 35-40.

[8] Krirkratthawit Wongkaew, Thanaporn Wannachod, Vanee Mohdee, Ura Pancharoen, Amornchai Arpornwichanop, Anchaleeporn W.Lothongkum, Mass transfer resistance and response surface methodology for separation of platinum (IV) across hollow fiber supported liquid membrane, Journal of Industrial and Engineering Chemistry 42 (2016) 23-35.

[9] Krirkratthawit Wongkaew, Katarína Fulajtárova, Milan Hronec, Vanee Mohdee, Ura Pancharoen, Kasidit Nootong, Measurement of the solubility of the salt of 2-

จุฬาลงกรณ์มหาวิทยาลัย
CHULALONGKORN UNIVERSITY

mercaptobenzothiazole with cyclohexylamine and tert-butylamine in various solvents at low temperatures: Models and thermodynamic parameters, Fluid Phase Equilibria 434 (2017) 141-151.

[10] Krirkratthawit Wongkaew, Vanee Mohdee, Ura Pancharoen, Amornchai Arpornwichanop, Anchaleeporn W.Lothongkum, Separation of platinum (IV) across hollow fiber supported liquid membrane using non-toxic diluents: Mass transfer and thermodynamics, Journal of Industrial and Engineering Chemistry 54 (2017) 278-289.

จุฬาลงกรณ์มหาวิทยาลัย
CHULALONGKORN UNIVERSITY